

ADIPONECTIN AS A REGULATOR OF VASCULAR REDOX STATE IN HUMAN ATHEROSCLEROSIS

by

Marios Margaritis

Thesis presented for the degree of

Doctor of Philosophy in Cardiovascular Medicine

at the University of Oxford

Green Templeton College

Division of Cardiovascular Medicine

Radcliffe Department of Medicine

University of Oxford

Level 6, John Radcliffe Hospital

Oxford, OX3 9DU

Supervisors: Professor Charalambos Antoniades,

Professor Barbara Casadei, Professor Keith M Channon

Trinity Term 2016

Acknowledgments

This page has probably been the hardest –and most enjoyable- to write in my thesis. There are several individuals whose help has been instrumental in completing my research project and to whom I need to extend special thanks. First and foremost to my supervisor and mentor, Professor Antoniades; his invaluable guidance and assistance have undoubtedly influenced and shaped my career for years to come. To my joint supervisors Professor Casadei and Professor Channon, for their advice and continued support through these years. To my colleagues at the Division of Cardiovascular Medicine, in no particular order: Dr Alexios Antonopoulos, Dr Fabio Sanna, Dr Patricia Ciccone, Dr Ioannis Akoumianakis, Miss Laura Herdman, Dr Regent Lee, Dr Costantinos Psarros, Miss Akansha Tarun; we survived through it all together!

My research would have been impossible without the financial support of the British Heart Foundation Centre of Research Excellence – Oxford. In addition, I received funding from Research Council UK and through the Medical Research Council – Green Templeton College joint partnership award. I feel that I should also list my parents as a significant funding source, thanks mum and dad!

The omnipresent frustrations, obstacles and vicissitudes of any research degree mandate strong social and emotional support. I would not have been able to achieve this much without the unwavering and unconditional support of my family, both immediate and extended. Thanks mum for constantly urging me to get on with my writing! Special thanks to (soon-to-be Dr) Anna Kotova, my best friend and Oxford confidante; we did end up submitting at about the same time eventually! To Dr O'Leary; for more than his taxi-driver services. To all my friends in Greece and around the world; thank you for enriching my life and infusing me with much-needed energy boosts and inspiration whenever I felt at my wits' end.

Finally, I would like to express my support and admiration to all ambitious, driven scientists in the world who have spent and will spend thousands of hours of their lives in the laboratory, in the library and on the field. Your research has formed the basis of my own and countless other fellow scientists'. Our collective drive, enthusiasm and energy keep the gears spinning in the eternal quest to broaden humanity's horizons.

Sic luceat lux.

Dedication

For my parents and my sister

In memory of my grandmother and my aunt,

who passed away during the course of my DPhil studies

Abstract

Atherosclerotic cardiovascular disease is a leading cause of death worldwide. Dysregulation of vascular redox state plays a crucial role in the atherosclerotic process. Increased production of vascular superoxide ($O_2^{\cdot-}$) and other reactive oxygen species (ROS) leads to endothelial dysfunction, a key early step in atherogenesis. Adipose tissue is a source of vasoactive, hormone-like molecules which are termed adipokines. One of the most important adipokines is adiponectin. Adiponectin has been shown to have antioxidant, anti-atherosclerotic effects in cell culture studies and animal models. However, its role in human cardiovascular disease has not been extensively investigated. More specifically, its effects on the human vascular wall and the mechanisms regulating its synthesis in adipose tissue have not been studied before in humans.

The aim of my thesis is to explore the role of adiponectin in human atherosclerosis. This was achieved through use of the Oxford CABG Bioresource: a well-phenotyped cohort and tissue bank of patients undergoing cardiac surgery. By employing a range of *in vivo* and *ex vivo* techniques, I demonstrate for the first time in humans that adiponectin has direct antioxidant effects in the vascular wall, by directly suppressing pro-oxidant vascular enzymes and restoring redox balance. These effects persist in type 2 diabetes, presence of which is linked to reduced circulating adiponectin levels. Indeed, a variety of stimuli affect adiponectin synthesis in human adipose tissue, with brain natriuretic peptide being a major driver of adiponectin synthesis. However, different adipose tissue depots demonstrate diverse responses to stimuli affecting adiponectin synthesis, owing to their functional and morphological differences. Of particular interest is the fact that synthesis of adiponectin in perivascular adipose tissue is driven by the oxidative stress status of the underlying vessel. This observation led me to document for the first time in humans the existence of a reciprocal, two-way interaction between perivascular adipose tissue and the vascular wall: high vascular oxidative stress leads to release of factors with the ability to up-regulate adiponectin expression in perivascular adipose tissue, acting as a local paracrine defence mechanism attempting to restore vascular redox state. My thesis provides proof-of-concept for this novel cross-talk between adipose tissue and the vascular wall. This can have significant impact in designing new therapeutic strategies against atherosclerosis.

List of Publications & Presentations

Original manuscripts contributing to DPhil thesis

Margaritis M*, Antonopoulos AS*, Digby J, Lee R, Reilly S, Coutinho P, Shirodaria C, Sayeed R, Petrou M, De Silva R, Jalilzadeh S, Demosthenous M, Bakogiannis C, Tousoulis D, Stefanadis C, Choudhury RP, Casadei B, Channon KM, Antoniades C. Interactions between vascular wall and perivascular adipose tissue reveal novel roles for adiponectin in the regulation of endothelial nitric oxide synthase function in human vessels. ***Circulation*** 2013;127(22):2209-21. *Joint first authors

Margaritis M*, Antonopoulos AS*, Coutinho P, Digby J, Patel R, Psarros C, Ntusi N, Karamitsos TD, Lee R, De Silva R, Petrou M, Sayeed R, Demosthenous M, Bakogiannis C, Wordsworth PB, Tousoulis D, Neubauer S, Channon KM, Antoniades C.Reciprocal effects of systemic inflammation and brain natriuretic peptide on adiponectin biosynthesis in adipose tissue of patients with ischemic heart disease. ***Arterioscler Thromb Vasc Biol*** 2014;34(9):2151-9. *Joint first authors

Margaritis M*, Antonopoulos AS*, Coutinho P, Shirodaria C, Psarros C, Herdman L, Sanna F, De Silva R, Petrou M, Sayeed R, Krasopoulos G, Lee R, Digby J, Reilly S, Bakogiannis C, Tousoulis D, Kessler B, Casadei B, Channon KM, Antoniades C. Adiponectin As A Link Between Type 2 Diabetes Mellitus And Vascular NADPH-Oxidase Activity In The Human Arterial Wall: The Regulatory Role Of Perivascular Adipose Tissue. ***Diabetes*** 2015;64(6):2207-19.*Joint first authors

Other published manuscripts during DPhil

Margaritis M*, Lee R*, Channon KM, Antoniades C.Evaluating oxidative stress in human cardiovascular disease: methodological aspects and considerations. ***Curr Med Chem***. 2012;19(16):2504-20. *Joint first authors

Cunnington C, Van Assche T, Shirodaria C, Kylintireas I, Lindsay AC, Lee JM, Antoniades C, **Margaritis M**, Lee R, Cerrato R, Crabtree MJ, Francis JM, Sayeed R, Ratnatunga C, Pillai R, Choudhury RP, Neubauer S, Channon KM. Systemic and vascular oxidation limits the efficacy of oral tetrahydrobiopterin treatment in patients with coronary artery disease. ***Circulation*** 2012;125(11):1356-66.

Antoniades C, Demosthenous M, Reilly S, **Margaritis M**, Zhang MH, Antonopoulos A, Marinou K, Nahar K, Jayaram R, Tousoulis D, Bakogiannis C, Sayeed R, Triantafyllou C, Koumallos N, Psarros C, Miliou A, Stefanadis C, Channon KM, Casadei B. Myocardial redox state predicts in-hospital clinical outcome after cardiac surgery effects of short-term pre-operative statin treatment. ***J Am Coll Cardiol*** 2012;59(1):60-70.

Margaritis M, Channon KM, Antoniades C. Statins and vein graft failure in coronary bypass surgery. ***Curr Opin Pharmacol*** 2012;12(2):172-80.

Margaritis M, Channon KM, Antoniades C. Statins as regulators of redox state in the vascular endothelium: beyond lipid lowering. ***Antioxid Redox Signal*** 2014;20(8):1198-215.

Margaritis M*, Antonopoulos AS*, Verheule S, Recalde A, Sanna F, Herdman L, Psarros C, Nasrallah H, Coutinho P, Akoumianakis I, Brewer AC, Sayeed R, Krasopoulos G, Petrou M, Tarun A, Tousoulis D, Shah AM, Casadei B, Channon KM, Antoniades C. Mutual Regulation of Epicardial Adipose Tissue and Myocardial Redox State by PPAR-γ/Adiponectin Signalling. ***Circulation Research*** 2016; 118(5): 842–855. *Joint first authors

Young Investigator Awards during DPhil

Winner of the Young Investigator Prize – British Atherosclerosis Society/British Society for Cardiovascular Research Joint Spring Meeting, London 2013:

M Margaritis et al. A novel cross-talk between perivascular adipose tissue and the arterial wall controls redox state in human atherosclerosis *Heart* 2013;**99**:A4-A5

Winner of the Young Investigator Award, Session Coronary Pathophysiology and Microcirculation, European Society of Cardiology Congress, Amsterdam 2013:

M. Margaritis et al. A novel cross-talk between perivascular adipose tissue and the arterial wall controls redox state in human atherosclerosis *Eur Heart J 2013*

Winner of the Young Investigator Award, Session Ageing and Senescence, European Society of Cardiology Congress, London 2015:

M. Margaritis et al. Telomere length predicts clinical outcomes post-revascularization procedures: its role as a novel biomarker of systemic oxidative stress and cardiovascular ageing *Eur Heart J 2015*

Conference abstracts and presentations related to DPhil thesis

European Society of Cardiology Congress, Munich 2012 (poster presentation):

M Margaritis et al. Adiponectin produced in perivascular adipose tissue as a defence mechanism against vascular oxidative stress in human vein grafts. *Eur Heart J 2012*

American Heart Association Scientific Sessions, Los Angeles, 2012 (oral presentation – one of the top five abstracts submitted from the UK, highlighted in a special "International Forum" session:

M Margaritis et al. Cross-Talk Between The Arterial Wall And Peri-Vascular Adipose Tissue Determines Redox State Of Internal Mammary Artery Grafts Used In Coronary Bypass Surgery: The role of NADPH-oxidase. *Circulation 2012*

American Heart Association Scientific Sessions, Los Angeles, 2012 (oral presentation):

M Margaritis et al. Adiponectin Improves Endothelial Redox State In Human Atherosclerosis By Phosphorylating eNOS And Improving Its Enzymatic Coupling. *Circulation 2012*

Finalist at the SET for BRITAIN competition organised by the Parliamentary & Scientific Committee of the House of Commons (18/03/2013, Houses of Parliament Terrace Marquee, Westminster, London):

M Margaritis , C Antoniades. A novel cross-talk between perivascular adipose tissue and the arterial wall controls redox state in human atherosclerosis.

American Heart Association Scientific Sessions, Dallas, 2013 (oral presentation):

M Margaritis et al. The interplay between perivascular adipose tissue and the arterial wall regulates NADPH-oxidase activity in human vessels. *Circulation 2013*

European Society of Cardiology Congress, Barcelona 2014 (oral presentation):

M Margaritis et al. Perivascular adipose tissue around the left internal mammary artery regulates oxidative stress in this graft through PI3k/Akt-mediated down-regulation of p22phox subunit of NADPH-oxidase. *Eur Heart J 2014*

Contents

Acknowledgments ii
Dedication iv
Abstract v
List of Publications & Presentations vi
Original manuscripts contributing to DPhil thesis vi
Other published manuscripts during DPhil vii
Young Investigator Awards during DPhil viii
Conference abstracts and presentations related to DPhil thesis ix
Contents x
List of figures xv
List of tables xviii
List of commonly used abbreviations xix
Chapter 1 Introduction 21
1.1 Atherosclerosis: a global health burden 21
1.2 Oxidative stress and atherogenesis 22
1.3 Sources of ROS in the human vasculature 26
1.3.1 NAPDH-oxidases 26
1.3.2 Endothelial nitric oxide synthase (eNOS) 29
1.3.3 Other enzymes 32
1.4 Adipose tissue: a source of adipokines 33
1.5 Adiponectin: a vasoprotective adipokine 35
1.5.1 Adiponectin gene and protein structure 35
1.5.2 Regulation of adiponectin biosynthesis 37
1.5.3 Adiponectin signalling 39
1.5.4 Metabolic effects of adiponectin 40
1.5.5 Anti-atherosclerotic effects of adiponectin 42
1.5.5.1 Anti-inflammatory effects of adiponectin 43
1.5.5.2 Anti-oxidant, endothelium-protecting effects of adiponectin 44
1.5.5.3 Inhibition of VSMC proliferation by adiponectin 46
1.6 Distinct properties of adipose tissue depots 46
1.6.1 Subcutaneous versus visceral adipose tissue 46
1.6.2 Perivascular adipose tissue and vascular redox state 48

1.7 Hypotheses and aims 51
Chapter 2 Study design & methods 52
2.1 The Oxford CABG Bioresource 52
2.2 Demographics, risk factors and in-hospital follow-up 54
2.3 Pre-operative assessment of endothelial function 56
2.4 Sample collection 59
2.4.1 Blood sampling 59
2.4.2 Tissue collection and processing 59
2.5 Adipose tissue explant cultures 62
2.6 Biomarker measurements 64
2.6.1 Enzyme-linked Immunosorbent Assay (ELISA) 64
2.6.2 Plasma malonyldialdehyde (MDA) measurements/TBARS assay 66
2.6.3 Medical laboratory measurements 67
2.7 Measurement of vascular superoxide production 68
2.7.1 Lucigenin-enhanced chemiluminescence 68
2.7.2 Dihydroethidium Staining & Confocal Microscopy 73
2.8 Organ bath vasomotor studies 75
2.9 DNA Extraction and Genotyping 80
2.9.1 DNA Extraction 80
2.9.2 Genotyping usingTaqMan® Probes 80
2.10 Gene Expression Studies 83
2.10.1 RNA Extraction 83
2.10.2 Reverse transcription of RNA – cDNA library creation 83
2.10.3 Gene expression studies using quantitative PCR 84
2.11 Detection of tissue protein expression using Western immunoblotting 87
2.12 Extraction of membrane-bound proteins and estimation of Rac1 translocation 90
2.13 Rac1 activation assay 91
2.14 Statistical analysis 92
2.15 Personal contribution 93
Chapter 3 Adiponectin and human vascular redox state 94
3.1 Introduction 94
3.2 Study population - Methods 94
3.2.1 Vascular biopterin measurements 96
3.2.2 Statistical analysis 98
3.3 Results 100
3.3.1 Adiponectin in the circulation and its role in vascular physiology 100

3.3.1.1 Circulating adiponectin and NO-mediated vasorelaxation in human vessels.....100
3.3.1.2 Circulating adiponectin and vascular superoxide generation 102
3.3.1.3 Circulating adiponectin and vascular NADPH-oxidases activity 103
3.3.1.4 Circulating adiponectin and eNOS coupling 104
3.3.2 Exploring causality: a Mendelian randomization approach 105
3.3.2.1 Background/Experimental design 105
3.3.2.2 Single nucleotide polymorphisms in the ADIPOQ locus, serum levels of adiponectin & endothelial function 106
3.3.2.3 Single nucleotide polymorphisms in the ADIPOQ locus & vascular redox state.....108
3.3.3 Exploring causality: *Ex vivo* mechanistic experiments.....109
3.3.3.1 Background/Experimental design 109
3.3.3.2 Direct effects of adiponectin on resting superoxide production and vascular NADPH-oxidases activity 110
3.3.3.3 Adiponectin and cellular signalling pathways: PI3K/Akt - AMPK 113
3.3.3.4 Mechanism of NADPH-oxidases activity suppression by adiponectin 115
3.3.3.5 Direct effects of adiponectin on eNOS coupling.....119
3.3.3.6 Mechanism of eNOS coupling restoration by adiponectin.....121
3.4 Discussion.....124
3.4.1 Adiponectin and the subcellular mechanisms mediating its effects.....125
3.4.2 Adiponectin and endothelial dysfunction in human atherosclerosis 127
3.5 Conclusions 129
Chapter 4 Vascular effects of adiponectin in type 2 diabetes 130
4.1 Introduction 130
4.2 Study population - Methods.....131
4.2.1 Total antioxidant capacity measurements.....132
4.3 Results.....133
4.3.1 Adiponectin genetic variability, type 2 diabetes and atherosclerosis 133
4.3.2 Exploring vascular adiponectin “resistance” in diabetic patients 136
4.3.2.1 Vascular and systemic oxidative stress in type 2 diabetes 137
4.3.2.2 Mechanisms of increased NADPH-oxidases activity in type 2 diabetes 139
4.3.2.3 Exploring vascular adiponectin “resistance” in type 2 diabetes 141
4.4 Discussion.....144
4.5 Conclusions 146
Chapter 5 Adiponectin as a biomarker – Regulation of adiponectin synthesis in adipose tissue...147
5.1 Introduction 147
5.2 Study population & Methods.....148

5.2.1 Immunohistochemistry of human adipose tissue sections 152
5.2.2 Statistical analysis 153
5.3 Results 155
5.3.1 Impact of left ventricular function on circulating adiponectin 155
5.3.1.1 Obesity, heart failure and adiponectin levels 155
5.3.1.2 Heart failure, circulating adiponectin levels and endothelial function 157
5.3.1.3 Determinants of circulating adiponectin in cardiovascular disease: role of BNP 158
5.3.2 Human adipose tissue as a source of adiponectin 160
5.3.2.1 Contribution of distinct adipose tissue sites to circulating adiponectin levels 160
5.3.2.2 *ADIPOQ* genetic variability and adiponectin gene expression in adipose tissue 162
5.3.2.3 Transcriptional control of adiponectin gene expression 163
5.3.3 BNP, inflammation & adiponectin synthesis in adipose tissue 165
5.3.4 Direct effects of inflammatory cytokines & BNP on adiponectin synthesis in human adipose tissue: *ex vivo* culture model 169
5.3.5 Morphological/Functional differences of femoral versus mesothoracic and subcutaneous adipose tissue in humans 171
5.3.5.1 Inflammatory cell marker gene expression measurements in adipose tissue 171
5.3.5.2 Immunohistochemistry of human adipose tissue 172
5.4 Discussion 174
5.4.1 Adiponectin as a biomarker in cardiovascular disease 175
5.4.2 Divergent characteristics of distinct human adipose tissue sites 177
5.5 Conclusions 179
Chapter 6 Cross-talk between perivascular adipose tissue and the vascular wall: the role of adiponectin 180
6.1 Introduction 180
6.2 Methods 181
6.3 Results 181
6.3.1.1 Adiponectin expression in PVAT and vascular $O_2^{\cdot -}$ generation 181
6.3.1.2 Adiponectin expression in PVAT and eNOS coupling 183
6.3.1.3 Adiponectin expression in PVAT and NADPH-oxidases activity 184
6.3.2 “Local” versus “Remote” adipose tissue and vascular redox state 185
6.3.3 Exploring the existence of a “vessel-to-adipose tissue” signal 187
6.3.4 Exploring the nature of the “vessel-to-adipose tissue” signal 189
6.3.4.1 MDA & 4-HNE vascular content in conditions of high oxidative stress 191
6.3.4.2 Effects of MDA & 4-HNE on adiponectin gene expression in PVAT 194
6.4 Discussion 196

6.4.1 Adiponectin expression in PVAT and vascular oxidative stress: a conundrum? 197
6.4.2 The role of 4-HNE as a mediator of the cross-talk between PVAT and the vascular wall 198
6.4.3 The role of PVAT in atherosclerosis 199
6.5 Conclusions 201
Chapter 7 Study limitations 203
7.1 Use of saphenous veins 203
7.2 Lack of an atherosclerosis-free "control" group in the clinical cohort 204
Chapter 8 Discussion – Future work 211
8.1 Clinical and therapeutic implications 211
8.1.1 Insights into the obesity "paradox" 211
8.1.2 Adiponectin and adiponectin pathways as a therapeutic target 212
8.1.3 The importance of graft perivascular tissue in CABG surgery 215
8.2 Future work 217
8.2.1 Adiponectin in human health and disease 217
8.2.2 The Oxford CABG Bioresource – Investigating novel adipokines 218
List of references 219
Appendix I 255
Appendix II 258

List of figures

Figure 1.1: Oxidative stress in atherogenesis.....24
Figure 1.2: NADPH-oxidase isoforms in the cardiovascular system.....27
Figure 1.3: eNOS coupling and uncoupling.....30
Figure 1.4: Primary structure of adiponectin.....35
Figure 1.5: Monomer, low-molecular weight and high-molecular weight adiponectin forms.....36
Figure 1.6: Endocrine, paracrine and vasocrine adipokine signalling on the vascular wall.....50
Figure 2.1: Overview of the AdipoRedox study recruitment process and sample collection.....54
Figure 2.2: Cardiovascular clinical research facility vascular studies room.....56
Figure 2.3: Flow-mediated dilatation experimental setup.....57
Figure 2.4: Representative FMD- analysis, Vascular Analyser software.....58
Figure 2.5: Pedicle internal mammary artery sample.....60
Figure 2.6: Saphenous vein sample.....60
Figure 2.7: Mesothoracic adipose tissue sample.....61
Figure 2.8: Saphenous vein rings sample.....61
Figure 2.9: Mesothoracic adipose tissue intended for *ex vivo* explant culture.....62
Figure 2.10: Schematic illustration of the adipose tissue explant culture experimental design.....63
Figure 2.11: Representative ELISA standard curve.....64
Figure 2.12: Representative MDA measurements standard curve.....67
Figure 2.13: Chemical reaction of lucigenin with superoxide.....69
Figure 2.14: Representative NADPH-stim/Vas2870-inhib $O_2^{\cdot -}$ generation luminometry.....71
Figure 2.15: Representative LNAME-inhibitable $O_2^{\cdot -}$ generation luminometrty.....72
Figure 2.16: Organ bath vasomotor studies experimental setup – detail.....75
Figure 2.17: Organ bath vasomotor studies experimental setup – overview.....76
Figure 2.18: Representative SV vasomotor study phenylephrine curve..... 77
Figure 2.19: Representative SV vasomotor study acetylcholine curve.....78
Figure 2.20: Representative SV vasomotor study sodium nitroprusside curve.....79
Figure 2.21: StepOne Plus ABI qPCR instrument.....81
Figure 2.22: Representative allelic discrimination plot – genotyping experiments.....82
Figure 2.23: Representative standard curve – quantitative PCR gene expression experiments.....85
Figure 3.1: HPLC instrument.....96
Figure 3.2: Representative BH4 standard chromatogram.....97
Figure 3.3: Representative BH2 and B standard chromatogram.....98
Figure 3.4: Serum adiponectin levels and flow-mediated dilatation of the brachial artery.....100
Figure 3.5: Serum adiponectin levels and organ bath vasomotor studies.....101
Figure 3.6: Serum adiponectin levels and resting vascular $O_2^{\cdot -}$ generation.....102

Figure 3.7: Serum adiponectin levels and NADPH-stimulated vascular $O_2^{\cdot -}$ generation.....103
Figure 3.8: Serum adiponectin levels and LNAME-inhibitable vascular $O_2^{\cdot -}$ generation.....104
Figure 3.9: Influence of *ADIPOQ* SNPs on serum adiponectin levels.....107
Figure 3.10: Influence of *ADIPOQ* SNPs on endothelial function.....107
Figure 3.11: Influence of *ADIPOQ* SNPs on vascular $O_2^{\cdot -}$ generation.....108
Figure 3.12: Direct effects of adiponectin on resting vascular $O_2^{\cdot -}$ generation.....110
Figure 3.13: Direct effects of adiponectin on NADPH-stimulated vascular $O_2^{\cdot -}$ generation.....111
Figure 3.14: DHE staining of adiponectin/Vas2870-treated vessels.....112
Figure 3.15: Adiponectin and vascular PI3K/Akt phosphorylation.....113
Figure 3.16: Adiponectin and vascular AMPK phosphorylation.....114
Figure 3.17: Adiponectin and vascular NADPH-oxidases subunits protein expression.....115
Figure 3.18: Adiponectin and vascular $p22^{phox}$ gene/protein expression.....116
Figure 3.19: Direct effects of adiponectin on Rac1 activation and membrane translocation.....117
Figure 3.20: Direct effects of adiponectin on vascular $p22^{phox}$ protein levels after 18 hours.....118
Figure 3.21: Direct effects of adiponectin on LNAME-inhibitable vascular $O_2^{\cdot -}$ generation.....119
Figure 3.22: DHE staining of adiponectin/LNAME-treated vessels.....120
Figure 3.23: Direct effects of adiponectin on eNOS phosphorylation at Ser1177.....121
Figure 3.24: Serum levels of adiponectin and vascular BH4 content in the clinical cohort.....122
Figure 3.25: Direct effects of adiponectin on vascular BH4 content.....123
Figure 3.26: Schematic illustration of the effects of adiponectin on vascular redox state.....129
Figure 4.1: Serum adiponectin levels and insulin resistance/type 2 diabetes.....133
Figure 4.2: *ADIPOQ* locus variability and obesity.....133
Figure 4.3: *ADIPOQ* locus variability and type 2 diabetes.....134
Figure 4.4: *ADIPOQ* locus variability and extent of coronary artery disease.....135
Figure 4.5: Type 2 diabetes and circulating oxidative stress biomarkers.....137
Figure 4.6: Type 2 diabetes and vascular oxidative stress.....138
Figure 4.7: Type 2 diabetes and vascular p47phox/Rac1 translocation 139
Figure 4.8: Type 2 diabetes and vascular PI3K/Akt activity.....140
Figure 4.9: Type 2 diabetes and gene expression of adiponectin receptors in the vasculature.....142
Figure 4.10: Effects of adiponectin on PI3K/Akt activity in the presence of type 2 diabetes.....143
Figure 4.11: Effects of adiponectin on vascular $O_2^{\cdot -}$ in the presence of type 2 diabetes.....144
Figure 5.1: Chapter 5 study design.....150
Figure 5.2: Leica confocal microscope used in immunohistochemistry experiments.....153
Figure 5.3: Serum levels of adiponectin and BMI in subjects with preserved LVEF.....155
Figure 5.4: Serum levels of adiponectin and BMI in subjects with impaired LVEF.....156
Figure 5.5: Serum levels of adiponectin across Chapter 5 study groups.....156
Figure 5.6: Serum levels of adiponectin & FMD in subjects with preserved & impaired LVEF..157

Figure 5.7: Serum levels of adiponectin and levels of BNP, IL-6 and MCP-1.....159
Figure 5.8: Serum levels of adiponectin and *ADIPOQ* expression in adipose tissue depots.....161
Figure 5.9: *ADIPOQ* locus variability and *ADIPOQ* expression in adipose tissue depots.....162
Figure 5.10: *ADIPOQ* expression and *PPARγ/CD36* gene expression in adipose tissue depots...164
Figure 5.11: Plasma BNP levels and *ADIPOQ* expression/release from adipose tissue depots.....166
Figure 5.12: Serum IL-6 levels and *ADIPOQ* expression/release from adipose tissue depots.....167
Figure 5.13: Plasma MCP-1 levels & *ADIPOQ* expression/release from adipose tissue depots...168
Figure 5.14: Direct effects of inflammation on *ADIPOQ* gene expression in adipose tissue.....170
Figure 5.15: Gene expression of inflammatory cell markers in adipose tissue depots.....172
Figure 5.16: Immunohistochemistry of adipose tissue depots.....173
Figure 6.1: *ADIPOQ* gene expression/release in PVAT and resting vascular $O_2^{\cdot -}$.....182
Figure 6.2: *ADIPOQ* gene expression/release in PVAT and LNAME-inhibitable $O_2^{\cdot -}$.....183
Figure 6.3: *ADIPOQ* gene expression in PVAT and NADPH-stimulated vascular $O_2^{\cdot -}$.....184
Figure 6.4: *ADIPOQ* gene expression/release in ScAT/MtAT and NADPH-stim vascular $O_2^{\cdot -}$...186
Figure 6.5: Co-incubation of IMA & PVAT experiment.....188
Figure 6.6: Effects of H_2O_2 exposure on *ADIPOQ* gene expression in PVAT.....189
Figure 6.7: Vascular $O_2^{\cdot -}$ generation and vascular 4-HNE protein adduct content.....191
Figure 6.8: NADPH-stimulated vascular $O_2^{\cdot -}$ generation and vascular 4-HNE protein adducts....192
Figure 6.9: Presence of type 2 diabetes and vascular 4-HNE /MDA protein adducts.....193
Figure 6.10: Effects of MDA on *ADIPOQ* gene expression in PVAT.....195
Figure 6.11: Effects of 4-HNE on *ADIPOQ* gene expression in PVAT.....196
Figure 6.12: Cross-talk between PVAT and the vascular wall: role of 4-HNE and adiponectin...202
Figure 7.1: Adiponectin levels and expression in patients undergoing CABG vs. valve surgery..208

List of tables

Table 2.1 ELISA kits used in this project.....65
Table 2.2 Single Nucleotide Polymorphism TaqMan® genotyping assays.....82
Table 2.3 TaqMan® gene expression probes used in this project 86
Table 2.4 Primary immunoblotting antibodies used in this project.....89
Table 2.5 Secondary (HRP-conjugated) antibodies used in this project.....89
Table 3.1 Demographic characteristics of study participants.....95
Table 3.2 Expected & observed frequencies of SNP alleles in the study population.....106
Table 3.3 Pharmacological inhibitors used in vascular *ex vivo* mechanistic experiments.....109
Table 4.1 Demographic characteristics of study participants.....131
Table 5.1 Demographic characteristics of study participants.....151
Table 7.1: Demographics of patients undergoing valve surgery compared to CABG patients.....206

List of commonly used abbreviations

4-HNE: 4-hydroxy-nonenal

AdN: Adiponectin

AMP: Adenosine monophosphate

AMPK: AMP-activated protein kinase

ApoE: Apolipoprotein E

BH2: Dihydrobiopterin

BH4: Tetrahydrobiopterin

BMI: Body mass index

BNP: Brain natriuretic peptide

CABG: Coronary artery bypass graft

CAD: Coronary artery disease

CVD: Cardiovascular disease

cGMP: Cyclic guanosine monophosphate

DHE: Dihydroethidium

EID: Endothelium-independent dilatation

ELISA: Enzyme-linked immunosorbent assay

eNOS: Endothelial nitric oxide synthase

FemAT: Femoral adipose tissue

FMD: Flow-mediated dilatation

GSH: Glutathione

GTP: Guanosine Triphosphate

HDL: High density lipoprotein

HMW: High molecular weight

HsCRP: High-sensitivity C-reactive protein

IL-6: Interleukin-6

IMA: Internal mammary artery

LDL: Low density lipoprotein

LNAME: NG-nitro-L-arginine methyl ester

LVEF: Left ventricular ejection fraction

MCP-1: Monocyte chemoattractant protein 1

MDA: Malonyldialdehyde

MtAT: Mesothoracic adipose tissue

NADPH: Nicotinamide adenine dinucleotide phosphate

NF-kB: Nuclear factor kappa b

NO: Nitric oxide

$O_2^{\cdot -}$: Superoxide anion

$ONOO^{\cdot -}$: Peroxynitrite

OxLDL: Oxidised low density lipoprotein

PCR: Polymerase chain reaction

PI3K: Phosphatidylinositol-4,5-bisphosphate 3-kinase

PPAR: peroxisome proliferator-activated receptor

PVAT: Perivascular adipose tissue

ROS: Reactive oxygen species

ScAT: Subcutaneous adipose tissue

SNP: Single nucleotide polymorphism

SNPr: Sodium nitroprusside

SV: Saphenous vein

TD2M: Type 2 diabetes mellitus

TNFα: Tumor necrosis factor-a

VSMC: Vascular smooth muscle cell

HUVEC: Human umbilical vein endothelial cells

VAT: Visceral adipose tissue

WAT: White adipose tissue

BAT: Brown adipose tissue

Chapter 1
Introduction

This chapter discusses the role of oxidative stress in atherosclerosis and presents the most important enzymatic sources of reactive oxygen species in the human vasculature. It explores the role of adipose tissue as an endocrine organ, reviews the current literature on adiponectin and discusses the potential divergent properties of distinct adipose tissue sites.

1.1 Atherosclerosis: a global health burden

Atherosclerosis is a major worldwide health problem. Despite major advances in both primary and secondary prevention which led to a reduction in mortality in the years between 1990 and 2010, atherosclerotic cardiovascular disease is still the leading global cause of death[1]. While the number of cardiovascular disease-related deaths has been in decline in higher-income countries, it has been increasing rapidly in low- and middle-income countries. In 2008 the percentage of premature deaths attributable to cardiovascular disease was approximately 4% in high-income countries but rose to almost 42% in low-income countries[2]; there are rapidly expanding inequalities in the incidence and clinical outcomes of cardiovascular disease among different countries and across different socioeconomic classes.

Our understanding of atherogenesis has dramatically improved over the last decade, allowing the identification of new drug targets and the development of novel therapeutic strategies. Despite the immense worldwide research efforts in identifying the molecular causes of atherosclerosis and the many paradigm-shifting interventions that have been introduced as a result, there are still a great number of unanswered questions. Some of these concern the role of oxidative stress and the mechanisms controlling vascular redox

state in the atherosclerotic process, as well as the relations between obesity, diabetes, adipose tissue and the pathogenesis of atherosclerosis.

1.2 Oxidative stress and atherogenesis

Reactive oxygen species (ROS) are chemically reactive molecules containing oxygen. In biology, they are considered a byproduct of oxygen metabolism, with additional roles in physiological cell signalling and host immunity. The precursor of most ROS is superoxide ($O_2^{\cdot -}$), produced from the reduction of molecular oxygen (O_2). Oxidative stress is defined by the imbalance between the production of ROS and the endogenous antioxidant mechanisms to counteract the effects of ROS or to repair the resulting damages[3]. Under physiological conditions, several tightly controlled oxidative pathways contribute towards ROS productions, while several intra- and extra- cellular antioxidant enzymatic mechanisms account for ROS elimination[3]. ROS are responsible for direct damage of cellular structures within the vascular wall and they are also capable of triggering a number of redox sensitive transcriptional pathways.

Endothelium has been identified as a major source of ROS in human blood vessels[4] and endothelial function is closely linked to homeostasis of ROS formation within the vascular wall[5]. Endothelial dysfunction is widely regarded as one of the key early events in the atherosclerotic process. Endothelial dysfunction is characterised by reduced availability of nitric oxide (NO). NO is a gaseous molecule which diffuses to the VSMCs, triggers an increase in intracellular cyclic GMP and induces vasorelaxation. It has a major role in the regulation of vascular tone, as it opposes the actions of vasoconstricting factors such as endothelin-1. Moreover, NO is implicated in the regulation of other vascular processes, such as platelet aggregation and leukocyte adhesion, thus playing an integral role in vascular homeostasis[6].

Low density lipoprotein (LDL) is the critical element in the prevailing theories of atherogenesis. Oxidation of circulating LDLs particles occurs primarily at the vascular endothelium rather than in plasma, which is enriched with innate antioxidant defense mechanisms[7]. This occurs mainly in the subendothelial space, at sites of endothelial dysfunction (i.e. branching points of the circulation where turbulent flow occurs) where endothelial permeability is disturbed. LDL becomes entrapped in the sub-endothelial space where it is subject to oxidative modifications by ROS to form oxidized LDL (oxLDL). This is then readily internalized by macrophages through the "scavenger receptor" pathway originally described by Brown and Goldstein[8], leading to the accumulation of foam cells and subsequent atherogenesis[8].

Risk factors for atherosclerosis such as smoking, hypertension and diabetes mellitus, are associated with an increased production of ROS by the endothelium. As LDLs traverse the sub-endothelial space in lesion prone arterial segments, oxidative damage caused by these ROS occurs and involves the process of lipid peroxidation and apolipoprotein B-100 modification, leading to the formation of oxLDL. OxLDLs are involved in many atherogenic steps in the vascular wall such as endothelial dysfunction, migration of macrophages and smooth muscle cells and release of inflammatory cytokines, and are avidly internalized by macrophages via scavenger-receptor pathways. In addition, oxLDL also induces further oxidative stress to the endothelial cells, smooth muscle cells and foams cells, thus perpetuating the cycle of atherogenesis.

Further to its involvement in atherogenesis, circulating oxLDL has also been implicated in the pathogenesis of metabolic disorders such as obesity and diabetes mellitus[9]. The critical role of oxLDL in atherogenesis was highlighted by a recent study based on apolipoprotein E (ApoE) deficient mice, which demonstrated that atherosclerotic progression could be completely inhibited by ectopic hepatic expression of lectin-like

oxLDL receptor 1 (LOX-1). Decreased levels of plasma lipid peroxides and monocyte chemotactic protein-1 (MCP-1) levels were observed in the same mice, suggesting a positive effect on oxidative stress by selective clearance of oxLDL[10]. A schematic illustration which highlights the role of oxLDL throughout the stages of atherogenesis is shown in Figure 1.1.

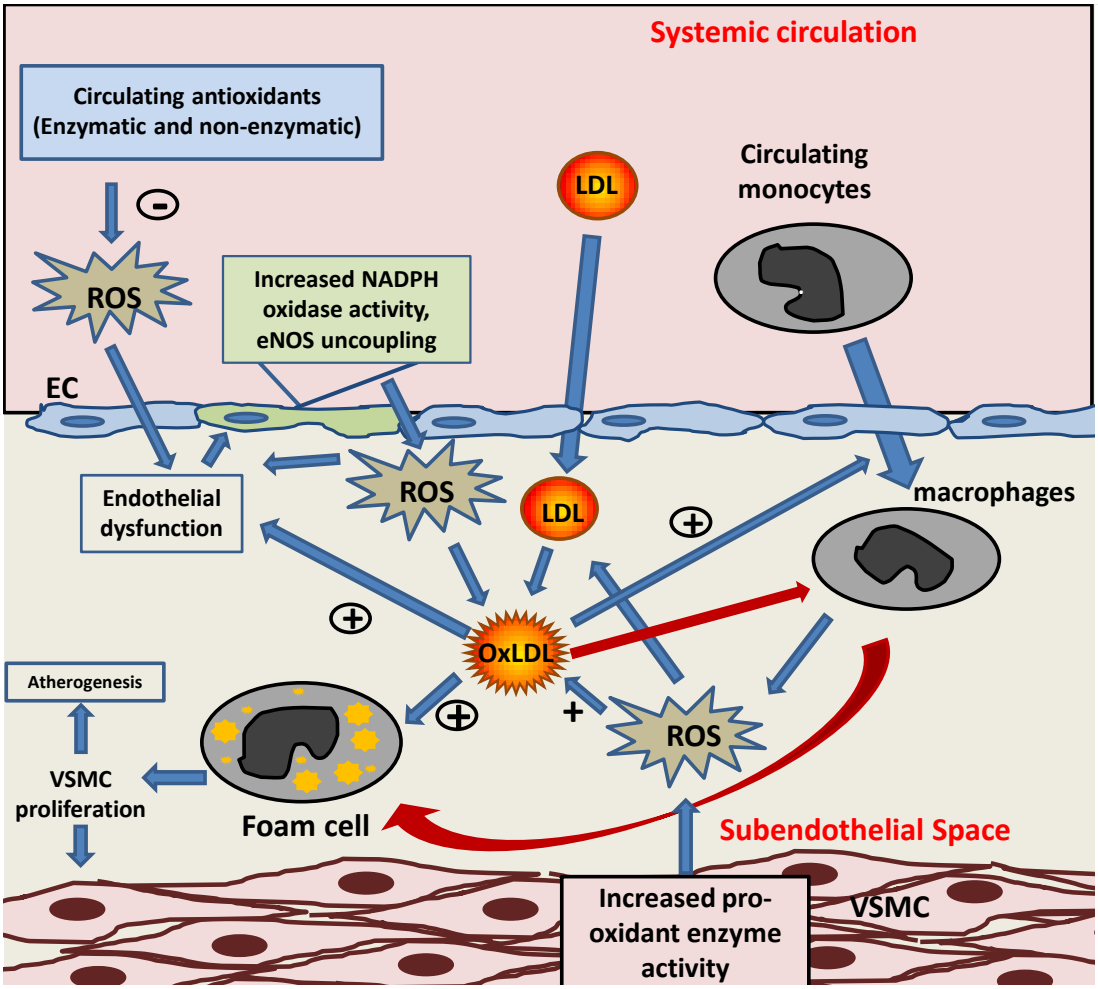


Figure 1.1: *The central role of low density lipoprotein (LDL) and atherogenesis. LDL is protected from oxidative modification in systemic circulation due to the abundant native circulating anti-oxidants. Once trapped in the sub-endothelial space, reactive oxidant species (ROS) reacts with LDL and leading to formation of oxidized LDL (oxLDL). oxLDL is chemoattractant to circulating monocytes and also transcytosed by them via scavenger receptor pathways, leading to the formation of foam cells. Accumulation of foam cells and subsequent vascular smooth muscle cell (VSMC) sequestration/proliferation is the cornerstone of atherogenesis. The chain of events is amplified in a feed- forward fashion as oxLDL contributes towards endothelial dysfunction and further ROS formation. Adapted from* ***Margaritis et al. Curr Med Chem 2012;19(16):2504-20****.*

ROS also act as transcriptional regulators in the vascular wall. Indeed, studies have revealed that they regulate many key redox sensitive transcriptional pathways interfering with growth, survival and/or apoptosis, differentiation and inflammation[11, 12]. Prolonged exposure of the endothelium to increased levels of ROS can result into a proatherogenic endothelial phenotype[11]. Apart from the endothelium, vascular smooth muscle cells can also be influenced by ROS-mediated signalling which has been shown to regulate differentiation, hypertrophy and growth, all key processes in the pathophysiology of atherosclerosis[3]. The cellular mechanisms governing these regulatory properties of ROS are thought to include protein-protein interactions as well as protein phosphorylation and glutathiolation[3].

The pathway of NF-kB is a well-studied example of redox signalling. In the absence of physiological stimuli, NF-kB is neutralised by its suppressor, IkB, and the pathway is blocked. ROS interfere with the phosphorylation and subsequent degradation of IkB, allowing NF-kB to freely move to the nucleus, where it regulates the transcription of many key proatherogenic genes, such as cytokines and vascular smooth muscle cell growth-related genes [11].

The pathway of AP1 is another example of redox sensitive signalling. AP1 is a protein participating in the regulation of cell differentiation and growth in the vascular wall. Its subunits are proteins of the c-Fos and c-Jun family, arranged in homodimers as well as heterodimers [11]. It has been demonstrated that oxLDL and ROS production can reduce AP1 signaling. The cellular mechanisms of this reduction are not fully understood, but possibly related to the c-Jun N-terminal kinase (JNK) pathway [11].

1.3 Sources of ROS in the human vasculature

1.3.1 NAPDH-oxidases

NADPH-oxidases were first characterized in phagocytic cells, where they play a pivotal role in host defense by generating $O_2^{\cdot -}$ through the transfer of electrons from NADPH to O_2[13]. The phagocytic NADPH-oxidase consists of two membrane-bound subunits: $p22^{phox}$ and $gp91^{phox}$ (together comprising the cytochrome b558 complex), and four cytosolic subunits: $p40^{phox}$, $p47^{phox}$, $p67^{phox}$ and a small GTP-binding protein (Rac1 or 2), which upon stimulation translocates to flavocytochrome b558 and activates the enzymatic complex. Several distinct NADPH-oxidases have been described in various cells of mesodermal origin, based on the presence of seven different homologues of the $gp91^{phox}$ membrane subunit (Figure 1.2). These homologues have been termed NOX1 to 5 and Duox1-2. Homologues of two cytosolic subunits have also been discovered: NOXO1 is a homologue of $p47^{phox}$ and NoxA1 shares considerable similarity with $p67^{phox}$[14]. Human cardiovascular cells express NOX1, NOX2 (which is the homologue of phagocyte NADPH-oxidase), NOX4 and NOX5[15]. However, this expression profile varies considerably in different cells of the vascular wall, as well as in different vessels. More specifically, endothelial cells have been shown to express all NOX isoforms, but mainly NOX2 and NOX4, with NOX2 being the most abundant isoform in human vein endothelium [4]. In VSMCs, NOX4 is the most abundant NOX isoform of NADPH oxidase, located mainly in the medial layer of human arteries[13]. NOX1 is also expressed in lower amounts in VSMC, where its activity and expression can be stimulated by angiotensin II and platelet-derived growth factor (PDGF)[16]; there are also reports of NOX2[17] and NOX5[18] expression in these cells. NOX5 is Ca^{2+}-sensitive and it is thought to have a detrimental role in vascular function, contributing to the pathogenesis of hypertension and atherosclerosis[18]. Interestingly, although $p47^{phox}$ has been detected in all vascular cells[15],

p67^{phox} has been found in the endothelium[19] but not in aortic smooth muscle cells[20]. However, its functional homologue NoxA1 has been shown to be present in mouse aortic VSMCs, indicating that it replaces p67^{phox} in the media of large vessels[21]. It has been reported that immunoreactive NoxA1 is present in intimal and medial smooth muscle cells of human early carotid atherosclerotic lesions, suggesting involvement of this particular subunit in the regulation of redox signaling and maintenance of the VSMC phenotype[22]. Human cardiac tissue mainly expresses NOX2 and NOX4[23]. Figure 1.2 presents an illustration of different NADPH-oxidase isoforms and their distribution in the cardiovascular system.

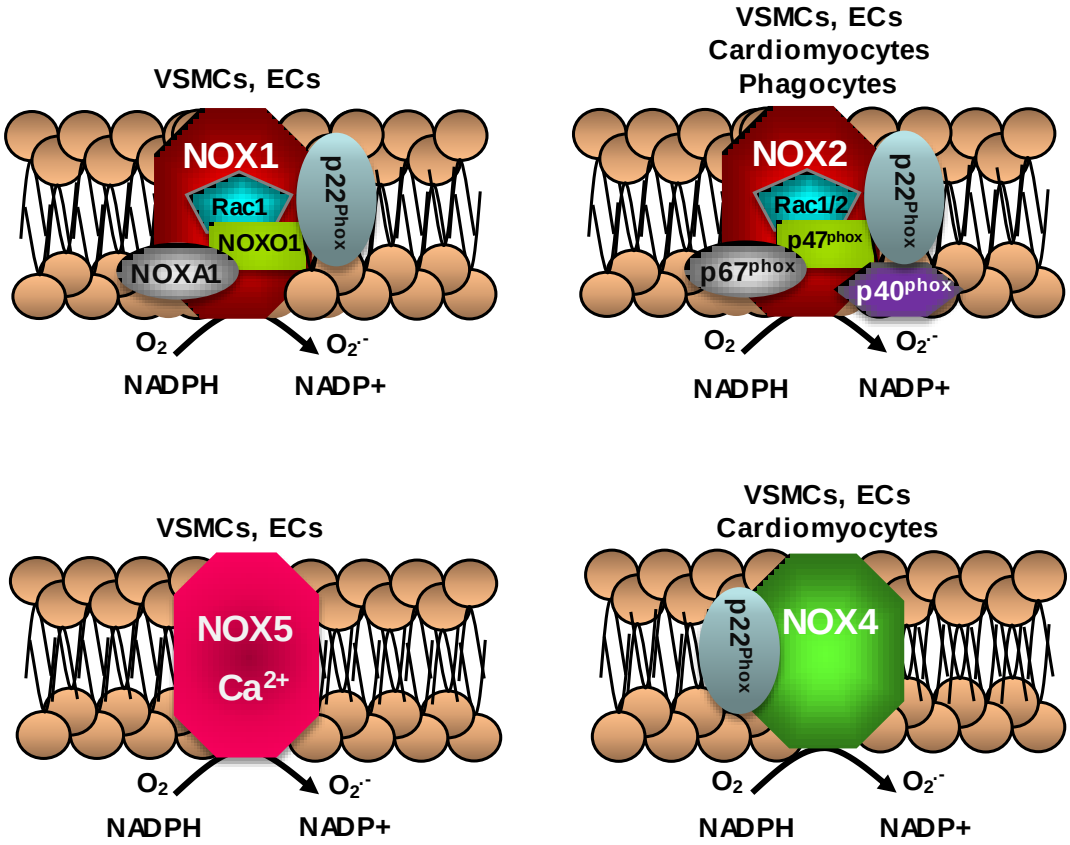


Figure 1.2: *NADPH-oxidase isoforms in the cardiovascular system. The NOX1-containing isoform (consisting of NOX1, p22phox, NOXA1, NOXO1 and Rac1) are present in vascular smooth muscle (VSMCs) and endothelial cells (ECs). The NOX2-containing isoform (comprising NOX2, p22phox, p67phox, p47phox, p40phox and Rac1/2) is present in phagocytes, VSMCs, ECs and cardiomyocytes. The NOX4-containing isoform consists only of the membrane subunits p22phox and NOX4 and is present in VSMCs, ECs and cardiomyocytes. NOX5 is calcium-dependent and has been found in VSMCs and ECs.*

Contrary to the phagocytic NADPH-oxidase, the vascular isoforms are constitutively active, generating a low but steady amount of $O_2^{\cdot -}$, the production rate of which is ~1-10% of that in phagocytes[15]. This rate can be increased by a number of agonists and stimuli, such as angiotensin II, thrombin, tumor necrosis factor-a (TNFα), interleukin-1, vascular endothelial growth factor (VEGF) or mechanical forces like shear stress, although the resulting amounts of ROS are still only a fraction of the phagocytic ROS generation[24]. In *Nox2-/-* mice, inflammatory stimuli such as TNFα and angiotensin II fail to elicit an increase in $O_2^{\cdot -}$ production in ECs[25]. In addition to a sustained activation of the enzyme, these agonists, as well as oxLDL, have been shown to up-regulate gene expression of the oxidase subunits[15, 26].

The constitutive and rather low activity of vascular NADPH-oxidases suggests that, under physiological conditions, they are involved in physiological vascular redox signaling. In disease states however, it is well-established that elevated expression and activity of NADPH-oxidase isoforms in the vasculature, together with the resulting increased ROS production, contribute to the initiation and maintenance of the atherosclerotic process. In particular, high activity and/or expression of NOX2 in cardiovascular tissues has been heavily implicated in the pathogenesis of hypertension, endothelial dysfunction and atherosclerosis[3]. However, it should be noted that recent studies have unveiled a distinct, potentially beneficial role for NOX4 NADPH-oxidase isoform in the vascular wall, by enhancing vasodilation in a hydrogen peroxide-mediated way[27]. This underlies the fact that controlled ROS production in specific cellular compartments may be beneficial for vascular homeostasis, serving as signaling molecules mediating multiple biological processes.

1.3.2 Endothelial nitric oxide synthase (eNOS)

The major enzymatic source of NO in the vasculature is endothelial nitric oxide synthase (eNOS), which is located predominantly in endothelial cells. eNOS is a complex homodimer that uses L-arginine and molecular O_2 as substrate to produce NO and L-citrulline (Figure 1.3). This is achieved through the transfer of electrons, using NADPH as a donor, from the flavins of the reductase domain on one monodimer to the oxidase domain of the other, where the iron-containing heme active site is located[13]. The presence of calmodulin, which is activated by calcium-binding, increases the rate of electron flow. At the heme site, the electrons are utilized to reduce and activate O_2, which is in turn used to produce NO through a two-step oxidation of L-arginine. This process requires the binding of the essential co-factor tetrahydrobiopterin (BH_4).

The enzymatic activity of eNOS is delicately regulated. Increased calcium concentration induces the binding of modulatory calmodulin (CaM) to eNOS, whereas heat-shock protein 90 (hsp90) acts as an allosteric regulator and caveolin–1 as a tonic inhibitor of eNOS[28]. Apart from protein interactions, eNOS is also regulated by phosphorylation at several amino acid residues. One such site is Ser1177, phosphorylation of which facilitates electron transport within the enzyme and increases its sensitivity to calcium. Ser1177 can be phosphorylated through different pathways, including the Ser/Thr kinases Akt, AMP-activated kinase (AMPK), Ca^{2+}/calmodulin-dependent protein kinase II (CaMKII) and Protein Kinase A (PKA)[28]. Thr495 is another phosphorylation site which interferes with CaM binding. It is phosphorylated under resting-state conditions acting as an inhibitor; stimuli that increase eNOS activity are accompanied by dephosphorylation of this residue. Dephosphorylation of Thr495 is also thought to increase eNOS uncoupling[28]. Ser633 is another phosphorylation site of human eNOS which increases eNOS activity and is important for maintenance of NO production after initial phosphorylation of Ser1177[29].

When BH4 is bound to eNOS, the enzyme is considered to be "coupled"[30]. Coupling of eNOS is essential for the physiological function of the human vessel. Degradation of BH4 by ROS, especially peroxynitrite ($ONOO^{\cdot-}$), leads to what is known as "uncoupling" of the enzyme: in the absence of BH4, the flow of electrons within eNOS is disturbed; this leads to dissociation of the ferrous-dioxygen complex, causing eNOS to convert O_2 into superoxide radicals instead of producing NO[31]. $O_2^{\cdot-}$ reacts with NO to form $ONOO^{\cdot-}$, which can further oxidize BH4, creating a vicious cycle of eNOS uncoupling (Figure 1.3).

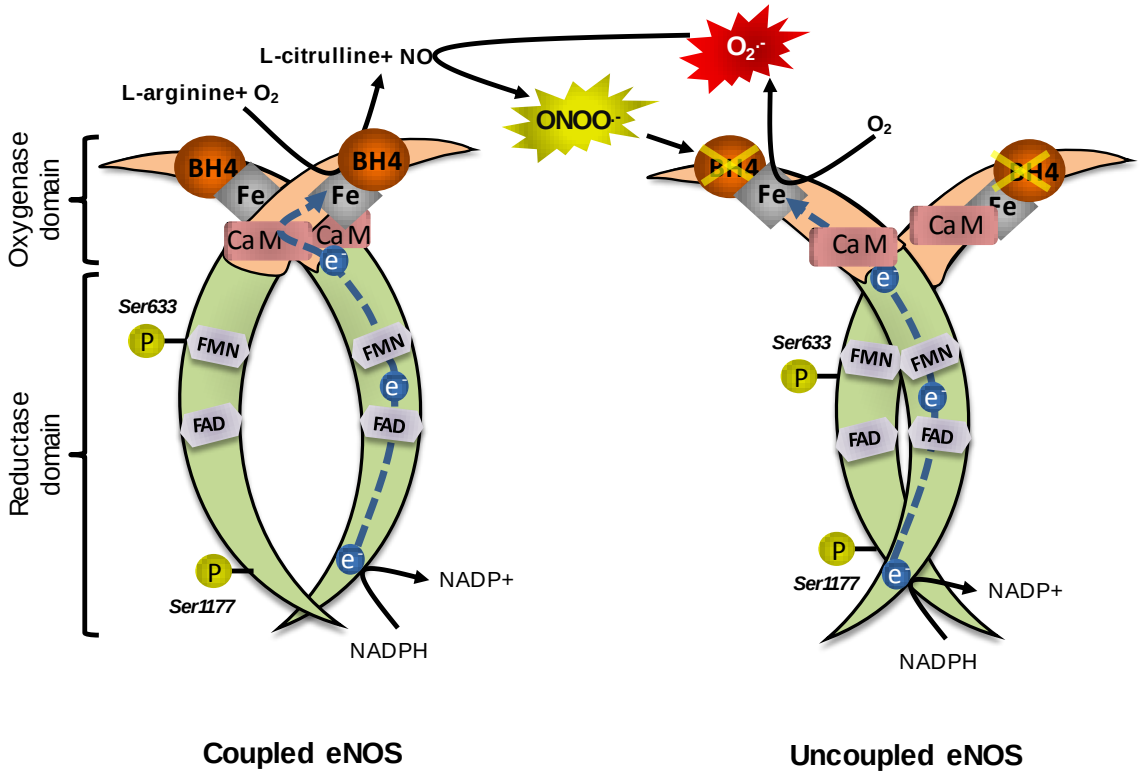


Figure 1.3: *In the presence of BH4, eNOS shuttles electrons from the flavins of the reductase domain of one monodimer to the oxygenase domain of the other monodimer, in a two-step reaction that produces L-citrulline and NO from L-arginine and O_2. BH4 is sensitive to degradation by ROS, especially $ONOO^{\cdot-}$. In the absence of BH4, eNOS is uncoupled: electrons are transferred to O_2, producing $O_2^{\cdot-}$. $O_2^{\cdot-}$ reacts rapidly with NO to form $ONOO^{\cdot-}$, which can further oxidize BH4, creating a vicious circle that leads to endothelial dysfunction. Ser1177 and Ser633 are activation phosphorylation sites. Abbreviatons: eNOS: endothelial nitric oxide synthase; BH4: tetrahydrobiopterin; $O_2^{\cdot-}$: superoxide; $ONOO^{\cdot-}$: peroxynitrite; CaM: Calmodulin. Adapted from* ***Margaritis et al. Antioxid Redox Signal 2014; 20(8):1198-215.***

The resulting drop in production of NO inhibits endothelium-dependent vasorelaxation, disturbs vascular homeostasis and leads to endothelial dysfunction[30]. In addition, ONOO- has well-established roles in LDL-oxidation and is also responsible for the nitration of various cellular components; accumulation of nitrated proteins is a potent marker of oxidative/nitrosative cellular damage. $ONOO^{\cdot -}$ can induce cellular apoptosis and even necrosis at high concentrations, further aggravating endothelial dysfunction[32].

Another mechanism by which eNOS function is negatively affected is through the effects of the endogenous eNOS inhibitor asymmetric dimethylarginine (ADMA). ADMA is produced as a by-product of protein metabolism through methylation of L-arginine residues, and its production is greatly increased by LDL in ECs[33]. ADMA is metabolized by the enzyme dimethylarginine dimethylaminohydrolase (DDAH) and eliminated through urinary excretion[34]. Due to its close resemblance in structure to L-arginine, ADMA inhibits activity of eNOS, either through inhibition of cellular L-arginine uptake or direct competitive inhibition for binding to eNOS[35]. *In vitro* experiments using purified neuronal NOS suggest that ADMA acts more as a direct inhibitor rather than an uncoupling-inducer[36]. ADMA induces eNOS uncoupling only in the presence of partial BH4 deficiency [36], which is a common condition in the human vascular endothelium in advanced disease states. In line to this observation, exposure of EC cultures to ADMA increases ROS generation[33] and accelerates cell senescence[37], possibly through an induction of eNOS uncoupling in vivo. High levels of ADMA have been associated with impaired endothelial function and increased ROS generation in the human vasculature[35], while in prospective studies, circulating ADMA is independently related to increased mortality and worse clinical outcome in patients with atherosclerosis or diabetes[38].

1.3.3 Other enzymes

Xanthine oxidase (XO), one of the two forms of xanthine oxidoreductase – the other being xanthine dehydrogenase (XDH), is present in endothelial cells in pathophysiological conditions [39]. It is responsible for the reduction of xanthine and hypoxanthine, leading to the formation of O_2^- radicals and hydrogen peroxide (H_2O_2). This ROS formation appears to be more significant in human arteries than veins [40]. The amount of ROS production depends on the XO/XHD ratio, which is increased by mechanical stress, hypoxia and the action of proinflammatory mediators [39, 41]. Moreover, XO activity is further augmented by NADPH-oxidases-induced H_2O_2 production, possibly in a calcium-dependent manner, thus promoting the generation of ROS *via* a positive feedback mechanism [39].

Myeloperoxidase is an enzyme predominantly expressed in neutrophils. It catalyzes the conversion of hydrogen peroxide and chloride anion to hypochlorous acid, as well as tyrosine to tyrosyl radical; both products are known to be highly cytotoxic. Circulating levels of the enzyme have been associated with the presence of coronary artery disease[42] and myeloperoxidase-triggered inflammatory processes have been linked to atherogenesis and plaque rupture[43].

Lipoxygenases are enzymes which oxidize fatty acids into fatty acid hydroperoxides. The lipoxygenase pathway is responsible for production of various signaling lipids, both pro-inflammatory and anti-inflammatory, such as 15-epilipoxin-A(4).

Cyclooxygenases convert arachidonic acid to prostaglandin H2, a precursor molecule to synthesis of prostanoid fatty acids. They are important enzymes implicated in the triggering and maintenance of pro- and anti-inflammatory and thrombotic processes.

1.4 Adipose tissue: a source of adipokines

Adipose tissue is loose connective tissue characterized by the presence of adipocytes. Two histological types of adipose tissue exist: white adipose tissue (WAT) and brown adipose tissue (BAT). Adipocytes of WAT contain a single large lipid droplet, whereas adipocytes of BAT consist of multiple smaller lipid droplets and abundant mitochondria. Adipose tissue is also characterized by the presence of rich vasculature, with a vascular-stromal component comprising endothelial cells, fibroblasts, infiltrating immune cells and pre-adipocytes[44]. Pre-adipocytes are derived from multipotent stem cells of mesodermal origin and mature into adipocytes via the action of two families of transcriptional factors: the peroxisome proliferator-activated receptor (PPAR) and sterol regulatory element-binding proteins (SREBP)[45,46]. In particular, PPARγ is expressed in high quantities and is regarded as the master differentiator of adipose tissue; PPARγ knock-out mice are characterized by total absence of adipose tissue and are non-viable[47].

Brown adipose tissue, so called because of its dark appearance in histological preparations due to the presence of multiple mitochondria in its adipocytes, comprises up to 5% of total body weight in human infants, but diminishes with age. It is located mainly in the lower neck and supraclavicular regions in human adults. Contrary to the function of WAT as fatty acid storage, the main function of BAT is the consumption of energy through beta-oxidation in order to generate heat. Brown adipocytes exclusively express uncoupling chain protein-1 (UCP-1), also known as thermogenin, which enables the cells' mitochondria to uncouple oxidative phosphorylation and utilize substrates to generate heat rather than ATP. The main stimulus for this process is exposure to cold, which induces the sympathetic nervous system to elevate the circulating catecholamine levels, which in turn upregulate the expression of UCP-1 in BAT. This heat generation process is termed "non-shivering thermogenesis", in contrast to the heat produced via the shivering of skeletal

muscles. Until recently, it was thought that functional brown adipose tissue was practically nonexistent in human adults. Two studies using PET/CT imaging combined with open biopsies proved the existence of functional brown adipose tissue in healthy human adults and demonstrated a negative correlation of active BAT with BMI [48], [49]. The roles of brown adipose tissue in the regulation of energy expenditure and development of obesity remain to be elucidated.

It has been traditionally believed that the primary roles of WAT are insulation and cushioning of the body, as well as maintenance of the energy status, via the storage and release of free fatty acids after food intake and fasting respectively. However, during the past decades, the perception of adipose tissue as a simple energy storage depot has shifted to that of a tissue with a much more dynamic involvement in the regulation of lipid and glucose metabolism, as well as the inflammatory status of the body. Adipose tissue has been shown to be an active, endocrine organ, producing hormones and cytokines, collectively termed adipokines, which elicit a variety of local and systemic responses [50]. A plethora of adipokines have been identified over the last decades. Some exert vasoprotective, anti-atherogenic effects, whereas others are thought to promote atherosclerotic disease processes. Several of the adipokines that have been identified are leptin, omentin, apelin, visfatin, resistin and others. The most well-studied, however, is undoubtedly adiponectin.

1.5 Adiponectin: a vasoprotective adipokine

1.5.1 Adiponectin gene and protein structure

Adiponectin (also referred to as GBP-28, apM1, AdipoQ and Acrp30) is an adipokine first identified in 1995 in differentiating 3T3-L1 adipocytes[51]. It is synthesized mainly by adipocytes and is one of their most abundant products. Adiponectin is not expressed by human pre-adipocytes and differentiation into adipocytes is necessary to induce its expression[52]. It was initially thought that adiponectin is produced exclusively by adipocytes[51]; however, more recent evidence suggests that it is also produced by other tissues, such as skeletal muscle cells[53] and cardiomyocytes[54].

The adiponectin gene has been mapped to chromosome 3q27 and its regulatory sequences contain a classical CCAAT box and several putative binding sites for transcription factors but no typical TATA box[55]. Adiponectin is a protein of 244 amino acids consisting of four domains (Figure 1.4):

- an amino-terminal signal sequence that targets adiponectin for secretion,
- a variable region that differs between species,
- a 65-amino acid long collagen-like fibrous domain and
- a C1q-complement-like carboxy-terminal globular domain[56].

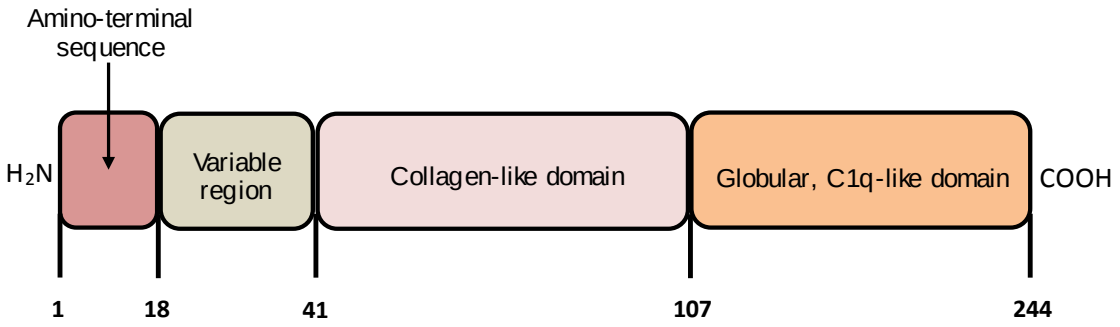


Figure 1.4: *Schematic representation of the primary structure of a full-length adiponectin protein molecule. The numbers represent amino acid positions in the sequence.*

After its translation, specific residues in adiponectin peptide are hydroxylated and glycosylated, a step critical to the biological functions of the molecule. While the gene sequence bears similarities to complement C1q, the final protein structure closely resembles TNF-α, despite significant differences in the amino acid sequences[56].

In humans, circulating adiponectin self-assembles into trimeric forms, which further assemble into hexamers and polymeric high molecular weight (HMW) adiponectin[57]. The globular form of adiponectin, which results from proteolytic cleavage of the full molecule, is only measurable at low levels in human serum[58]. Figure 1.5 provides a visualization of the various forms of circulating adiponectin.

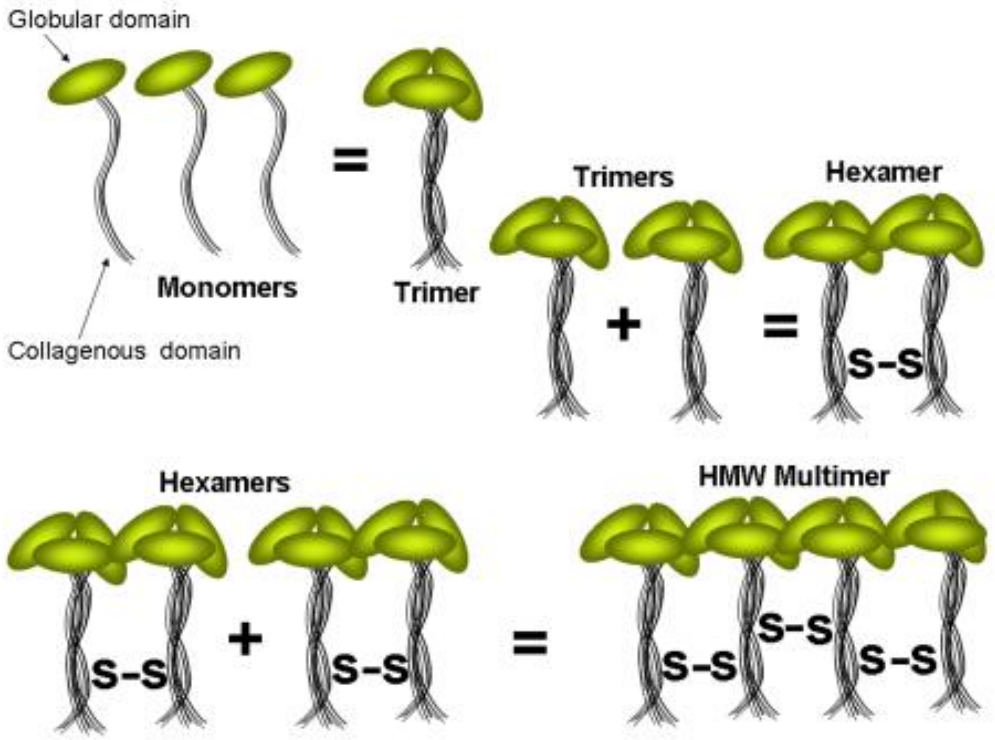


Figure 1.5: *Adiponectin monomers self-assemble into trimers, which further assemble into hexamers, oligomers and high molecular-weight (HMW) multimers. Reproduced with permission from* ***Antonopoulos et al. Obes Rev 2009;10(3):269-79.***

1.5.2 Regulation of adiponectin biosynthesis

Physiological levels of adiponectin in the human bloodstream are approximately 0.5–10 μg/mL at a concentration of around 0.01% of all plasma protein[59], although the levels can vary greatly based on underlying disease status. It is important to note that the serum/plasma concentration of adiponectin is almost 1,000-fold higher than most other adipokines and hormones, including insulin[59]. In animal studies the half-life of circulating adiponectin has been reported to be approximately 75 minutes, with liver mainly responsible for its clearance[60]. This process is markedly slower for the HMW forms of adiponectin; as a consequence, levels of this form of the molecule are fairly stable in serum/plasma[60].

The mechanisms involved in the regulation of adiponectin synthesis are not fully understood. Adiponectin production is induced via distinct signaling pathways and involves various transcriptional factors. Analysis of the adiponectin promoter revealed putative binding sites for the adipogenic transcription factors adipocyte determination/ differentiation-dependent factor 1 (ADD1) / sterol regulatory element - binding protein 1c (SREBP1c)[61, 62], PPARγ[63] and CCAAT enhancer-binding proteins (C/EBP)[64].

In vitro studies have shown that increased oxidative stress[65], sympathetic nervous system activity via β-adrenergic stimulation[66] and proinflammatory cytokines[67] suppress adiponectin synthesis in adipocytes, whereas caloric restriction up-regulates adiponectin expression[68]. In a clinical setting, several traditional atherosclerotic risk factors have been linked to reduced levels of adiponectin in the circulation. Clinical data suggest that lower adiponectin levels are associated with the male gender (possibly due to an androgen or lack of estrogen effect)[69] and smoking habit[70], while Mediterranean diet[71] and exercise[72] increase adiponectin circulating levels. Importantly, adiponectin levels are inversely correlated with body weight or body mass index (BMI) and are elevated after weight

loss[73]. On the other hand, disease-states such as heart failure,[74, 75] alcohol abuse and chronic viral hepatitis C[76] are associated with a striking increase in circulating adiponectin levels. Several pharmacological interventions have also been shown to affect adiponectin levels. PPARα[77], PPARγ[78] and PPARδ[79] agonists up-regulate adiponectin expression in animal studies; in humans, treatment with thiazolidinediones is well-documented to cause an increase in circulating adiponectin levels in healthy, obese and diabetic patients[80]. Other types of medication commonly administered in patients suffering from cardiac disease such as statins and angiotensin converting enzyme inhibitors have been shown to affect adiponectin levels, although different studies have shown conflicting results[81].

Genetic variability appears to be another crucial determinant of adiponectin gene expression. Numerous single nucleotide polymorphisms (SNPs) have been identified on the *ADIPOQ* gene, some of them having a functional effect on adiponectin gene expression and circulating adiponectin levels.[82, 83] Genome-wide association studies have uncovered SNPs affecting adiponectin levels in other loci as well, such as the *CDH13* locus encoding for the adiponectin receptor T-cadherin (albeit mostly in Asian populations)[84]. Nevertheless, literature on the importance of adiponectin gene variability has not been consistent on whether SNPs affecting adiponectin levels are also linked to obesity, type 2 diabetes mellitus and cardiovascular disease.

Adiponectin has been shown to be expressed in all adipose tissue depots in the human body. Some studies would seem to suggest that subcutaneous adipose tissue demonstrates higher production of the hormone compared to visceral fat but this is lost in the presence of diabetes[85]. Conversely, obesity appears to suppress adiponectin expression more in visceral adipose tissue compared to subcutaneous[86]. In any case, the depots mainly responsible for contributing to adiponectin plasma pool have not been clearly determined yet. This issue is explored in depth in my thesis.

1.5.3 Adiponectin signalling

Adiponectin signalling is receptor-mediated. The first adiponectin receptors identified were AdipoR1 and AdipoR2, which are seven-transmembrane proteins responsible for internalization of the adiponectin molecule and further downstream signaling. The amino acid sequence of AdipoR1 and AdipoR2 is approximately two-thirds identical between the two proteins[87]. Both receptors are integral membrane proteins with an internal N-terminus and an external C-terminus; this topology resembles classic G-protein coupled receptors, but in reverse[88]. The crystal structures of both receptors were only very recently reported by Tanabe et al.[89]: the seven-transmembrane helices enclose a cavity in which three conserved histidine residues coordinate a zinc ion, which is thought to have an important role in downstream signaling. AdipoR1 is widely expressed in human cells but its higher expression can be found in skeletal muscle, whereas AdipoR2 is highly expressed in the liver[88]. Both receptors are expressed in human vascular[90] and cardiac tissue[23].

The downstream signalling of AdipoR1 and AdipoR2 receptors is not fully elucidated. AdipoR1 exerts many of its downstream effects through Ca^{2+}/calmodulin-dependent protein kinase kinase (CAMKK) and AMPK pathways[91], whereas AdipoR2 is linked to activation of PPARα pathways in the liver[92]. The first protein found to directly interact with adiponectin receptors is APPL1, an adaptor protein consisting of a PH pleckstrin homology domain, a phosphotyrosine binding domain, and a leucine zipper motif[93]. APPL1 has the ability to couple adiponectin receptors with their downstream signalling cascades. The intracellular N-terminal portion of the adiponectin receptor interacts with the phosphotyrosine binding domain of APPL1, resulting in further downstream adiponectin signalling. APPL1 itself appears to play an important role in adiponectin-dependent insulin-signalling pathways in skeletal muscle cells, facilitating the

binding of insulin receptor substrate (IRS) 1/2 to the insulin receptor, thus enhancing insulin sensitivity[94]. Targeted disruption of AdipoR1 and AdipoR2 in mice causes impaired adiponectin-stimulated AMPK and PPARα signaling respectively. Simultaneous disruption of both receptors in mice causes an increase in hepatic triglyceride infiltration, inflammation and oxidative stress, leading to insulin resistance and glucose intolerance[92]. Furthermore, adiponectin has been shown to act through AMPK-independent pathways. AdipoRs may stimulate ceramidase activity, leading to changes in ceramide and sphingosine content; the balance of these two bioactive lipids acts as a critical cellular rheostat. Holland et al.[95] demonstrated that sphingosine-1-phosphate may be a critical mediator of adiponectin effects in the cell and possibly also involved in AMPK phosphorylation and/or Ca^{2+} influx and CAMKK activation.

After the discovery of AdipoR1 and AdipoR2, a third receptor for adiponectin was identified, T-cadherin (CDH13). T-cadherin is a glycosyl phosphatidylinol-linked cell surface molecule, first identified as modulator of neural crest cell migration and axon guidance molecule[96]. In 2004, T-cadherin was shown to be a receptor of hexameric and HMW-forms of adiponectin, expressed in endothelial cells and VSMCs[97]. The activated form of T-cadherin has been shown to protect endothelial cells against apoptosis triggered by oxidative stress through activation of the PI3K/Akt/mTOR survival signal pathway and concomitant suppression of the p38 Mitogen-Activated Protein Kinase (MAPK) proapoptotic pathway[98].

1.5.4 Metabolic effects of adiponectin

Adiponectin has well-documented insulin-sensitizing, anti-diabetic effects. It plays a key role in the control of energy homeostasis, through its regulatory actions on the metabolism of carbohydrates and lipids. Experiments in mice demonstrate that adiponectin induces fatty-acid uptake and stimulates phosphorylation of acetyl coenzyme A

carboxylase and oxidation in myocytes via sequential activation of AMPK, p38MAPK and PPARα[99]. It also reduces tissue triglyceride content in skeletal muscle and liver, ameliorating insulin resistance by promoting fat oxidation[100] and increasing hepatic IRS-2 expression[101]. In an interesting study Liu et al.[102] studied the metabolomic profile of high-fat diet exposed, adiponectin-knockout murine skeletal muscle: they reported pathological changes in fatty acid and glucose uptake, as well mitochondrial function, all of which were reversed after treatment with exogenous adiponectin. Presence of insulin resistance has also been shown to be linked to adiponectin resistance in liver and muscle via down-regulation of AdipoR2[103], suggesting that development of type 2 diabetes may be pathophysiologically linked to diminished tissue signalling of adiponectin.

Activated AdipoR1 and AdipoR2 have been shown to increased fatty acid oxidation in liver and skeletal muscle, enhance biogenesis of mitochondria, increase glucose metabolism and suppress hepatic gluconeogenesis. These effects are linked to markedly improved metabolic function and protect against obesity and type 2 diabetes[99, 104]. Interestingly though, it has been suggested that AdipoR1 and AdipoR2 may display seemingly opposing effects on glucose and lipid metabolism pathways. In one study, AdipoR1 knock-out mice demonstrated increased diet-induced adiposity associated with fat and glucose intolerance. Conversely, AdipoR2-null mice appeared to resist the pathophysiological changes induced by a high-fat diet, maintaining a lean and insulin-sensitive phenotype[105]. In a second study, AdipoR2 knock-out mice exhibited reduced dyslipidaemia and insulin resistance induced by a high-fat diet, but progressed to type 2 diabetes as high-fat feeding continued[106]. The exact function of individual adiponectin receptors in mediating the metabolic effects of this adipokine requires further investigation. Other mechanisms through which adiponectin prevents insulin resistance are promotion of beta-cell viability[107], reduction of local inflammation in adipose tissue[108] and

inhibition of release of insulin resistance-inducing factors by adipose tissue in an autocrine fashion[108].

In clinical studies, high circulating adiponectin levels have been linked to reduced risk of type 2 diabetes in healthy individuals, as demonstrated by a large meta-analysis of almost 15,000 prospective study participants[109]. The crucial involvement of adiponectin in promoting insulin sensitivity is also documented by a recent study which showed an association between reduced levels of the hormone and increased incidence of prediabetes, defined as impaired glucose tolerance and/or impaired fasting glucose[110].

1.5.5 Anti-atherosclerotic effects of adiponectin

Ever since its discovery, a large number of clinical studies have linked adiponectin to atherosclerotic disease. Adiponectin knock-out mice were an extremely useful tool in investigating the role of this adipokine in atherosclerosis. Deletion of adiponectin leads to impaired regulation of vascular tone[111] and increased neointimal thickening after arterial injury *in vivo*[112]. Conversely, adenovirus-mediated overexpression of full-length adiponectin[113] and transgenic overexpression of globular adiponectin[114] in Apolipoprotein-E (ApoE) deficient mice leads to marked reduction in atherosclerotic burden. Similarly, adenovirus-mediated local overexpression of adiponectin in atherosclerotic rabbits led to a significant reduction in plaque size[115].

The anti-atherosclerotic effects of adiponectin are generally thought to be mediated through anti-inflammatory, anti-oxidant, endothelium-protecting effects and through its ability to inhibit VSMC proliferation and migration, as discussed in the following paragraphs.

1.5.5.1 Anti-inflammatory effects of adiponectin

Numerous basic science studies have demonstrated a plethora of anti-inflammatory effects of adiponectin. In endothelial cells, adiponectin inhibits TNF-α-induced IkBa phosphorylation and subsequent NF-kB activation through cAMP-PKA-dependent signaling[116]. The same pathway leads to an adiponectin-mediated reduction in interleukin-8 synthesis in endothelial cells[117]. It also has the ability to prevent TNF-α induced expression of the adhesion molecules vascular cell adhesion molecule 1 (VCAM-1), intracellular cell adhesion molecule 1 (ICAM-1) and E-selectin[118], thus reducing migration of inflammatory cells.

Adiponectin also displays several function- and phenotype-modulating effects in macrophages. In these cells, it reduces production of the pro-inflammatory cytokines TNF-α and IL-6[119] and increases expression of the anti-inflammatory molecules interleukin-10 (IL-10) and Interleukin-1 receptor antagonist (IL-1Ra)[120]. This enhanced expression of IL-10 has been associated with increased tissue inhibitor of metalloproteinases-1 (TIMP-1) expression in human monocyte-derived macrophages[121], which is associated with increased plaque stability. Furthermore, several studies have demonstrated that adiponectin inhibits transformation of macrophages to foam cells. This is achieved through lipid uptake and metabolism modifications in monocyte-derived macrophages: adiponectin leads to reduced class A scavenger receptor expression[122], increased high density lipoprotein (HDL)-mediated cholesterol efflux via a PPARγ/ Liver X Receptor/ ATP-binding cassette transporter ABCA1 signaling pathway[123], as well as downregulation of sterol O-acyltransferase 1, which catalyzes formation of cholesterol esters[124]. The net effect is a reduction in lipid accumulation in macrophages, which protects against foam cell transformation.

1.5.5.2 Anti-oxidant, endothelium-protecting effects of adiponectin

The physiological effects of adiponectin on the various redox regulatory systems in the vasculature have been extensively studied. A direct stimulation of NO production by eNOS has been demonstrated in adiponectin-treated bovine aortic endothelial cell cultures, mediated through a phosphatidylinositol 3-kinase (PI3) dependent pathway involving phosphorylation of eNOS by AMPK[125]. Treatment of human umbilical vein endothelial cells (HUVEC) with globular adiponectin leads to both activation and upregulation of eNOS[126]. Another human endothelial cell culture study showed a marked attenuation of TNF-α induced production of ADMA after treatment with adiponectin[127]. Adiponectin has been found to stimulate the binding of heat shock protein HSP90 to eNOS, contributing to higher NO production[128]. This mechanism also mediates the protective action of adiponectin against angiotensin II-induced apoptosis of endothelial cells in HUVEC cultures[129].

Several experimental models of adiponectin deficiency have further elucidated the roles of this adipokine in the regulation of redox-sensitive pathways in the vessel wall. One study has demonstrated increased $O_2^{\cdot -}$ and $ONOO^{\cdot -}$ formation as well as reduced vasodilatory response to acetylcholine in vascular rings obtained from adiponectin knock-out mice[130]. eNOS expression was found to be normal, but eNOS phosphorylation and NO production were significantly reduced. The researchers conclude that adiponectin deficiency causes endothelial dysfunction via reduced NO bioavailability. Adiponectin deficiency has also been associated with reduced endothelial NO and increased interactions between leukocytes and the endothelium in adiponectin knock-out mice, through elevated expression of vascular adhesion molecules[131]. Treatment with globular adiponectin reverses these effects; however, simultaneous blocking of eNOS with N(omega)-nitro-L-arginine methyl ester (L-NAME) does not have the same result. This

suggests that some of the anti-inflammatory actions of adiponectin are mediated through enhanced eNOS activity.

The role of adiponectin has also been researched in various experimental disease-state models. Adiponectin is able to suppress ROS generation in endothelial cells exposed to hyperglycemia[132] or palmitate[133] through a cAMP/AMPK mediated pathway. In bovine endothelial cell cultures treated with oxLDL, globular adiponectin suppresses cellular proliferation and $O_2^{\cdot -}$ generation through inhibition of NADPH-oxidases and enhanced eNOS activity[134]. Adiponectin also attenuates oxLDL-induced endothelial dysfunction in HUVECs via an increase in intracellular GSH levels[135]. In hyperlipidaemic rats treatment of vascular segments with adiponectin improves eNOS and inhibited inducible NOS (iNOS) activity, leading to increased bioavailability of NO and reduced oxidative and nitrosative stress[136]. This adiponectin-mediated inhibition of iNOS has also been observed in adventitial fibroblasts treated with lipopolysaccharide (LPS), where adiponectin prevented fibroblast proliferation and migration into the intima by reducing $ONOO^-$ production[137]. In obese Sprague-Dawley rats, treatment of aortic segments with globular adiponectin reverses the observed endothelial dysfunction via amelioration of eNOS activity through AMPK-mediated phosphorylation[138]. This mechanism is also responsible for the stimulated revascularization observed in a murine hindlimb ischemia model, where adiponectin levels were elevated through caloric restriction versus control[139]. Interestingly, another study in obese Sprague-Dawley rats demonstrated reduced phosphorylated AMPK and eNOS, despite normal or elevated levels of circulating adiponectin after 8 weeks on a high-fat diet[140]. This suggests that obesity and hyperlipidemia may inhibit the protective actions of adiponectin on the vasculature.

In clinical studies, reduced levels of adiponectin in the circulation have been shown to predict endothelial dysfunction in coronary[141] and peripheral arteries[111], independently

of other cardiac risk factors, such as BMI, blood cholesterol levels and insulin resistance. Indeed, early studies showed that high levels of adiponectin in the circulation are associated with lower risk of myocardial infarction[142], reduced incidence of early-onset coronary artery disease and multi-vessel disease[143], as well as reduced overall coronary artery disease in men[144].

1.5.5.3 Inhibition of VSMC proliferation by adiponectin

As mentioned previously, VSMC proliferation and migration to the intima is one of the steps in the atherosclerotic process. Adiponectin has been shown to interfere with this process by inhibiting several pro-atherogenic growth factors, such as basic fibroblast growth factor (FGF) and platelet-derived growth factor BB (PDGF-BB)[145]. This is mediated by enhanced binding of these factors to the middle- and high-molecular weight forms of adiponectin in the circulation, which prevents receptor binding and triggering of pro-atherosclerotic intracellular cascades[146]. Adiponectin knock-out mice exhibit increased neointimal formation after external vascular cuff injury[147] or wire injury[112]; in the latter study, this was rescued via adenovirus-mediated supplementation with adiponectin.

1.6 Distinct properties of adipose tissue depots

1.6.1 Subcutaneous versus visceral adipose tissue

The majority of adipose tissue present in the human body is distributed in two depots: subcutaneous (ScAT) and visceral (VAT) adipose tissue. ScAT, as its name suggests, is located subcutaneously, whereas VAT intra-abdominally, surrounding the abdominal organs[44]. There is a considerable amount of clinical observations suggesting that central adiposity (characterized mainly by increased visceral fat in the trunk and/or abdomen, so called "male-patterned/apple-shaped") leads to higher risk of cardiovascular

disease than peripheral adiposity (which exhibits increased subcutaneous fat in the gluteal and femoral areas "female-patterned/pear-shaped"). It has been demonstrated that the waist-hip ratio positively correlates with triglycerides and negatively with HDL cholesterol[148] and is independently associated with prevalent atherosclerosis, providing better discrimination than either waist circumference or body mass index[149, 150]. Peripheral fat has been shown to possess antiatherogenic effects, as evidenced by evaluation of aortic calcification in elderly women[151]. Removal of excess femoral fat in obese females via liposuction did not confer improvement in systemic inflammatory markers, blood pressure or insulin sensitivity, despite a considerable decrease in body fat[152]. In fact, loss of fat in the gluteal and femoral area versus the abdominal area has been linked to worsening of coronary heart disease risk factors in obese females following a 14-week weight loss intervention [153]. On the contrary, surgical removal of excess abdominal visceral fat in rat models has been shown to lead to improvements in hepatic insulin resistance and glucose tolerance[154]. Evidence of a link between increased VAT and macrovascular disease has been reported, such as increased carotid intima/media thickness in centrally obese versus lean women[155] and a positive correlation with angiographically assessed coronary artery disease incidence [156]. A number of studies indicate that obese children are at a higher risk of developing metabolic syndrome and related disorders in adulthood, with the risk being more closely associated with intraabdominal rather than subcutaneous adipose tissue accumulation [157], [158]. Moreover, human adipose tissue distribution has been shown to be altered in type 2 diabetes mellitus, with increased VAT and intramuscular adipose tissue compared to ScAT[159].

The aforementioned clinical observations have led to the hypothesis that there exists a functional rather than simply a topographic distinction between the different adipose tissue depots. A number of studies have reported a discordant expression of various

adipokines between ScAT and VAT. Human omental fat cells exhibit a higher secretion of adiponectin than subcutaneous adipocytes *in vitro*, but this secretion correlates negatively with body mass index[160]. Indeed, increased peripheral fat mass has been linked to higher circulating adiponectin levels in obese elderly women vs. central mass[161]. A number of pro-inflammatory mediators are expressed at higher levels in human VAT than in ScAT, such as complement factors and angiotensinogen[162]. It has been shown that VAT inflammation accelerates atherosclerosis in ApoE deficient mice[163]. In humans, visceral adipose tissue exhibits a higher degree of inflammatory cell infiltration which has been observed to be associated with hepatic fibroinflammatory lesions[164]. VAT has also been shown to be a major contributor of plasma IL-6 levels in extremely obese patients[165]. Owing to the fact that it drains directly onto the portal circulation, it has been hypothesized that the observed increased secretion of IL-6 may stimulate the liver into elevated production of inflammatory mediators and proteins involved in hemostasis, such as CRP and PAI-1[44], thus contributing to heightened systemic inflammation.

1.6.2 Perivascular adipose tissue and vascular redox state

Adipose tissue also exists at the adventitial border of human blood vessels. This depot, called perivascular or periadventital adipose tissue (PVAT), has traditionally been considered as structural support for the vessels it surrounds. During the last years, however, it has been increasingly implicated in the pathogenesis of atherosclerosis, owing to its close proximity to the vessel wall of coronary arteries and the aorta. However, the role of PVAT in the regulation of vascular redox state and atherosclerosis is highly controversial. A large number of studies have uncovered seemingly contradictory properties of PVAT, both pro- and anti-contractile, pro- and anti-atherogenic[166]. Indeed, increased PVAT has been observed to co-localize with atherosclerotic plaques and exhibit a high degree of inflammatory cell infiltration[167]. Human perivascular adipocytes

surrounding the coronaries exhibit reduced differentiation and a heightened proinflammatory biochemical profile, which clearly distinguishes them from other adipose tissue depots[168]. On the other hand, peri-aortic AT in rodents exhibits BAT-like characteristics: it displays thermogenic capabilities and increases triglyceride clearance after cold exposure[169]. Targeted deletion of PPARγ in VSMCs of rodents leads to developmental loss of PVAT, which in turn results in endothelial dysfunction and accelerated atherosclerosis[169]. However, while functional BAT exists in the aortic arch of non-obese adult humans, it has been shown in post-mortem samples that pericoronary AT displays an unequivocally white morphology and phenotype[168]; this highlights the fact that care should be taken when attempting to translate results from animal studies to humans.

Adipose tissue sites (such as gluteal, subcutaneous, visceral etc.) that are distal to larger vessels contribute to the circulating pool of each adipokine and are thus able to exert endocrine effects in remote target-organs. These include the vascular wall, allowing adipokines to trigger signaling from the vascular lumen to the endothelium and the VSMCs. On the other hand, perivascular adipose tissue (PVAT), owing to its close proximity to the vascular wall, potentially has direct, paracrine effects in the underlying vasculature, in an "outside-to-inside" way. Adipokines produced by PVAT, either from adipocytes or the vascular stromal fraction (which includes inflammatory cells) could directly diffuse to the wall of smaller vessels, in a paracrine manner. It is highly unlikely, however, that large molecules would be able to have deep penetration in the vascular wall in this manner, especially considering that several adipokines have very high molecular weights. A second mechanism that would allow such large molecules to reach the vascular wall from PVAT has been proposed: proof-of-concept for "outside-to-inside" signaling in vessels has been demonstrated by applying an IL-1b-eluting cotton mesh around coronary arteries in pigs: this contributed to alterations in the underlying vessels, including intimal

thickening, *in vivo*[170]. Similarly, in larger or atherosclerotic vessels, adipokines originating from PVAT could reach the inner cellular layers of the vasculature through vasa vasorum. This mechanism has been termed "vasocrine signaling" and was first shown in PVAT surrounding arterioles of rat muscle[171]. It could also be relevant to the-rich in vasa vasorum- coronary vascular system, both in the presence and absence of atherosclerotic plaques[172]. However, definitive existence for the presence of an interaction between PVAT and the underlying vessel in humans, as well as evidence on the potential mediators of such a cross-talk, has not been reported in the literature. Figure 1.6 presents the different mechanisms through which adipokines could interact with the vascular wall.

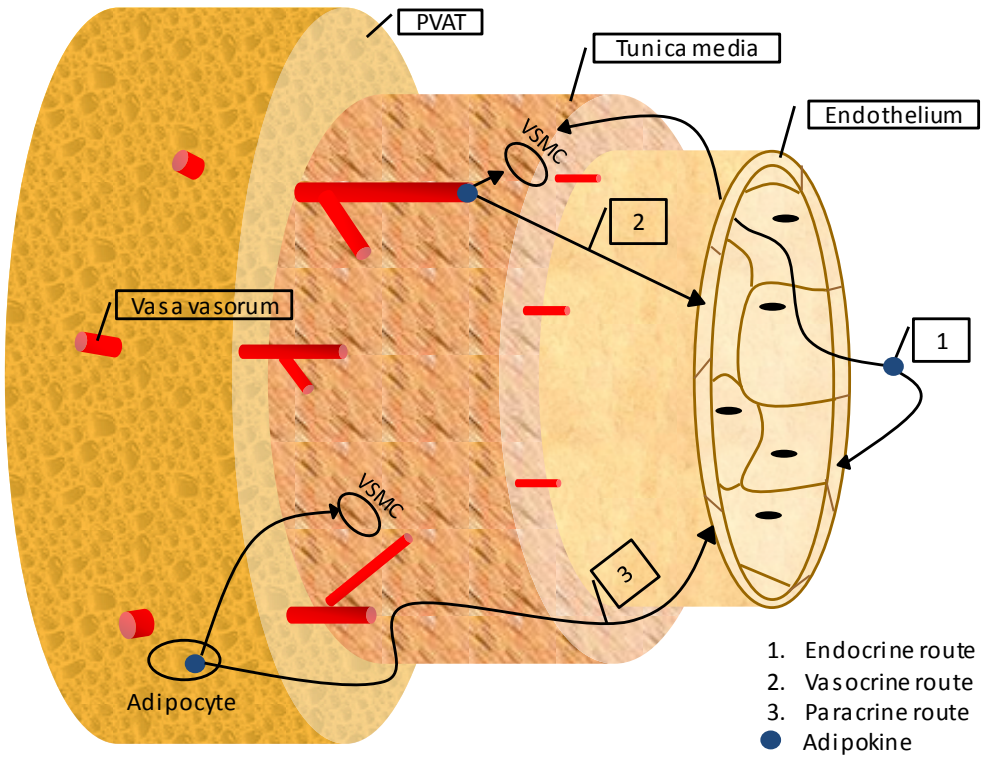


Figure 1.6: *Adipokines can reach endothelial cells in the endothelium or vascular smooth muscle cells (VSMCs) in the tunica media through three potential routes. Adipokines can be secreted from distal adipose tissue sites and reach the vascular wall via an endocrine path. They can be secreted from perivascular adipose tissue (PVAT) and reach the vascular wall through the vasa vasorum via a vasocrine mechanism, or they can diffuse to the vascular wall and reach VSMCs (and potentially the endothelium) through a paracrine route. (Special thanks to Dr. Ioannis Akoumianakis for his assistance in designing this figure).*

1.7 Hypotheses and aims

The main hypothesis of my thesis project is that adiponectin has direct antioxidant effects in the human vascular wall. I also hypothesized that the regulation of its synthesis in adipose tissue is delicately controlled by a variety of factors, with distinct adipose tissue depots being affected in diverse ways by different stimuli.

In order to investigate these hypotheses, this thesis aims to:

- Examine the factors influencing adiponectin synthesis in human adipose tissue.
- Explore the morphological and functional characteristics of distinct adipose tissue depots in relation to their adiponectin-producing ability.
- Investigate the effects of adiponectin on human vascular redox state, as a "first in humans" proof-of-concept.
- Determine the molecular pathways mediating the aforementioned effects.
- Evaluate the role of adiponectin as a mediator in a potential interplay between adipose tissue and the vascular wall in human atherosclerosis.
- Discuss and propose future work to further explore the findings from this thesis.

Chapter 2
Study design & methods

This chapter describes the recruitment process for patients taking part in the study, the demographic characteristics of the study participants, as well as the background and experimental conditions for methods used in this thesis. Each following chapter will outline techniques used exclusively for that particular chapter.

2.1 The Oxford CABG Bioresource

During my time as a DPhil student at the University of Oxford, I contributed significantly to the development of the Oxford Coronary Artery Bypass Grafting (CABG) Bioresource, an ongoing project at the Division of Cardiovascular Medicine, Radcliffe Department of Medicine, University of Oxford. This project aims to create a large, well-phenotyped cohort of patients undergoing cardiac surgery.

Inclusion criteria are:

- Patient willing and able to give informed consent for participation in the study
- Male or female, aged 18 years or above
- Diagnosed with cardiac disease and scheduled for elective coronary artery bypass graft surgery or valve replacement/repair surgery

Exclusion criteria are:

- Auto-immune diseases (eg rheumatoid arthritis)
- Active infectious diseases (eg hepatitis, HIV)
- End-stage liver or renal failure (requiring dialysis)
- Active malignancy
- Recent unstable coronary syndrome (within the previous 8 weeks)

- Patients receiving non-steroidal anti-inflammatory drugs, dietary supplements or antioxidant vitamins

Phase I of the Oxford CABG Bioresource is complete. It comprises 677 patients who were recruited in the period 2004-2011 in a collaborative effort between the University of Oxford and the University of Athens. Data on adipose tissue phenotype are available for a subset of 258 patients, recruited between the period 2007-2011 at the 1st Cardiology Unit, University of Athens Medical School. Phase II of this project (called the AdipoRedox study) began in September 2011 (NRES Committee South Central Oxford C – 11/SC/0140). Patients undergoing CABG or valve surgery are recruited at the Department of Cardiothoracic Surgery, John Radcliffe Hospital, Oxford University Hospitals NHS Foundation Trust. I personally recruited the first patient in the AdipoRedox study (16th September 2011) and I have participated in the recruitment, sample collection and tissue processing for more than 400 patients since then. The final section of this chapter describes my personal contribution in detail.

The process of recruitment can be summarised as follows. Written informed consent is sought from all participants in the study (a copy of the research consent form is provided in Appendix I of this thesis). After obtaining consent, a full cardiovascular history is recorded and non-invasive echo-based imaging studies are performed on recruitment for each individual patient. During surgery, adipose tissue and vascular samples are collected (more details in paragraph 2.4). In the lab immediately after surgery, various bio-assays are performed routinely in fresh vascular and adipose tissue samples. Additional tissue samples and blood are snap-frozen and stored at -80^{o}C for subsequent experiments. Surplus fresh tissue is used for specific *ex vivo* experiments, as required. Figure 2.1 offers a visual representation of the recruitment process. Each individual experimental method is described in detail in separate sections of this chapter.

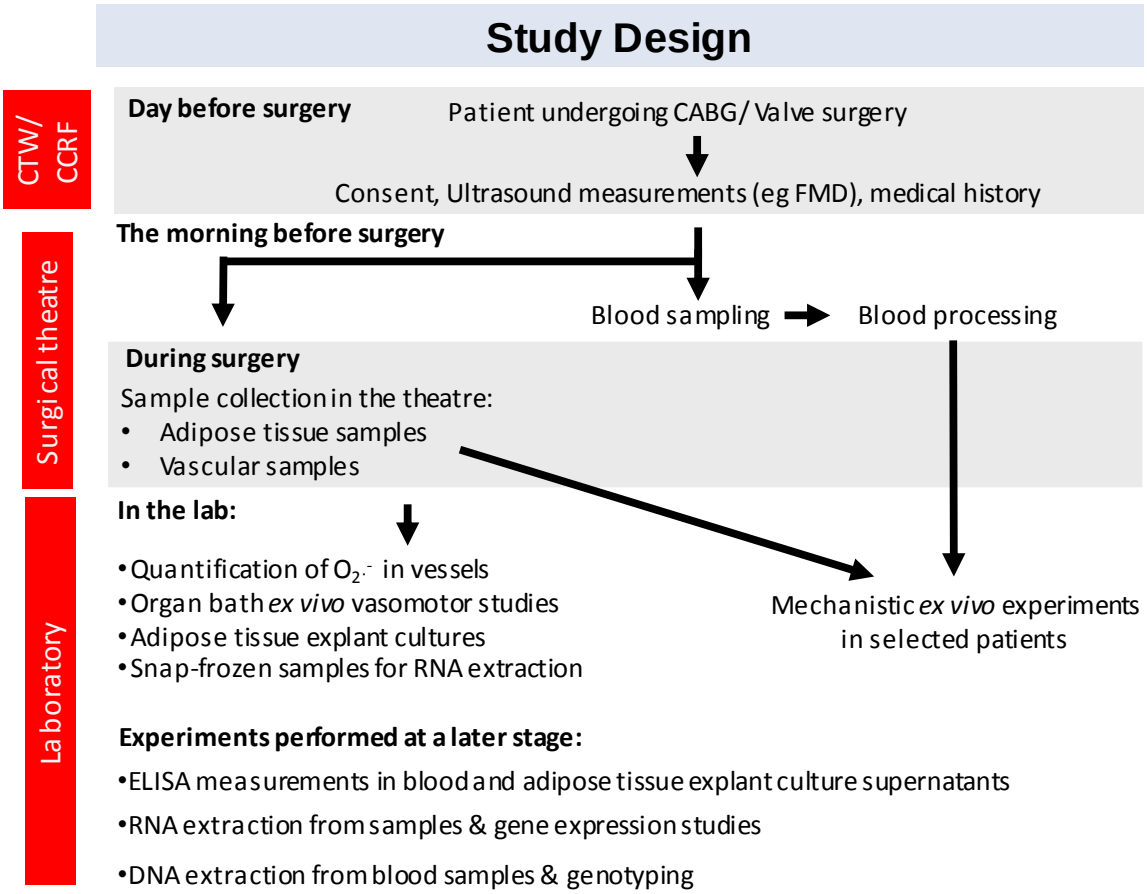


Figure 2.1: *An overview of the recruitment process & design of the AdipoRedox Study. CTW: Cardiothoracic Ward; CCRF: Cardiovascular Clinical Research Facility; CABG: Coronary Artery Bypass Grafting; FMD: Flow-mediated dilatation*

2.2 Demographics, risk factors and in-hospital follow-up

Different subsets of the Oxford CABG Bioresource have been used in each individual chapter of my thesis. This is due to the fact that specific tissue samples (for example adipose tissue or internal mammary artery samples) were not available for all patients. Each individual results chapter includes a table outlining the demographic/anthropometric characteristics of the population used in the experiments presented in that particular chapter.

Information regarding risk factors (hypertension, hyperlipidaemia, diabetes mellitus, smoking status), family history of cardiac disease, New York Heart Association (NYHA) classification of heart failure, Canadian Cardiovascular Society (CCS) grading of angina pectoris and medication profile were obtained either through the medical records or through discussion with the study subject. Additional information was obtained through the medical records regarding angiographic extent of coronary artery disease, left ventricular ejection fraction, previous myocardial infarctions and their territories, previous transient ischaemic attacks (TIA)/stroke, presence of peripheral vascular disease (PVD), previous percutaneous transluminal coronary angioplasty (PTCA) and any other relevant medical conditions. This information was recorded on an AdipoRedox study Case Report Form (CRF), a template copy of which can be found in Appendix II. Values for cholesterol, high-density lipoprotein (HDL) and triglycerides were obtained through the medical records of the patient, and represent the most recent laboratory value that could be retrieved. Measurement of body mass index (BMI), waist, hip, arm and chest circumference was performed by nursing staff or the researcher on the day before surgery.

After the procedure, information regarding EUROSCORE, on- or off-pump CABG, clamp/total bypass time (in case of on-pump), number of vein and number of arterial grafts used were obtained from the operative note filed in the medical records. As part of the AdipoRedox study, the patients were followed-up in-hospital for events such as post-operative atrial fibrillation, need for inotropic support and days spent in the cardiothoracic critical care unit (CTCC). While this information is not used in my thesis, it constitutes an integral part of the data available for patients recruited in the Oxford CABG Bioresource.

2.3 Pre-operative assessment of endothelial function

Peripheral arteries, especially the brachial artery, respond to physical and chemical stimuli by adjusting vascular tone and regulating blood flow. Increased blood flow in peripheral arteries leads to increased shear stress stimuli, increased NO production, and vasodilation. The vasorelaxation response of the brachial artery to increased shear stress is called flow mediated dilation (FMD) and is an indirect, *in vivo* estimation of the ability of endothelium to produce NO.

The process of obtaining FMD measurements in subjects taking part in the AdipoRedox study was as follows. After a 12 hour fasting period, the subject was positioned in a supine position, in the vascular measurements room of the Cardiovascular Clinical Research Facility. Level 1, Heart Centre, JR Hospital, Oxford (Figure 2.2).



Figure 2.2: *Setup of the room used for flow-mediated dilatation of the brachial artery measurements, Cardiovascular Clinical Research Facility, Level 1, Heart Centre, John Radcliffe Hospital.*

The temperature in the room was maintained constant and the patient kept their arm in a comfortable position to assess the brachial artery. ECG leads were attached to the patient's chest. The vessel was imaged in the longitudinal plane above the antecubital fossa, using a linear array transducer (7–12 MHz frequency) attached to a Phillips CX50 ultrasound system (Figure 2.3). The diameter of the brachial artery was determined at rest and blood flow estimated by time averaging the pulsed Doppler velocity signal obtained from a mid-artery sample volume. After baseline brachial artery diameter determination, ischaemia was produced by inflating a cuff placed at the distal forearm, at a pressure 50 mm Hg greater than the systolic blood pressure. The release of the ischaemia cuff after five minutes leads to an increase in blood flow, resulting in a vasodilatory effect due to shear stress on the brachial artery.

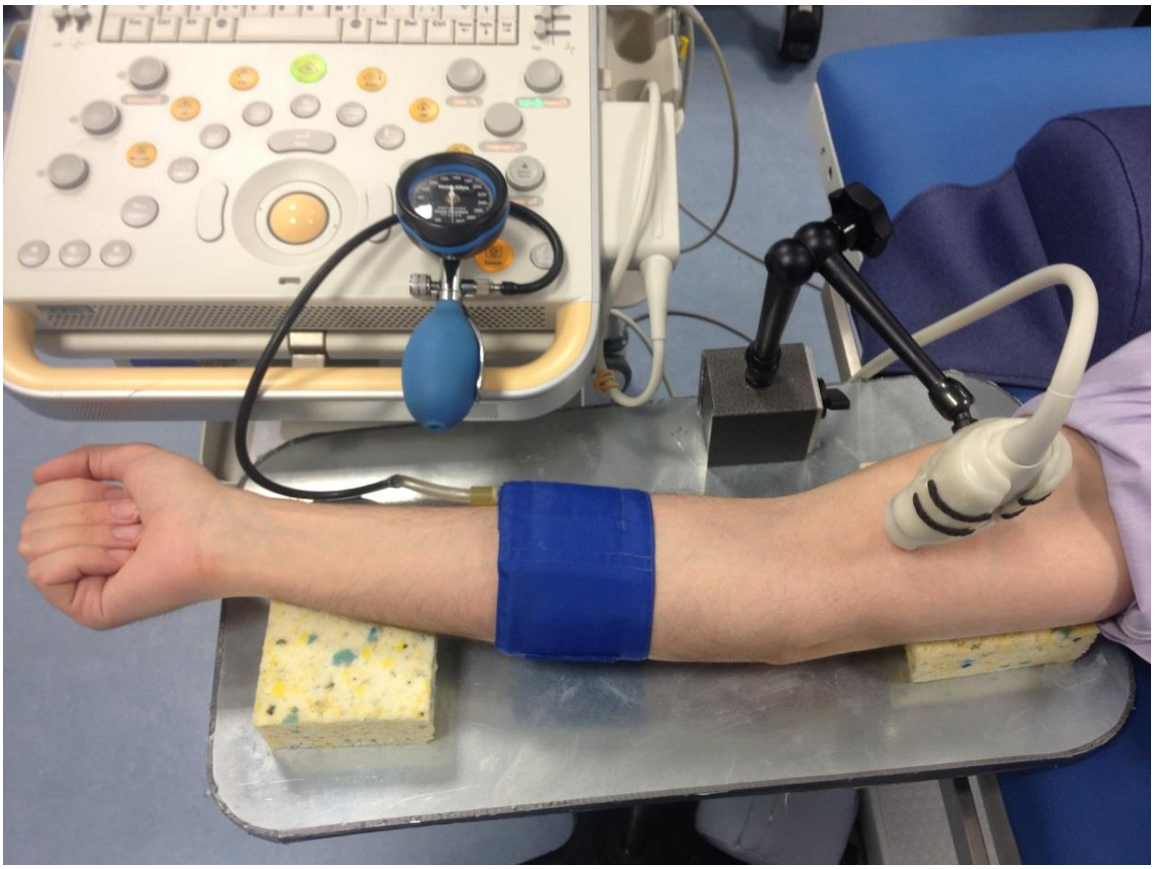


Figure 2.3: *Positioning of the ultrasound probe over the brachial artery, above the antecubital fossa. The ischaemia cuff is placed distally around the forearm. After 5 minutes of ischaemia, the cuff is released, causing endothelium-dependent vasodilation.*

The maximum diameter of the brachial artery was determined approximately 60 seconds after release. The diameter of the brachial artery was always measured at the starting frame of the QRS wave, to avoid any effect of arterial compliance on the measurements. FMD was defined as the percentage change of the brachial artery diameter from rest to the diameter 60 seconds after ischaemia cuff release. A further measurement was made three minutes after a sublingual spray of glyceryl trinitrate (GTN 400 µg), to estimate endothelium-independent vasodilation.

The diameter of the brachial artery was calculated off-line using edge detection software. (Vascular Analyser, Medical Imaging Applications LLC) (Figure 2.4). FMD and endothelium-independent dilatation (EID) of the brachial artery were defined as the % change in vessel diameter after forearm ischaemia or sublingual GTN, respectively.

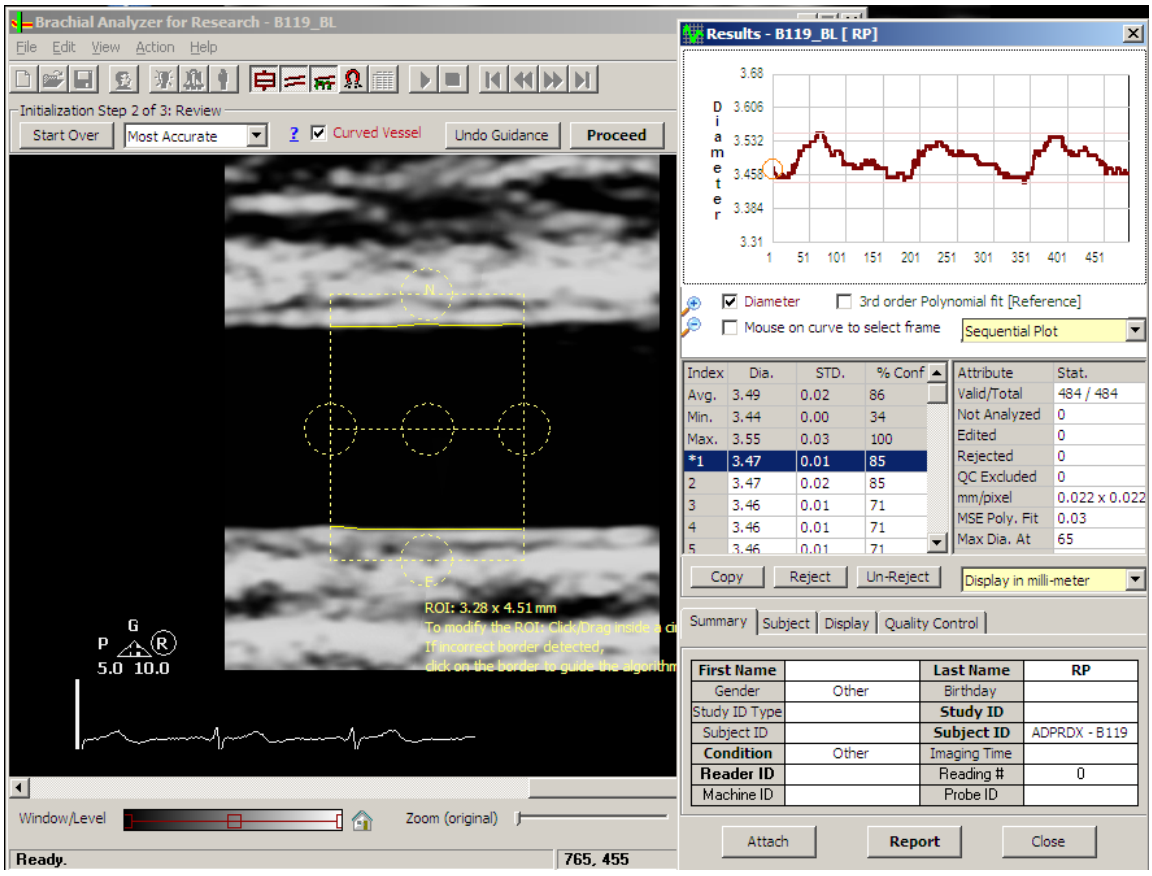


Figure 2.4 *Representative screenshot of flow-mediated dilatation (FMD) analysis using Vascular Analyser software.*

2.4 Sample collection

Unless otherwise specified, all reagents used were purchased from Sigma-Aldrich (UK).

2.4.1 Blood sampling

Venous blood samples were obtained after 8 hours of fasting, on the morning of surgery, from the central line cannula. The samples were immediately distributed to standard BD Vacutainer tubes, either for serum collection (orange Serum Separator Tubes) or for plasma collection using different anti-coagulants (Lavender- K_2EDTA; Blue – Citrate; Green – Li^+/Heparin). The samples were immediately transferred to the CCRF laboratory. Two K_2EDTA vials of whole blood were frozen at -80^{o}C for future DNA extraction. The remainder of the plasma vials were spun at 3000 g at 4°C for 15 minutes using a Labofuge 400R (Heraeus Instruments) centrifuge. Serum vials were kept at room temperature for 30 min, to allow blood to clot according to serum collection protocol; after 30 min, the tubes were spun at 3000 g for 15 min and serum was collected. Plasma and serum were split into aliquots in barcode-labelled vials and kept at -80^{o}C until further processing.

2.4.2 Tissue collection and processing

On the day of surgery, sterile vials containing ice-cold Krebs Henseleit buffer (KHLB: NaCl 120 mM, KCl 4.7 mM, $CaCl_2$ 2.5 mM, $MgSO_4$ 1.2 mM, KH_2PO_4, $NaHCO_3$, and glucose 5.5 mM, pH 7.4), oxygenated for 5 min (95% O_2/5% CO_2), were prepared in order to allow transfer of samples from theatre to the laboratory.

Tissue samples were harvested by the surgeon performing the procedure and transferred to the sterile vials in theatre. Samples collected were as follows:

- A sample of the pedicle left internal mammary artery (IMA), with its perivascular adipose tissue (peri-IMA PVAT) attached (Figure 2.5).
- A sample of the long saphenous vein (SV, Figure 2.6), with its perivascular adipose tissue attached (Peri-SV PVAT).
- Subcutaneous adipose tissue (ScAT), collected from the site of the sternotomy, superiorly to the sternum.
- Mesothoracic adipose tissue (MtAT), which was obtained from the mediastinum in the intrathoracic cavity, inferiorly to the sternum but superiorly to the pericardial sac (Figure 2.7).
- A sample of femoral adipose tissue (FemAT), which was obtained from the leg incision site, distally to the SV.
- A piece of the right atrium appendage (RAA), if excised during on-pump CABG or valve procedures (not used in my thesis but part of the Oxford CABG Bioresource).

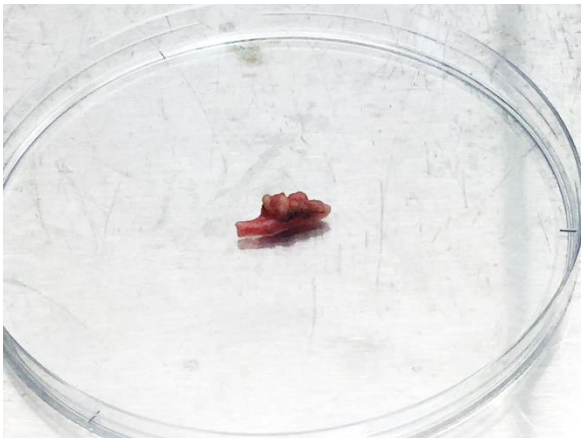


Figure 2.5: *Sample of internal mammary artery (IMA) with its perivascular adipose tissue (PVAT) attached, obtained from a patient undergoing CABG surgery, recruited in the AdipoRedox study.*

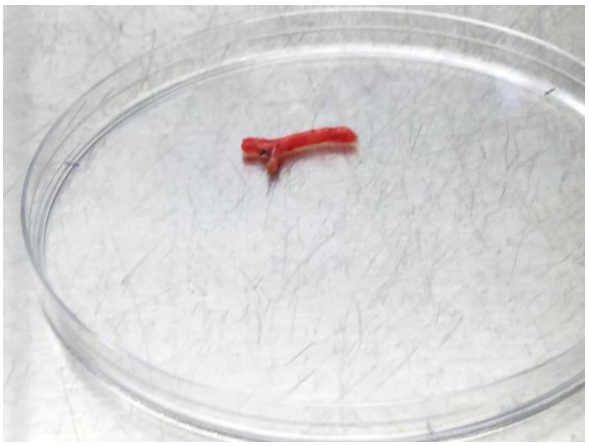


Figure 2.6: *Sample of long saphenous vein (SV) separated from its perivascular adipose tissue, obtained from a patient undergoing CABG surgery, recruited in the AdipoRedox study.*

All surgical samples were obtained before cannulation of the right atrium and before heparin administration. To limit the possible impact of anaesthesia on the study results, the same anaesthetic agents were used in all cases (propofol/rocuronium bromide/remifentanil). Each sample was always obtained at the same stage of the operation

to limit inter-patient variability. Sample collection lasted approximately 30 min and all samples were kept on wet ice during the process, after which they were transferred to the laboratory. To minimise the possible impact of surgical manipulations on the integrity and overall biology of the study samples, the vessels collected in this study (SVs and IMAs) were harvested by using a "no touch" technique and explanted with their adipose tissue.

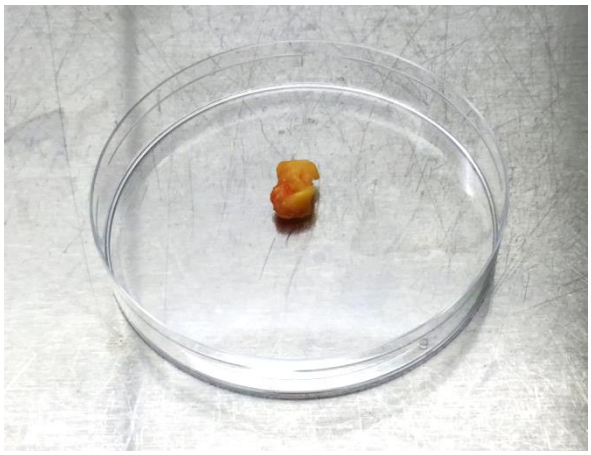


Figure 2.7: *Sample of mesothoracic adipose tissue (MtAT) obtained from a patient undergoing CABG surgery, recruited in the AdipoRedox study.*

SV and IMA samples were placed in a petri dish with a small amount of KHLB and gently flushed with sterile saline using a 25G needle and 5 mL syringe to remove blood and clots. The perivascular adipose tissue surrounding the vessel was carefully dissected using sterile forceps and scalpel. The vessels were carefully cut into rings with a single slice using a 15 scalpel blade (Figure 2.8). Two vessel rings were used for luminometry experiments to estimate superoxide generation, as described in paragraph 2.7. Up to four additional SV rings were used for organ bath vasomotor studies, to estimate endothelial function, as described in paragraph 2.8. Additional vascular rings were used for mechanistic *ex vivo* experiments, as required.

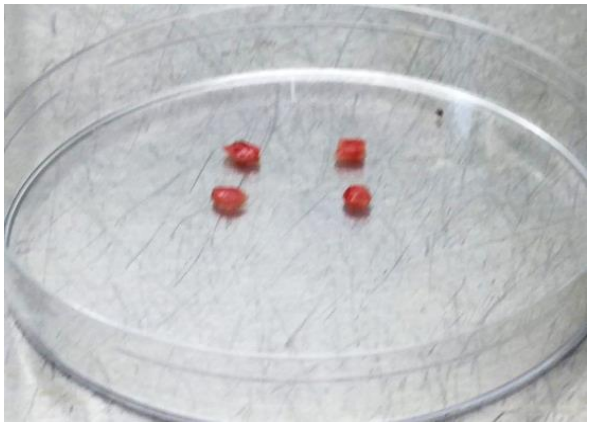


Figure 2.8: *Sample of long saphenous vein cut in 4 separate vessel ring, obtained from a patient undergoing CABG surgery, recruited in the AdipoRedox study*

All adipose tissue samples were cut into separate pieces using sterile scissors and/or scalpel. The pieces were washed in sterile phosphate buffered saline (PBS). Adventitia and connective tissue were removed and discarded. Adipose tissue pieces of approximately 100 mg were stored in -80^{o}C for further assays. One of these pieces was kept in QIAzol (QIAgen) for future RNA extraction. For ScAT, MtAT, Peri-SV PVAT and FemAT, where a large sample was obtained, additional pieces (ranging from 200-500 mg) were used for adipose tissue explant culture, as described below.

2.5 Adipose tissue explant cultures

Samples of ScAT, MtAT, Peri-SV-AT and FemAT were used in an *ex vivo* explant culture protocol, to estimate the biosynthetic rate for various adipokines. Adipose tissue samples were obtained as mentioned previously and separated in up to four pieces, each weighing 200-500 mg (Figure 2.9).



Figure 2.9: *Sample of mesothoracic adipose tissue (MtAT) obtained from a patient undergoing CABG surgery recruited in the AdipoRedox study, cut in 4 pieces, intended for adipose tissue explant culture.*

After obtaining an exact weight using micro-scales, the samples were cut in ~1-2 mm^3 cubes using scissors and scalpel, washed with sterile PBS and equilibrated for 1 hour at 37 ^{o}C in Medium-199 containing HEPES 25 mM, gentamycin 50 µg/mL and fatty acid-free bovine serum albumin 1% in the presence of protease inhibitor (Roche Applied

Science) in a cell culture incubator with 5% CO_2 atmosphere. At the end of the equilibration period, the medium was discarded by filtering the samples through a micro-sieve and washing with additional medium (kept at 37°C), to remove cellular debris. Then, a weight-adjusted volume of fresh medium was added to the tissue (1 mL per 200 mg tissue), followed by a 4 hour incubation under the same conditions. At the end of the incubation period, the medium was separated from the adipose tissue by using a micro-sieve. The culture supernatants and the adipose tissue were collected, filtered and stored at -80°C. Sterile conditions were maintained throughout. The experimental process is illustrated in Figure 2.10. At a later stage, the supernatants were thawed and the levels of adipokines in the supernatant were measured using enzyme-linked immunosorbent assays (ELISA), as described in the following paragraph.

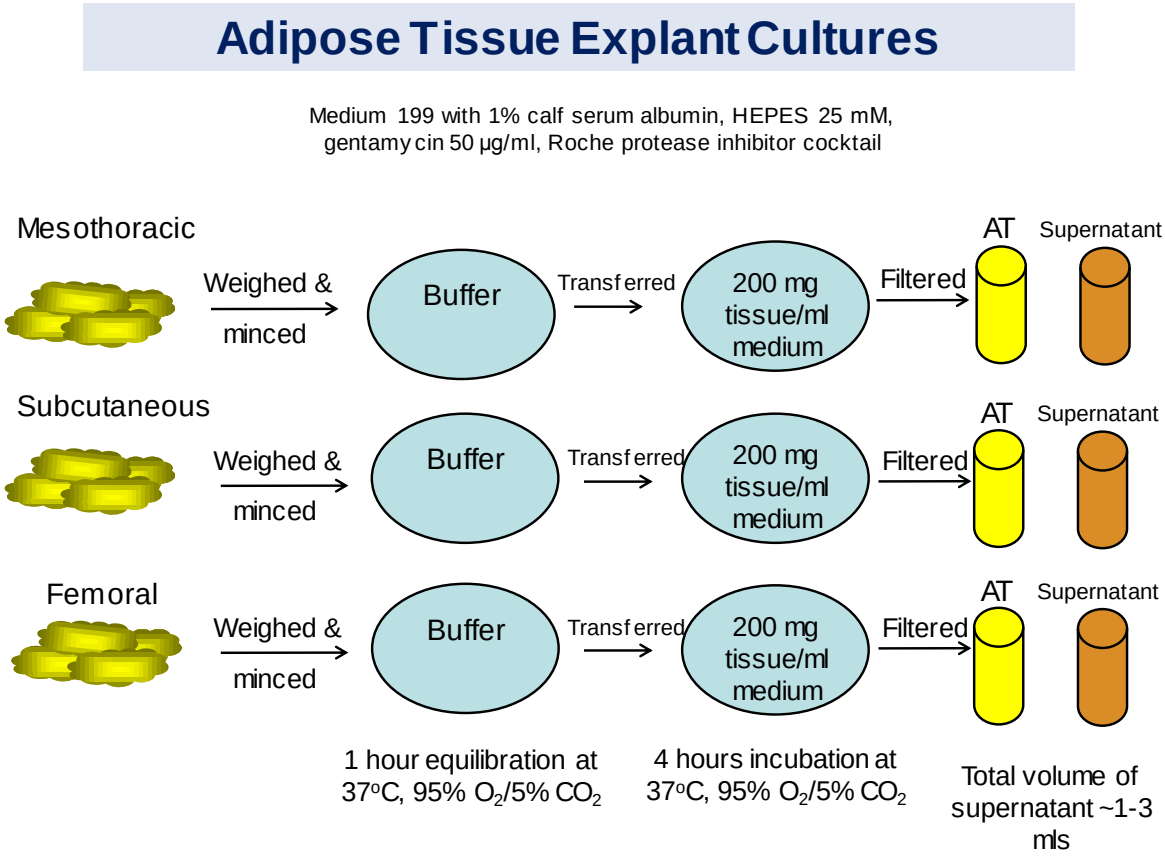


Figure 2.10: *Schematic illustration of the adipose tissue explant culture experimental design.*

2.6 Biomarker measurements

2.6.1 Enzyme-linked Immunosorbent Assay (ELISA)

Commercially available sandwich ELISAs were used to measure the levels of biomolecules in the circulation or in the adipose tissue explant culture supernatants (obtained using the method described in paragraph 2.5). The general principle of this widely used assay is as follows: samples, standards and quality controls are incubated in microplate wells pre-coated with anti-human anti-target biomarker antibody. After incubation (time depends on each kit) which allows capture of the target molecule on the antibodies coating the plate wells, the plate is washed to remove the remainder of the sample. Then, a solution containing anti-human anti-target antibody conjugated with horseradish peroxidase (HRP) (conjugate) is added to the wells and incubated for 60 minutes. Following another washing step, a substrate solution is added, which allows the conjugate HRP to react. Typically this step requires protection from light exposure. After a kit-specific incubation time, the reaction is stopped by addition of a stop solution and absorbance of the resulting product is measured, at a kit-specific wavelength. The absorbance is proportional to the concentration of the target biomarker. A standard curve is constructed by plotting absorbance values against concentrations of standards (representative curve in Figure

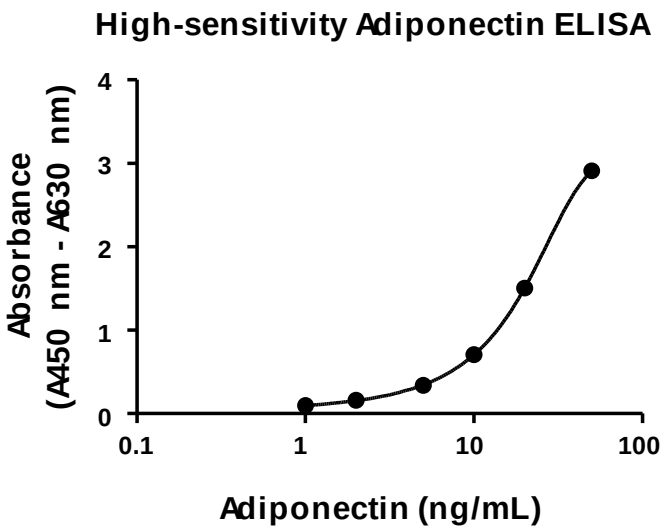


Figure 2.11: *Representative standard curve from a high-sensitivity adiponectin ELISA kit (BioVendor).*

2.11). The absorbance measured is corrected for blank wells and the concentrations of unknown samples are determined based on this standard curve. An internal quality control is used for all plates (pooled serum/plasma sample created from randomly chosen patients).

In my project, ELISA kits were used to measure:

- full-length total adiponectin (including globular and HMW forms) in human serum and in adipose tissue explant culture supernatants,
- interleukin-6 (IL-6) in human serum,
- monocyte-chemoattractant protein-1 (MCP-1) in human plasma,
- 4-hydroxynonenal (4-HNE), a lipid oxidation product, in human plasma.

A list of ELISA kit manufacturers and kit catalogue numbers can be found in Table 2.1. All reaction conditions (solutions/dilutions used, incubation times, absorbance wavelength) were according to the manufacturer-specified instructions in the kit manual.

Table 2.1 ELISA kits used in this project

Biomarker	Manufacturer	Catalogue No.
Total adiponectin	BioVendor, Brno, Czech Republic	RD195023100
High-sensitivity total adiponectin	BioVendor, Brno, Czech Republic	RD191023100
MCP-1	R&D, Abingdon, UK	DCP00
IL-6	R&D, Abingdon, UK	D6050
4-HNE	MyBioSource, San Diego, CA	MBS006597

2.6.2 Plasma malonyldialdehyde (MDA) measurements/TBARS assay

Malonyldialdehyde (MDA) is an *in vivo* product of lipid peroxidation, widely used as a marker of oxidative stress in biology. Lipid peroxides are unstable and decompose to form a series of compounds, including reactive carbonyl compounds. MDA is the by-product of the arachidonate cycle and a principle aldehyde product of lipid peroxidation.

The thiobarbituric acid reactive substances (TBARS) assay is one of the most reliable and was employed to quantify plasma MDA in K_2EDTA-anticoagulated samples obtained from patients recruited in the Oxford CABG Bioresource. The assay is based on the reaction of thiobarbituric acid with MDA which produces a pink coloured MDA-(TBA2) Schiff base adduct, which can be measured colourimetrically or fluorometrically.

The assay was performed as follows: 50 µl of plasma sample were added to 1 mL H_2O and 1 mL TBA solution (made up of 0.418 g TBA into 50 mL pure acetic acid and 50 mL H2O). Serial dilution standards were created based on an MDA standard formed by dissolving 120 µl of 1,1,3,3-tetratethoxypropane (TEP) in 25 mL ethanol. The samples were mixed and heated for 1 hour at high temperature (95-100^{o}C) to allow the formation of MDA-(TBA2) adduct. Molecules of MDA and TBA bind in 1:2 ratio in this thermodynamic energy-driven reaction. To increase the sensitivity of the assay, the MDA-(TBA2) adduct was then extracted in 3.5 mL n-butanol and centrifuged at 1500g for 10 min to separate and discard the butanol phase. The pink extract was then measured using a FLUOstar Omega (BMG Labtech) fluorometer/spectrophotometer, with an excitation wavelength of 525 nm and emission wavelength of 547 nm. The linear standard curve was plotted (Figure 2.12) and unknown samples were extrapolated from the curve.

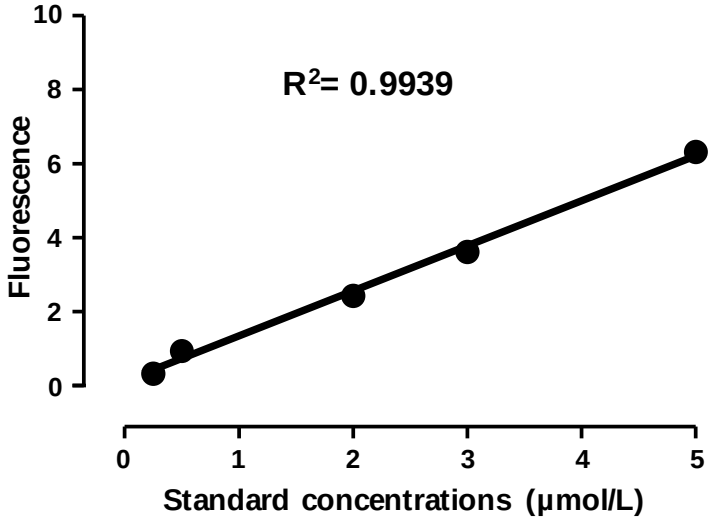


Figure 2.12: *Representative standard curve from an MDA measurement experiment.*

2.6.3 Medical laboratory measurements

The values of some circulating biomarkers were determined using standardized laboratory assays employed in routine clinical practice in a hospital setting. They were retrieved for use in the study from the medical records of the patients enrolled in the Oxford CABG Bioresource.

High sensitivity C-Reactive Protein (hsCRP) was measured by a high-sensitivity latex enhanced immunoturbidimetric assay (ADVIA, Bayer HealthCare LLC). Plasma BNP was quantified by chemiluminescent-microparticle immunoassay (Architect BNP, Abbott, Germany). Serum insulin was measured by chemiluminescent-microparticle immunoassay and serum glucose by the hexokinase method using commercial kits (ABBOTT, Wiesbaden Germany).

2.7 Measurement of vascular superoxide production

Superoxide generation was measured in vascular tissue samples by using two different methods:

- lucigenin-enhanced chemiluminescence
- oxidative fluorescent microtopography (dihydroethidium staining).

2.7.1 Lucigenin-enhanced chemiluminescence

2.7.1.1 Background

The term chemiluminescence describes the phenomenon of light emission as a result of a chemical reaction, due to the presence of excited electrons on one of the reaction products, which leads to emission of a photon upon return of the electrons to the stable ground state. A chemiluminescent probe is employed which, upon reaction with a biological free radical, releases a photon that can be detected by a luminometer. This allows for quantification of free radical generation in the sample[173].

The most commonly used chemiluminescent probe is lucigenin (bis-*N*-methylacridinium nitrate), which is cell-permeable and specific to superoxide radical [174]. The first step in this reaction is the reduction of lucigenin by an $O_2^{\cdot -}$ radical to the lucigenin radical cation, which in turn reacts with a second $O_2^{\cdot -}$ radical to form the unstable lucigenin dioxetane. This molecule breaks down into two *N*-methylacridone molecules, one of which is electronically excited and emits a photon upon decaying to the stable ground state[175] (Figure 2.13). Lucigenin is extremely sensitive for the detection of $O_2^{\cdot -}$, with the rate constant of the first reaction being $\approx 10^8$ mol/L per second [176], much higher than other assays such as cytochrome C reduction[174].

The validity of the lucigenin-enhanced chemiluminescence assay has been discussed extensively in the past. The main issue is a phenomenon called redox-cycling, which relates to the formation of $O_2^{\cdot -}$ after reaction of the lucigenin radical cation with molecular

oxygen, thus leading to an overestimation of the total $O_2^{\cdot -}$ generated by the sample[177]. This reaction can be observed at all concentrations of lucigenin, though much more strongly so at high concentrations (up to 250 µmol/L) [174]. It also depends on the total levels of $O_2^{\cdot -}$ present in the sample, with higher pre-existing concentrations of $O_2^{\cdot -}$ leading to smaller contribution of redox-cycling to the total superoxide generated[174]. Despite these concerns, redox-cycling has been proven to account for an insignificant amount of the total $O_2^{\cdot -}$ generated in cardiovascular biology experiments, due to the low concentrations of lucigenin used (usually 5 µmol/L and not higher than 20 µmol/L)[178].

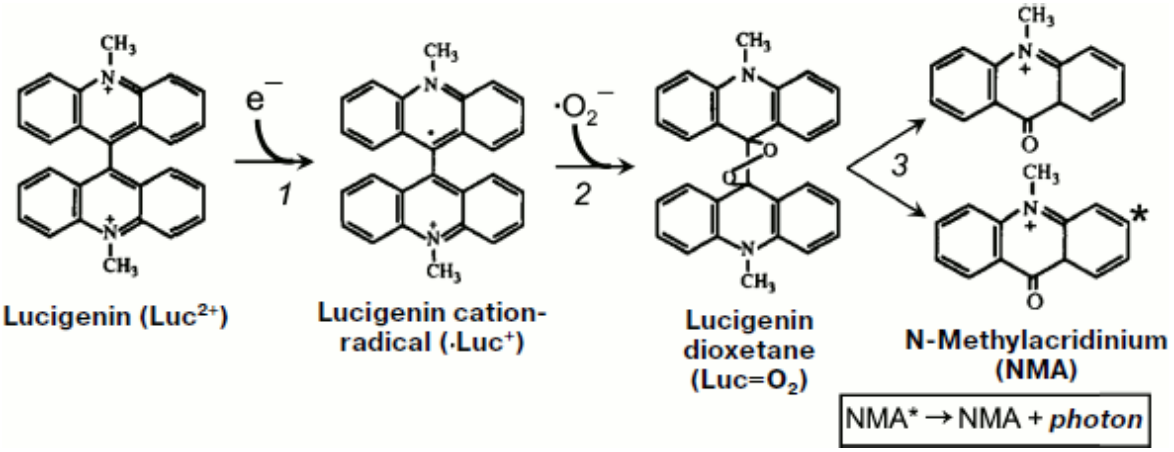


Figure 2.13: *Reaction of a lucigenin molecule with an $O_2^{\cdot -}$ radical forms lucigenin dioxetane, which breaks down into two N-Methylacridinium molecules, one of which emits a photon. (Vladimirov & Proskurnina, Bull Exp Biol Med. 2007;144(3):390-6.)*

The assay can be modified to allow for quantification of $O_2^{\cdot -}$ fraction attributed to each specific enzymatic system present in the vasculature, by using the appropriate substrate or inhibitor. For example, NADPH oxidase activity can be assessed after stimulation with NADPH[40] and/or inhibition with specific inhibitors, such as Vas2870[179]. The effect of uncoupled eNOS on ROS generation can be determined after inhibition with *NG*-nitro-L-arginine methyl ester (LNAME); elevated levels of uncoupled eNOS will result in a lower average count signal, because inhibition of the uncoupled form of the enzyme will lead to lower $O_2^{\cdot -}$ formation[180].

2.7.1.2 Resting vascular $O_2^{\cdot -}$ generation measurements

All lugicenin-enhanced chemiluminescence experiments presented in this thesis were performed using a single-tube FB12 Titertek-Berthold luminometer, kept in a dark box to minimize light interference and modified to maintain sample concentration at 37°C using a pump-fitted water bath (Grant Instruments). A concentration of 5 µmol/L of lucigenin was used in all experiments.

Fresh samples of SV or IMA transferred from the operating theatre were opened longitudinally to expose the endothelial surface and then equilibrated for 20 minutes at 37°C in 2 mL of oxygenated (95% O_2/5% CO_2) Krebs-HEPES buffer (KHB, 99 mM NaCl, 4.7 mM KCl, 1.2 mM $MgSO_4$, 1 mM KH_2PO_4, 1.9 mM $CaCl_2$, 25 mM $NaHCO_3$, 11.1 mM Glucose and 20 mM HEPES; pH-7.4). The assay was performed as follows:

First, the background measurement corresponding to the reaction vial containing the buffer (2 mL) and dark-adapted lucigenin (5 µmol/L) was recorded (Figure 2.14, Arrow 1, left green circle). This is later subtracted from the tissue reading. Then, the sample was added, allowed to equilibrate and the new signal was measured at a resting plateau (Figure 2.14, Arrow 2, right green circle). The counts detected by the luminometer are expressed as relative light units (RLU/second) normalized to tissue weight.

2.7.1.3 NADPH-stimulated/Vas2870-inhibitable $O_2^{\cdot -}$ generation measurements

After a stable resting $O_2^{\cdot -}$ generation measurement was obtained, 100 µmol of NADPH were added to the luminometer vial to estimate activity of NADPH-oxidases. Adding NADPH to the vial results in a signal spike, which eventually equilibrates to a plateau. (Figure 2.14, Arrow 3, blue circle). Both the 10 minute reading, as well as the plateau reading was obtained.

After obtaining a plateau NADPH-stimulated reading, 20 µL of Vas2870 (Enzo Life sciences) solution were added to the luminometer vial, to a final concentration of 40

µmol/L. Vas2870 is a cell-permeable and specific pan-NADPH oxidases (NOX) inhibitor. Adding Vas2870 leads to a gradual reduction in the NADPH-stimulated signal, which stabilizes to a plateau after approximately 30 min (Figure 2.14, Arrow 4, yellow circle). The new inhibited plateau signal is obtained and subtracted from the NADPH-stimulated plateau, to estimate the fraction of signal attributed to NADPH-oxidases.

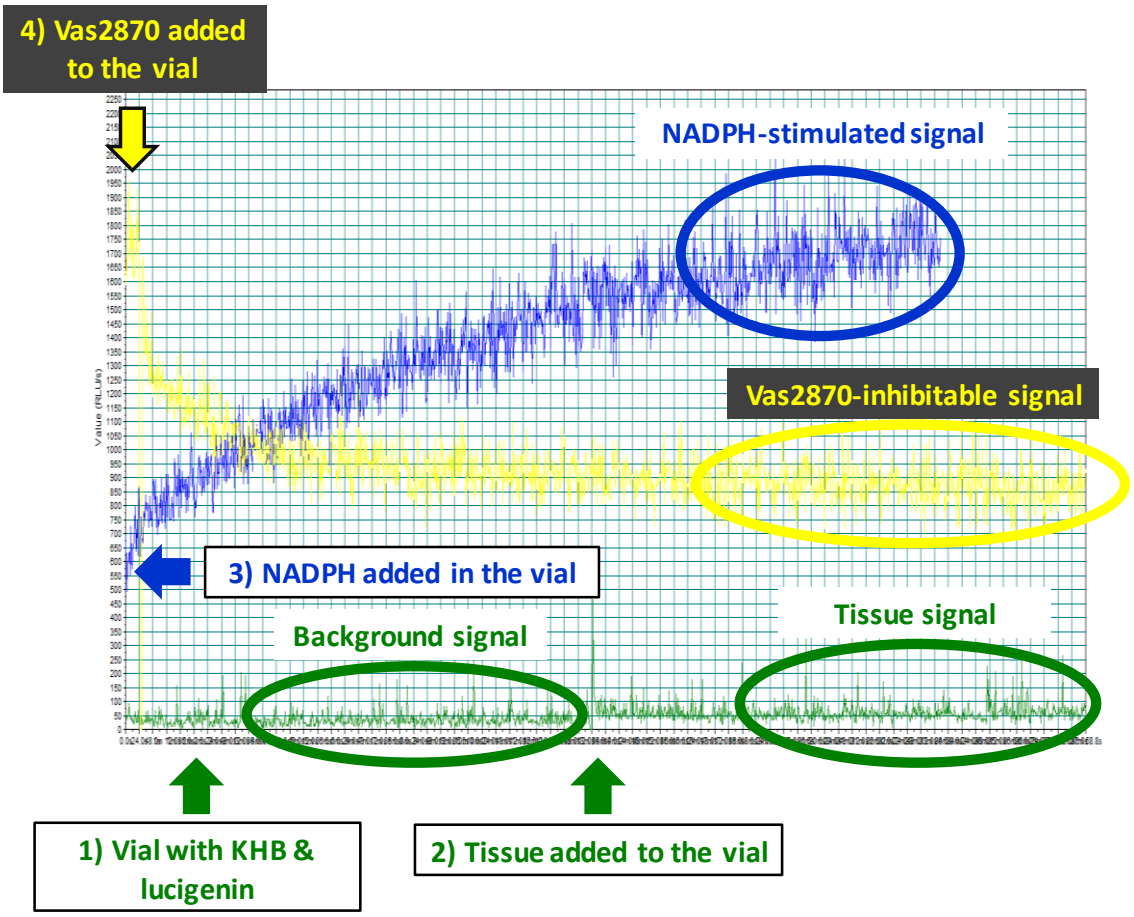


Figure 2.14: *Representative trace from a luminometry experiment. The X axis shows time (28 minutes) and Y axis shows Relative Light Units (RLUs). Whenever a full 28 min trace is acquired, the new trace starts from X=0 again, in order of green→ blue→ yellow. This means that the above experiment represents a continuous trace of a single experiment, broken down into three separate coloured lines, each accounting for 28 minutes of signal measurement by the luminometer. The numbered arrows correspond to the sequence of events. The circles indicate the traces used as final readout for every step of the experiment. First, a background signal of the vial plus KHB and lucigenin is obtained (left green circle). Then, the tissue is added in the vial and a tissue signal is obtained (right green circle). Then, in the same vial, NADPH is added and a signal is obtained (blue circle). Finally, Vas2870 is added and the readout is obtained (yellow circle).*

2.7.1.4 LNAME-inhibitable superoxide generation measurements

In the experiments presented in this thesis, N-Nitro-L-arginine methyl ester hydrochloride (L-NAME) – a nonspecific competitive NOS inhibitor - was used to estimate uncoupled eNOS, due to the ability of L-NAME to competitively block NOS in both its "coupled" and "uncoupled" functional states. A second vessel ring from the same patient was used for these experiments, in addition to the one used for resting and NADPH/Vas2870 measurements. The vessel ring was cut open longitudinally, as mentioned before, and was equilibrated for 30 minutes at 37°C in 2 mL of oxygenated KHB, with the addition of 100 µmol/L LNAME, to inhibit NOS enzymes. The background measurement corresponding to the reaction vial containing the buffer (2 mL), dark-adapted lucigenin (5 µmol/L) and 100 µmol/L LNAME was recorded. Then, the sample was transferred to the luminometer vial and allowed to reach resting plateau (Figure 2.15).

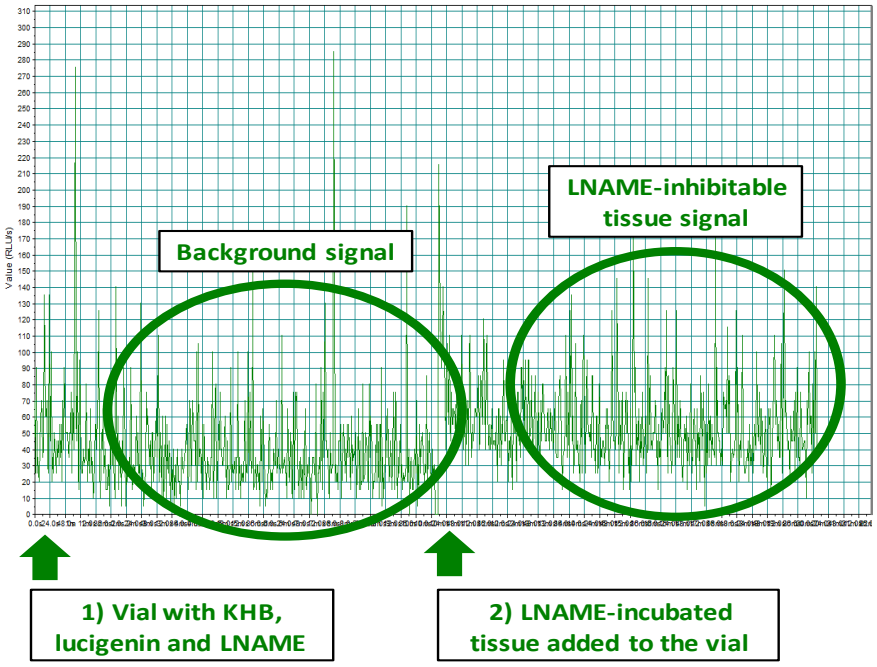


Figure 2.15: *Representative trace from a luminometry experiment. X axis represents time (28 minutes per full coloured trace) and Y axis shows Relative Light Units (RLUs). The numbered arrows correspond to the sequence of events. The circles indicate the traces used as final readout for every step of the experiment.*

The background signal was subtracted from this reading, adjusted to tissue weight, and the final reading was in turn subtracted from the resting, weight-adjusted $O_2^{\cdot -}$ reading obtained using the other vascular ring. The LNAME-inhibitable $\Delta O_2^{\cdot -}$ was thus calculated. A lower, negative value indicates that eNOS is largely uncoupled in this vascular sample, because LNAME led to an overall inhibition in superoxide generation. On the contrary, a higher, positive value indicates that eNOS is largely coupled, because inhibition of the enzyme led to an increase in superoxide generation, by reducing NO levels and thus diminishing its $O_2^{\cdot -}$-scavenging effects.

2.7.2 Dihydroethidium Staining & Confocal Microscopy

Dihydroethidium (DHE) staining is a technique used for the detection of intracellular $O_2^{\cdot -}$ generation in whole tissue samples. The principle underlying the method was believed to be the reaction of the cell-permeable dihydroethidium with $O_2^{\cdot -}$, leading to generation of ethidium which binds to nuclear DNA and exhibits red fluorescence[181]. This was detected by fluorescence microscopy and semi-quantified based on the intensity of the signal. In more recent years, however, it has been shown that DHE reacts specifically with $O_2^{\cdot -}$ to form a distinct product, 2-hydroxyethidium, whereas the ethidium that is produced from DHE is thought to arise from a variety of other reactions that reflect the total redox status of the cell[182]. Due to the fact that 2-hydroxyethidium has a different molecular weight than DHE and ethidium, HPLC can be employed to accurately detect and quantify the product, which represents the total intracellular generation of $O_2^{\cdot -}$[183].

In my thesis, in situ $O_2^{\cdot -}$ production was determined in vessel cryosections with oxidative fluorescent dye dihydroethidium (DHE) as part of *ex vivo* experiments in select patients. Serial SV and IMA rings were incubated with/without certain interventions (more details in Chapter 3), snap frozen in Optimal Cutting Temperature (OCT) Compound (VWR, USA) and kept at -80^{o}C until assaying. Cryosections (30 μm) were obtained by

using a microcryotome (-25^{o}C) housed at the Wellcome Trust Centre for Human Genetics, Old Road Campus, University of Oxford. The sections were mounted onto glass slides, marked with a PAP pen and incubated with KHB alone or KHB + LNAME (100 µmol/L to inhibit nitric oxide synthases) or KHB+Vas2870 (40 µmol/L to inhibit NADPH-oxidases) for 30 minutes at 37^{o}C. The buffer was then removed and the sections were incubated in the dark with DHE (2 µmol/L) for 5 minutes at 37^{o}C. At the end of the 5 minute incubation period, the buffer was quickly aspirated and the reaction stopped with fresh ice-cold KHB. The sections were secured with a cover slip and kept in the dark until visualisation under the microscope.

Fluorescence images of the endothelium and tunica media were obtained from each vessel quadrant by using a Zeiss LSM 510 META laser scanning confocal microscope, housed at the Wellcome Trust Centre for Human Genetics, Old Road Campus, University of Oxford. Images were obtained by using an excitation wavelength of 488 nm and an emission wavelength of 585 nm. In each case, segments of vessel rings (±L-NAME or ±Vas2870) were analysed in parallel with identical imaging parameters in a blinded fashion.

2.8 Organ bath vasomotor studies

In order to estimate endothelial function in an *ex vivo* setup, I performed organ bath vasomotor studies using SV rings from patients undergoing CABG surgery, recruited in the Oxford CABG Bioresource. The experimental premise is the ability of acetylcholine to induce endothelium-dependent NO-mediated dilatation on vascular rings.

A Radnotti double-walled 15-mL glass chamber organ bath set-up was used to perform vasomotor studies. Each experimental chamber is fitted with a thin metal hook fixed on an immobile support (Figure 2.16). A second hook is attached to a non-absorbable suture, in turn attached to a force transducer (AD Instruments). The force transducer is connected to an amplifier (Octal Bridge Amp – AD Instruments) and reader (PowerLab 8/35 – AD Instruments), which is in turn connected to a desktop computer using LabChart software (AD Instruments). Tension exerted on the force transducer is converted into an electric signal, which is translated into grams of tension by the software.

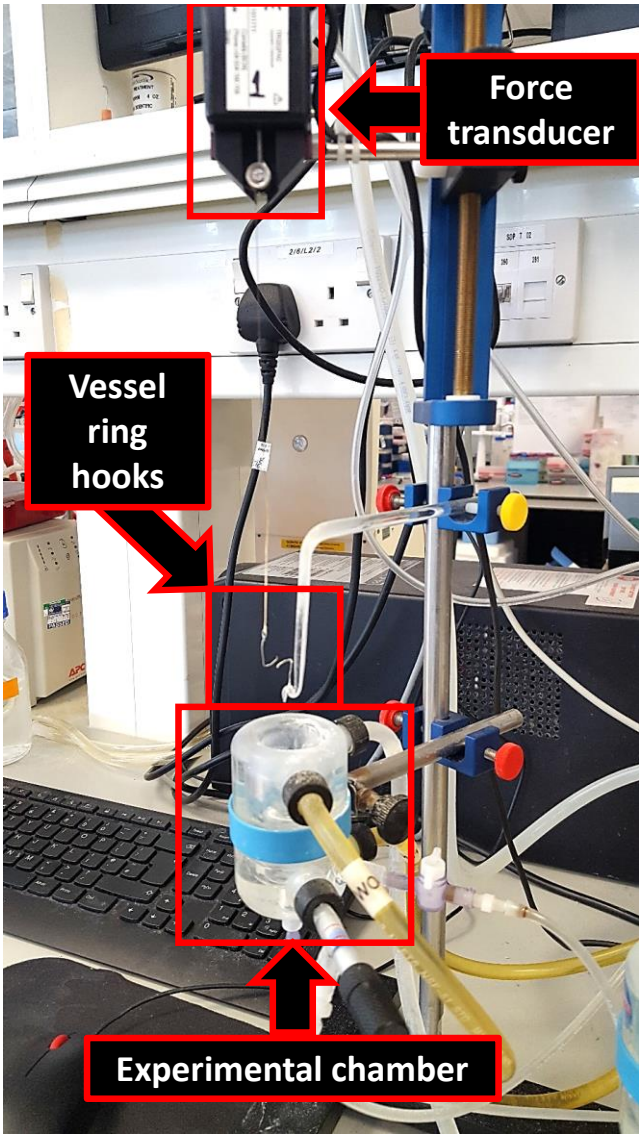


Figure 2.16: *Detail of the experimental setup used for organ bath vasomotor studies.*

For each patient, up to 4 SV rings were used. The two metal hooks shown in Figure 2.16 were sequentially inserted through the lumen of each vessel ring, applying just enough tension to secure the ring in place. The chamber was then raised, immersing the vessel in 15 mL of warm KHLB buffer. The temperature was maintained at 37°C thanks to warm water flowing through the double-walled glass chambers via a pump-fitted water bath (Grant Instruments). The buffer was oxygenated with 95% O_2/5% CO_2 via a built-in air delivery system. The KHLB buffer was stored in a water tank above the individual chambers, kept at 37°C using the same pump-fitted water bath. By opening water valves adjacent to the individual experimental chambers, the chambers can be emptied and then filled with fresh, warm KHBL, flowing down from the water tank due to a hydrostatic pressure differential. The full experimental setup is shown in Figure 2.17.

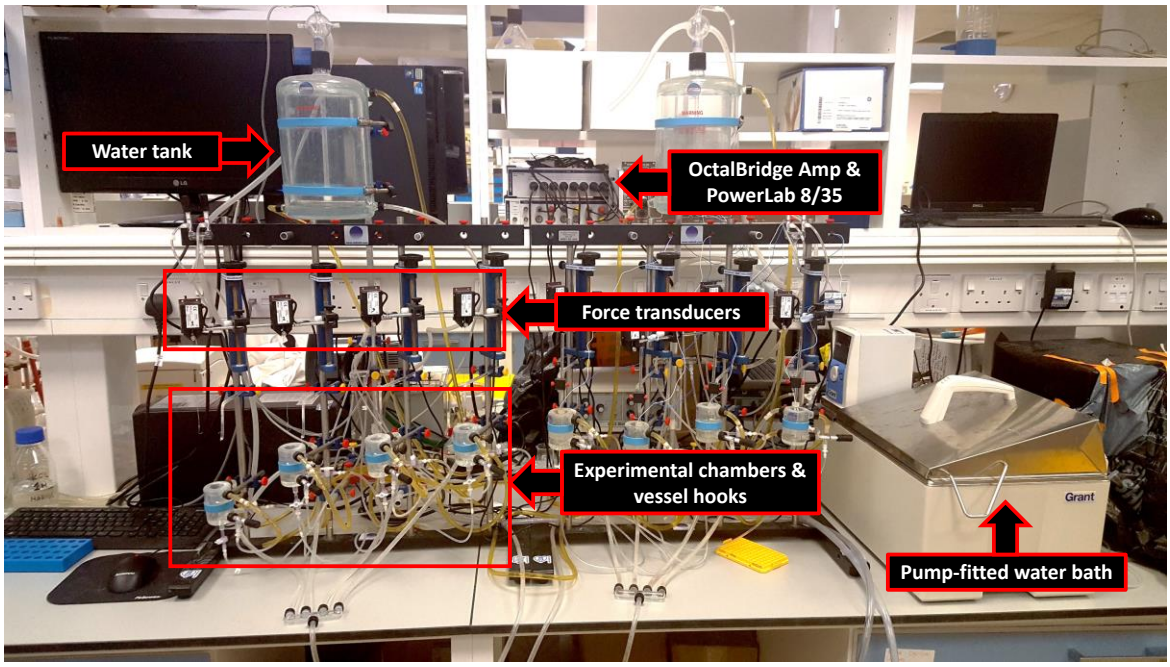


Figure 2.17: *Organ bath vasomotor study setup, located in the Division of Cardiovascular Medicine laboratory, Level 5, West Wing, John Radcliffe Hospital, Oxford. Force exerted on the vessel hooks is transmitted to the force transducer, which is connected to the OctalBridge amplifier and PowerLab 8/35 reader. This is, in turn, connected to a computer running LabChart software. Temperature is maintained via 37°C-heated water flowing from a pump-fitted water bath to the double-walled Radnotti glass chambers. The water tank contains warm KHLB, used to wash the experimental chambers after each intervention. 95% O_2/5% CO_2 is supplied via a built-in air delivery system (not pictured).*

Vessels were equilibrated at minimal tension in the organ bath for 20 minutes and then subjected to passive stretching in 1 g increments until a resting tension of 3g was achieved. Contractile responses and vessel viability were tested by exposure to potassium chloride (KCl 60 mmol/L). All vessel rings which did not respond to KCl were deemed non-viable and the experiment was aborted. SV rings which exhibited response to KCl were washed three times with buffer and allowed to return to a resting 3 g tension. A phenylephrine (PE)-induced constriction dose-response curve was created by adding increasing concentration of PE in the experimental chamber (PE, 10^{-9} M to 10^{-5} M, Figure 2.18).



Figure 2.18: *Representative LabChart file showing a phenylephrine (PE) curve obtained from 2 saphenous vein rings belonging to a patient recruited in the AdipoRedox study. The x axis represents time and the y axis vessel tension. Each vertical dotted line is a marker representing the point where increasing concentrations of PE were added to the experimental chamber. The last vertical line represents the time point where washing of the chambers with fresh buffer was performed and the vessels were allowed to return to resting tension.*

At the end of the PE curve, the vessels were washed and allowed to relax back to 3 g resting tension. They were then pre-contracted with phenylephrine ($3x10^{-6}$ M) and an endothelium-dependent relaxation curve was created by using increasing concentrations of acetylcholine (ACh, 10^{-9} M to 10^{-5} M, Figure 2.19). After the final dose of ACh was added to the organ bath chambers and a reading was obtained, the vessels were washed and allowed to equilibrate back to 3 g resting tension.

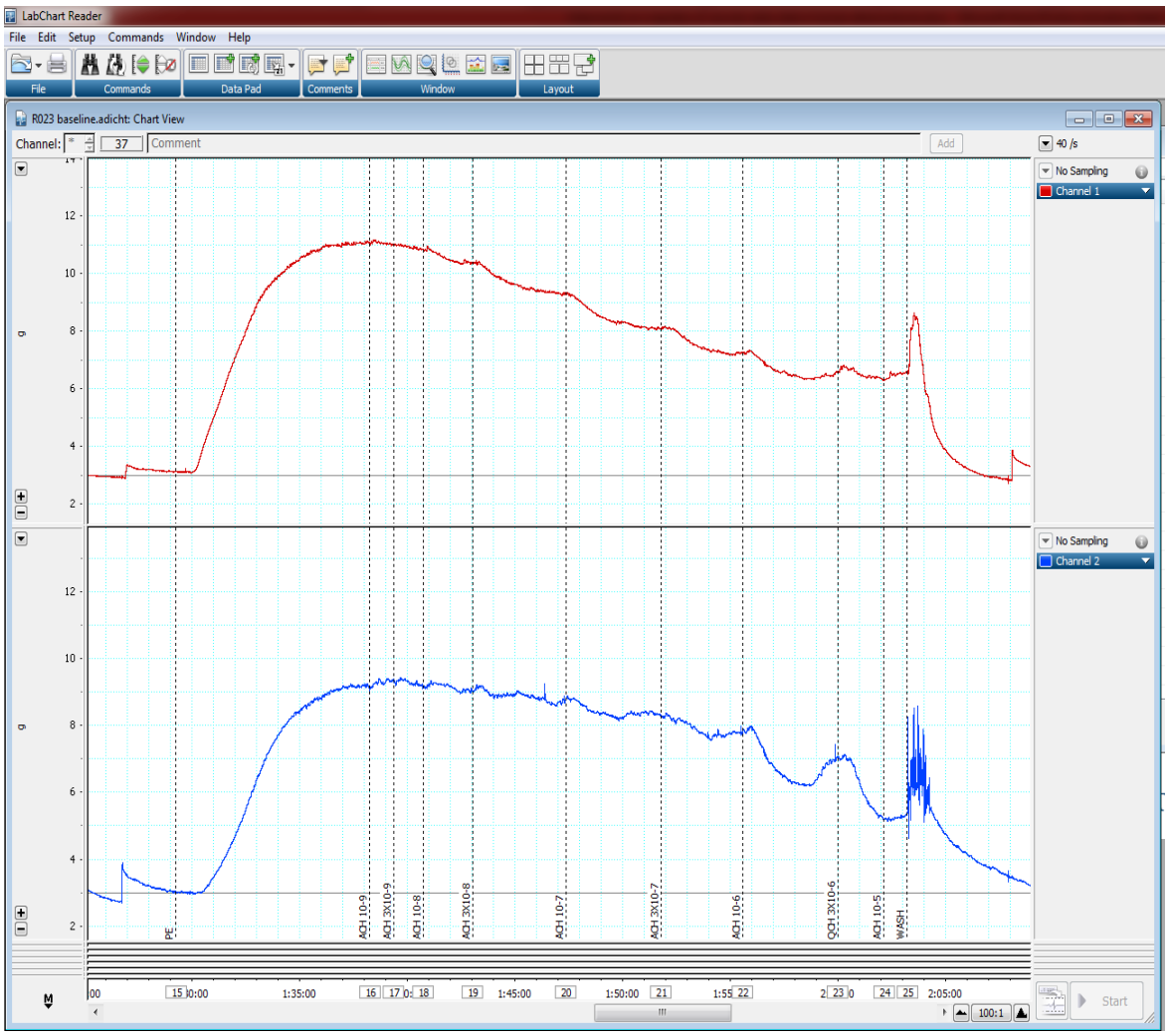


Figure 2.19: *Representative LabChart file showing an acetylcholine (ACh) curve obtained from 2 saphenous vein rings belonging to a patient recruited in the AdipoRedox study. The x axis represents time and the y axis vessel tension. The first vertical line on the left represents the time point where preconstriction with phenylephrine $3x10^{-6}$ M was initiated. Each subsequent vertical dotted line is a marker representing the point where increasing concentrations of acetylcholine were added to the experimental chamber. The last vertical line represents the time point where washing of the chambers with fresh buffer was performed and the vessels were allowed to return to resting tension.*

The vessels were pre-contracted again with phenylephrine ($3x10^{-6}$ M) and exposed to the NOS inhibitor NG-nitro-L-arginine methyl ester (L-NAME; 100 µmol/L). After an in-chamber incubation of 20 minutes, relaxations to the endothelium-independent NO donor sodium nitroprusside (SNPr, 10^{-10} M to 10^{-6} M, Figure 2.20) were evaluated. Readings were recorded using LabChart software. Vasodilatory responses were measured off-line from the LabChart file and expressed as a percentage of the preconstricted tension.

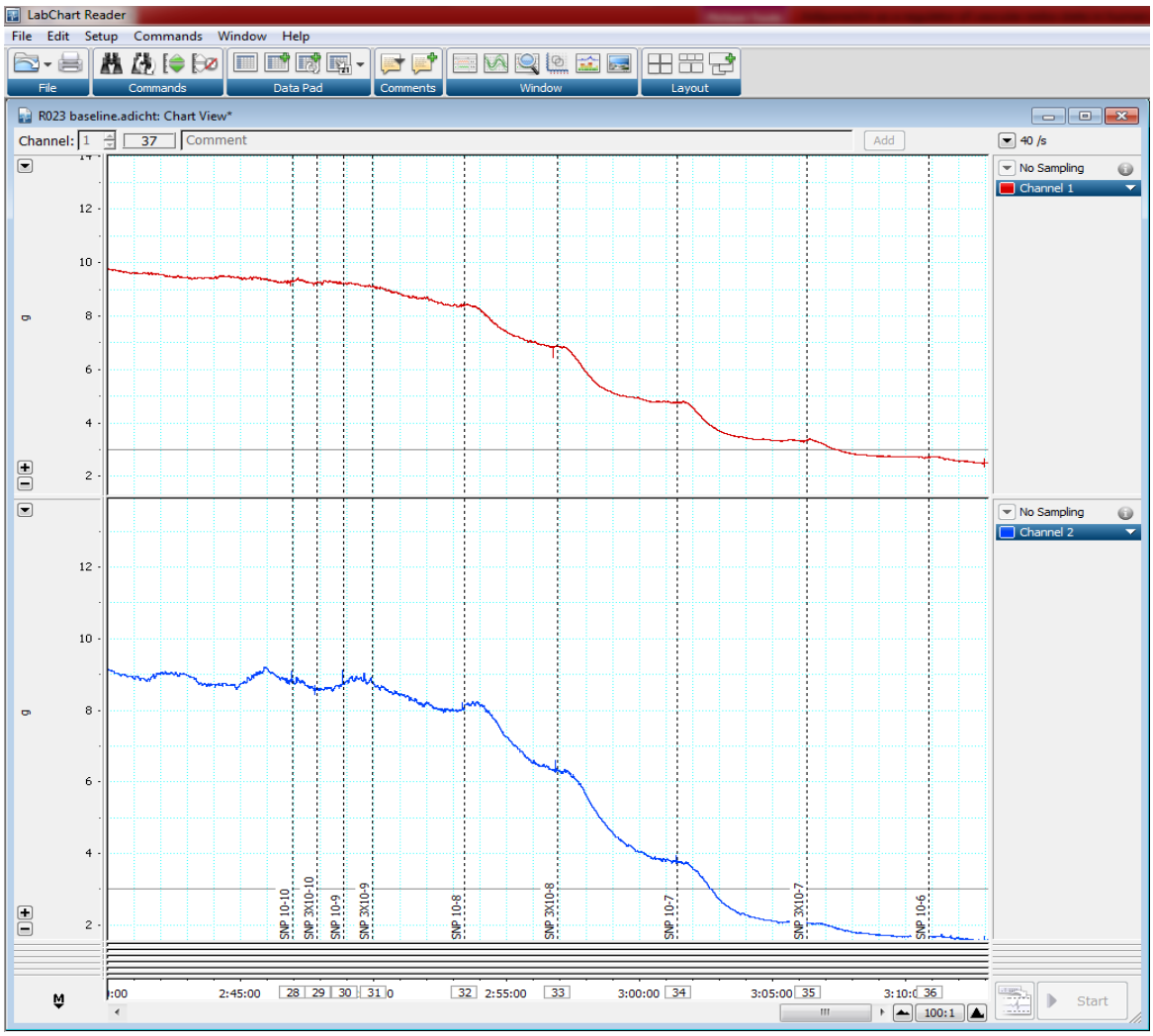


Figure 2.20: *Representative LabChart file showing a sodium nitroprusside (SNPr) curve obtained from 2 saphenous vein rings belonging to a patient recruited in the AdipoRedox study. The x axis represents time and the y axis vessel tension. The vessels were preconstricted with phenylephrine $3x10^{-6}$ M. After a stable plateau was reached, the NOS inhibitor NG-nitro-L-arginine methyl ester was added (L-NAME; 100 µmol/L). After 20 minutes, an SNPr curve was created. Each vertical dotted line is a marker representing the point where increasing concentrations of SNPr were added to the experimental chamber.*

2.9 DNA Extraction and Genotyping

2.9.1 DNA Extraction

Genomic DNA was extracted from whole blood using a commercial kit (QIAamp DNA blood Midi kit, QIAgen) following the protocol provided by the manufacturer. Briefly, K_2-EDTA anti-coagulated whole blood samples were thawed from storage. 2 mL of whole blood were mixed with 200 µL of Proteinase K (QIAgen) and 2.4 mL of buffer AL and incubated at 70^{o}C for 10 minutes. Then, 2 mL of absolute ethanol were mixed into the lysate and the samples were transferred to the QIAamp Midi columns. After sequential centrifugation and wash steps with buffers AW1 and AW2, the DNA was eluted using nuclease-free water. Quantification and quality check of DNA was performed using a Nanodrop® ND-1000 Spectrophotometer. Samples with a 260/280 ratio of less than 1.8 were re-extracted until DNA of sufficient quality was obtained. The samples were carefully plated into 96-well working plates for further experiments. The remainder of the sample was stored in barcoded cryovials at 2-8^{o}C as part of the Oxford CABG Bioresource.

2.9.2 Genotyping using TaqMan® Probes

Genotyping for single nucleotide polymorphisms (SNPs) in or near the *ADIPOQ* locus, encoding for adiponectin, was performed using ready-made TaqMan® probes (Life Technologies). The assay is based on the premise of allele-specific probe sequences carrying distinct fluorophore dyes (FAM and VIC). Homozygous individuals for either allele are expected to display an exponential increase in fluorescence over 40 PCR amplification cycles corresponding to just one of the two different fluorescent dyes. Conversely, heterozygous individuals should display an increase in the fluorescence of both dyes. This assay has significant advantages over other genotyping assays, such as

restriction fragment length polymorphisms, namely high sensitivity/specificity and a high-throughput nature, allowing a large number of samples to be assayed at the same time.

The assay was run according to manufacturer's conditions, on an ABI StepOne Plus PCR system (Figure 2.21), using blank template as negative control. More specifically, 1 µl of genomic DNA was used per reaction, mixed with 5 µl of TaqMan® Genotyping Master Mix, 0.5 µl of TaqMan® probe (x40 concentrated) and 3.5 µl of nuclease-free water. Approximately 15-20 ng/µl of genomic DNA were used per reaction. Due to the high sensitivity and specificity of the assay, the samples were run as a single reaction. Allelic discrimination was automatically performed through the StepOne Plus software built-in algorithm (Figure 2.22). Whenever a result was deemed undetermined, the assay was repeated with a higher concentration of DNA until a successful read was performed, otherwise the sample was not included in the final analysis. A list of SNPs investigated in this study and their respective TaqMan® Genotyping probes can be found in table 2.2.

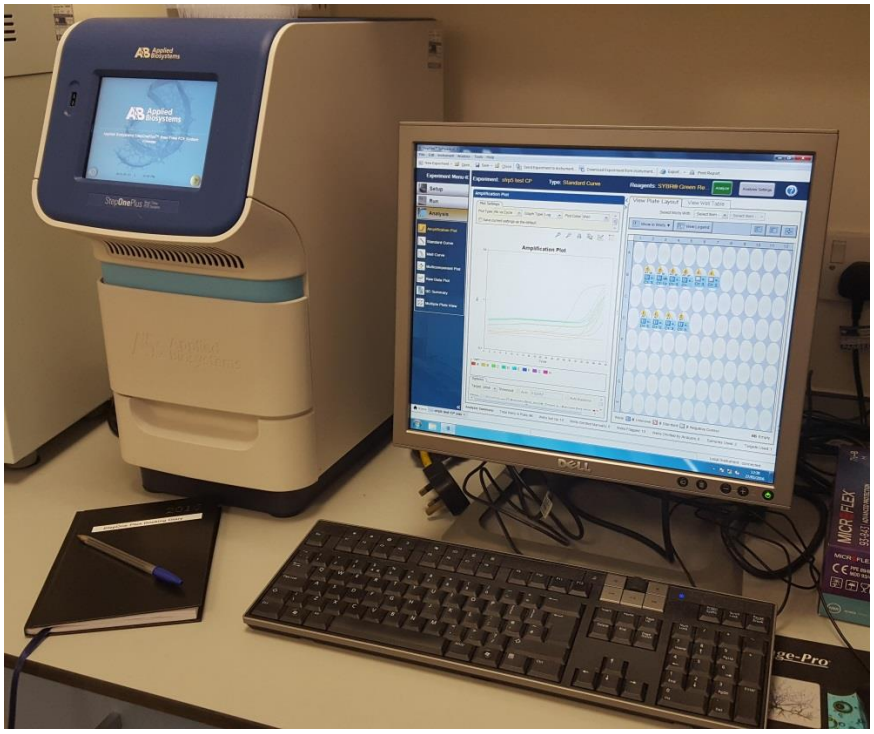


Figure 2.21: *The StepOne Plus instrument used for genotyping experiments in my thesis, housed at the Cardiovascular Medicine Lab, Level 5, West Wing, John Radcliffe Hospital.*

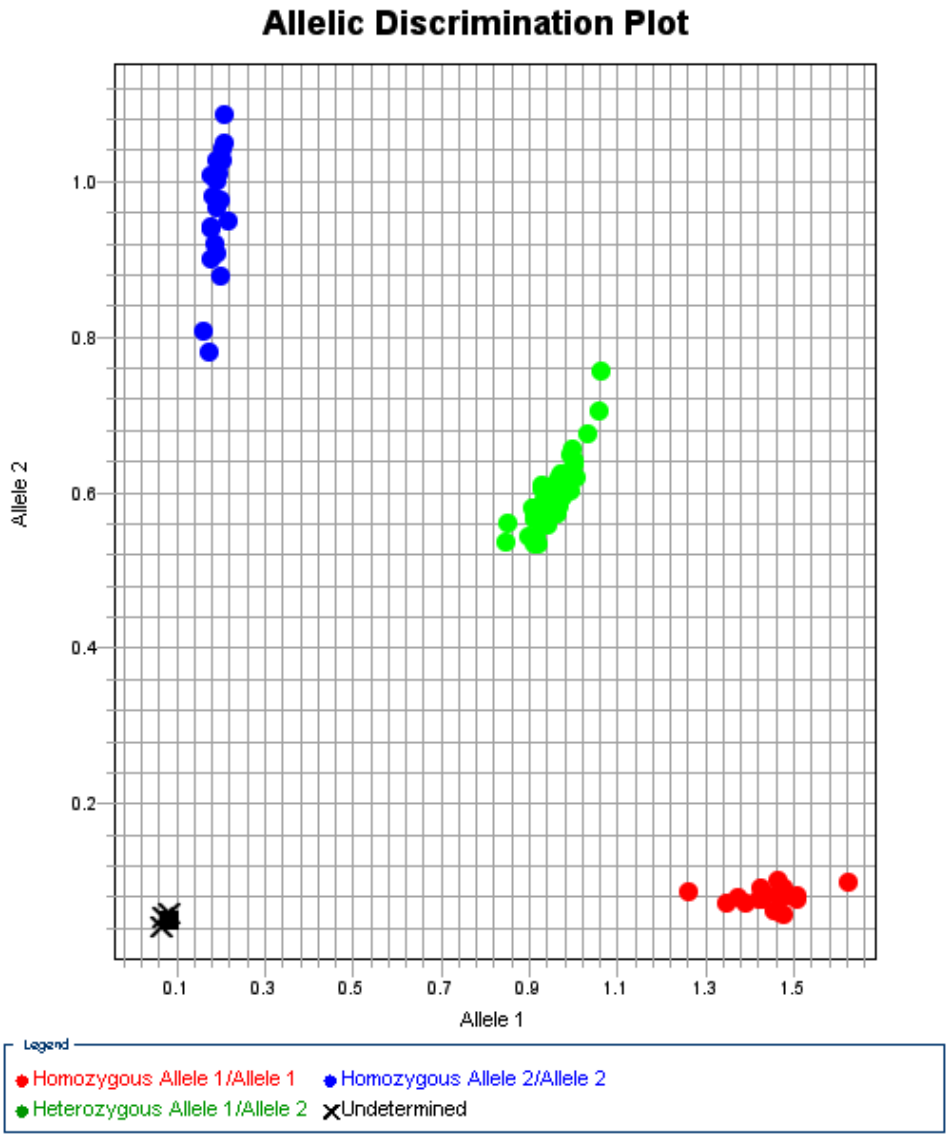


Figure 2.22: *A representative allelic discrimination plot created by StepOnePlus Software. A call for homozygosity or heterozygosity is made automatically based on the FAM or VIC relative fluorescence. Red samples are homozygous for the VIC-carrying probe, blue samples for the FAM-carrying probe, and green samples are heterozygous.*

Table 2.2 Single Nucleotide Polymorphism TaqMan® genotyping assays

Target SNP	Probe ID
rs17366568	C-33187752-10
rs266717	C-8288442-10

2.10 Gene Expression Studies

2.10.1 RNA Extraction

Samples of vascular or adipose tissue were snap frozen in 1 mL of QIAzol (QIAgen, Stanford, CA) and stored at -80^{o}C until processed. RNA was extracted by using the RNeasy Micro or Mini kit (QIAgen) depending on tissue weight. The kit is designed to extract only larger RNA molecules, generally larger than 200 nucleotides. Smaller RNA molecules (for example microRNAs) are not retained by the column silica membrane.

In brief, samples were homogenized for 1 min using a pre-cooled Polytron homogeniser (Kinematica AG). Chloroform was added (20% of QIAzol volume used, usually 200 µl for 1 mL of QIAzol), the samples were vigorously shaken by hand and allowed to rest at room temperature for 2-3 min. The samples were then spun at 13,000 rpm for 15 min, at 4^{o}C. The clear, aqueous phase containing the RNA was transferred to a separate RNAse free vial. One unit of ethanol 70% (approximately 500-700 mL, depending on the volume of the aqueous phase obtained from the previous step) was added and vigorously mixed. The sample was then passed through the RNeasy columns, following the appropriate washing steps. RNA was eluted from the column using nuclease-free water. RNA quality and quantity were determined using a Nanodrop® ND-1000 Spectrophotometer. A 260/280 ratio higher than 2.0 was achieved in more than 98.5% of the samples extracted and all samples failing to meet that threshold were either discarded or re-extracted from additional tissue samples.

2.10.2 Reverse transcription of RNA – cDNA library creation

Ribonucleic acid was reverse transcribed using the Quantitect Reverse Transcription kit (QIAgen), with the addition of the optional genomic DNA wipeout step, to eliminate any genomic DNA contamination. Up to 1 g of RNA was reverse transcribed at every

reaction and the reactions were performed in duplicate for every sample type, with the total cDNA being pooled together at the end of the reaction. Reaction conditions were as follows: 2 min at 42°C (gDNA elimination step), 30 min at 42°C (cDNA synthesis step) and finally 3 min at 95°C (reverse transcriptase inactivation step).

A cDNA library was created by diluting the cDNA sample using TE buffer (10 mmol/L Tris HCl, 1 mmol/L EDTA, pH 8.0) to a final cDNA concentration of 1.67 µg/µl. The samples were stored in deep 1.8 mL 96-well "stock" plates. Prior to freezing at -80°C, "working" plates were created, by distributing 100 µl of sample in regular V-bottom PCR plates, and stored at -20°C until further processing.

2.10.3 Gene expression studies using quantitative PCR

TaqMan® probes were used for all gene expression studies presented in this thesis. This method carries several advantages over conventional qPCR using SYBR Green. The most important is the increased specificity of the signal detected, achieved through the use of the fluorophore-binding probe, which allows specific detection of target mRNA, whereas SYBRGreen binds non-specifically to double-stranded cDNA. In addition, all TaqMan probes used in my experiments were designed to span exon junctions, thus eliminating the chance of detecting genomic DNA which might have contaminated the sample (in spite of the gDNA wipeout step during reverse transcription).

All reactions were performed in triplicate in 384-well plates, using 5 ng of cDNA per reaction (3 µl of diluted cDNA sample from the "working" plates, 3 µl of Invitrogen TaqMan® Gene Expression Master Mix and 0.3 µl of TaqMan assay probe). A standard sample was created by pooling together a small volume of undiluted sample from all samples across the cDNA library. A standard curve was created based on serial dilutions of the standard sample (1:10, 1:25, 1:100, 1:200, 1:400). The standards were run in quadruplicate. The experiments were performed on an ABI 7900HT Fast Real-Time PCR

System (Applied Biosystems) housed at the Wellcome Trust Centre for Human Genetics, Old Road Campus, University of Oxford.

The Pfaffl method[184] was used to calculate relative gene expression, with PPIA (cyclophilin) used as housekeeping gene for adipose tissue experiments and GAPDH for vascular tissue experiments. A standard curve was created by plotting log(Standard dilution) on the X axis and the Ct value of the standard samples on the Y axis (Figure 2.23). Efficiency of the reaction was calculated by using the formula E = Power(10, -1/*a*), where E is efficiency and *a* is the slope of the standard curve. If *a* is approximately equal to -3.3, then E=2, which denotes 100% efficiency (each copy of target mRNA becomes exactly 2 copies at the end of each cycle). If E=2, then the Pfaffl method yields identical results to the $2^{-\Delta\Delta CT}$ method, which is based on the assumption that efficiency is 100% for all reactions. Using inventoried TaqMan gene expression probes is generally guaranteed by Life Technologies to yield 100±10% efficiency. The experiments performed for my thesis are in keeping with this claim, as all qPCRs performed had an efficiency of >90%.

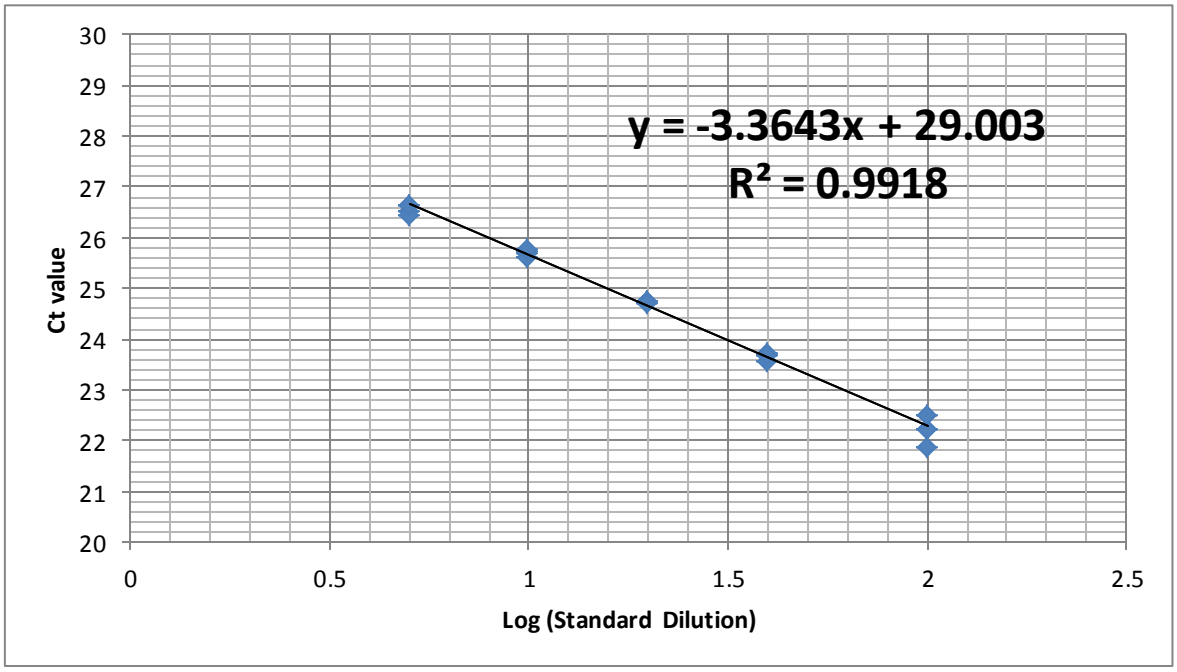


Figure 2.23: *An example of a qPCR standard curve. The efficiency for this qPCR reaction based on the curve is E= 1.98 (98%). The target gene presented in this graph was PPARγ, but similar curves were obtained for all target genes examined in my thesis.*

A list of TaqMan gene expression probes used in this thesis can be found in the table below (Table 2.3). All probes used were inventoried, "best-coverage" probes.

Table 2.3 TaqMan® gene expression probes used in this project

Target Gene	Probe ID
GAPDH	Hs02758991_g1
PPIA (Cyclophilin)	Hs04194521_s1
ADIPOQ	Hs00605917_m1
PPARG	Hs01115513_m1
CD36	Hs01567185_m1
CD68	Hs02836816_g1
CCR7	Hs01013469_m1
MRC1 (CD206)	Hs00267207_m1
IL6-R	Hs01075666_m1
ADIPOR1	Hs01114951_m1
ADIPOR2	Hs00226105_m1
NOX1	Hs01071088_m1
CYBB (NOX2)	Hs00166163_m1
NOX4	Hs01558199_m1
CYBA ($p22^{phox}$)	Hs00609145_m1
NCF1 ($p47^{phox}$)	Hs00165362_m1
NCF2 ($p67^{phox}$)	Hs01084940_m1
RAC1	Hs01588892_g1

2.11 Detection of tissue protein expression using Western immunoblotting

Protein levels were semi-quantified using Western immunoblotting analysis, which is based on protein separation using gel electrophoresis and specific binding of primary antibody directed against a target protein. All immunoblotting experiments presented in this thesis were performed on human vascular tissue homogenates.

Vascular tissue samples (15-20 mg) were homogenized for 30 seconds using a precooled electric Polytron homogenizer in 300 µl of CelLytic MT Cell Lysis Reagent containing a protease inhibitor cocktail (1 tablet in 10 mL of lysis buffer; Complete Mini EDTA-free, Roche, UK). For experiments involving detection of phosphorylated forms of proteins, a phosphatase inhibitor (PhosSTOP, 1 tablet per 10 mL buffer) was also added to the cell lysis reagent. Homogenates were spun at 13,000 rpm for 15 minutes at 4 ºC. The protein concentration of the supernatant was then measured using a commercially available bicinchoninic acid assay (BCA™ Protein Assay kit, Pierce, UK).

Mass-adjusted protein lysates (1-20 µg) were mixed with Laemmli buffer and denatured by incubation at 95°C for 5 minutes. Precast 10- or 12-well 8%, 10% or 4-20% gradient Bis-Tris/SDS gels (Thermo Scientific, UK) were positioned in a BioRad Mini-PROTEAN® Tetra electrophoresis system. An equal amount of protein lysate was loaded in every well of each precast gel. The tank was filled with MOPS (3-(N-morpholino)propanesulfonic acid) buffer and electrophoresis at 120 Volts for 1.5 hours was performed by using a BioRad PowerPac Basic. After separation, the proteins were transferred to nitrocellulose membranes (Amersham Protran 0.2 µm, GE Healthcare, UK) by using a BioRad wet transfer system (90V for >1 hour at 4°C). Presence of protein bands was confirmed with visual inspection after staining with Ponceau S. This was followed by blocking with 5% skimmed milk (Blotting grade blocking agent, BioRad). The membranes

were washed with Tris-Buffered Saline/Tween 20 buffer (TBST) and incubated overnight at 4^{o}C with a primary antibody, at the dilution recommended by the manufacturer. Either 5% skimmed milk or bovine serum albumin (BSA) was used as diluent for the primary antibody, according to the manufacturer's recommendation. A list of primary antibodies used can be found in Table 2.4. After overnight incubation, the membranes were washed three-times with TBST over 30 minutes and incubated for 1 hour with anti-IgG-horseradish-peroxidase (HRP) secondary antibody corresponding to the species source for the primary antibody (Table 2.5). After incubation, the membranes were washed with TBST. Enhanced chemifluorescence (SuperSignal® West Dura Extended Duration Substrate or SuperSignal® West Pico Chemiluminescent Substrate, Thermo Scientific, UK) was used to activate the HRP enzyme. The immunological signal was visualised by film exposure (Amersham Hyperfilm ECL, GE Healthcare) in a dark room or with a BioRad Chemidoc MP Imaging System.

For detection of phosphorylated forms of proteins, the membranes were first exposed to the anti-phospho primary antibody. After visualisation of the bands, the membranes were stripped using Restore^{TM} Western Blotting Stripping Buffer (ThermoScientific). They were then blocked with 5% milk again, incubated with anti-total protein primary antibody and visualised as above. Finally, the phospho-protein to total protein ratio was calculated based on the two protein bands obtained from the same membrane. For all other proteins, adjustments were made in relation to the house-keeping protein, GAPDH, visualised on the same membrane.

Image analysis was performed using the open source image processing software Image J.

Table 2.4 Primary immunoblotting antibodies used in this project

Target	Manufacturer	Source Species	Catalogue no.
Total eNOS	BD Biosciences	Mouse	610297
Phospho-eNOS (Ser1177)	Cell Signaling	Rabbit	#9570
Total Akt	Cell Signaling	Rabbit	#4691
Phospho-Akt (Ser473)	Cell Signaling	Rabbit	#9271
Total AMPKα	Cell Signaling	Rabbit	#2532
Phospho-AMPK α (Thr172)	Cell Signaling	Rabbit	#2535
4-HNE protein adducts	R&D Systems	Mouse	MAB3249
MDA protein adducts	Abcam	Rabbit	ab27642
Rac1	Merck-Millipore	Mouse	05-389
NOX1	Abcam	Rabbit	ab55831
NOX2	MyBioSource	Rabbit	MBS153418
NOX4	Abcam	Rabbit	ab109225
$p47^{phox}$	Cell Signaling	Rabbit	#4312
$p67^{phox}$	Cell Signaling	Rabbit	#3923
$p22^{phox}$	Santa Cruz Biotechnology	Rabbit	sc-20781
GAPDH (HRP-conjugated)	Sigma-Aldrich	Mouse	G9295

Table 2.5 Secondary (HRP-conjugated) antibodies used in this project

Target	Manufacturer	Source Species	Catalogue no.
Anti-Rabbit IgG	Sigma-Aldrich	Goat	A6154
Anti-Mouse IgG	Sigma-Aldrich	Rabbit	A9044

2.12 Extraction of membrane-bound proteins and estimation of Rac1 translocation

As mentioned in Chapter 1, Rac1 is a small GTP-ase and a subunit of NADPH-oxidase complexes NOX1 and NOX2. Rac1 activation and translocation to the membrane is necessary for production of $O_2^{\cdot -}$ radicals from these isoforms of the enzyme. In order to establish the effects of adiponectin on Rac1-incorporating NADPH-oxidases activity, I needed to estimate the translocation of Rac1 to the cellular membrane in vascular samples. To achieve this, I used differential centrifugation to isolate membrane proteins as described below. Vascular samples were homogenized in ice-cold HEPES buffer (20 mmol/L HEPES, 150 mmol/L NaCl, and 1 mmol/L EDTA, pH 7.4), to which 1 tablet of protease inhibitor cocktail per 10 mL of buffer (Roche, UK) was added just before homogenization. Cell nuclei and unbroken cells were removed by centrifugation of the homogenates at 2.800 g at 4°C for 20 min.

The supernatants were further centrifuged at 100.000 g for 60 min at 4°C to separate the membrane proteins using an OptimaMAX XP ultracentrifuge (Beckman Coulter). The pellets, which contained the membrane protein fraction, were re-suspended in HEPES buffer containing 1% Triton for 20 min on ice and used for the measurement of membrane-translocated Rac-1 protein by Western immunoblotting, as described in paragraph 2.11.

2.13 Rac1 activation assay

In order to estimate Rac1 activation in vascular samples, I performed a commercially available affinity precipitation assay using the PAK1-PBD conjugated glutathione agarose beads, according to the manufacturer's instructions (Millipore, Temecula, USA). The rationale behind this method is as follows. The PAK1-PBD beads selectively bind to the active form of GTP-ase proteins, such as activated Rac1. By adding the beads to a vascular lysate, incubating and centrifuging, the activated GTP-ases are pulled down in the pellet. After eluting the bead-bound proteins in LaemmLi buffer and separating them using gel electrophoresis, western blotting is performed to semi-quantify the GTP-ase in question, in this case Rac1.

For the experiments presented in my thesis, vascular samples were homogenized on ice in 500 µL of lysis buffer. Positive controls were created by incubating a small volume of pooled sample with GTP for 30 minutes, according to the protocol provided by Millipore. Similarly, negative controls were created by incubating a small volume of pooled sample with GDP for 30 minutes. After a pre-clearing step with glutathione beads, pull-down of GTP-bound Rac1 was performed by incubating tissue lysates (100 µg) with GST fusion protein corresponding to the p21-binding domain of PAK-1 bound to glutathione-agarose for 1 h at 4°C. The beads were washed three times with lysis buffer, and the protein bound to the beads was eluted with LaemmLi buffer and analyzed for the amount of GTP-bound Rac1 by immunoblotting using a Rac1 monoclonal antibody (Millipore, USA). Rac1 activation was defined as the ratio of GTP-Rac1/total Rac1. Total Rac1 was measured in whole samples from the same subjects by Western immunoblotting, as described in paragraph 2.11.

2.14 Statistical analysis

In all experiments presented in the following chapters, continuous variables were tested for normal distribution using the Kolmogorov-Smirnov test. Non-normally distributed variables were log-transformed for analysis and are presented as median [25^{th}-75^{th} percentile] or on log-transformed scale. Normally distributed variables are presented as mean ± SEM.

In the clinical association studies, continuous variables between 3 groups were compared by using one-way ANOVA followed by Bonferoni post-hoc test for individual comparisons, while comparisons between 2 groups were performed by unpaired t-tests. Categorical variables were compared by using χ^2 test, as appropriate. Correlations between continuous variables were assessed by using bivariate analysis, and Pearson's coefficient was estimated. Whenever a non-normally distributed variable failed to normalise after log-transformation, non-parametric analysis was used and Spearman's coefficient was estimated.

For all *ex vivo* experiments where paired samples were used, Wilcoxon's signed rank and paired Student's t-test were used for individual comparisons between groups. Whenever more than one comparison was made, Bonferoni post-hoc correction was performed.

Power calculations and specific tests used are presented in a separate statistical analysis section in each chapter. All statistical tests were performed by using SPSS v20.0 (IBM Analytics). $P<0.05$ was considered statistically significant.

2.15 Personal contribution

All experiments presented in my thesis were performed on human clinical samples obtained from patients undergoing coronary artery bypass graft (CABG) surgery or valve surgery. Routine experiments (vascular superoxide measurements, organ bath vasomotor studies, adipose tissue explant cultures) performed on fresh human tissue from patients belonging to **Phase I** (2004-2011) of the Oxford CABG Bioresource were not performed by me. However, additional experiments on frozen/preserved samples from Phase I patients (genotyping, RNA extraction from adipose/vascular tissue and gene expression studies) were performed by me at the University of Oxford Cardiovascular Medicine Division laboratory, level 5, West Wing, John Radcliffe Hospital, Oxford. Routine experiments performed on fresh human tissue (vascular luminometry experiments, organ bath vasomotor studies, adipose tissue explant cultures) from patients belonging to **Phase II** (2011-2015) were performed by me at the same laboratory. All *ex vivo* tissue incubations and laboratory experiments associated with them that are presented in this thesis were performed by me, using fresh vascular and adipose tissue samples collected from Phase II patients (AdipoRedox study). Pre-operative echo measurements, including FMD of the brachial artery, were performed by Dr. Alexios Antonopoulos and Miss Laura Herdmann. DNA extractions and ELISAs were performed by Dr Alexios Antonopoulos.

Chapter 3
Adiponectin and human vascular redox state

Chapter 3 outlines the observations in the clinical cohort regarding the effects of adiponectin on vascular redox state and endothelial function, and presents the mechanistic results obtained by using an *ex vivo* human tissue model.

3.1 Introduction

As mentioned in Chapter 1, experimental studies in cell cultures and animal models suggest that adiponectin improves endothelial function by stimulating nitric oxide (NO) production.[126] This is believed to be due to endothelial NO synthase (eNOS) activation through AMPK and PI3K/Akt-mediated phosphorylation.[128,130] However, under conditions of increased vascular oxidative stress, such as those observed in human atherosclerosis, eNOS is "uncoupled" mostly due to oxidation of its co-factor tetrahydrobiopterin (BH4) and produces superoxide radicals ($O_2^{\cdot -}$) instead of NO.[185-187] In this biological setting, activation of eNOS by adiponectin may increase $O_2^{\cdot -}$ generation from uncoupled eNOS[188] if there is no parallel increase of vascular BH4. The effects of adiponectin on NADPH-oxidases activity and the subsequent impact on BH4 bioavailability have not been investigated before.

3.2 Study population - Methods

Sample collection, flow-mediated dilatation of the brachial artery measurements, vascular superoxide measurements, vasomotor studies, biomarker measurements, Western immunoblotting and genotyping were performed as described in the Methods chapter. Additional techniques used in this chapter only are presented below. The clinical cohort in this chapter corresponds to the entire population of Phase I of the Oxford CABG

Bioresource. *Ex vivo* study samples were obtained from patients recruited as part of the AdipoRedox study in Oxford. Demographic characteristics and medication profile can be found in Table 3.1.

Table 3.1 Demographic characteristics of study participants

	Clinical Cohort	***Ex vivo* studies**
Participants (n)	677	46
Age (years)	66.1±0.3	63.2±1.5
Males gender (%)	563 (83)	35 (78)
Hypertension, n (%)	465 (68)	36 (80)
Hyperlipidaemia, n (%)	433 (64)	22 (49)
Diabetes mellitus, n (%)	221 (33)	12 (27)
Smoking (active/ex), n (%)	161/325 (24/48)	8/20 (18/44)
BMI (Kg/m^2)	27.6±0.17	29.3±0.72
Cholesterol (mg/dl)	177.7±2.0	155.8±16.3
HDL (mg/dl)	38.6±0.5	36.3±3.9
Triglycerides (mg/dl)	124 [94-166]	107 [56-128]
Serum adiponectin (µg/ml)	10.1 [1.2-28.7]	-
Medication (%)		
ACEi/ARBs	65	62
Beta blockers	73	71
Aspirin/clopidogrel	80	95
Statins	76	79
CCBs	32	24
Metformin/Oral hypoglycaemics	33	27
Insulin	16	12

BMI: Body mass index; ACEi: Angiotensin converting enzyme inhibitors; ARBs: Angiotensin receptor blockers; CCBs: Calcium channel blockers. Values are expressed as mean ± SEM or median [25^{th}-75^{th} percentiles].

3.2.1 Vascular biopterin measurements

BH4, BH2 and biopterin (B) levels in vascular tissue were determined by HPLC followed by electrochemical (for BH4) and fluorescent (for BH2 and B) detection.

Vascular rings of SV and IMAs were snap-frozen and stored at -80°C until assayed. To measure biopterins, these vessel rings were subjected to 3 freeze/thaw cycles in re-suspension buffer (50 mM phosphate buffered saline, 1 mM Dithioerythritol (DTE), 1mM EDTA, pH 7.4), and centrifuged for 15 min at 13,000 rpm at 4°C. The vascular supernatants were transferred to new, cooled micro tubes and precipitated with cold H3PO41M, trichloroacetic acid (TCA) 2M and DTE 1mM. Samples were vigorously mixed and then centrifuged for 15 min at 13,000 rpm, 4°C.

Samples were injected onto an isocratic HPLC system and quantified using sequential electrochemical (Coulochem III, ESA Inc., UK) and fluorescence (Jasco, UK) detection. The setup can be seen in figure 3.1. HPLC separation was performed using a 250 mm, ACE C-18 column (Hichrom, UK) and mobile phase comprising 50 mM sodium acetate, 5 mM citric acid, 48 µM EDTA, and 160 µM DTE (pH=5.2) (ultrapure electrochemical HPLC grade) at a flow rate of 1.3 ml/min. BH4 was measured directly by the electrochemical detector (background



Figure 3.1: *The HPLC system used in the biopterin experiment measurements, housed at the Wellcome Trust Centre for Human Genetics, Old Road Campus, University of Oxford.*

currents of +500 nA and -50 nA were used for the detection of BH4 on electrochemical cells E1 and E2, respectively). 7,8-BH2 and biopterin were measured as separate chromatographic picks, in the same sample using a Jasco FP2020 fluorescence detector, serially connected to the electrochemical detector. Quantification of BH4, 7,8-BH2 and B was by comparison with external standards. The standards (1 nmol/L – 1 µmol/L) were prepared from a stock solution containing authentic 10 µmol/L BH4, 7,8-BH2 and B (Schircks, Zurich) in ice-cold re-suspension buffer. All samples were loaded in the HPLC auto-sampler in random coded batches (of up to 24 samples), blinded to the group identity of each sample. Similarly, all analytical processing to determine biopterin levels was performed blinded to the sample identity. Each batch was run with an individual standard curve for BH4, BH2 and B. Representative pictures from the top standard peaks are shown in Figures 3.2 & 3.3. Biopterin levels were expressed as pmol/g of vascular tissue.

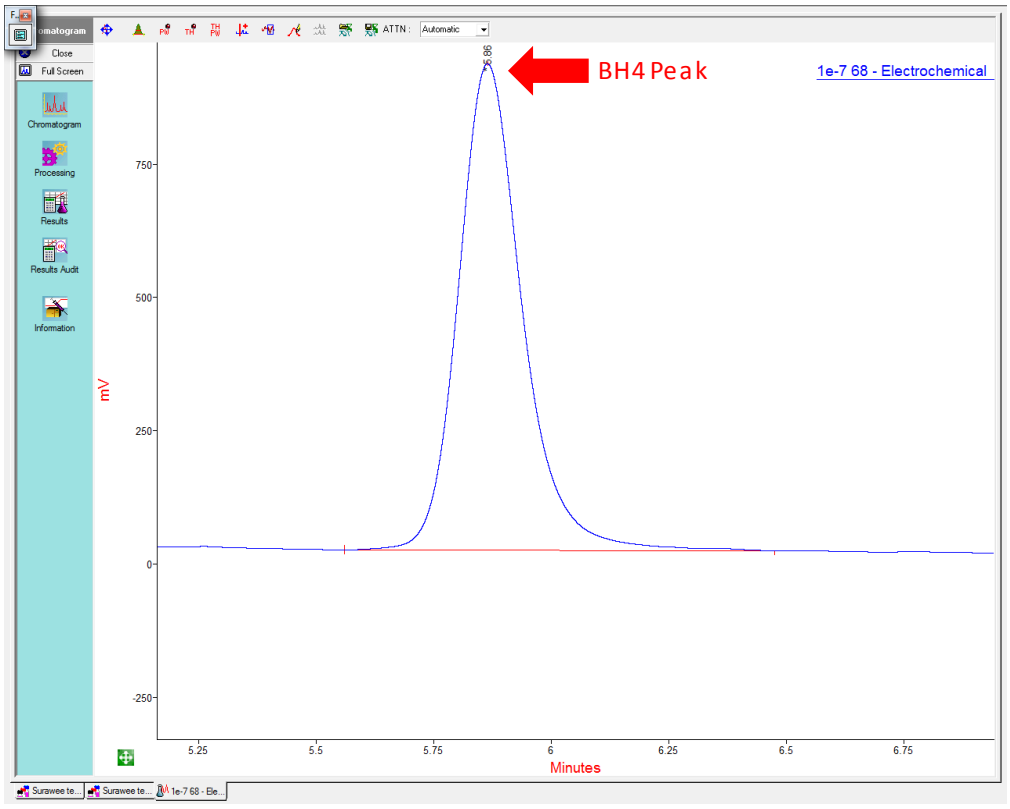


Figure 3.2: *Measurement of biopterins using HPLC. Representative figure showing the tetrahydrobiopterin (BH4) peak of the highest standard used in the experiment (electrochemical detection).*

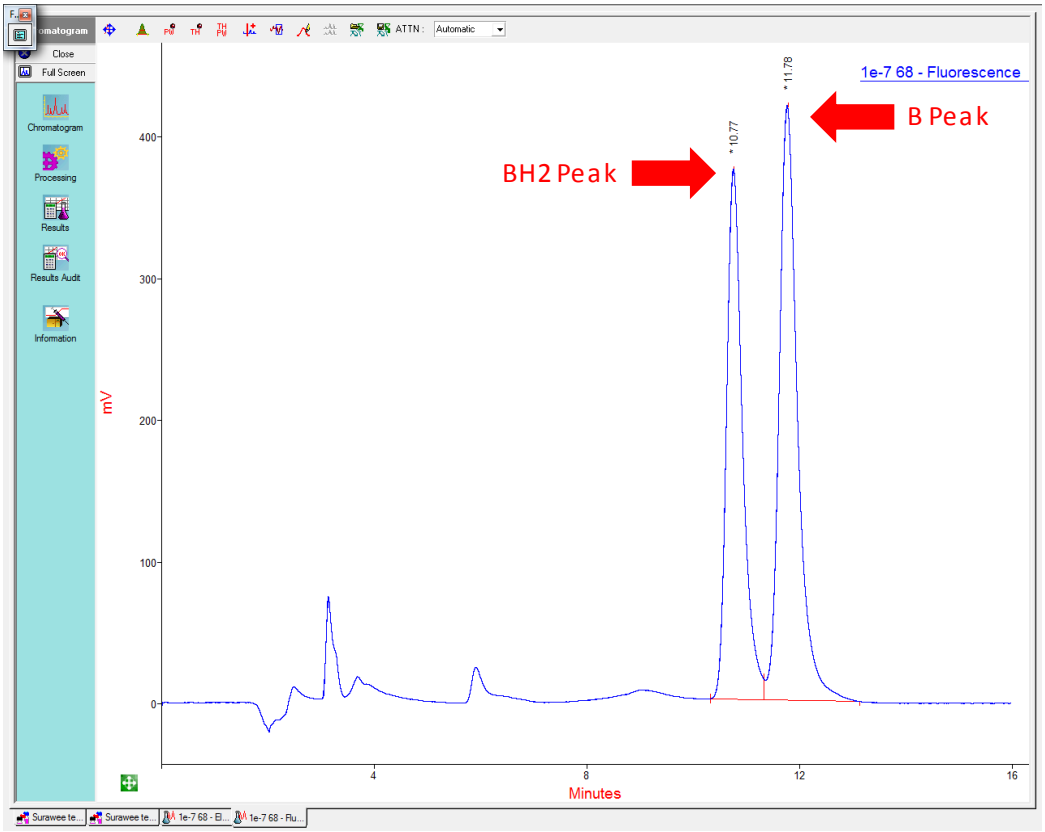


Figure 3.3: *Measurement of biopterins using HPLC. Representative figure showing the 7,8-dihydrobiopterin (BH2) and biopterin (B) peaks of the highest standard used in the experiment (fluorescent detection).*

3.2.2 Statistical analysis

Sample size calculations were based on previous data from my laboratory. For the clinical studies it was estimated that a total number of 500 subjects would allow detection of a 2.38 absolute difference in FMD between the highest and the lowest tertile of circulating adiponectin with α=0.05, power 0.9 and assumed SD 2.3. For the *ex vivo* experiments, sample size calculations were performed based on previous experience on this model,[189] and estimated that with a minimum of 5 pairs of samples (serial rings from the same vessel) I would be able to identify a change of $\log(O_2^{\cdot-})$ by 0.48 with α=0.05, power 0.9 and SD for a difference in the response of the pairs of 0.25.

Continuous variables were tested for normal distribution using the Kolmogorov-Smirnov test. Non-normally distributed variables were log-transformed for analysis and

are presented as median [25^{th}-75^{th} percentile] or on log-transformed scale. Normally distributed variables are presented as mean ± SEM.

In the clinical studies, continuous variables between 3 groups were compared by using one-way ANOVA followed by Bonferoni post-hoc test for individual comparisons, while comparisons between 2 groups were performed by unpaired t-test. Categorical variables were compared by using χ^2 test, as appropriate. Correlations between continuous variables were assessed by using bivariate analysis, and Pearson's coefficient was estimated. For the organ bath experiments, the effect of "serum adiponectin tertile" on vasorelaxations in response to acetylcholine (ACh) was evaluated by using two-way ANOVA for repeated measures (examining the effect of "ACh or SNPr concentration" x "serum adiponectin tertile or genotype" interaction on "vasorelaxations"), in a full factorial model. Linear regression was performed by using FMD or log(vascular $O_2^{\cdot -}$) as dependent variables, and as independent variables, log(serum adiponectin) and those of the clinical demographic characteristics (age, gender, diabetes, smoking, dyslipidemia, hypertension) that showed a simple association with the dependent variable at the level of 15%. A backward elimination procedure was then used by having p=0.1 as threshold to remove a variable from the respective model.

For the *ex vivo* experiments where serial rings from the same vessel were incubated with multiple interventions, repeated measures ANOVA was performed, as well as paired t-test for individual comparisons, followed by Bonferoni post-hoc correction for multiple testing as appropriate.

All statistical tests were performed by using SPSS v20.0 and $P<0.05$ was considered statistically significant.

3.3 Results

3.3.1 Adiponectin in the circulation and its role in vascular physiology

In the first part of my project, I measured circulating adiponectin in the blood samples stored from subjects enrolled in Phase I of the Oxford CABG Bioresource and identified associations between levels of the hormone in the bloodstream and vascular phenotypic markers.

3.3.1.1 Circulating adiponectin and NO-mediated vasorelaxation in human vessels

I first examined the association between serum adiponectin and endothelial function, as evaluated both *in vivo* by estimating the flow-mediated dilatation (FMD) of the brachial artery FMD, as well as *ex vivo* by estimating the responses of SV rings to acetylcholine (ACh) in an organ bath setting. There was a significant positive association between levels of serum adiponectin and higher FMD of the brachial artery (Figure 3.4, Panel A). On the other hand, there were no associations between adiponectin levels in the circulation and endothelium independent dilatation of the brachial artery (Figure 3.4, Panel B).

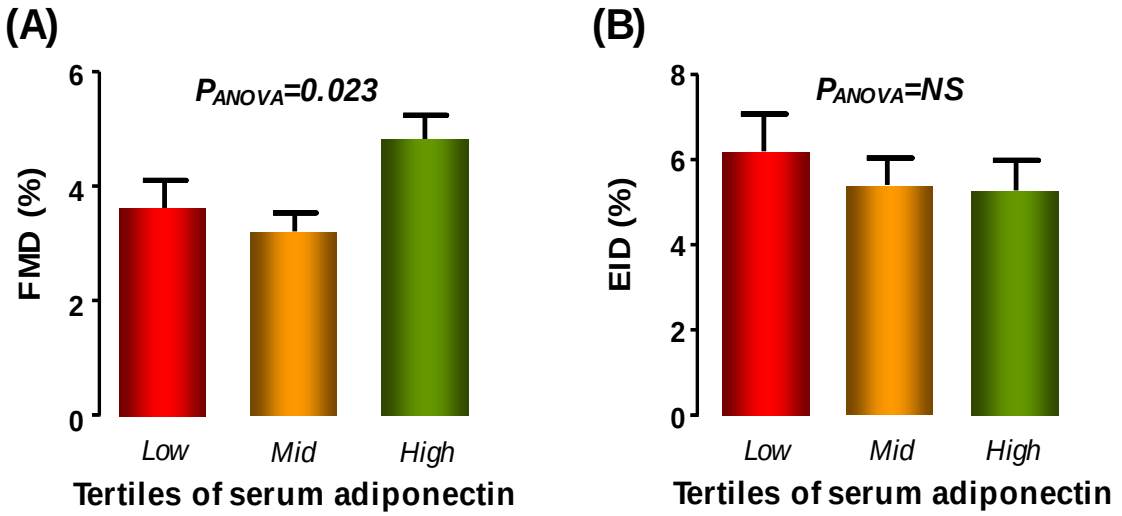


Figure 3.4: *Flow mediated dilation (FMD) was higher in patients with elevated circulating adiponectin (A), but endothelium independent dilation (EID) was not related with circulating adiponectin (B) in n=230 subjects of Phase I of the Oxford CABG Bioresource. Values are expressed as mean ± SEM.* ***(Margaritis et al. Circulation 2013;127(22):2209-21)***

In multivariable analysis, the independent predictors of FMD were: log(serum adiponectin) (β(SE): 1.75(0.69), P=0.012), hypertension (β(SE): -2.16(0.47), P=0.0001) and smoking (β(SE):-1.51(0.31), P=0.0001).

These findings were confirmed in organ bath vasomotor studies performed routinely on SV segments obtained from patients undergoing bypass surgery. The vasorelaxation responses of SV segments after treatment with increasing concentrations of acetylcholine (ACh) were significantly greater in vessels from patients in the highest tertile of circulating adiponectin compared to patients in the lowest tertile (Figure 3.5, Panel A). Similarly to the FMD/EID observations, there were no associations between circulating adiponectin and vasorelaxations of SVs in response to sodium nitroprusside (SNPr) *ex vivo* (Figure 3.5, Panel B). These findings suggest that high levels of adiponectin in the circulation could potentially be causally linked to improved endothelial function in the human vascular wall, although they do not provide proof of causality *per se*.

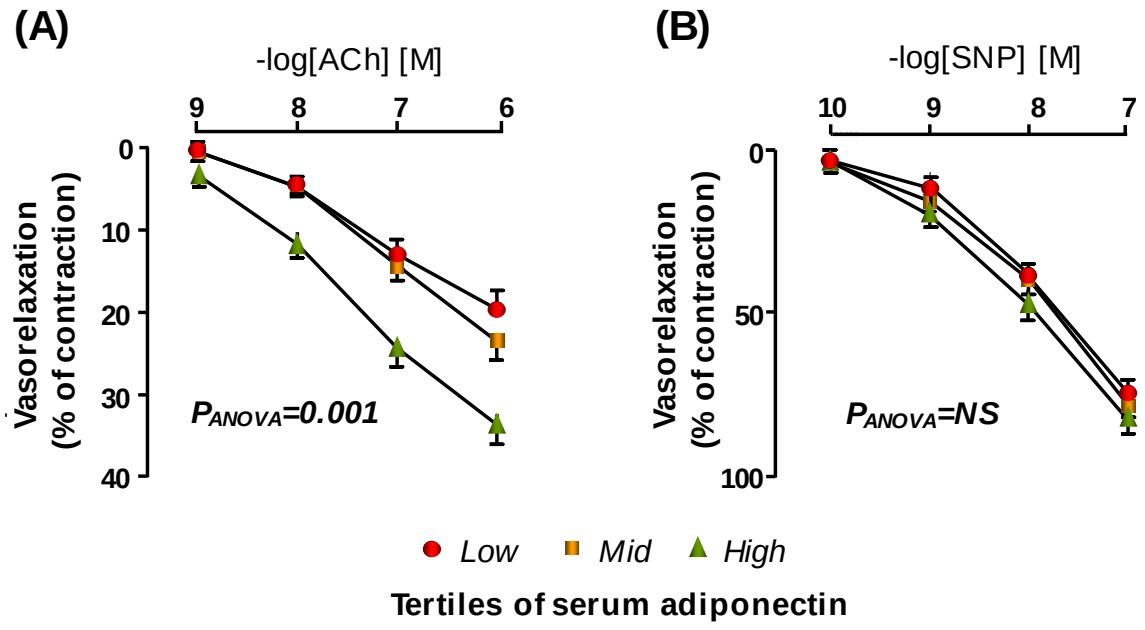


Figure 3.5: *High levels of serum adiponectin were positively associated with improved acetylcholine (ACh)-induced vasorelaxation of SV rings obtained from patients undergoing CABG (A, n=230). On the contrary, endothelium-independent vasorelaxation as a response to sodium-nitroprusside (SNPr) was not related to adiponectin levels in the circulation (B). Values are expressed as mean ± SEM* ***(Margaritis et al. Circulation 2013;127(22):2209-21)***

3.3.1.2 Circulating adiponectin and vascular superoxide generation

Following the previous observations, I then examined whether serum levels of adiponectin were related to vascular $O_2^{\cdot -}$ generation in human internal mammary arteries and saphenous veins. I found that circulating adiponectin was closely related with basal $O_2^{\cdot -}$ generation in both vessel types, as measured by lucigenin-enhanced chemiluminescence (Figure 3.6, Panel A for SVs and Panel B for IMAs).

In multivariable analysis, the independent predictors of $\log(O_2^{\cdot -})$ in SV were log(circulating adiponectin) (β(SE):-0.2984(0.06), P=0.0001), smoking (β(SE):0.068 (0.024), P=0.005) and treatment with statins (β(SE):-0.219(0.044), P=0.0001). Similarly, the independent predictors of $\log(O_2^{\cdot -})$ in IMAs were log(circulating adiponectin) (β(SE):-0.265(0.077), P=0.001), statin treatment (β(SE):-0.199(0.061), P=0.001), diabetes (β(SE): 0.112(0.047), P=0.019) and smoking (β(SE):0.053 (0.032), P=0.097).

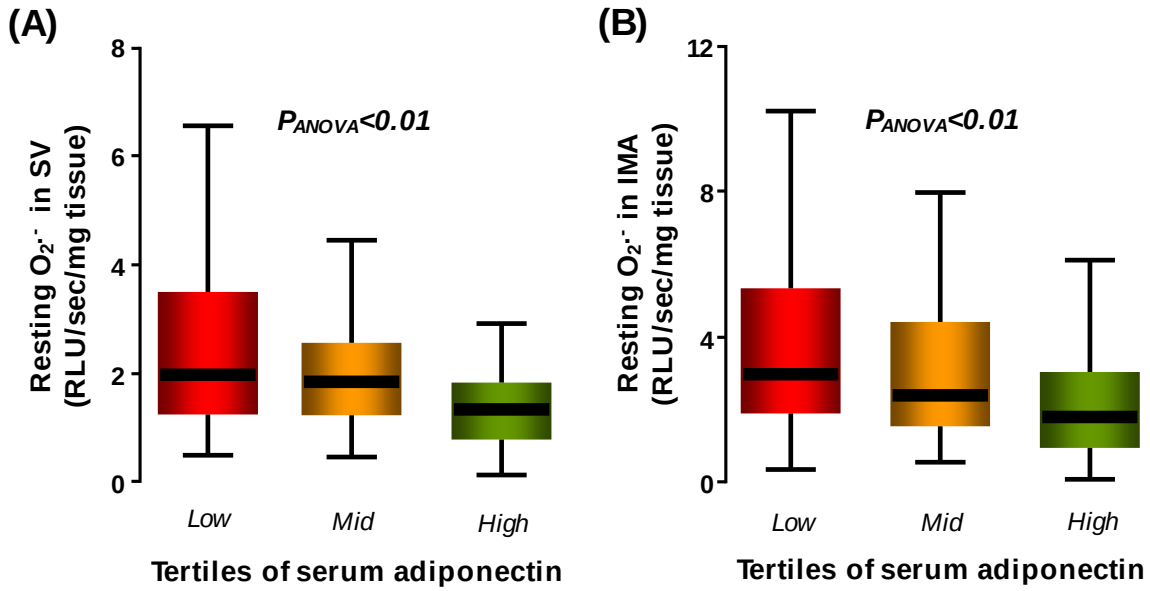
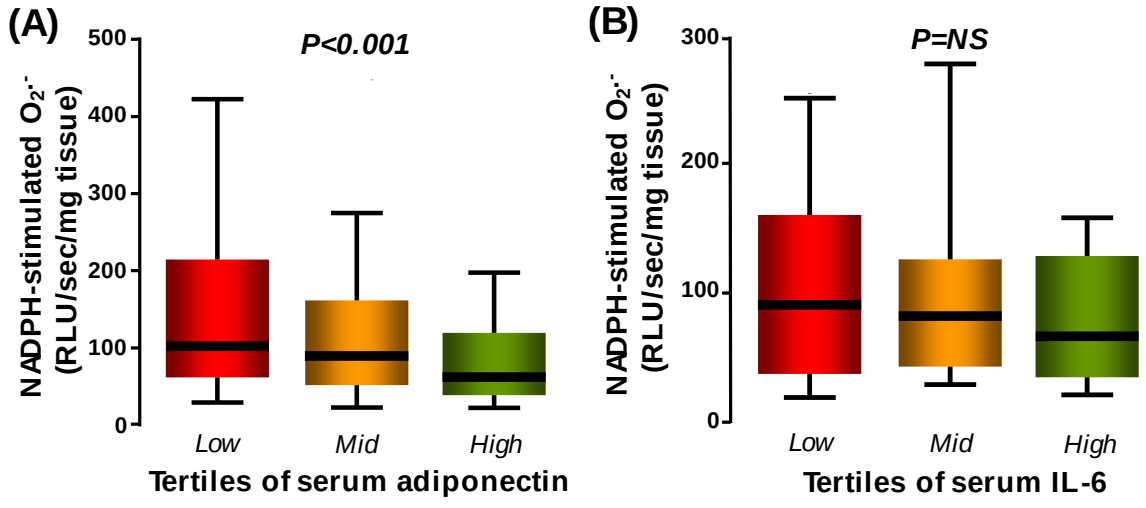


Figure 3.6: *Patients with high serum levels of adiponectin had significantly lower vascular superoxide ($O_2^{\cdot -}$) generation in both saphenous veins (SV, n=396, Panel A) and internal mammary arteries (IMA, n=257, Panel B). Values are expressed as median [25th-75th percentiles].* ***(Margaritis et al. Circulation 2013;127(22):2209-21)***

3.3.1.3 Circulating adiponectin and vascular NADPH-oxidases activity

I then hypothesized that circulating adiponectin was related to NADPH-oxidases activity in human vascular tissue, given that these enzymes are one of the main vascular sources of $O_2\cdot^-$. To assess this hypothesis, I examined the relation between serum levels of adiponectin and NADPH-stimulated $O_2\cdot^-$ generation as measured by lucigenin-enhanced chemiluminescence. I found that NADPH-stimulated $O_2\cdot^-$ generation was significantly lower in patients with high circulating adiponectin (Figure 3.7, Panel A). This suggests an association between high levels of adiponectin in the bloodstream and reduced activity of vascular NADPH-oxidases. In multivariable analysis, log(circulating adiponectin) was an independent predictor of log(NADPH-stimulated-$O_2\cdot^-$) in IMAs (β(SE): -0.233(0.074), P=0.002), independently of type 2 diabetes (β(SE):0.112(0.047) P=0.017), hypertension (β(SE):0.108(0.048), P=0.026) and smoking (β(SE):0.088(0.031), P=0.004). On the contrary, NADPH-oxidases activity in IMAs was not linked to circulating levels of interleukin-6 (IL-6), a marker of inflammation (Figure 3.7, Panel B).

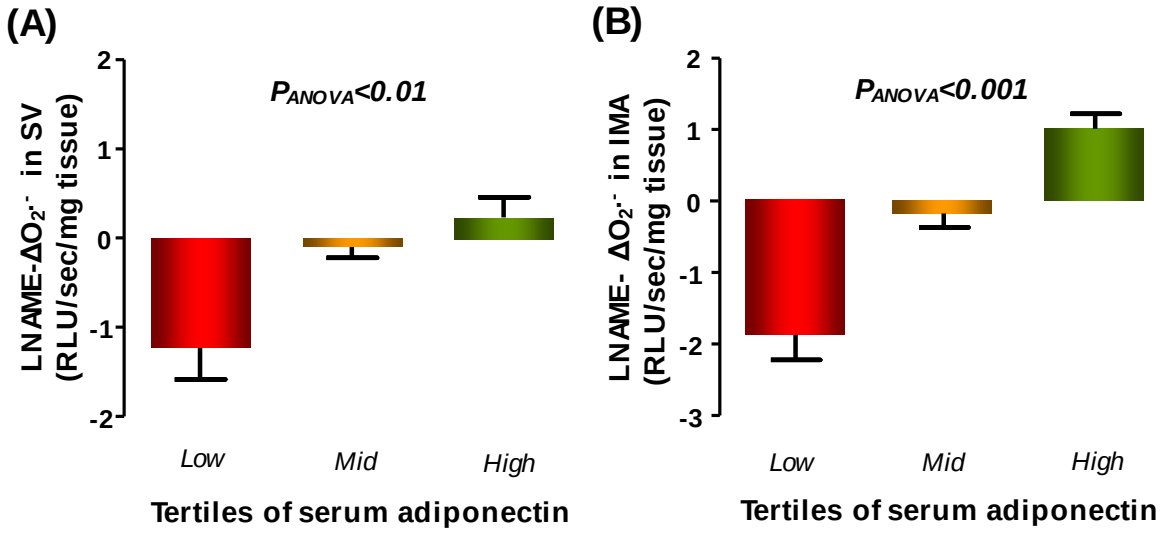


d

superoxide ($O_2\cdot^-$) generation in the vascular wall of their left internal mammary artery (n=257, Panel A), whereas serum interleukin 6 (IL-6) levels did not show any association (n=257, Panel B). Values are expressed as median [25th-75th percentiles]. ***(Margaritis et al. Diabetes 2015;64(6):2207-19)***

3.3.1.4 Circulating adiponectin and eNOS coupling

Another important source of $O_2^{\cdot-}$ radicals in the vasculature is uncoupled eNOS. To assess whether there are interactions between circulating adiponectin and eNOS coupling, I examined the association between adiponectin levels in the bloodstream and LNAME-inhibitable vascular $O_2^{\cdot-}$ (which provides an estimate of eNOS uncoupling). I observed that low circulating adiponectin levels were related to greater LNAME-inhibitable $O_2^{\cdot-}$ in both SV and IMA segments, which is indicative of more eNOS uncoupling (Figure 3.8). In multivariable analysis, the independent predictors of LNAME-$\Delta(O_2^{\cdot-})$ in IMAs were log(circulating adiponectin) (β(SE): 4.37(0.73), P=0.0001) and treatment with statins (β(SE):2.73(0.57), P=0.0001) whereas the predictors of LNAME-$\Delta(O_2^{\cdot-})$ in SVs, were also log(circulating AdN) (β(SE): 2.12(0.54), P=0.0001) and statin treatment (β(SE): 2.25(0.39), P=0.0001). These findings suggest that increased circulating adiponectin and regular statin treatment are independently associated with improved eNOS coupling in human arteries and veins.



levels of LNAME-inhibitable vascular superoxide ($O_2^{\cdot-}$) in both saphenous veins (SV, n=244, Panel A) and internal mammary arteries (IMA, n=182, Panel B). Values are expressed as mean ± SEM. ***(Margaritis et al. Circulation 2013;127(22):2209-21)***

3.3.2 Exploring causality: a Mendelian randomization approach

3.3.2.1 Background/Experimental design

The aforementioned observations provide a link between high circulating adiponectin levels and improved endothelial function/redox state in human vascular tissue. However, they are purely associations and neither prove an actual causal relationship, nor pinpoint the direction of causality. In order to prove the existence of causal relations, I first used a Mendelian Randomization approach. This approach can be summarized as follows: whenever a biomarker (in this study: circulating adiponectin levels) is associated with a certain phenotype (in this study: endothelial function and vascular oxidative stress), if we can identify a genotype that is linked to levels of the biomarker in question and show that this genotype is also associated with the observed phenotype, then the association between the biomarker and the phenotype is causal, with direction of causality from the biomarker to the phenotype. This is owing to the fact that the alleles that form the genotype are randomly distributed during gametogenesis, an event uninfluenced by socioeconomic, environmental and behavioural factors. This is the reason why Mendelian Randomization studies have been dubbed, and rightly so, "nature's clinical trials"[190].

In my study I genotyped the Oxford CABG Bioresource Phase I population for two common single nucleotide polymorphisms (SNPs) on chromosome 3. The first one is rs17366568, located within an intron in the *ADIPOQ* locus leading to a transition substitution (A<G). The second SNP is rs266717, located in the intergenic region between *ADIPOQ* and *RFC4* locus and also causing a transition substitution (C<T). Both SNPs have been shown to affect circulating adiponectin levels in genome wide association studies.[82, 191] Individuals bearing the G allele for the rs17366568 SNP and the T allele for the rs266717 SNP have been shown to be genetically predisposed towards higher circulating adiponectin levels. These two polymorphisms are not in linkage

disequilibrium[82], so their effect on *ADIPOQ* gene expression could be independent from each other and therefore additive.

3.3.2.2 Single nucleotide polymorphisms in the ADIPOQ locus, serum levels of adiponectin & endothelial function

The observed frequency of the two distinct alleles in each SNP I examined in the Oxford CABG Bioresource Phase I population was in line with the results of the GWAS, as expected for a white-caucasian population of European descent, based on data available online on the dbSNP National Center for Biotechnology Information (NCBI) database (Table 3.2).

Table 3.2 Expected & observed frequencies of SNP alleles in the study population

SNP	Homozygotes (Allele 1) Frequency	Heterozygotes Frequency	Homozygotes (Allele 2) Frequency
rs17366568	AA *Expected:4.2%* Observed: 1.7% (n=11)	AG *Expected:20.8%* Observed: 22.3% (n=151)	GG *Expected: 75%* Observed: 76.0% (n=515)
rs266717	CC *Expected: 22.5%* Observed: 25.0% (n=169)	CT *Expected: 50%* Observed: 49.5% (n=335)	TT *Expected: 27.5%* Observed: 25.5% (n=173)

I first established that the rs17366568G and rs266717T alleles had an additive effect on serum adiponectin, accounting for approximately 30% of the observed variance between the extreme genotypes (Figure 3.9), thus confirming the relevance of the GWAS findings in my study population.

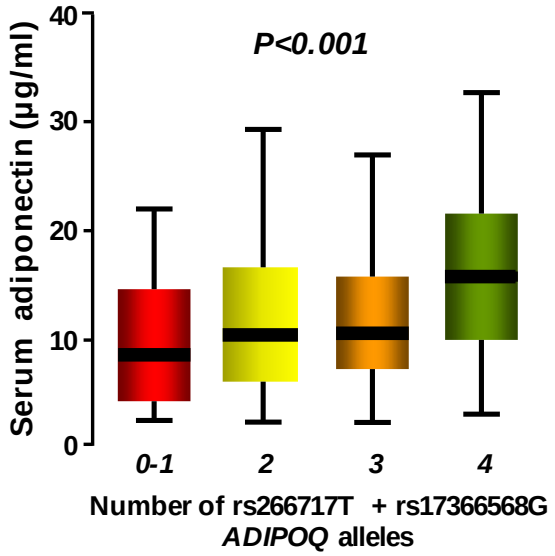


Figure 3.9: *The additive number of rs17366568G and rs266717T alleles for rs266717 was associated with significantly higher serum levels of adiponectin (0-1 alleles n=43, 2 alleles n=117, 3 alleles n=296, 4 alleles n=221). Values are expressed as median [25th-75th percentiles].* ***(Margaritis et al. Diabetes 2015;64(6):2207-19)***

I then proceeded to show that the additive number of rs266717T & rs17366568G alleles was also positively associated with FMD of the brachial artery (Figure 3.10, Panel A) and the *ex vivo* endothelium-dependent vasorelaxation response of SV rings to acetylcholine obtained from patients undergoing bypass surgery (Figure 3.10, Panel B). These findings document for the first time that genetically-determined hypo-adiponectinemia may actually lead to endothelial dysfunction in human vessels.

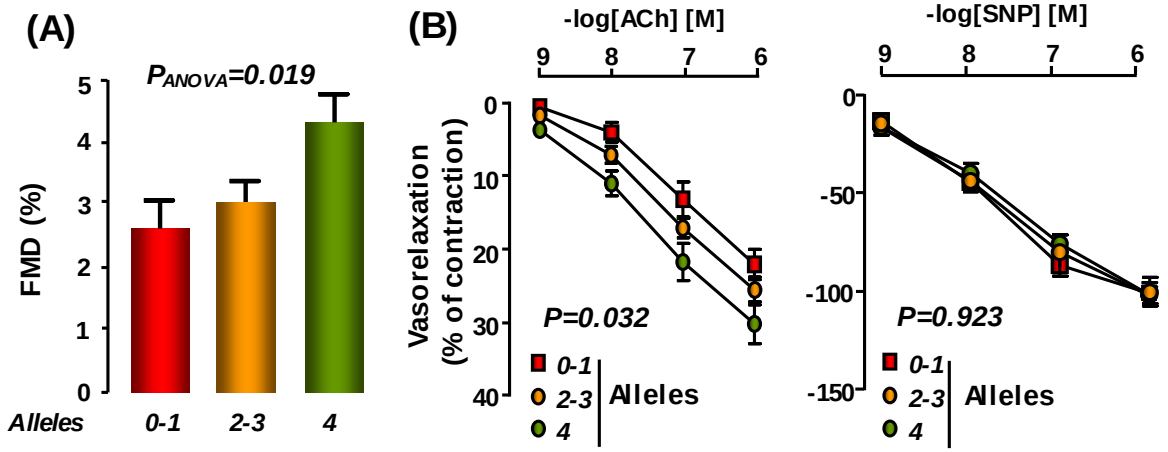


Figure 3.10: *The number of rs17366568G and rs266717T alleles was positively associated with flow mediated dilation of the brachial artery (FMD, Panel A) and vasorelaxations of SVs (n=230) in response to acetylcholine (ACh, Panel B) but not to sodium nitroprusside (SNPr). Values are expressed as mean ± SEM.* ***(Margaritis et al. Circulation 2013;127(22):2209-21)***

3.3.2.3 Single nucleotide polymorphisms in the ADIPOQ locus & vascular redox state

Continuing from the previous observations, I found that the additive number of rs17366568G and rs266717T alleles was also negatively related with resting $O_2^{\cdot -}$ generation (Figure 3.11, Panel A) and LNAME-inhibitable $O_2^{\cdot -}$ in SV and IMA segments (Figure 3.11, Panel B). In addition, these alleles were also linked to reduced NADPH-stimulated $O_2^{\cdot -}$ in IMA segments (Figure 3.11, Panel C). However, they had no significant impact on systemic oxidative stress as estimated by plasma malonyldialdehyde (MDA) levels (Figure 3.11, Panel D).

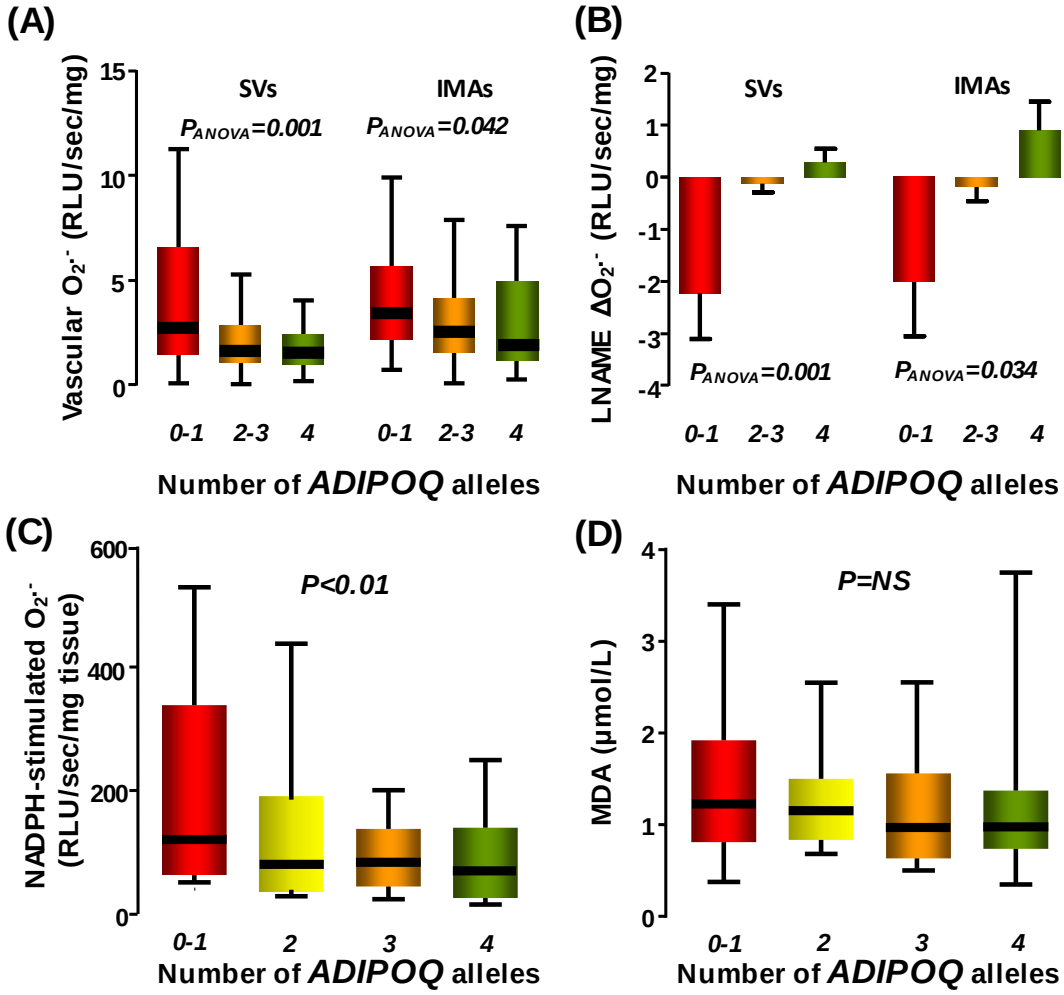


Figure 3.11: *The number of rs17366568G and rs266717T alleles related with lower vascular superoxide generation ($O_2^{\cdot -}$, Panel A) and less LNAME-inhibitable $O_2^{\cdot -}$ (Panel B) in both SVs (n=396) and internal mammary arteries (IMAs, n=257). Values expressed as median [25^{th}-75^{th} percentiles] Panels A, C&D or mean ± SEM for panel B.* ***(Margaritis et al. Circulation 2013;127(22):2209-21); Margaritis et al. Diabetes 2015;64(6):2207-19)***

3.3.3 Exploring causality: *Ex vivo* mechanistic experiments

3.3.3.1 Background/Experimental design

A second approach I used to explore the causal association between adiponectin and endothelial function/vascular redox state was to perform *ex vivo* incubations of paired tissue samples. The source of tissue was patients enrolled in the AdipoRedox study, which constitutes Phase II of the Oxford CABG Bioresource. In these experiments, I incubated paired human vascular segments (SVs and/or IMAs) obtained from patients undergoing CABG surgery with or without recombinant human full-length adiponectin 10 μg/ml for 6 hours. This concentration was chosen because it corresponds to physiological levels of adiponectin in the circulation, based on observations made in the cohort as well as the literature available[192]. Human recombinant adiponectin was purchased from Biovendor (Brno, Czech Republic). At the end of the incubation period, the samples were either used fresh in an experiment or snap frozen and stored at -80^{o}C for further assays. By using this experimental design, I was able to examine the direct effects of adiponectin on human vascular redox state. In order to explore the sub-cellular mechanisms mediating my initial findings, as mentioned below, in select experiments a third vascular sample was used from the same patient. That sample was exposed to recombinant human adiponectin plus a pharmacological inhibitor, as dictated each time by the specific biological question. The inhibitors used and their biological targets can be found in Table 3.3 below.

Table 3.3: Pharmacological inhibitors used in vascular *ex vivo* mechanistic experiments

Inhibitor	Biological Target	Concentration	Supplier
Wortmannin	PI3K/Akt	100 nmol/L	SigmaAldrich
DAHP (2,4-diamino hydroxyl pyrimidine)	GTP-Cyclohydrolase	1 mmol/L	SigmaAldrich

3.3.3.2 Direct effects of adiponectin on resting superoxide production and vascular NADPH-oxidases activity

In the first set of experiments, I observed that incubation of human vascular tissue with adiponectin led to a significant reduction in resting $O_2^{\cdot -}$ generation in both SVs and IMAs, as evidenced by lucigenin-enhanced chemiluminescence (Figure 3.12). This proves that adiponectin has a direct antioxidant effect on the human vascular wall.

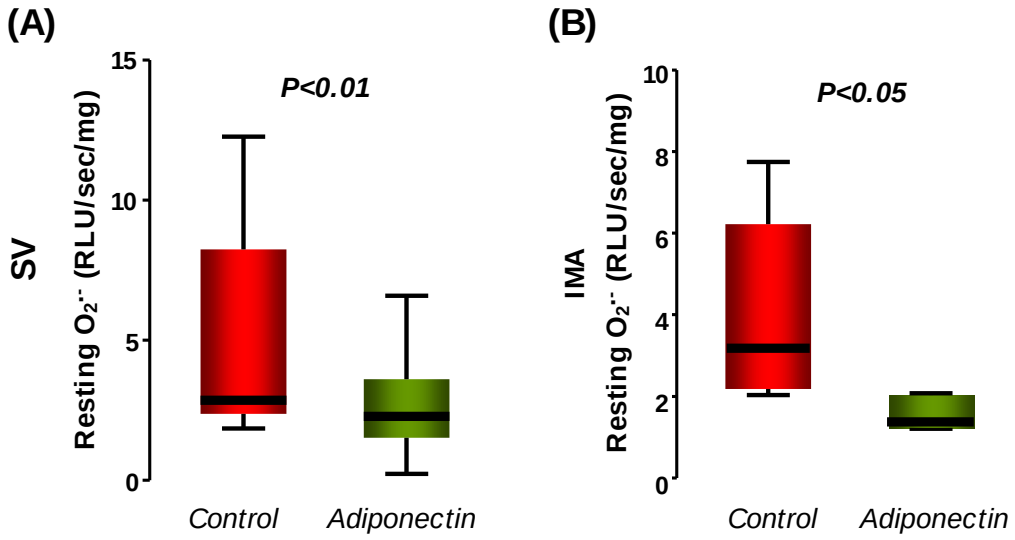


Figure 3.12: *Ex vivo incubation of human saphenous veins (SV – Panel A, n=9) and internal mammary arteries (IMA – Panel B, n=5) with adiponectin 10 μg/ml for 6 hours led to a significant reduction in resting superoxide $O_2^{\cdot -}$ generation. Values expressed as median [25th-75th percentiles]* ***(Margaritis et al. Circulation 2013;127(22):2209-21)***

I then proceeded to show that adiponectin led to reduction in NADPH-stimulated-$O_2^{\cdot -}$ generation in IMAs, suggesting reduced NADPH-oxidases activity (Figure 3.13, Panel A). Given the low specificity of NADPH-stimulated signal as a measure of activity of these enzymes, I used the specific inhibitor Vas2870 and found that incubation with adiponectin led to significant reduction in the Vas2870-inhibitable signal (Figure 3.13, Panel B). Importantly, these effects were reversed by the PI3K/Akt signalling inhibitor wortmannin, implying that Akt is a crucial mediator of the antioxidant effects of adiponectin.

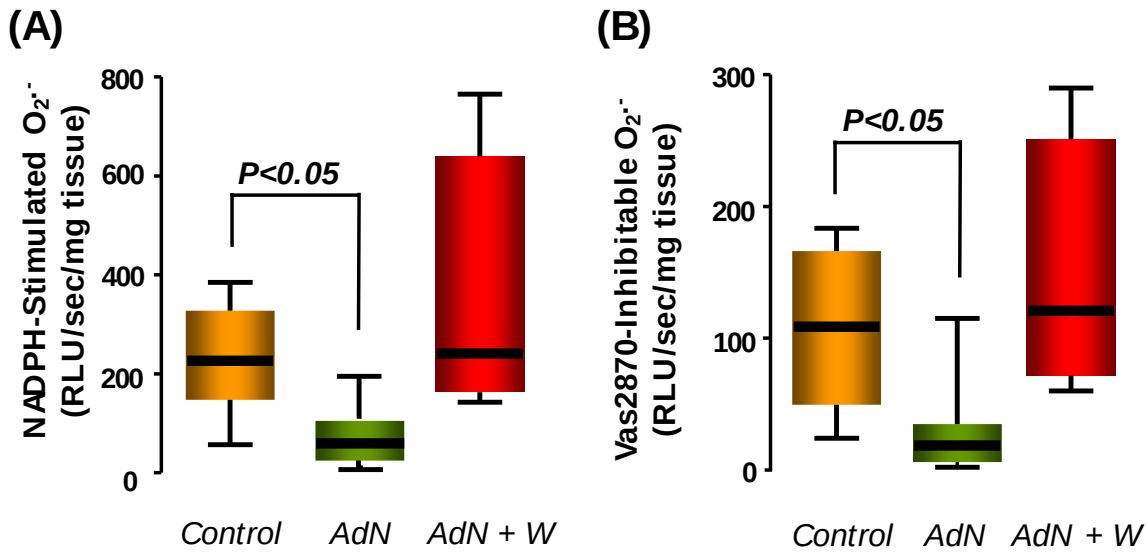


Figure 3.13: *Ex vivo incubation of human internal mammary arteries (n=10) with adiponectin (AdN) 10 μg/ml for 6 hours led to a significant reduction in NADPH-stimulated (A) and Vas2870-inihibitable superoxide ($O_2^{\cdot-}$) generation (B), effects reversed by the PI3K/Akt inhibitor Wortmannin (W). Values expressed as median [25^{th}-75^{th} percentiles]* ***(Margaritis et al. Diabetes 2015;64(6):2207-19)***

The results from the previous experiment were confirmed by using a different technique to estimate vascular $O_2^{\cdot-}$ generation, namely dihydroethidium (DHE) staining. This technique, coupled with confocal microscopy, allows visualisation of $O_2^{\cdot-}$ generation in tissue cryosections, as described in Chapter 2. Figure 3.14 shows results of such a DHE staining experiment: paired IMA samples, which had been incubated with or without adiponectin 10 μg/ml for 6 hours and stored in OCT were cut in sections and incubated with Vas2870 for 30 min, to inhibit NADPH-oxidases. DHE was then added according to the protocol mentioned in Chapter 2, and the resulting fluorescence was visualised using confocal microscopy. The findings were similar to the ones obtained using the luminometry experiment: adiponectin led to a reduction in $O_2^{\cdot-}$ generation throughout the vascular wall compared to control (Figure 3.14, Panels A&B). However, inhibition of NADPH-oxidases with Vas2870 before exposure to DHE led to a lack of significant

difference between the control and adiponectin-treated samples (Figure 3.14, Panels C&D). This leads to the conclusion that inhibition of NADPH-oxidases plays a major role in the direct antioxidant effects of adiponectin in the vascular wall.

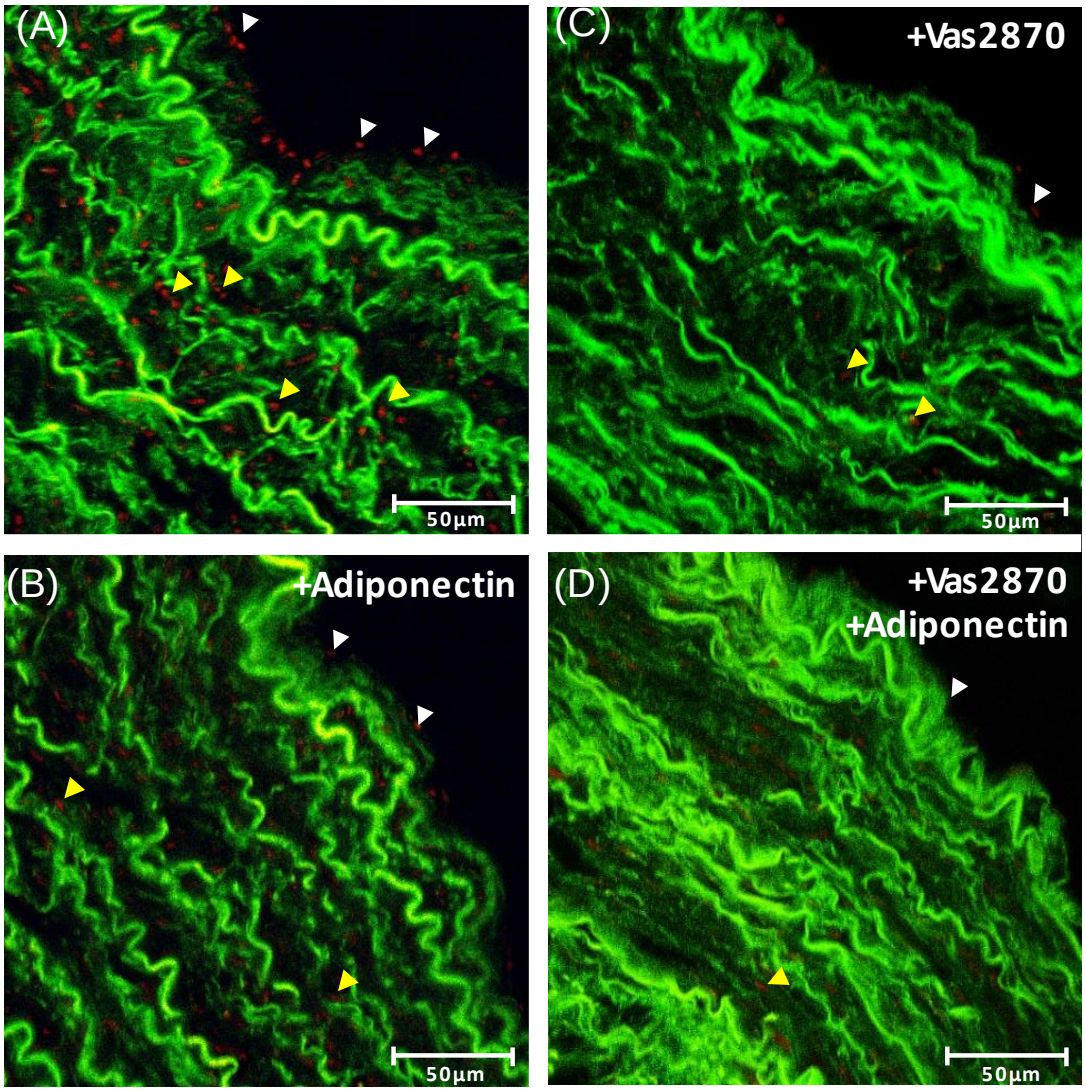


Figure 3.14: *Ex-vivo incubation of serial human left internal mammary artery (IMA) segments (n=4) with adiponectin 10 µg/ml for 6 h resulted into reduction of superoxide ($O_2^{\cdot-}$, red dots) production in both the vascular endothelium (white arrow heads) and the wall (yellow arrow heads, Panels A & B). Inhibition with Vas2870 supressed $O_2^{\cdot-}$ production in both the endothelium and the vascular wall (Panels C and D) suggesting that adiponectin supressed NADPH-oxidase derived $O_2^{\cdot-}$ signal throughout the entire vascular wall. Images of dihydroethidium staining viewed through a Zeiss LSM 510 META laser scanning confocal microscope at 40x magnification.* ***(Margaritis et al. Diabetes 2015;64(6):2207-19)***

3.3.3.3 Adiponectin and cellular signalling pathways: PI3K/Akt - AMPK

The results of the experiments presented in figure 3.13 give indirect evidence that adiponectin relies on the PI3K/Akt pathway to mediate its antioxidant effects in the vasculature. Activation of Akt by adiponectin has been previously shown in cell culture models[193]. To fully investigate the hypothesis that PI3K/Akt is an integral component of the adiponectin cellular signalling pathway in the human vascular wall, I incubated additional segments of human SVs and IMAs with adiponectin 10 μg/ml for 6 hours and proceeded to perform western immunoblotting for the Ser473-phosphorylated form of Akt, which is an activated form of the protein. In both veins and arteries, incubation with adiponectin led to a significant increase in vascular levels of phospho-Akt at Ser473, effects which were, as expected, fully suppressed with wortmannin (Figure 3.15).

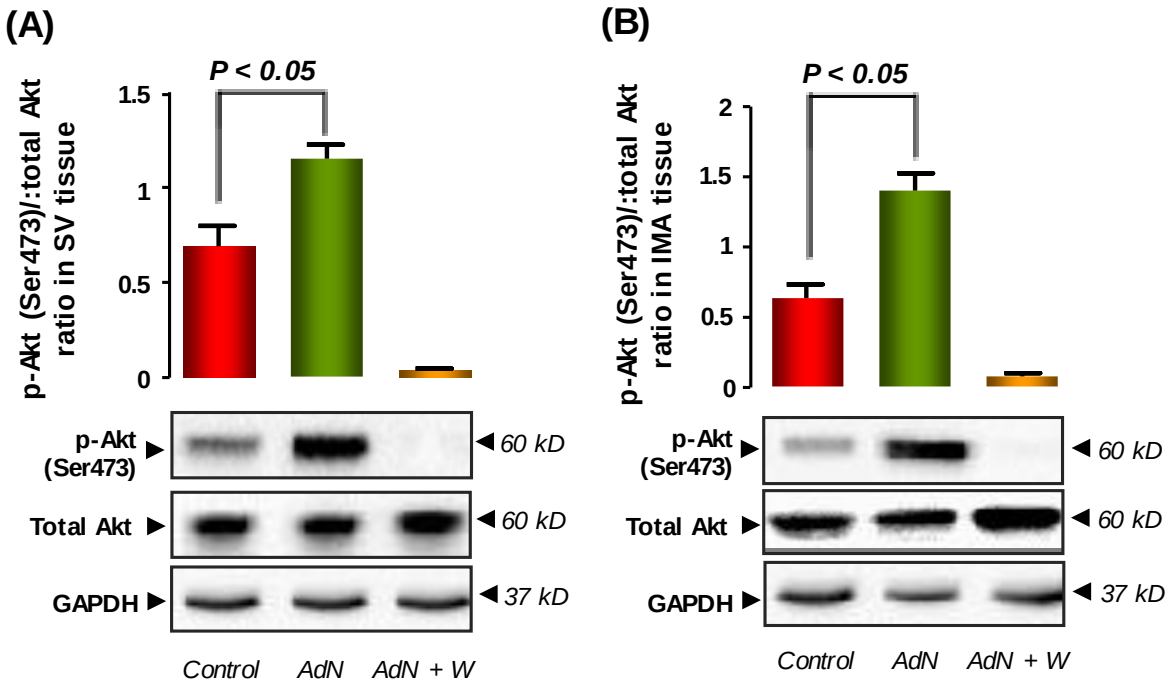


Figure 3.15: *Ex vivo incubation of serial saphenous vein segments (SV, n=11, Panel A) and internal mammary artery segments (IMA, n=5, Panel B) with adiponectin (AdN, 10μg/ml for 6h) increased phosphorylation of Akt at Ser473, an activation site. Values are expressed as mean ± SEM.* ***(Margaritis et al. Circulation 2013;127(22):2209-21)***

In addition to Akt, there is significant literature supporting a role for AMP kinase (AMPK) as a crucial mediator of the effects of adiponectin in vascular cells[125], skeletal muscle[194] and adipocytes[195]. To investigate a potential effect of adiponectin in human vascular tissue, I used the same experimental design as before and incubated additional segments of human SVs with adiponectin 10 μg/ml for 6 hours. I then proceeded to perform Western immunoblotting for the Thr172-phosphorylated form of AMPK. Thr172 is an activation phosphorylation site and leads to increased activity of the enzyme. However, as can be seen in Figure 3.16, I was unable to observe any significant change in phosphorylation of vascular AMPK at Thr172 after incubation of human saphenous veins with adiponectin. This finding is discussed in detail in paragraph 3.4.1.

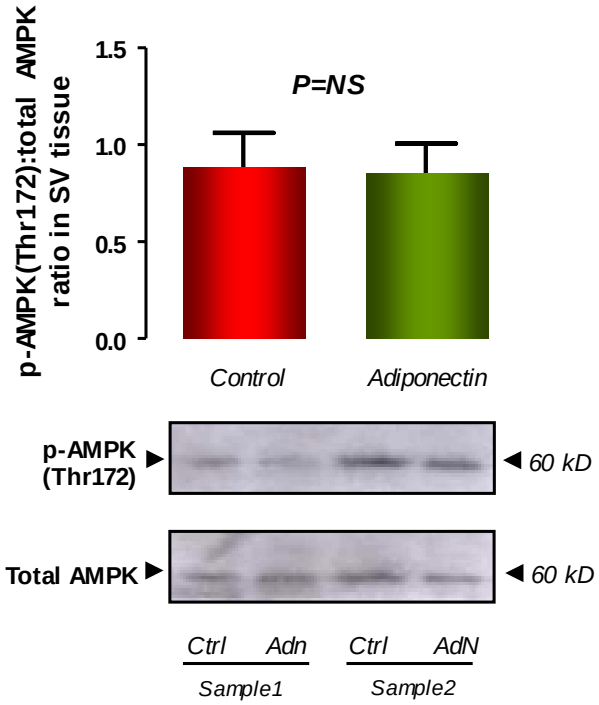


Figure 3.16: *Ex vivo incubation of serial saphenous vein segments (SV, n=4) with adiponectin (AdN, 10μg/ml for 6h) did not lead to significant changes in phosphorylation of AMP kinase (AMPK) at Thr172. Representative blots from two paired samples are shown. Values are expressed as mean ± SEM.*

3.3.3.4 Mechanism of NADPH-oxidases activity suppression by adiponectin

My previous experiments led to the conclusion that adiponectin directly suppresses NADPH-oxidases via a PI3K/Akt-mediated pathway. To further explore the molecular mechanisms by which adiponectin exerts these effects, I first examined its impact on the expression of NADPH-oxidases subunits. I observed that incubation of internal mammary artery segments with adiponectin 10 μg/ml for 6 hours had no effect on either gene expression (p=NS for all targets) or total protein levels of Rac1, NOX1, NOX2, NOX4, $p47^{phox}$ and $p67^{phox}$ (Figure 3.17).

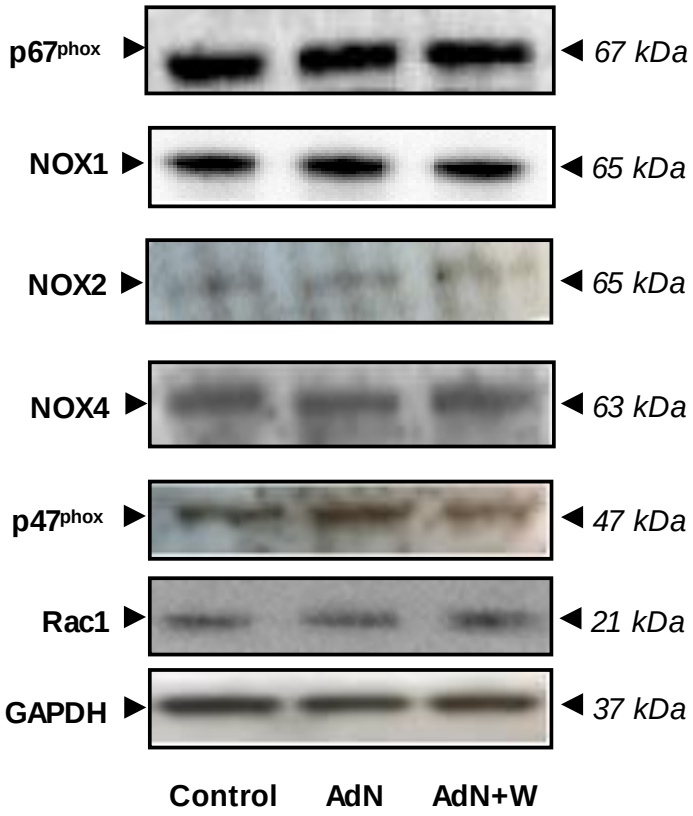


Figure 3.17: *Incubation of human internal mammary artery segments with adiponectin (AdN, 10 μg/ml for 6 hours, n=5) did not lead to significant differences in protein levels of the NADPH-oxidase subunits p67phox, NOX1, NOX2, NOX4 or P47phox. Addition of wortmannin (W) also did not lead to any appreciable effects.*

On the contrary, there was a significant reduction in gene expression of the CYBA gene, which encodes for the $p22^{phox}$ subunit, a necessary component of the NOX1, NOX2 and NOX4-containing enzymatic complexes (Figure 3.18, Panel A). Interestingly, this effect of adiponectin was prevented by wortmannin, suggesting that PI3K/Akt plays a crucial role in mediating these actions of adiponectin. However, I was initially surprised to discover that that the reduction in gene expression of the CYBA gene was not translated into an actual reduction of vascular $p22^{phox}$ protein levels after 6 hours of incubation with adiponectin (Figure 3.18, Panel B). This could be due to the relatively short incubation period, which would not be sufficient to lead to actual protein level changes. As such, these observations could not explain the significant and rapid PI3K/Akt-mediated decrease in NADPH-stimulated and Vas2870-inhibitable $O_2^{\cdot -}$ generation observed in these vessels after 6 hours of incubation with adiponectin, as shown in section 3.3.3.2 and Figure 3.13.

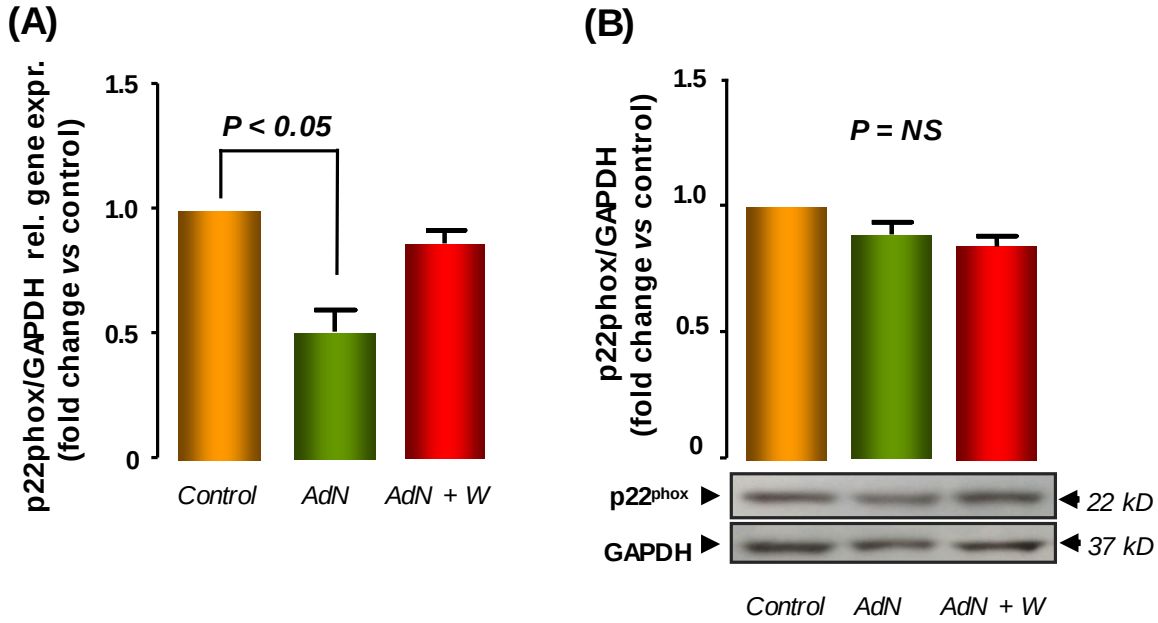


Figure 3.18: *Incubation of human internal mammary arteries (n=8) with adiponectin (AdN) 10 μg/ml for 6 hours led to a significant reduction in gene expression of the gene encoding for the $p22^{phox}$ subunit of NADPH-oxidase (A). Importantly, the PI3K/Akt inhibitor wortmannin (W) prevented this effect. However, this 6-hour incubation failed to lead to any significant changes in protein levels of $p22^{phox}$ in the vascular wall, as evidenced by Western immunoblotting (B). Values are expressed as mean ± SEM.* ***(Margaritis et al. Diabetes 2015;64(6):2207-19)***

In search of an alternative mechanism to explain the rapid antioxidant effects of adiponectin, I hypothesized that adiponectin could potentially inhibit activation of the small GTPase Rac1, a necessary subunit of the NOX1- and NOX2-containing isoforms of NADPH-oxidase. To explore this hypothesis, I estimated the activation of Rac1 and its translocation to the membrane in samples incubated with/without adiponectin ± wortmannin, using the methods described earlier in this chapter. I found that incubation of IMA samples with adiponectin for 6 hours led to a reduction in GTP-bound Rac1, (Figure 3.19, Panel A) and subsequently reduced translocation of this subunit to the membrane (Figure 3.19, Panel B). Both of these effects were reversed by wortmannin. These findings suggest that adiponectin suppresses NADPH-oxidases activity in the human arterial wall through a PI3K/Akt-mediated inhibition of Rac1 activation.

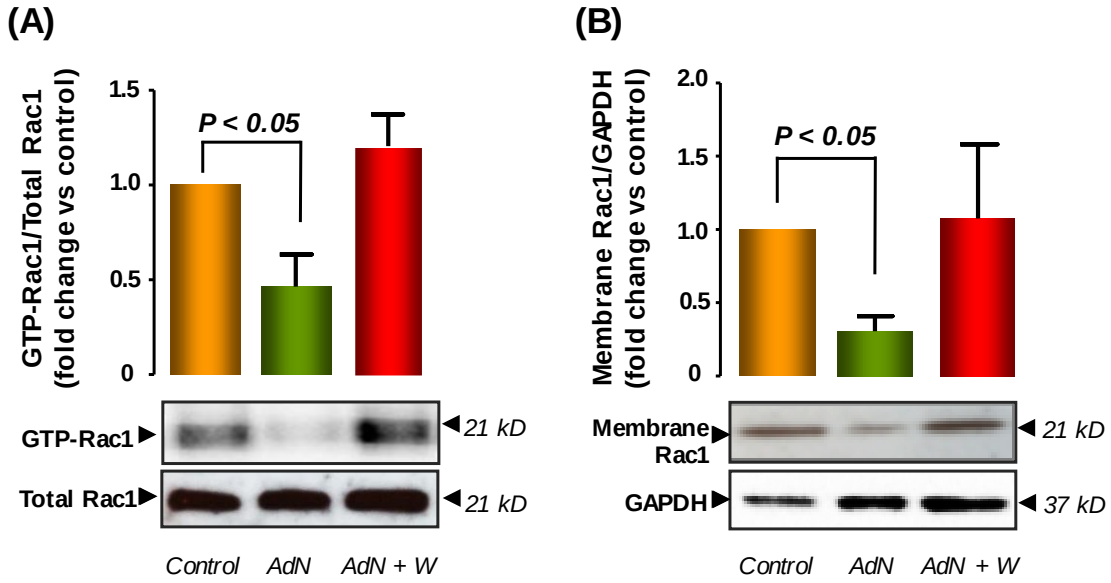


Figure 3.19: *Incubation of human internal mammary arteries (n=7) with adiponectin (AdN) 10 μg/ml for 6 hours led to significantly reduced activation of Rac1, as evidenced by a reduction in the ratio of GTP-Rac1/Total Rac (Panel A). This was linked to reduced translocation of Rac1 to the membrane (Panel B). Both of these effects of adiponectin were prevented after PI3K/Akt inhibition with wortmannin (W), suggesting that this pathway is crucial in mediating the actions of adiponectin in the vasculature. Values are expressed as mean ± SEM.* ***(Margaritis et al. Diabetes 2015;64(6):2207-19)***

Given the observations presented in Figure 3.18 that $p22^{phox}$ gene expression (but not its protein level) was downregulated in a PI3K/Akt-dependent way after 6 hours of incubation of human IMAs with adiponectin, I performed longer-term incubations, for 18 hours, to investigate for a potential effect of adiponectin on $p22^{phox}$ protein levels after more long-term exposure. Indeed, I confirmed that the effect of adiponectin on NADPH-stimulated (Figure 3.20, Panel A) and Vas2870-inhibitable $O_2\cdot^-$ (Figure 3.20, Panel B) in these vessels persisted after 18 hours of incubation. Importantly, I now demonstrated a PI3K/Akt-dependent reduction in the vascular protein level of the $p22^{phox}$ subunit of NADPH-oxidases (Figure 3.20, Panel C), documenting a second sub-acute effect of adiponectin on NADPH-oxidase.

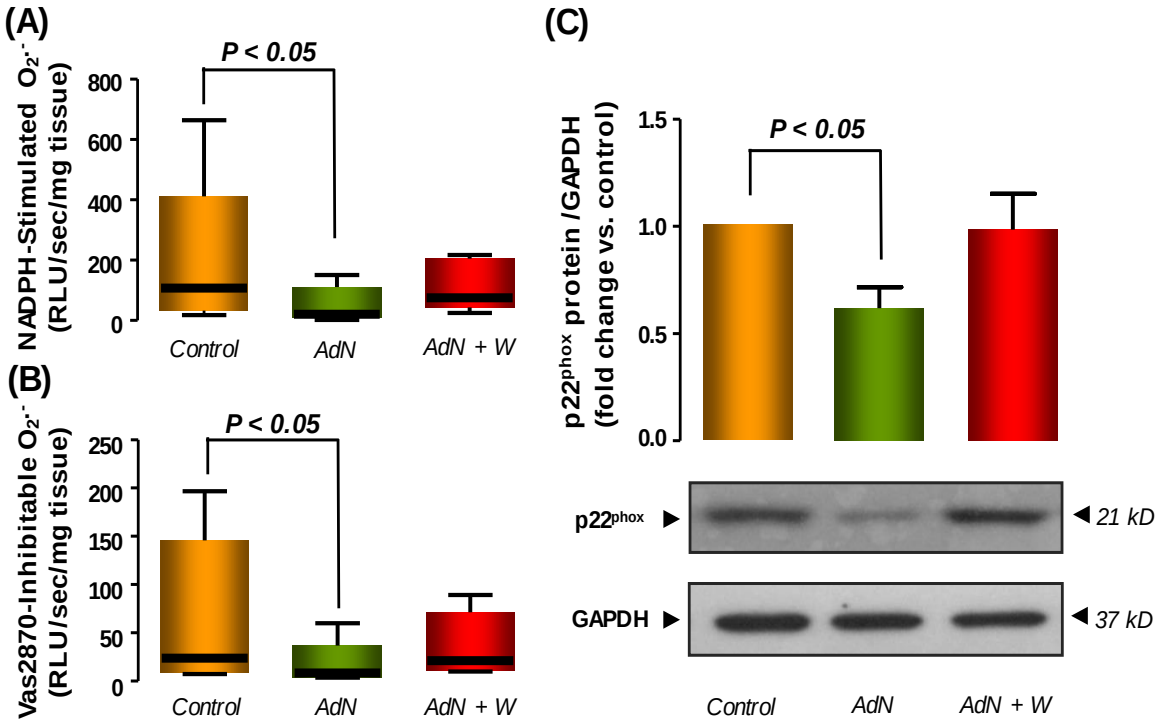


Figure 3.20: *The effect of adiponectin (AdN) 10 μg/ml on NADPH-stimulated superoxide ($O_2\cdot^-$, Panel A) and its Vas2870-inhibitable fraction (Panel B) remained significant after 18h of ex vivo culture of human internal mammary artery segments and this effect was again partly reversed by wortmannin (W, 100 nmol/L) (n=9). In these experiments, the reduction of $p22^{phox}$ protein levels was significant and this effect was prevented by wortmannin (Panel C). Values are expressed as median [25^{th}-75^{th} percentiles] (Panels A &B) or mean ± SEM (Panel C).* ***(Margaritis et al. Diabetes 2015;64(6):2207-19)***

3.3.3.5 Direct effects of adiponectin on eNOS coupling

As mentioned in the introduction, uncoupled eNOS is an important source of superoxide in the vasculature. One of the major mechanisms leading to eNOS uncoupling is oxidative degradation of its essential co-factor BH4. Having demonstrated that adiponectin has NADPH-oxidases-suppressing capabilities, I hypothesized that the resulting reduction in $O_2^{\cdot -}$ generation from this enzyme could potentially lead to an improvement in eNOS coupling by protecting BH4 from oxidation. To investigate this hypothesis, I first sought to establish whether *ex vivo* incubation of human vessels with adiponectin does indeed restore eNOS coupling status. Indeed, employing the same paired sample experimental setup used throughout this chapter, I found that incubation with adiponectin for 6 hours significantly restored eNOS coupling in human SVs and IMAs, as evidenced by increase in the LNAME-inhibitable signal obtained through lucigenin-enhanced chemiluminescence (Figure 3.21).

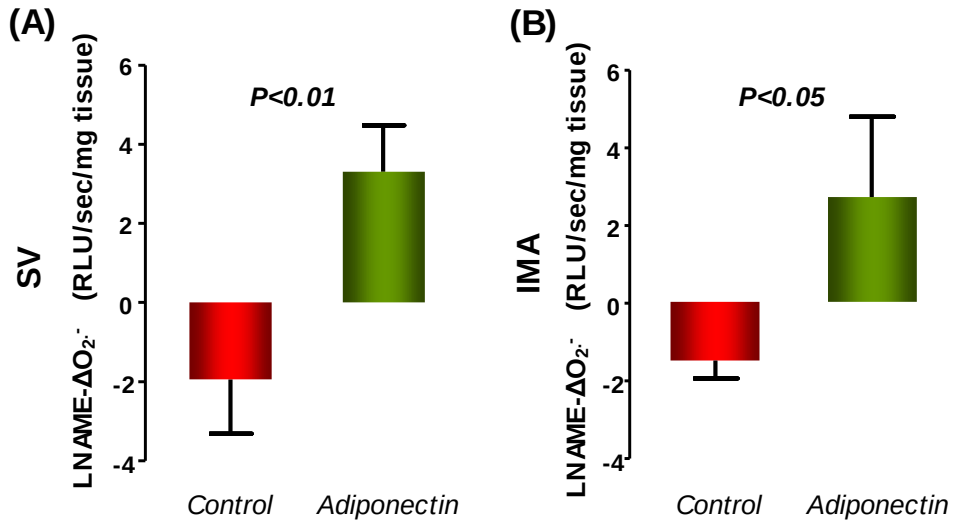


Figure 3.21: *Ex vivo incubation of human saphenous veins (SV – Panel A, n=9) and internal mammary arteries (IMA – Panel B, n=5) with adiponectin 10 μg/ml for 6 hours led to an increase in LNAME-inhibitable $O_2^{\cdot -}$ generation as measured by lucigenin chemiluminescence, which denotes improved eNOS coupling. Values are expressed as mean ± SEM.* ***(Margaritis et al. Circulation 2013;127(22):2209-21)***

This effect was also confirmed and visualised by using dihydroethidium (DHE) staining and confocal microscopy in these vessels. Treatment with adiponectin reduced $O_2^{\cdot -}$ generation in the endothelium. This was accompanied by a reversal in the endothelium-derived LNAME-induced $O_2^{\cdot -}$ generation inhibition, which denotes improvement in eNOS coupling (Figure 3.22).

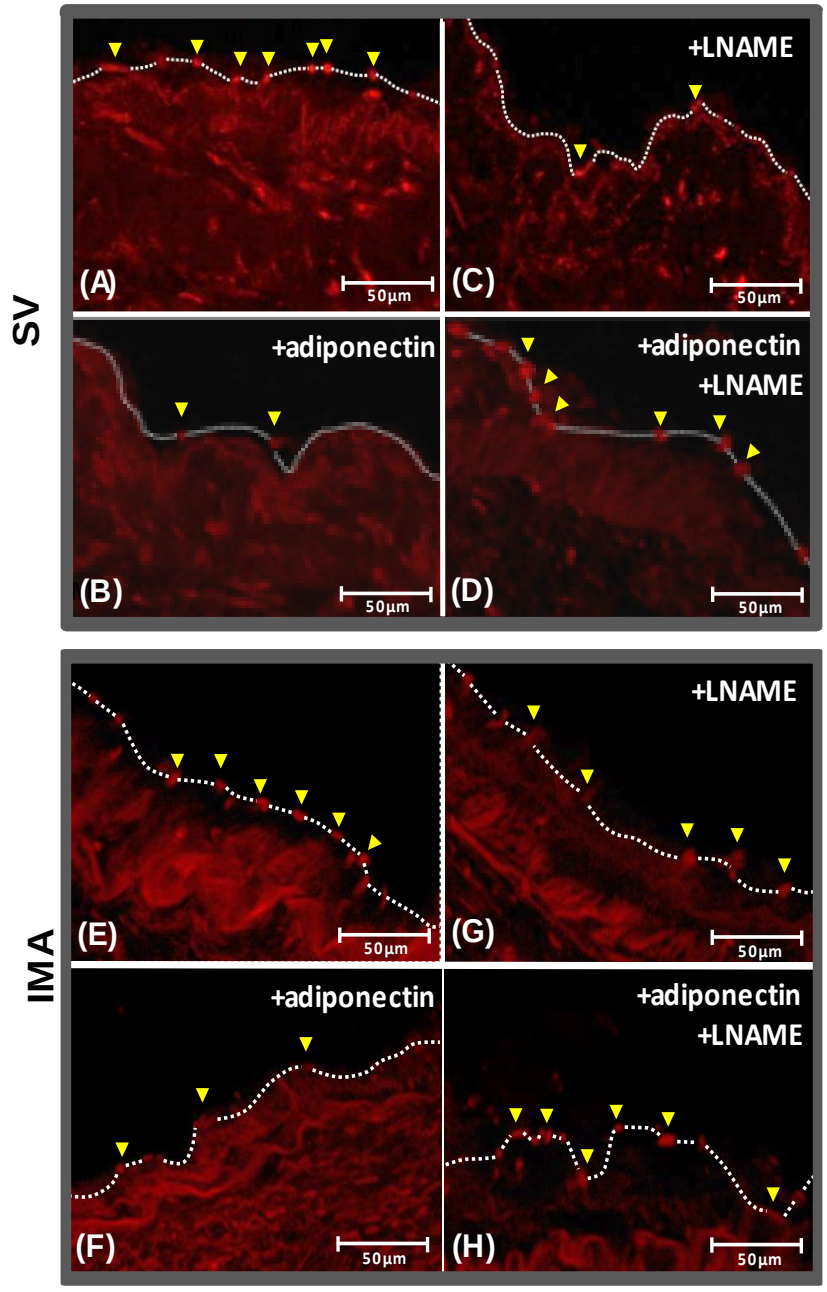


Figure 3.22: *Ex vivo incubation of serial human saphenous vein (SV, n=4) and internal mammary artery (IMA, n=4) rings with adiponectin (10μg/ml for 6 h) led to a reduction in endothelium-derived $O_2^{\cdot -}$. (Panel A control SV versus Panel B adiponectin-treated SV & Panel E control IMA versus Panel F adiponectin-treated IMA). After inhibition of eNOS with LNAME, the signal reduction observed in LNAME-treated control vessels (Panels C & G) was reversed after treatment with adiponectin + LNAME (Panels D & H), underlying improved eNOS coupling status in these vessels. The dotted lines define the endothelium. Yellow arrows denote $O_2^{\cdot -}$ generation in the endothelium. Images viewed through a Zeiss LSM 510 META laser scanning confocal microscope at 40 x magnification.* ***(Margaritis et al. Circulation 2013;127(22):2209-21)***

3.3.3.6 Mechanism of eNOS coupling restoration by adiponectin

Having established that adiponectin has the ability to restore eNOS coupling in human veins and arteries, I sought to explore the mechanisms by which adiponectin affects eNOS physiology in the human endothelium. The first step was to investigate the impact of adiponectin on eNOS phosphorylation. *Ex vivo* incubation of human SVs and IMAs with adiponectin increased eNOS phosphorylation at Ser1177 (Figure 3.23). The effect of adiponectin on eNOS phosphorylation was blocked by wortmannin, suggesting that adiponectin induces a PI3-Akt-mediated phosphorylation of eNOS, resulting in its activation. The ability of adiponectin to induce eNOS phosphorylation remained unchanged in the presence of DAHP (an inhibitor of GTP-cyclohydrolase, blocking the biopterins biosynthetic pathway), suggesting that a reduction in vascular BH4 levels does not modify the effect of adiponectin on eNOS phosphorylation.

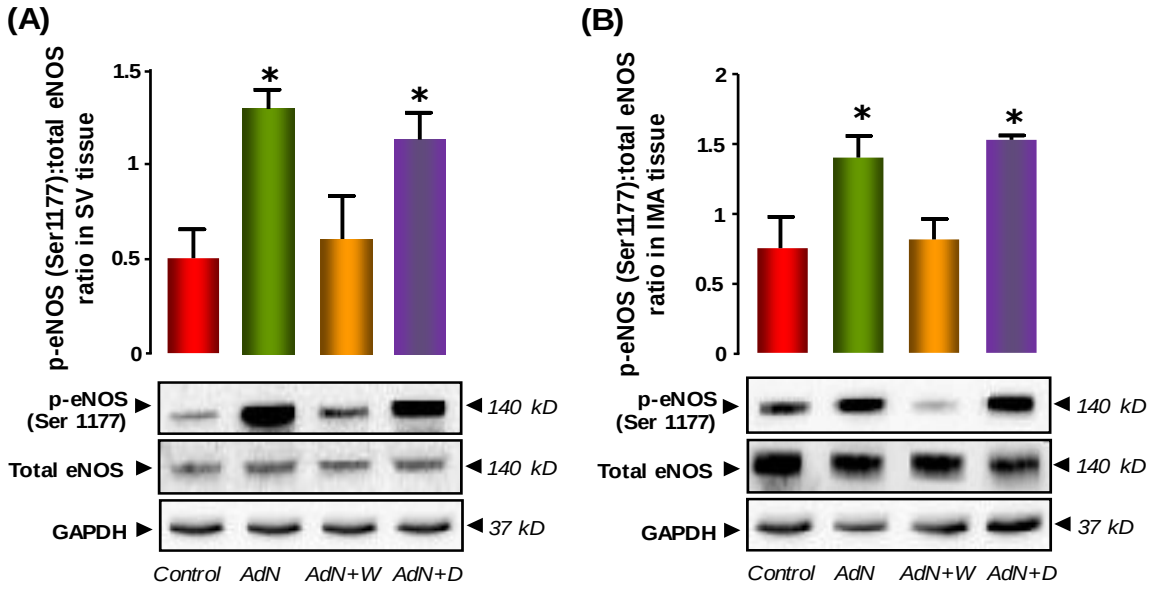


Figure 3.23: *Ex vivo incubation of serial saphenous vein segments (SV, n=11, Panel A) and internal mammary artery segments (IMA, n=5, Panel B) with adiponectin (AdN 10μg/ml for 6h) increased eNOS phosphorylation at Ser1177. The PI3K/Akt inhibitor wortmannin (W, 100 nmol/L) prevented these effects. DAHP (D, an inhibitor of GTP-cyclohydrolase blocking BH4 biosynthesis) did not modify the effects of AdN on eNOS phosphorylation. Values are expressed as mean ± SEM. *P<0.05 versus control* ***(Margaritis et al. Circulation 2013;127(22):2209-21)***

However, activation of eNOS by Ser1177 phosphorylation does not necessarily increase NO synthesis, since phosphorylated eNOS in the presence of BH4 deficiency may actually lead to increased $O_2^{\cdot -}$ generation by the uncoupled form of the enzyme.[188] Therefore, I hypothesized that adiponectin increases BH4 levels in the vasculature through its antioxidant, NADPH-oxidases-suppressing properties, and leads to restoration of eNOS coupling through this mechanism. To investigate this hypothesis, I first sought to examine whether there are links between high levels of adiponectin in the circulation and high vascular BH4 content. To this aim, I performed bivariate analysis of these two variables in the population recruited in phase I of the Oxford CABG Bioresource. Vascular biopterin measurements were available in 173 patients in this cohort. In this subgroup, serum levels of adiponectin were significantly (albeit weakly) positively correlated with BH4 and the BH4/total biopterins ratio in both SV and IMA segments (Figure 3.24). This association suggests that adiponectin could be causally linked to higher BH4 levels in the vasculature.

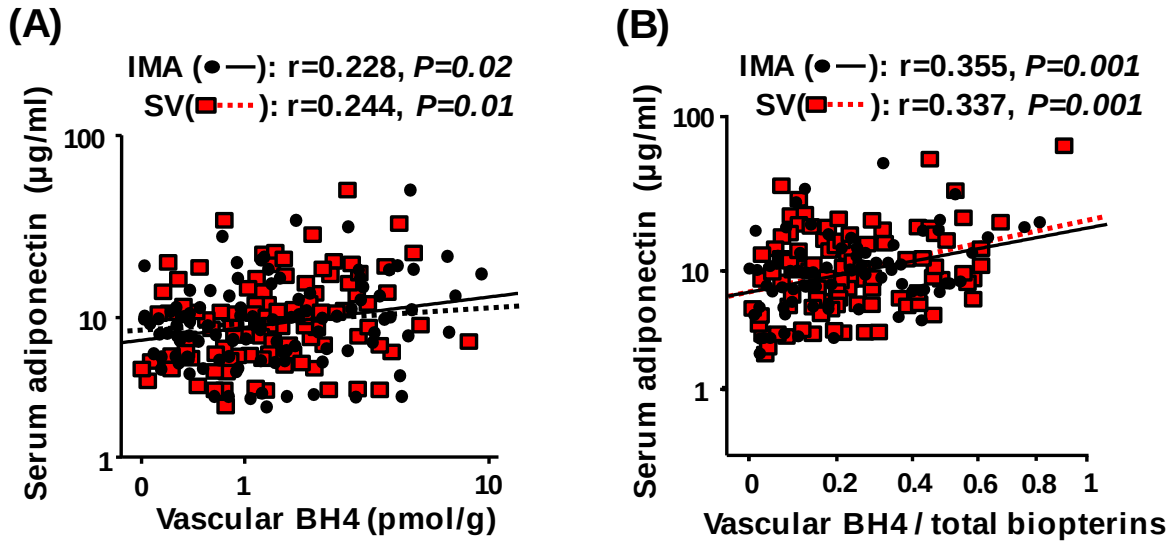


Figure 3.24: *Circulating AdN was significantly positively correlated with vascular tetrahydrobiopterin content (BH_4, Panel A) and BH_4/total biopterins ratio (Panel B) in both saphenous veins (SV) and internal mammary arteries (IMA) from n=173 patients in Phase I of the Oxford CABG Bioresource. Bivariate analysis on log-transformed values was performed and Pearson's r co-efficient was calculated.* ***(Margaritis et al. Circulation 2013;127(22):2209-21)***

To establish whether there is a true causal association between adiponectin and increased vascular BH4, I employed the *ex vivo* vascular mechanistic model: I incubated human SVs and IMAs with adiponectin 10 μg/ml for 6h and then measured vascular BH4 using the HPLC method described in paragraph 3.2.1 of this chapter. Adiponectin caused a significant increase in vascular BH4 (Figure 3.25, Panels A&B), as well as the BH4/total

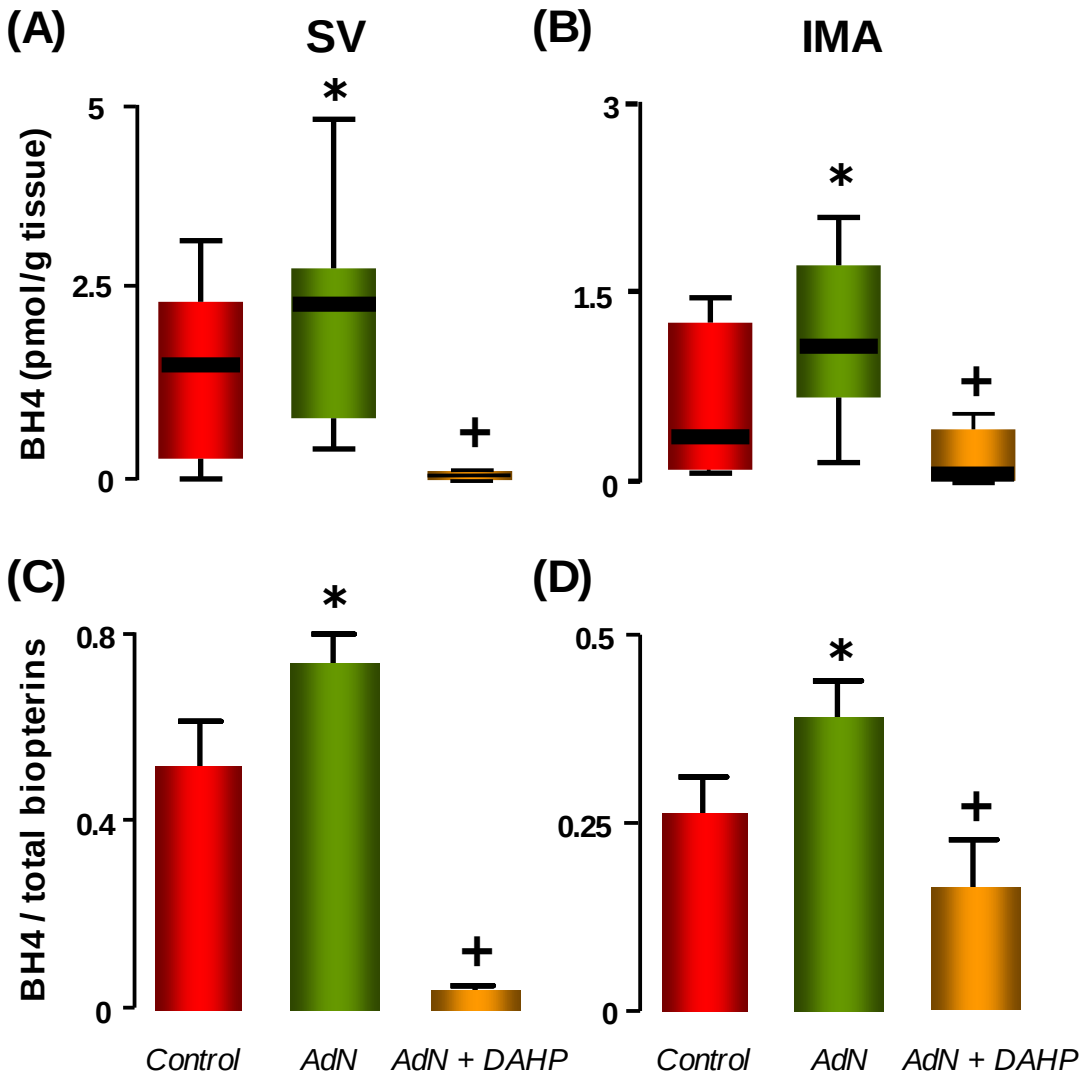


Figure 3.25: *Ex vivo incubation of serial saphenous vein (SV, n=13) and internal mammary arteries (IMA, n=7) rings with adiponectin (AdN) 10μg/ml for 6 hours significantly increased vascular BH_4 (Panels A and B) and BH4/total biopterins ratio (Panels C and D. Both vascular BH_4 and BH_4/total Biopterins ratio were significantly reduced by DAHP 1 mM. Values are expressed as median [25^{th}-75^{th} percentiles] (Panels A&B) and as mean ± SEM (Panels C&D). *P<0.05 vs control; +P<0.05 vs adiponectin* ***(Margaritis et al. Circulation 2013:127(22):2209-21)***

biopterins ratio (Figure 3.25, Panels C&D). Inhibition of GTP-cyclohydrolase with DAHP resulted in the expected reduction of vascular BH4 levels, even in the presence of adiponectin.

Interestingly, total biopterin levels were unchanged (P=NS) after incubation with adiponectin, suggesting that adiponectin "protects" BH4 from oxidation through antioxidant mechanisms, rather than through an increase in its total biosynthesis. This is strongly supported by the fact that adiponectin displays NADPH-oxidases suppressing capabilities, as shown in paragraphs 3.3.3.2 to 3.3.3.4.

3.4 Discussion

In this chapter, I examined the role of circulating adiponectin in the regulation of vascular redox state in patients with atherosclerosis. I demonstrated for the first time in humans that serum adiponectin is linked to improved endothelial function and is inversely related with vascular $O_2^{\cdot -}$ generation, NADPH-oxidases activity and uncoupled eNOS levels in human arteries and veins, independently of atherosclerosis risk factors. The causal relationship behind high adiponectin levels and reduced vascular oxidative stress was confirmed through Mendelian randomization: genetic variability of the *ADIPOQ* locus predisposing towards higher circulating adiponectin levels is linked to improved endothelial function, reduced vascular $O_2^{\cdot -}$ generation, reduced NADPH-oxidases activity and improved eNOS coupling in human vessels. By employing an *ex vivo* tissue model, I demonstrated for the first time in humans that adiponectin directly suppresses NADPH-oxidases through a PI3K/Akt-mediated double mechanism: acutely by reducing activation of Rac1 and its subsequent translocation to the membrane, and subacutely by reducing $p22^{phox}$ gene and protein expression. I also showed that the effect of adiponectin on eNOS coupling is mediated by its combined impact on PI3/Akt-mediated phosphorylation of eNOS at Ser1177 and increased vascular BH4 bioavailability.

3.4.1 Adiponectin and the subcellular mechanisms mediating its effects

My experiments provide evidence for a direct NADPH-oxidases suppressing effect of adiponectin in the human vasculature, leading to reduced vascular oxidative stress. Studies on adiponectin-knockout mice[81] corroborate these findings by showing increased NADPH-oxidases activity in these animals. In this chapter, I demonstrated two distinct mechanisms that lead to reduced NADPH-oxidases activation by adiponectin. The first one is a reduction in activation of Rac1. Indeed, adiponectin has been described in the literature as a regulator of various small G-proteins. One of the downstream effectors of adiponectin, APPL1, has been shown to interact with the small GTP-binding protein Rab5, leading to increased GLUT4 membrane translocation[93]. Similarly, adiponectin has been shown to trigger pro-survival pathways through activation of the small GTP-binding protein Ras[196]. My results show that adiponectin has the ability to "switch" Rac1 to its inactive GDP-bound form, an effect reversed by wortmannin, suggesting involvement of Akt in this pathway. In a study by Kwon et al.[197], Akt was shown to reduce Rac1-GTP binding through phosphorylation at Ser71 of Rac1, by directly inhibiting its GTP-binding activity without any significant change in GTP-ase activity. My data are in line with this study: they show that inhibiting the adiponectin-induced activation of Akt using wortmannin also prevents the switch of Rac1 to its inactive GDP-bound form.

The second mechanism leading to reduced NADPH-oxidases activation by adiponectin is a reduction in expression of the $p22^{phox}$ subunit of the enzymatic complex. Several studies have shown that adiponectin knock-out mice exhibit aggravated increases in $p22^{phox}$ mRNA levels after exposure to angiotensin II, compared to wild-type animals exposed to angiotensin II[198, 199]. A recent study by Fujishima et al.[200] showed that adiponectin knock-out mice display a marked up-regulation of $p22^{phox}$ expression which is prevented by supplementation with adiponectin. These effects of adiponectin are mediated

by activation of an Akt/GSK3β/β-catenin pathway. It is possible that similar Akt-dependent pathways displaying the ability to modify gene expression are active in the human vasculature; my data shows for the first time in humans that the effects of adiponectin on $p22^{phox}$ gene expression in human arteries are reversed by wortmannin, suggesting that Akt is critically involved in this process.

In addition to Akt, AMPK has been shown to be an important mediator of the vascular effects of adiponectin in cell culture and animal studies. A direct stimulation of NO production by eNOS has been demonstrated in adiponectin-treated bovine aortic endothelial cell cultures, mediated through increased phosphorylation of eNOS by AMPK[125]. In an obese rat model, globular adiponectin increased vascular eNOS activity through AMPK-mediated phosphorylation of the enzyme[138]. Despite these observations, I was unable to document a significant effect of adiponectin on AMPK activity in human vascular tissue, as demonstrated by phosphorylation of its activation site Thr172. There could be several explanations for this finding. Firstly, this could be due to the fact that human physiology is different to animal physiology, thus highlighting the potential pitfalls of animal studies. Secondly, in my experiments I used whole vascular tissue homogenates, without isolating the endothelial cells from the vascular smooth muscle cells (VSMCs). Therefore, an effect of adiponectin on AMPK may indeed be present in humans but that effect could be confined to the vascular endothelium alone, and would therefore be massively diluted by the presence of VSMC AMPK in my tissue homogenates. Interestingly, Ouchi et al.[193] have reported that adiponectin mediates its angiogenic effects by promoting a cross-talk between AMPK and Akt signaling in human umbilical vein endothelial cells. A similar interplay between the two molecular pathways could be relevant to human vascular tissue as well.

3.4.2 Adiponectin and endothelial dysfunction in human atherosclerosis

Adiponectin is an adipokine with antiatherogenic properties in experimental models, but has a controversial role in the clinical setting.[81] Although circulating adiponectin is reduced in obesity[201] and is related with reduced cardiovascular risk in the general population,[142] increased circulating adiponectin is inversely correlated with mortality and the overall clinical outcome in advanced cardiovascular disease states such as heart failure.[202] Moreover, pharmacological treatments that improve endothelial function and reduce cardiovascular risk (such as lipophilic statins) appear to reduce circulating adiponectin in patients with hypercholesterolaemia.[203, 204] This discordance between experimental data and clinical observations has introduced the concept that adiponectin may behave as a "rescue hormone" in advanced disease states.[81]

Experimental evidence suggests that adiponectin stimulates eNOS-derived NO production in endothelial cells through stimulation of PI3/Akt-mediated eNOS phosphorylation.[128, 205] In keeping with these first observations from cell culture models, adiponectin knock-out mice exhibit reduced eNOS phosphorylation status (at Ser1177) and impaired endothelial function.[130] In clinical studies, circulating adiponectin is directly related with endothelial function in the general population,[206] but this association is reversed in patients with type 2 diabetes mellitus and diabetic nephropathy,[207] introducing further controversy into the role of adiponectin in different clinical disease states.

In this chapter, I have demonstrated that serum levels of adiponectin are an independent predictor of endothelial function in the Oxford CABG Bioresource, a well-phenotyped cohort of patients with coronary artery disease without renal or heart failure. To further investigate the molecular mechanisms underlying this observation, I exposed human SVs and IMAs to AdN *ex vivo* and observed a rapid PI3/Akt-mediated increase in eNOS phosphorylation at Ser1177, which is known to activate the enzyme.[188, 208]

Although eNOS is the source of NO in the vascular endothelium, deficiency of its co-factor BH4 leads to its uncoupling, turning it into a source of $O_2^{\cdot -}$ instead of NO. Evidence from cell culture models suggests that activation of eNOS via Ser1177 phosphorylation, leads to either increased $O_2^{\cdot -}$ or NO, depending on the underlying coupling status of the enzyme.[188] Given that vascular BH4 is oxidised by free radicals and the balance between its synthesis and oxidation defines its net bioavailability,[185] any change in vascular redox state could drive eNOS uncoupling and trigger a pro-atherogenic vicious cycle. In this chapter, I demonstrated for the first time in humans that adiponectin increases vascular BH4 through a PI3K/Akt mediated mechanism. It is very likely that the NADPH-oxidases-suppressing effect of adiponectin plays a crucial role in protecting vascular BH4 against oxidative degradation, by reducing total vascular $O_2^{\cdot -}$ production. Indeed, my experiments showed that total biopterin levels are unchanged after incubation with adiponectin, suggesting that adiponectin "protects" BH4 from oxidation through antioxidant mechanisms, rather than through an increase in its synthesis.

Previous reports suggest that BH4 administration increases circulating adiponectin in an animal model.[209] In this chapter, I found evidence of a weak but significant positive correlation between serum levels of adiponectin and vascular BH4 content in veins and arteries. Although the biological significance of circulating adiponectin in the regulation of vascular BH4 bioavailability in humans *in vivo* needs further validation, my finding is compatible with the strong association observed between circulating adiponectin and eNOS coupling in human arteries and veins. Therefore it is likely that even this rather "weak" effect of adiponectin on vascular biopterins may have a significant impact on eNOS coupling *in vivo*. The combined increased phosphorylation of eNOS and its enzymatic coupling could be the driving force behind the striking association between high levels of circulating adiponectin and improved endothelial function in humans.

3.5 Conclusions

Adiponectin has direct antioxidant effects on the vascular wall. It suppresses NADPH-oxidases activity, increases vascular BH4 content, thus improving eNOS coupling, and increases activity of eNOS through a PI3K/Akt-mediated mechanism. The result is an increase in NO bioavailability, which manifests as improved endothelial function (Figure 3.26). Given that endothelial dysfunction is an important step in the atherosclerotic process, I conclude that adiponectin displays atheroprotective effects in the human vasculature.

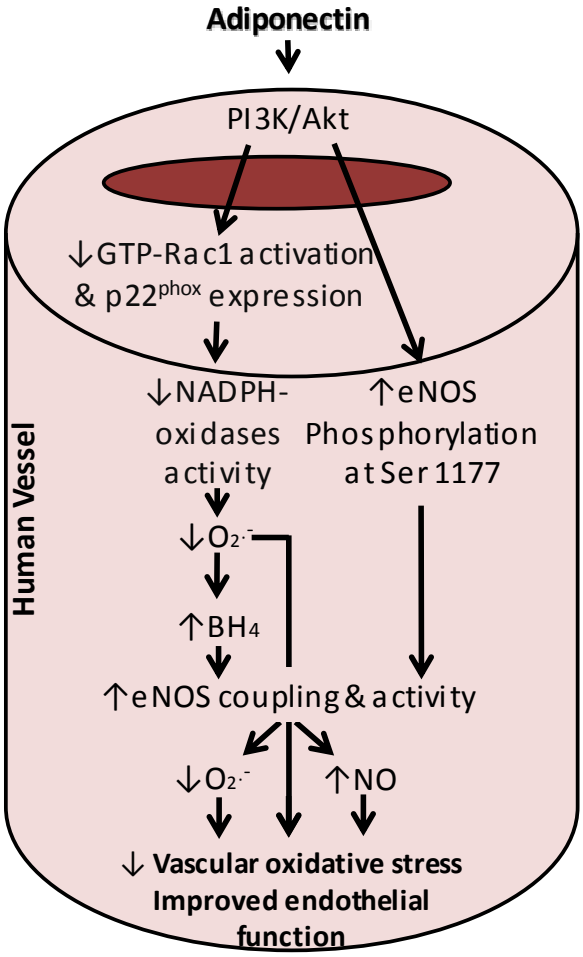


Figure 3.26: *The effects of adiponectin on human vascular redox state & endothelial function.*

Chapter 4
Vascular effects of adiponectin in type 2 diabetes

Chapter 4 outlines the observations in the clinical cohort regarding the association between adiponectin & type 2 diabetes mellitus and explores the existence of vascular adiponectin resistance in the presence of this important cardiovascular risk factor.

4.1 Introduction

It is well-established that circulating levels of adiponectin are reduced in type 2 diabetes and obesity [81]. While some studies support a causal link between low adiponectin and impaired glucose tolerance[210] others have failed to find such evidence[211]. Low circulating adiponectin levels have been associated with increased cardiovascular risk and future incidence of type 2 diabetes in healthy individuals[192]. However, in already established advanced cardiovascular disease states, circulating adiponectin is increased as a "stress hormone", high levels of which become predictive of adverse clinical outcome[212].

The presence of diabetes has been related to increased activity of NADPH-oxidases in the vascular wall[213]; this phenomenon is considered to play a key role in the development of vascular complications of type 2 diabetes[214]. To make matters worse, the presence of type 2 diabetes has been linked to adiponectin "resistance" in peripheral tissues (adipose tissue and skeletal muscle), due to reduced expression of adiponectin receptors[103]. However, it is unclear whether such a mechanism is relevant to human vascular pathophysiology. Given the ability of adiponectin to suppress NADPH-oxidases activity that I demonstrated in the previous chapter, I sought to explore the vascular effects of adiponectin in the presence or absence of type 2 diabetes and to investigate the existence of vascular adiponectin "resistance" in diabetic patients.

4.2 Study population - Methods

Unless otherwise specified, the chapter employs a subset of phase I of the Oxford CABG Bioresource; it includes all patients for whom full data on metabolic risk factors (insulin, glucose, cholesterol) as well as IMA O_2^- measurements were available (Table 4.1). *Ex vivo* experiments were performed on samples from AdipoRedox study patients.

Table 4.1: Demographic characteristics of study participants

	Clinical Cohort	***Ex vivo* studies**
Participants (n)	386	67
Age (years)	65.8±0.5	65.5±1.3
Male gender (%)	83.7	97.0
Hypertension (%)	68.9	76.1
Hyperlipidaemia (%)	62.4	77.6
Type 2 diabetes (%)	32.9	26.9
Smoking (active/ex) (%)	22.8/46.6	4.4/59.7
Body mass index (Kg/m^2)	27.7±0.2	29.4±0.5
Cholesterol (mg/dl)	177.3±2.4	146.9±12.4
Glucose (mg/dl)	125.4±3.1	97.2±5.4
Insulin (µU/ml)	15.49±1.43	13.98±2.01
HOMA-IR	5.39±0.54	3.36±0.03
High density lipoprotein (mg/dl)	38.8±0.6	42.5±7.7
Triglycerides (mg/dl)	141.4±4.9	149.7±40.7
Serum adiponectin (µg/ml)	11.2 [5.1-42.3]	-
Medication (%)		
ACEi	58.5	46.2
ARBs	9.8	16.4
Beta blockers	75.3	88.0
Aspirin/Clopidogrel	82.1	93.6
Statins	78.2	88.0
CCBs	24.9	41.7
Metformin/Oral hypogylcaemics	32.9	26.9
Insulin	19.6	17.3

ACEi: Angiotensin converting enzyme inhibitors; ARBs: Angiotensin receptor blockers; CCBs: Calcium channel blockers. HOMA-IR: Homeostatic model of insulin resistance.

Sample collection, vascular superoxide measurements, biomarker measurements, Western immunoblotting, genotyping, gene expression studies were performed as described in the Methods chapter. Statistical analysis was performed as described in Chapters 2 & 3. Additional techniques employed in this chapter only are presented below.

4.2.1 Total antioxidant capacity measurements

Total antioxidant capacity (TAC) is a measure of the cumulative effects of the antioxidants present in a biological fluid or tissue homogenate [215]. It is not a simple sum of all the known and unknown antioxidants contained, but rather an integrated parameter which reflects the complex interactions among these substances and their effect on the redox balance of the sample[216]. While unable to measure either the activity of endogenous antioxidant enzymes (SOD, catalase etc.) or metal binding proteins[217], TAC assays measure the contribution of low molecular weight antioxidants, which possess the ability to break oxidation chain reactions, namely the water-soluble urate, conjugated bilirubin, vitamin C and thiols, as well as the lipid-soluble flavonoids, carotenoids and vitamin E. Therefore, while not representing the actual total antioxidant capabilities of each biological sample, TAC measurements can serve as an efficient tool for evaluating differences in oxidant status among different samples[218].

There are several assays that can be employed to estimate TAC. In my study, in order to investigate differences in the total antioxidant capacity of IMAs from patients with/without type 2 diabetes, a commercially available kit was used (Cell Biolabs, San Diego, CA). This kit quantifies Cu^{2+}-reducing equivalent/mg protein as an index of the overall antioxidant capacity of the tissue. The Cu^{2+} ion is converted to Cu^{+} by low-molecular weight antioxidants and the reduced Cu^{+} ion is chelated with a colorimetric probe, giving a broad absorbance peak around 570 nm, proportional to the TAC.

4.3 Results

4.3.1 Adiponectin genetic variability, type 2 diabetes and atherosclerosis

I first explored the association between serum adiponectin levels and insulin resistance (IR), as defined by HOMA-IR >2.7 (based on previously published studies[219, 220]), and type 2 diabetes in the clinical cohort. I found that both are associated with reduced circulating adiponectin levels, in keeping with the results widely reported in the literature[81] (Figure 4.1).

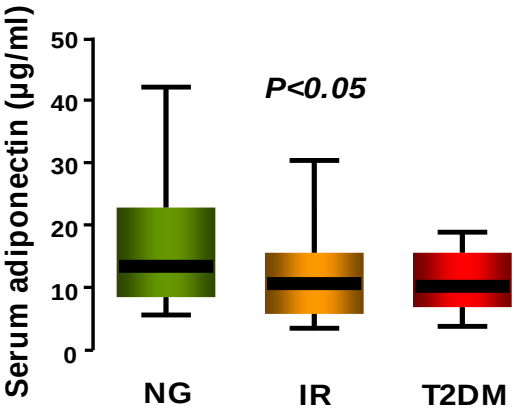


Figure 4.1: *Patients with insulin resistance (IR) or type 2 diabetes mellitus (T2DM) had significantly lower serum levels of adiponectin in their circulation (n=368). Values are expressed as median [25th-75th percentile].* ***(Margaritis et al. Diabetes 2015;64(6):2207-19)***

In Chapter 3, I described the design of a Mendelian randomization study based on the genetic variability of the *ADIPOQ* locus. I showed that the additive effect of rs266717T and rs17366568G alleles was associated with adiponectin levels, as well as vascular $O_2^{\cdot -}$ and endothelial function. This delineates a causal relationship between adiponectin levels and vascular phenotype.

Given the relationship between adiponectin and diabetes, I performed additional analysis on this model to uncover links between the genetic variability of the *ADIPOQ* locus and metabolic risk factors affecting cardiovascular risk. Firstly, I observed that the additive number of rs17366568G and rs266717T alleles was associated with lower body mass index (BMI) (Figure 4.2).

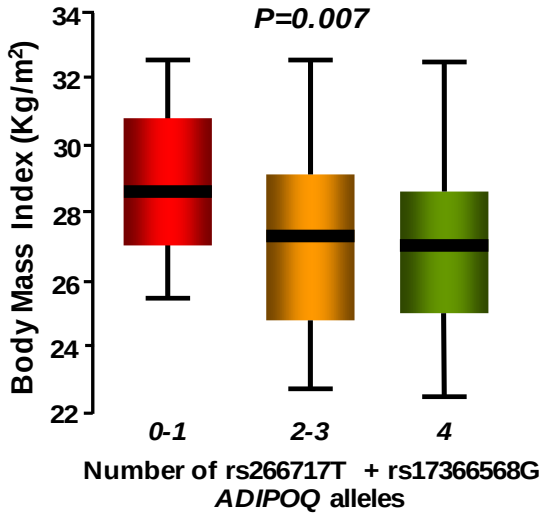


Figure 4.2: *The number of rs266717T and rs17366568G alleles was linked to reduced body mass index in the clinical cohort (n=368). Values are expressed as median [25th-75th percentile].*

Furthermore, the additive effect of these alleles was also associated with reduced presence of type 2 diabetes in the Oxford CABG Bioresource Phase I population (Figure 4.3). These observations seem to support the notion that the genetic variability of the *ADIPOQ* locus could be a risk factor for development of obesity and type 2 diabetes.

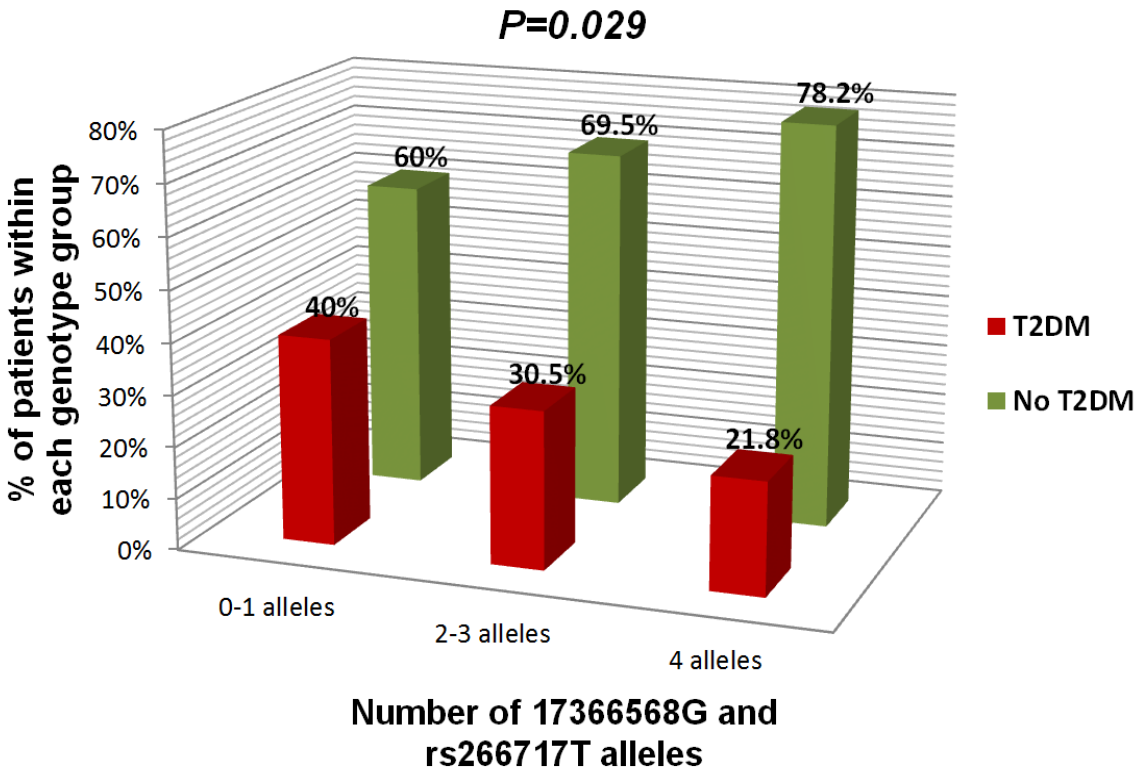


Figure 4.3: *Across the study population enrolled in the Oxford CABG Bioresource, there were a greater proportion of diabetic patients (T2DM) among the participants with 0-1 alleles compared to those with 4 alleles. P value derived from Pearson's* χ^2 *test. Values are expressed as % of total study population within each genotype group (n=677).*

Given that obesity and type 2 diabetes are important risk factors for development of coronary artery disease, I then sought to establish whether there might be an association between the genetic variability of the *ADIPOQ* locus and angiographic extent of coronary atherosclerosis (classified as 1, 2 or 3 coronary arteries with significant stenosis >50%). This information was obtained from the study subjects' medical records. As expected for patients undergoing elective CABG surgery, the proportion of individuals with triple vessel disease (63.7%) was higher compared to individuals with 2-vessel (24.3%) or single

vessel disease (12%). Interestingly, I observed that the additive effect of the rs17366568G and rs266717T alleles was inversely correlated with the extent of coronary artery disease, as documented by higher proportion of patients suffering from triple-vessel disease among those study subjects bearing none or 1 of the high-adiponectin-related alleles (Figure 4.4).

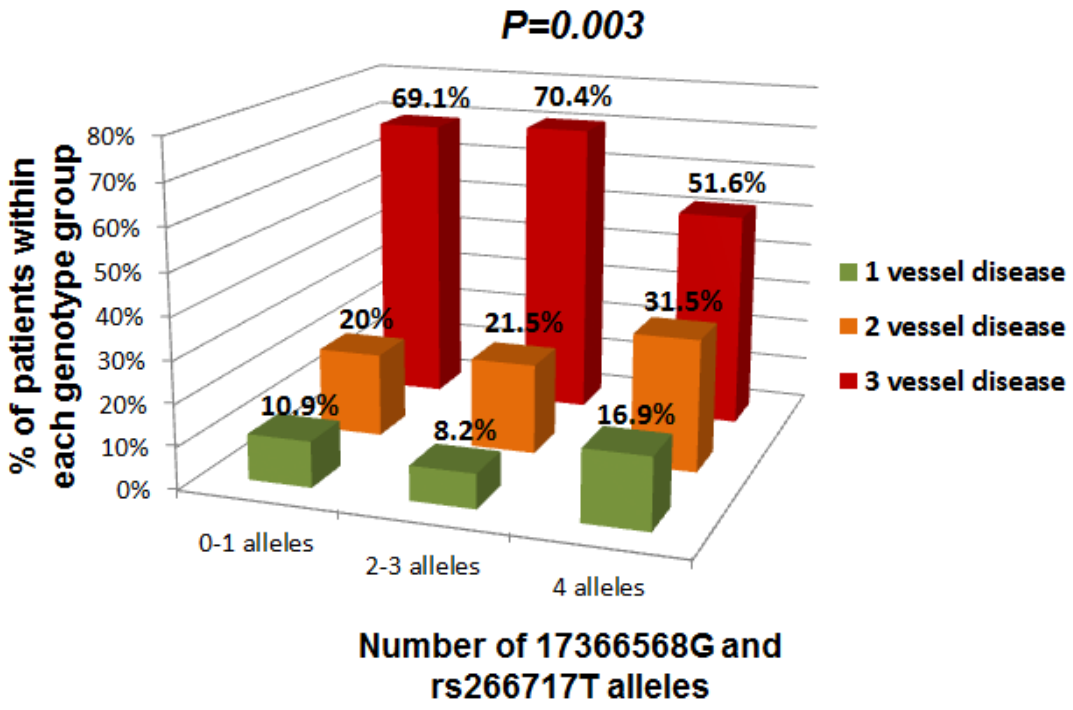


Figure 4.4: *There were a significantly lower proportion of patients with triple vessel disease among patients undergoing CABG whose genotype bears 4 of the rs17366568G and rs266717T alleles, compared to patients with 0-1 of these alleles. P value derived from Pearson's χ^2 test. Values are expressed as % of total study population within each genotype group (n=677).*

However, these associations do not show a direct causal link between *ADIPOQ* genotypes and the extent of coronary atherosclerosis, because the impact of this genotype on the atherosclerotic burden could be confounded via its impact on type 2 diabetes or obesity risk shown previously. To further explore this finding, multivariable analysis was performed in which the angiographic extent of coronary artery disease was used as the dependent variable. As independent variables I used the *ADIPOQ* genotype, along with those of the patients' clinical characteristics (BMI, age, gender and risk factors such as

hypercholesterolemia, type 2 diabetes and smoking) that showed an association with the dependent variable at the level of $P < 0.1$ in univariate analysis. The analysis was followed by a backward elimination procedure using the threshold of 0.1 to remove variables from the model. I found that the strongest independent predictors of the angiographic extent of coronary artery disease in this cohort were the rs266717/rs17366568 genotype (β(SE):-0.124(0.051), P=0.016), smoking (β(SE): 102(0.041) P=0.012), female gender (β(SE): 0.170(0.078), P=0.029) and type 2 diabetes (β(SE): 0.207(0.065), P=0.001). These results show that the genetic variability of ADIPOQ is associated with the severity of coronary atherosclerosis independently of conventional risk factors such as diabetes and raised BMI. As such, they lend support to the notion that the atheroprotective effects of adiponectin on the vasculature (demonstrated in Chapter 3) are not affected by the presence of type 2 diabetes.

4.3.2 Exploring vascular adiponectin "resistance" in diabetic patients

The experimental observations and conclusions derived in the previous paragraph would seem to contrast existing literature reports which describe adiponectin resistance in skeletal muscle and adipocytes in the presence of diabetes[103], as mentioned in the introduction of this chapter.

To investigate this conundrum further, the initial step was to explore the effects of type 2 diabetes on vascular redox state and more specifically the role of NADPH-oxidases, as well as the cellular pathways mediating these effects. Then, by employing the *ex vivo* mechanistic vascular tissue culture model used in Chapter 3, I looked at whether the antioxidant effects of adiponectin documented previously persist in the presence of diabetes or are blunted due to the vascular pathophysiological changes caused by this disease-state.

4.3.2.1 Vascular and systemic oxidative stress in type 2 diabetes

I first sought to establish the relationship between presence of type 2 diabetes and NADPH-oxidases activity in the human arterial wall in patients enrolled in the Oxford CABG Bioresource. I observed that insulin resistance and type 2 diabetes were associated with increased NADPH-stimulated $O_2^{\cdot -}$ generation in the human IMA (Figure 4.5, Panel A), which can be used to estimate NADPH-oxidases activity in the vasculature. These results are in keeping with reports suggesting increased activity of this pro-oxidant enzyme in the presence of diabetes[214]. In addition, IMAs from patients with type 2 diabetes also displayed significantly reduced total antioxidant capacity (Figure 4.5, Panel B), suggesting depletion of endogenous vascular antioxidant systems in diabetes.

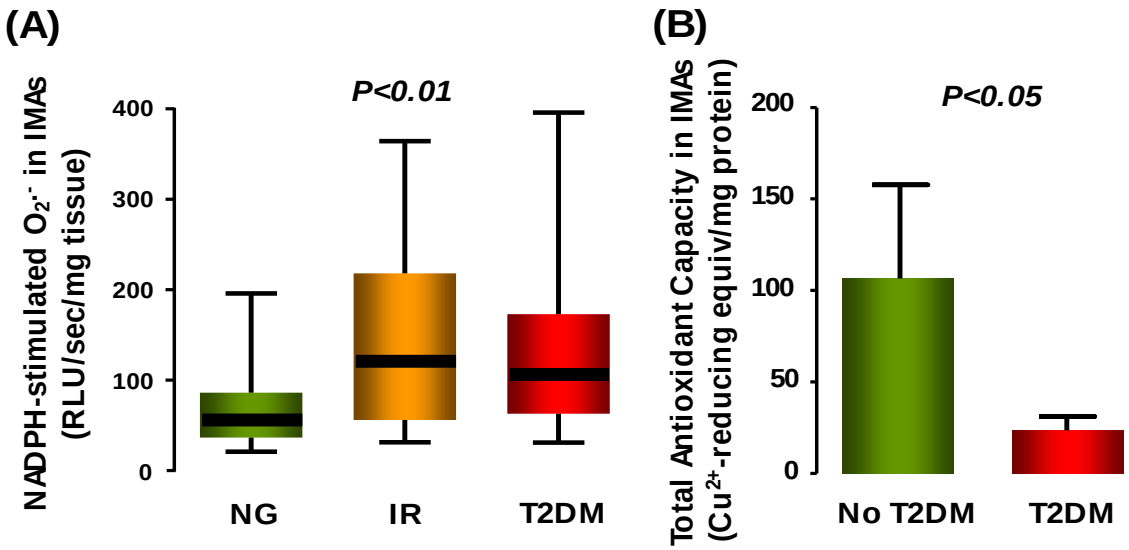


Figure 4.5: *Presence of insulin resistance (IR) or type 2 diabetes mellitus (T2DM) was associated with significantly higher NADPH-stimulated superoxide ($O_2^{\cdot -}$) generation in the vascular wall of the internal mammary artery (IMA, n=386, Panel A). Similarly, IMAs obtained from patients with T2DM (n=4) had significantly lower total antioxidant capacity compared to non-diabetic patients (n=4). Values are expressed as median [25th-75th percentile] (Panel A) and mean ± SEM (Panel B).* ***(Margaritis et al. Diabetes 2015;64(6):2207-19)***

However, I did not observe any significant association between insulin resistance or type 2 diabetes and circulating malonyldialdehyde (MDA, Figure 4.6, Panel A) or 4-hydroxynonenal (4-HNE, Figure 4.6, Panel B), both markers of systemic oxidative stress. This would imply that the impact of type 2 diabetes and insulin resistance on vascular redox state cannot be accurately monitored by circulating biomarkers of oxidative stress.

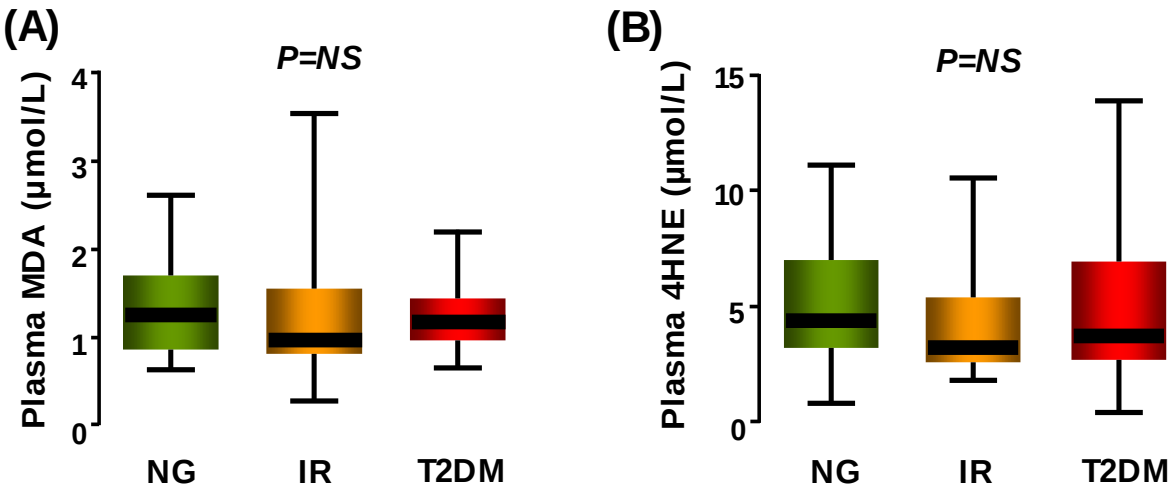


Figure 4.6: *There was no significant association between insulin resistance (IR)/type 2 diabetes (T2DM) and plasma malonyldialdehyde (MDA) (Panel A) or 4-hydroxynonenal (4-HNE) levels (Panel B), both markers of systemic oxidative stress (n=386). Values are expressed as median [25th-75th percentile].* ***(Margaritis et al. Diabetes 2015;64(6):2207-19)***

In addition, I was unable to find any significant correlation between plasma MDA levels and NADPH-stimulated $O_2 \cdot^-$ generation in IMAs from the same patients (r=0.076, P=0.448). This would suggest that NADPH-oxidases activity in the IMA is independent of what is conventionally defined as "systemic oxidative stress".

4.3.2.2 Mechanisms of increased NADPH-oxidases activity in type 2 diabetes

To explore the mechanisms leading to increased NADPH-oxidases activity in the presence of type 2 diabetes, I collected IMA samples from patients with or without diabetes and performed differential centrifugation, membrane protein isolation and Western immunoblotting by using the techniques mentioned in Chapter 2. I established that presence of type 2 diabetes was related with increased membrane translocation of the cytosolic subunits $p47^{phox}$ and Rac1, which form part of the NOX1 and NOX2-containing isoforms of NADPH-oxidase in the vascular wall (Figure 4.7). This would explain the increased NADPH-stimulated $O_2\cdot^-$ generation in the IMA wall observed in diabetic patients in the clinical cohort.

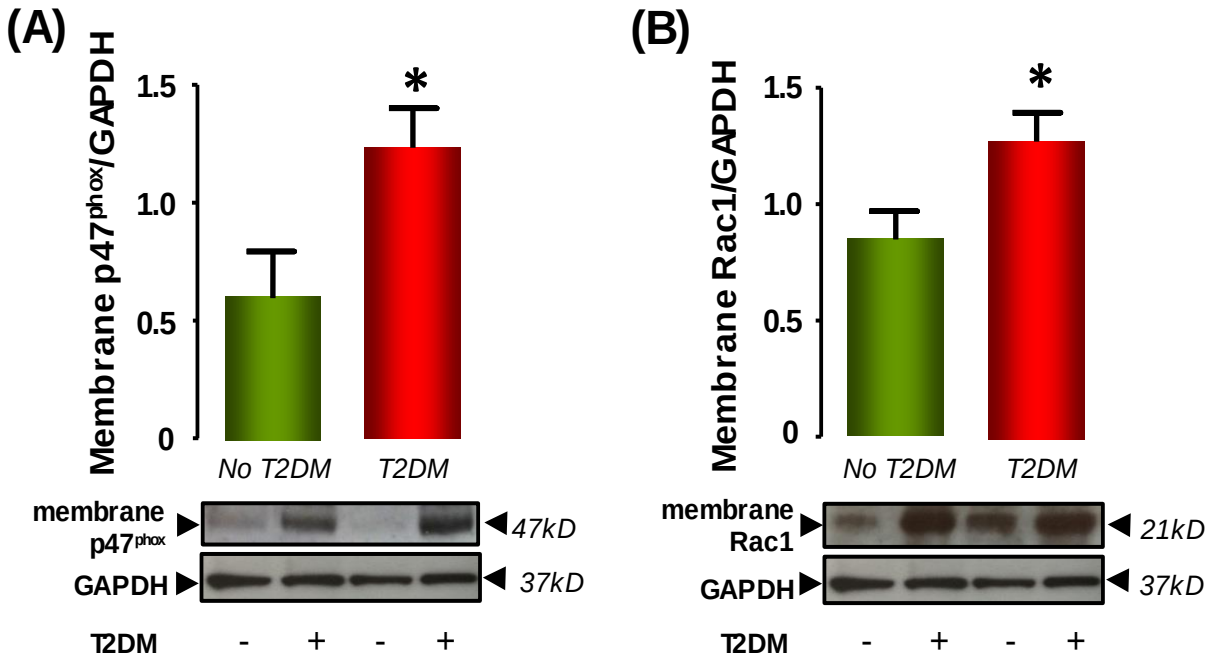


Figure 4.7: *Membrane translocation of $p47^{phox}$ subunit of NADPH-oxidases (Panel A) and Rac1 (Panel B) was significantly higher in internal mammary arteries (IMAs) from patients with type 2 diabetes (T2DM, n=4) compared to patients without T2DM (n=5). Values are expressed as mean ± SEM. Representative blots from four patients.*P<0.05 versus no T2DM.* ***(Margaritis et al. Diabetes 2015;64(6):2207-19)***

Decreased activity of the PI3K/Akt pathway in skeletal muscle and adipose tissue, manifested by reduced Akt phosphorylation, is a hallmark of diabetes and is linked to insulin resistance[221]. I hypothesized that activity of the PI3K/Akt pathway might also be blunted in human internal mammary artery tissue from diabetic patients compared to non-diabetic patients. Indeed, after performing Western immunoblotting, I observed reduced reduced Akt phosphorylation at Ser473 in IMAs obtained from CABG patients with type 2 diabetes compared to those without diabetes (Figure 4.8).

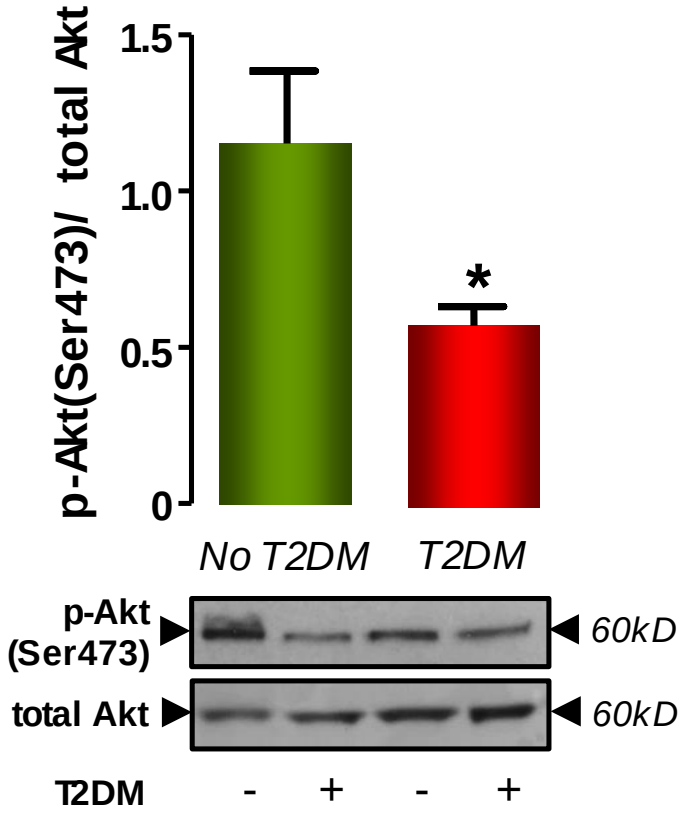


Figure 4.8: *The ratio of phosphorylated Akt at Ser473 (p-Akt) to total Akt was significantly lower in internal mammary arteries from patients with type 2 diabetes (T2DM, n=4) compared to those with no T2DM (n=5), suggesting reduced activity of Akt in the presence of T2DM. Values are expressed as mean ± SEM. Representative blots from four patients.*P<0.05 versus no T2DM.* ***(Margaritis et al. Diabetes 2015;64(6):2207-19)***

Taken together, these results lead to the conclusion that activity of the PI3K/Akt pathway is indeed reduced in the vascular wall of diabetic patients, and this is associated with increased activity of NADPH-oxidases and increased oxidative stress.

4.3.2.3 Exploring vascular adiponectin "resistance" in type 2 diabetes

In the previous Chapter, I presented the results from *ex vivo* experiments in which I exposed paired vascular samples to human recombinant adiponectin 10 μg/ml for 6 hours and/or 18 hours and documented direct NADPH-oxidases-suppressing effects mediated by the PI3K/Akt pathway. In those experiments, I did not select the patients *a priori* based on presence or absence of type 2 diabetes, or indeed other risk factors. Having demonstrated in the previous paragraph (4.3.2.2) that diabetes is associated with reduced activation of the PI3K/Akt pathway and increased NAPDH-stimulated $O_2^{\cdot -}$ generation in the IMA wall, I hypothesized that the vascular antioxidant effects of adiponectin might be blunted in the presence of diabetes.

There are several mechanisms through which diabetes-induced vascular adiponectin "resistance" might be mediated. Firstly, the expression of adiponectin receptors AdipoR1, AdipoR2 and T-cadherin may be reduced in the vascular wall of patients suffering from type 2 diabetes. This would, in turn, lead to diminished ability of adiponectin to exert its receptor-mediated effects. To explore this hypothesis, I first performed gene expression studies in vascular tissue samples obtained from patients belonging to the AdipoRedox study. I extracted RNA from internal mammary artery tissue which had been frozen as part of the Oxford CABG Bioresource and performed qRT-PCR to quantify the relative gene expression of the adiponectin receptors AdipoR1, AdipoR2 and T-cadherin (CDH13). I then grouped the patients based on presence or absence of known diagnosis of type 2 diabetes and compared the gene expression of the genes between the groups.

My results show that there were no significant differences in expression of these gene targets between the two patient groups in this study population (Figure 4.9), even though there was a small observable trend towards reduced expression in patients suffering from type 2 diabetes.

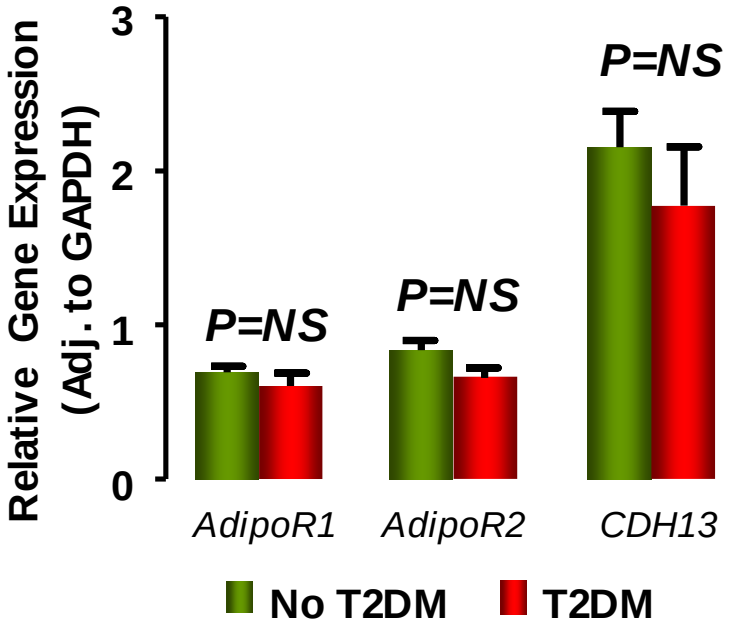


Figure 4.9: *In human internal mammary arteries, the gene expression of adiponectin receptors AdipoR1, AdipoR2 and CDH13 was not different between patients with diabetes (T2DM, n=23) compared to those with no T2DM (n=71). Values are expressed as mean ± SEM.* ***(Margaritis et al. Diabetes 2015;64(6):2207-19)***

Given the fact that the effects of adiponectin are receptor-mediated, a lack of significant difference in their gene expression in the presence of diabetes would imply that the existence of a potential adiponectin resistance would have to be identified in the subcellular mechanisms regulating its vascular actions. I therefore hypothesized that pathophysiological alterations in cellular signalling pathways induced by diabetes could potentially interfere with the ability of adiponectin to activate the PI3K/Akt pathway and thus prevent its antioxidant effects in the vasculature. To explore this second hypothesis, I performed additional paired IMA incubations with/without adiponectin ± wortmannin, using the same experimental design as before, but this time I selected patients *a priori*

based on their diabetic status. I then performed Western immunoblotting and calculated the phospho-Akt (Ser473) to total Akt ratio. I found that adiponectin was able to activate the PI3K/Akt pathway and induce a significant increase in vascular Akt phosphorylation irrespective of the presence of type 2 diabetes (Figure 4.10).

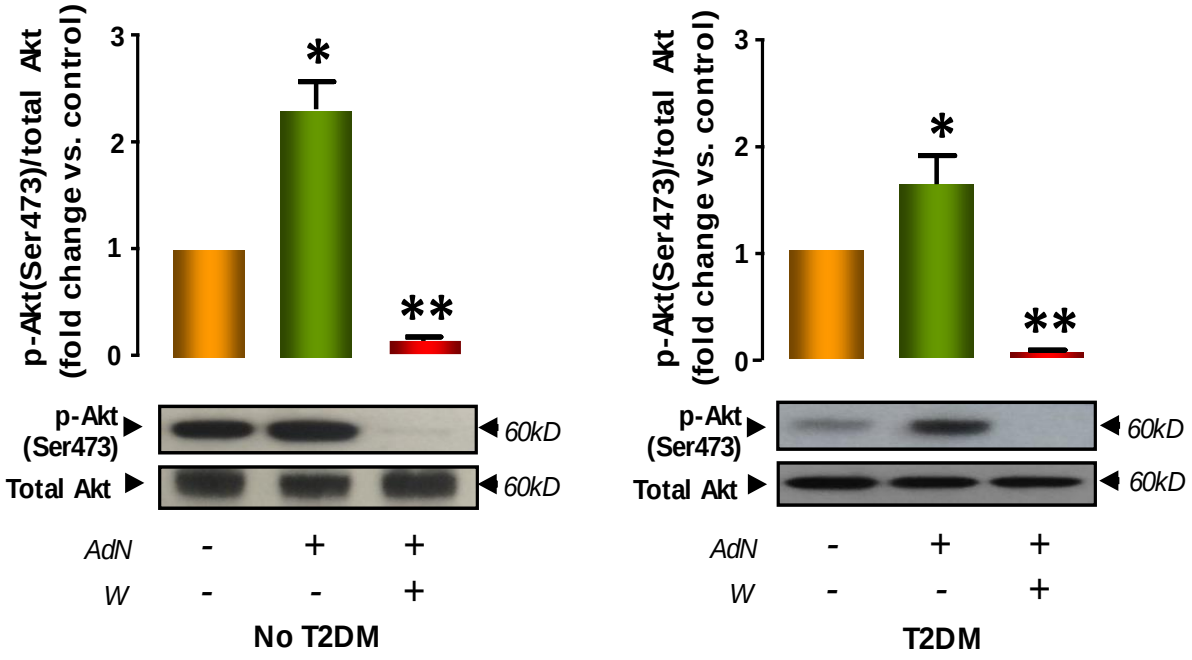


Figure 4.10: *Incubation of serial internal mammary artery segments with adiponectin (AdN, 10μg/ml for 6 hours) increased the p-Akt(Ser473)/total Akt ratio irrespective of presence of type 2 diabetes (T2DM.) As expected, the effect was abolished by exposure to the PI3K/Akt inhibitor wortmannin (W, 100 nmol/L) (n=8). Values are expressed as mean ± SEM. *P<0.05 versus control; **P<0.01 versus control.* ***(Margaritis et al. Diabetes 2015;64(6):2207-19)***

Based on these results, I came to the conclusion that both the vascular adiponectin receptor expression and the ability of adiponectin to induce PI3K/Akt in the vascular wall are unaffected by the presence of diabetes. To fully confirm that adiponectin maintains its vascular antioxidant, atheroprotective effects in diabetic patients, I repeated the *ex vivo* adiponectin incubation luminometry experiments presented in the previous Chapter, but this time I selected patients based on their diabetic status. I found that incubation of IMAs with adiponectin for 6 hours was able to significantly reduce vascular NADPH-stimulated

$O_2^{\cdot-}$ generation irrespective of the presence or absence of diagnosed diabetes in the patients from whom the samples originated (Figure 4.11). Based on these results, I can conclude that type 2 diabetes does not prevent the direct antioxidant effects of adiponectin in the human vasculature.

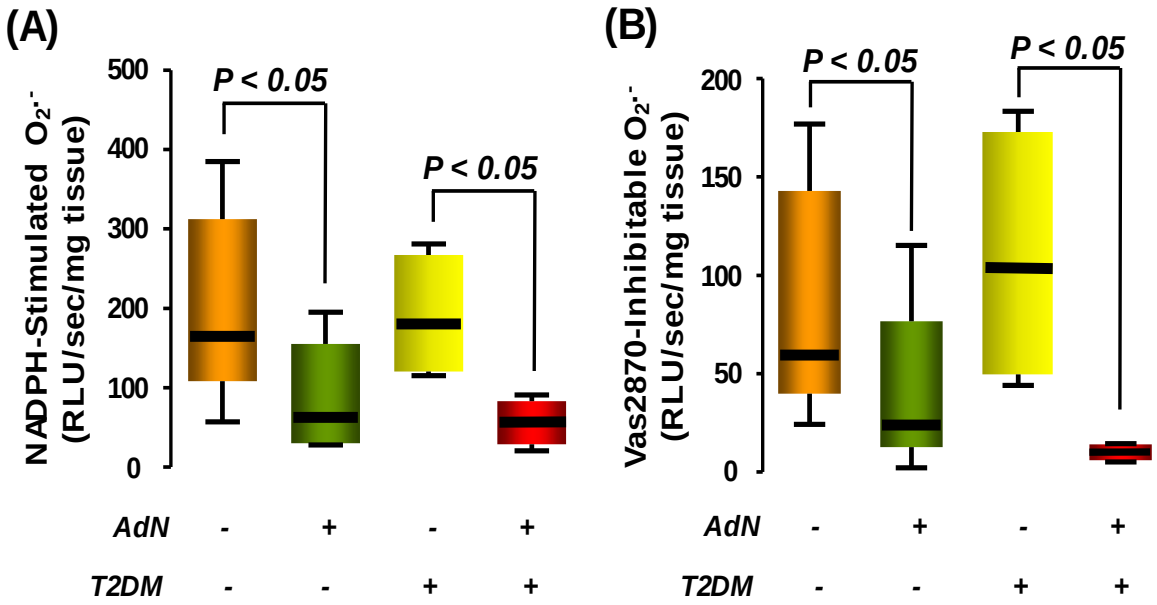


Figure 4.11: *Incubation of serial internal mammary arteries with adiponectin 10 μg/ml for 6 hours led to a significant reduction in NADPH-stimulated (Panel A) and Vas2870-inhibitable (Panel B) superoxide ($O_2^{\cdot-}$) generation, irrespective of presence or absence of type 2 diabetes (T2DM, n=4 and no T2DM, n=5). Values are expressed as median [25th-75th percentile].* ***(Margaritis et al. Diabetes 2015;64(6):2207-19)***

4.4 Discussion

In this chapter, I have shown patients with insulin resistance or type 2 diabetes display reduced serum levels of adiponectin. By using the genetic variability of the ADIPOQ locus, I demonstrated potential causal links between adiponectin and development of type 2 diabetes. Importantly though, the genetic variability of the locus encoding for adiponectin was linked to atherosclerotic burden independently from type 2 diabetes. This observation is fully in accordance with the results from *ex vivo* experiments,

which show increased NADPH-oxidases activity in presence of diabetes, yet preserved ability of exogenously administered adiponectin to exert antioxidant effects.

The link between circulating adiponectin levels and type 2 diabetes has been a matter of extensive study. A meta-analysis by Li et al. showed that higher adiponectin levels in the circulation are associated with lower risk of type 2 diabetes across diverse populations, consistent with a dose-response relationship[109]. However, a Mendelian randomization study failed to identify a causal link between genetically-determined lower circulating adiponectin and type 2 diabetes[211]. It is noteworthy that the 4-SNP model used in that study reportedly accounted for only 4% variation in adiponectin levels in multivariable analysis, which is lower than other studies, where multi-SNP models have accounted for a higher percentage of variation (for example 6.7% in the study by Heid et al.[82]). In a landmark meta-analysis, more than 45,000 multi-ethnic subjects from different GWAS were analysed in order to uncover SNPs influencing circulating adiponectin levels and risk of diabetes. A multi-SNP score was created, which was shown to be associated with increased risk of type 2 diabetes and increased waist-to-hip ratio[222]. Based on these reports, I sought to examine the association between adiponectin levels and insulin resistance/type 2 diabetes in the Oxford CABG Bioresource population. My results show that in this cohort, presence of type 2 diabetes is associated with reduced adiponectin levels in the circulation. What is more, genetic predisposition towards lower adiponectin levels is also linked to higher prevalence of type 2 diabetes, suggesting a potential causal relationship.

High circulating levels of adiponectin have been independently associated with reduced risk of type 2 diabetes in patients who had suffered a myocardial infarction[223], as well as decreased risk of type 2 diabetes and subsequently reduced risk of future cardiovascular events in a community-based prospective cohort of healthy individuals[224].

The Oxford CABG Bioresource population is a cohort of patients with established advanced coronary artery disease. In this population, genetically predetermined lower adiponectin was linked to extent of atherosclerotic burden in the coronary vasculature. Importantly, this association was shown to be independent from presence of type 2 diabetes and other risk factors, leading to the conclusion that adiponectin has direct effects in the vasculature that are not influenced by the presence of diabetes. Indeed, Dastani et al. have shown that adiponectin levels and coronary artery disease display a shared allelic architecture[225]. What is more, I proceeded to show using *ex vivo* tissue models that the ability of adiponectin to suppress NADPH-oxidases activity in human arteries is preserved in type 2 diabetes, and the expression of adiponectin receptors (AdipoR1, AdipoR2 and CDH13) is similar between patients with versus those without type 2 diabetes. Similarly, while vascular Akt activity is reduced in type 2 diabetes, exogenously administered adiponectin is able to activate Akt in the IMA wall.

The above results would seem to suggest that the increased Akt-mediated NADPH-oxidase activity observed in the human arterial wall in type 2 diabetes is not due to impaired responsiveness of these vessels to adiponectin, but mainly due to reduced adiponectin levels in the circulation. Presumably, this is a direct result of reduced production of adiponectin from adipose tissue in diabetic subjects. The mechanisms regulating adiponectin biosynthesis in human adipose tissue and the factors leading to up- or down-regulation are explored extensively in the following chapter.

4.5 Conclusions

Presence of type 2 diabetes is associated with increased oxidative stress in the human arterial wall. However, it is not related to development of vascular adiponectin resistance. The observed increased activity of NADPH-oxidases in diabetic patients is most likely due the reduced circulating levels of adiponectin observed in diabetic patients.

Chapter 5
Adiponectin as a biomarker – Regulation of adiponectin synthesis in adipose tissue

Having established the antioxidant effects of adiponectin through the experiments presented in the previous chapters, this chapter examines the factors influencing production of adiponectin in human adipose tissue and subsequently affecting its circulating levels. It explores the contribution of different adipose tissue depots to the circulating adiponectin pool and, based on those observations, presents findings regarding morphological/functional differences of distinct adipose tissue sites.

5.1 Introduction

The regulation of adiponectin biosynthesis in adipose tissue is complex. Previous studies have shown that exposure of cultured adipocytes to reactive oxygen species[226] or pro-inflammatory cytokines[227, 228] leads to downregulation of adiponectin gene expression. Similarly, induction of severe inflammation in experimental animal models downregulates expression of adiponectin in adipose tissue and reduces circulating adiponectin levels.[229] These observations provide insights into the well-established association between obesity and reduced levels of adiponectin in the circulation[230, 231]: obesity is thought to cause local inflammation and hypoxia in adipose tissue[232], which leads to suppression of adiponectin expression[233] and therefore a reduction in its circulating levels. Obesity has been shown to cause increased recruitment of macrophages to adipose tissue[234], as well as an increase in the ratio of M1-activated macrophages, which are the "classically activated" pro-inflammatory macrophages, versus M2-activated macrophages, which are involved in remodelling/repair of tissues[235, 236].

However, atherosclerosis-related low-grade inflammation has been associated with both increased[237] and decreased[238] circulating adiponectin in humans, while there is also evidence that advanced, chronic inflammation may even increase adiponectin levels.[239, 240] These conflicting findings suggest that mechanisms related with the underlying disease state may override the regulatory role of inflammation on adiponectin biosynthesis in advanced cardiovascular disease-states. Indeed, while high levels of circulating adiponectin are protective against future risk of cardiovascular disease[192], they predict worse clinical outcome in patients with established coronary artery disease (CAD)[202], chronic heart failure[241] and in patients undergoing elective cardiac surgery[242]. It has been proposed that stimulation of adiponectin synthesis by brain natriuretic peptide (BNP), a mechanism which has been demonstrated in cultured adipocytes[243], could explain the increased adiponectin levels in patients with heart failure despite the significant background inflammation. However, this link between BNP and adiponectin biosynthesis has never been demonstrated at the level of human adipose tissue.

5.2 Study population & Methods

A multi-study approach was used to examine the role of BNP and systemic inflammation as a regulator of adiponectin levels in advanced atherosclerosis with/without heart failure. In this chapter, Study 1 is a cross-sectional study, which included 575 subjects: 341 patients with angiographically documented CAD, 201 healthy individuals without any history or clinical signs of CAD and 33 patients with clinical syndrome of heart failure but without CAD (documented by coronary angiography). The patients with CAD were recruited as part of Phase I of the Oxford CABG Bioresource. The healthy volunteers and heart failure patients without CAD were recruited as part of an ongoing study at the 1st Cardiology Unit, University of Athens, Greece. The same inclusion and exclusion criteria as for the Oxford CABG Bioresource were applied. Written informed

consent was obtained for all study subjects. Blood samples were obtained as part of the study; biomarker measurements were performed as described in Chapter 2. Left ventricular ejection fraction (LVEF) was estimated by echocardiography as a routine outpatient measurement; the information was shared with the researchers under the terms of study participation. Endothelial function was estimated by measuring flow-mediated dilatation (FMD) of the brachial artery in subgroups of this population, as described in Chapter 2.

Study 2 is a clinical associations study in patients with known ischaemic heart disease. It consists of 258 patients undergoing CABG surgery, all belonging to phase I of the Oxford CABG Bioresource. This is the population subset mentioned in Chapter 2 (page 51), on which data on adipose tissue phenotype are available; these study subjects were recruited between the period 2007-2011 at the 1st Cardiology Unit, University of Athens Medical School. Sample collection, genotyping, adipose tissue explant cultures, biomarker measurements and gene expression studies were performed as described in Chapter 2. Immunohistochemistry of human adipose tissue sections was carried out as described in paragraph 5.2.1 below.

Study 3 is a mechanistic *ex vivo* study, comprising 13 patients undergoing CABG, recruited in Oxford in 2012-2013 as part of the AdipoRedox study (Phase II of the Oxford CABG Bioresource). The exact design of these experiments is described in the results paragraph of this chapter. Sample collection and gene expression studies were performed as described in Chapter 2.

The study design is summarized in Figure 5.1. Demographic data and measurements of participants for each study are presented in Tables 5.1 and 5.2.

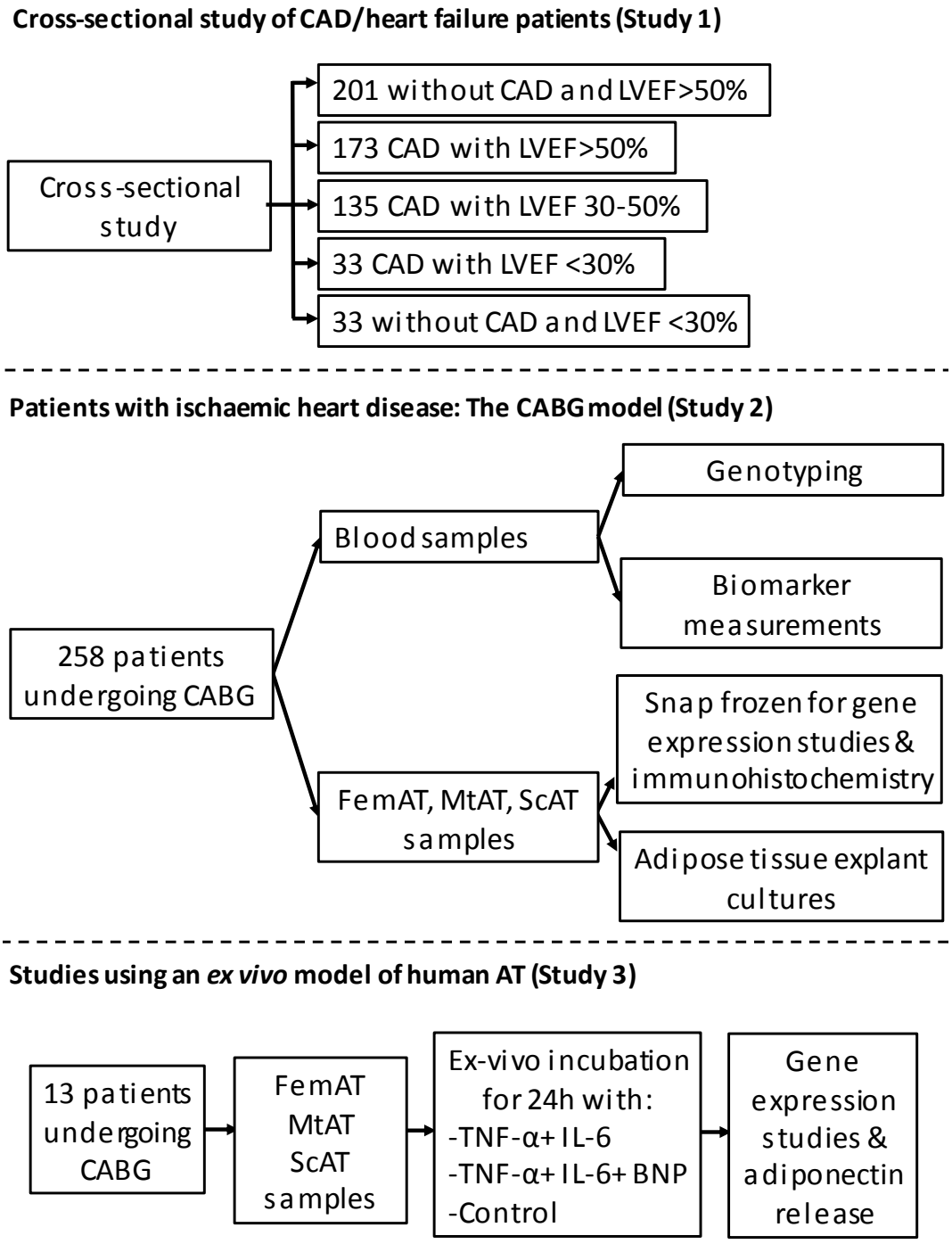


Figure 5.1: *The multi-design study employed in this chapter. Study 1 is a cross-sectional study of healthy volunteers, patients suffering from coronary artery disease (CAD) and patients with heart failure (Left Ventricular Ejection Fraction LVEF<30%) without CAD. Study 2 is a subset of the Oxford CABG Bioresource Phase I population, which includes all those patients for whom full adipose tissue sample sets were available. Study 3 corresponds to patients recruited in the AdipoRedox study and is an ex vivo adipose tissue incubation model. FemAT: femoral adipose tissue, MtAT: mesothoracic adipose tissue, ScAT: subcutaneous adipose tissue. TNFa: tumour necrosis factor alpha, IL-6: Interleukin-6, BNP: Brain Natriuretic Peptide*

Table 5.1 Demographic characteristics of study participants

		Study 1 *Cross-sectional study of CAD/HF patients*				**Study 2** *CABG patients*	**Study 3** *Ex vivo studies*
	Healthy controls	***CAD EF>50%***	***CAD EF 30-50%***	***CAD EF<30%***	***HF, no CAD***		
Participants, n(Males)	201 (171)	173(144)	135(123)	33(30)	33(30)	258 (208)	13(10)
Age (years)	66±0.7	65±0.7	64±0.9	67±1.6	67±1.5	67±0.7	63.1±3.7
Hypertension (%)	47	70	65	73	61	65	62
Dyslipidaemia (%)	24	64	67	58	49	69	77
T2DM (%)	7	28	27	30	19	32	15
Active/ Ex-smokers (%)	5/39	37/41	31/42	23/45	18/39	28/42	39 / 39
BMI (Kg/m^2)	27.4±0.3	27.6±0.4	27.7±0.5	27.4±0.6	26.0±0.6	27.7±0.3	29.9±0.9
hsCRP (mg/L)#	0.9 [0.5-1.8]	1.5 [0.8-3.4]‡	1.8 [0.8-4.1]‡	2.6 [1.3-4.7]‡	2.3 [0.8-3.6]†	1.8 [0.9-4.5]	0.9 [0.6-12.5]
Adiponectin (µg/ml)#	10.7 [2.4-23.6]	9.2 [2.7-19.9]	10.6 [3.1-19.0]	18.2 [8.4-68.7]*	24.7 [9.2-81.2]*	10.1 [1.9-18.8]	-
Medication (%)							
ACEi/ARBs	17/13	53/12	58/15	54/14	33/14	49/15	92
Beta blockers	6.5	78	80	63	42	70	70
Aspirin	1	80	81	88	42	61	100
Clopidogrel	0.5	32	43	44	16	42	92
Statins	11	84	84	74	52	69	54
CCBs	7.5	32	21	21	19	19	92
Metformin/Oral hypogl.	7	28	27	29	19	32	15
Insulin	0	16	13	20	11	18	11

ACEi: Angiotensin converting enzyme inhibitors; ARB: Angiotensin receptor blockers; BMI: Body mass index; CABG: Coronary artery bypass grafting; CAD: Coronary artery disease; CCBs: Calcium channel blockers T2DM: Type 2 Diabetes Mellitus; HF: Heart failure; Values expressed as mean±SEM; #Values expressed as median[25^{th}-75^{th} percentile]. *P<0.05; †P<0.01; ‡P<0.001 vs healthy controls;

5.2.1 Immunohistochemistry of human adipose tissue sections

Subcutaneous, mesothoracic and femoral adipose tissue samples were obtained from patients undergoing CABG surgery as described in Chapter 2. Stored in ice-cold phosphate-buffered saline (PBS), they were transferred to the lab within 30 minutes. There, they were washed and preserved in tissue cassettes by using optimal cutting temperature (OCT) media at -80ºC for future immunohistochemistry processing.

During processing, the samples were removed from their cassettes and loaded on a microcryotome (-20^{o}C). 15 micron sections were cut and mounted onto glass slides and allowed to air-dry for 15 minutes at room temperature. Initial inspection under the microscope was performed to ensure intact cells were present. The slides were fixed in pre-chilled (-20ºC) 70% ethanol twice for 15 seconds and then in pre-chilled acetone for 5 minutes, before being further air-dried at room temperature for 15 minutes. The sections were re-hydrated by briefly dipping in PBS-Tween (PBS-T). Non-specific antigen binding was blocked using serum-free protein block for 1-2 hours (#X0909, Dako CytoMation, Carpinteria, California, USA).

The samples were stained for CD68/CD40/CD206 expression with Monoclonal Mouse Anti-Human CD68, Monoclonal Mouse Anti-Human CD40 and Monoclonal Anti-Human CD206 antibodies respectively according to the manufacturer's instructions (Dako CytoMation, Carpinteria, California, USA; AbD Serotec, Kidlington, UK). The sections were incubated with primary antibody (1:50) overnight at 4ºC, washed with PBS-T and incubated with secondary antibody (Vectstain ABC-AP Kit (mouse IgG): Vector Laboratories, #PK-6200) for 1 hour at room temperature. The staining was developed using the DAB Substrate kit for Peroxidase (#SK-4100, Vector Laboratories, Burlingame, California, USA) according to the manufacturer's protocol. After counter-staining with haematoxylin the slides where dehydrated in graded ethanol (15 seconds), cleared with

Histo-clear (National Diagnostics, Atlanta, Georgia, USA) mounted with Neo-Mount (#109016, Merck KGaA, Darmstadt, Germany) and examined under a Leica TCS SP2 confocal microscope housed at the Cardiovascular Medicine laboratory, Level 5, West Wing, John Radcliffe hospital, Oxford.

Macrophage infiltration and cell size were quantified in a blinded fashion. Cell size was measured using the open source software Image J. For each patient 3 different fields were quantified per fat depot at 100x magnification for macrophage infiltration and 200x for cell size.



Figure 5.2: *The Leica TCS SP2 microscope used in the immunohistochemistry experiments*

5.2.2 Statistical analysis

Continuous variables were tested for normal distribution using the Kolmogorov-Smirnov test. Non-normally distributed variables were log-transformed for analysis and are presented as median [25^{th}-75^{th} percentile] or on log-transformed scale. Normally distributed variables are presented as mean ± SEM.

Comparisons between groups in study 1 were performed by using one-way ANOVA followed by Bonferroni post-hoc correction for individual comparisons vs healthy control group. Continuous variables were compared between 3 groups in Study 2 using one-way ANOVA. For comparisons of variables between 3 different adipose tissue depots from the same patient, repeated measures ANOVA was used followed by paired-t test and Bonferroni correction as described in the respective Figure legends. In Study arm 3 (ex vivo studies), changes of adiponectin release in culture supernatants or *ADIPOQ/PPARγ/CD36* gene expression in tissue were evaluated by using two-way ANOVA for repeated measures with [adipose tissue type] x [treatment group] interaction, followed by paired samples t-test for individual paired comparisons of each intervention vs control. Categorical variables were compared by using χ^2 test, as appropriate. Correlations between continuous variables were assessed by using bivariate analysis and Pearson's coefficient was estimated. When log-transformation of a non-normally distributed variable was not possible, the Spearman rho correlation coefficient was calculated. Comparisons of the correlation coefficients between groups were performed by calculating z-score.

In study arm 2, linear regression was performed by using log(serum adiponectin) as dependent variable and as independent variables those of the clinical demographic characteristics (age, gender, diabetes, smoking, dyslipidemia, hypertension, body mass index (BMI)) or circulating biomarkers [log(serum IL-6), log(plasma hsCRP) and log(plasma BNP)] that showed an association with the dependent variable at the level of 15%.

All statistical tests were performed using SPSS v20.0 and $P<0.05$ was considered statistically significant.

5.3 Results

5.3.1 Impact of left ventricular function on circulating adiponectin

5.3.1.1 Obesity, heart failure and adiponectin levels

I first examined the association between body mass index (BMI) and serum adiponectin levels in the cross-sectional study of patients with or without coronary artery disease (CAD) and/or systolic heart failure as evidenced by a low left ventricular ejection fraction (LVEF). I observed that BMI was inversely correlated with circulating adiponectin in healthy individuals, without CAD and with normal LVEF (Figure 5.3, Panel A). This was also true, although more weakly so, in patients with CAD and preserved or mildly reduced LVEF (Figure 5.3, Panel B).

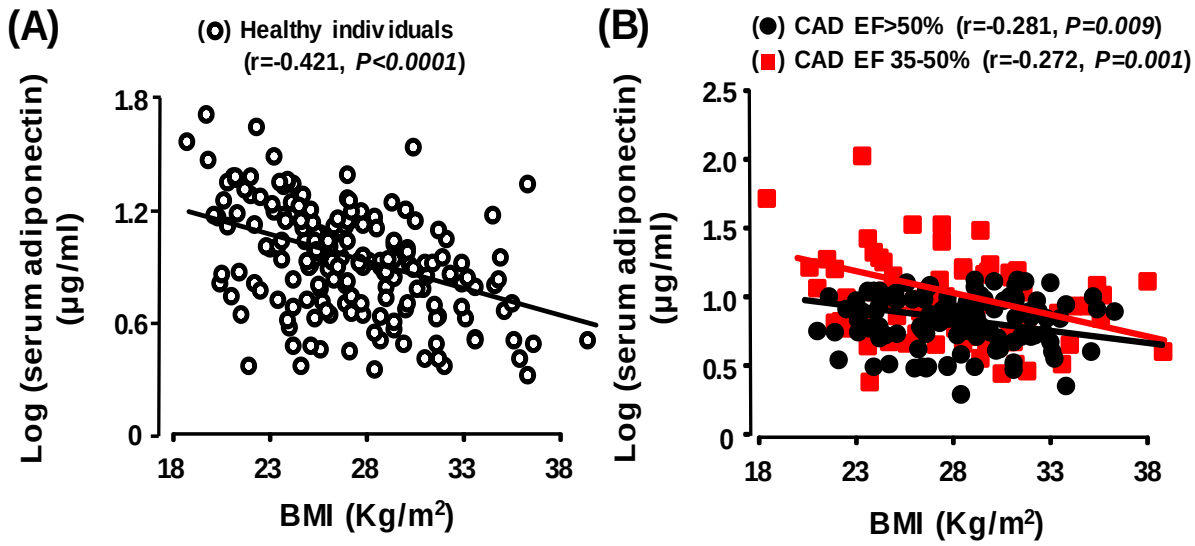


Figure 5.3: *In the population of Study 1, there was a significant inverse association between body mass index (BMI) and serum adiponectin levels among the healthy individuals (n=201, Panel A). This association was weaker but still significant in coronary artery disease (CAD) patients with normal (EF>50%, n=173) or mildly impaired left ventricular ejection fraction (EF=35-50%, n=135, Panel B). Pearson correlation coefficients and corresponding P values are presented for each study subject group.* ***(Margaritis et al. ATVB 2014;34(9):2151-9)***

However, this association was lost in patients with established left ventricular impairment (Figure 5.3); importantly, this was irrespective of presence or absence of CAD.

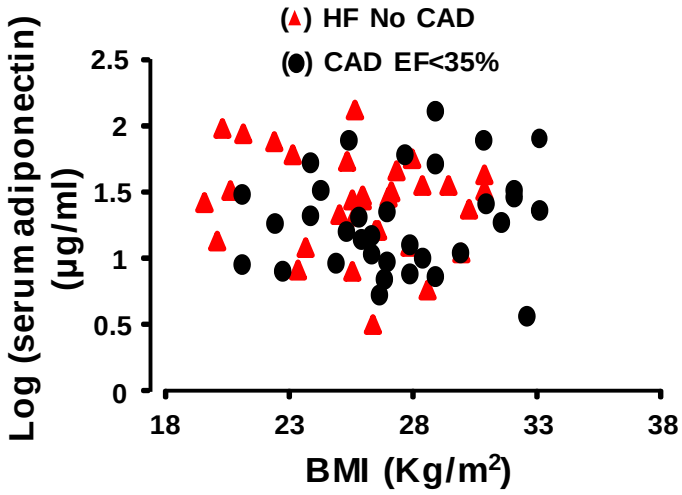


Figure 5.4: *There was no association between circulating adiponectin levels and body mass index (BMI) in patients with heart failure (HF) (severely impaired ejection fraction EF (<35%)) in the presence (n=33) or absence (n=33) of coronary artery disease (CAD).* ***(Margaritis et al. ATVB 2014;34(9):2151-9)***

Following these observations, I compared the levels of circulating adiponectin among the different study groups. I found that median serum adiponectin was not significantly different between CAD patients with normal or mildly impaired LVEF and healthy individuals (Figure 5.5). However, there was a strikingly significant association between elevated serum adiponectin levels and presence of heart failure as evidenced by impaired LVEF, either of ischaemic or non-ischaemic aetiology (Figure 5.5).

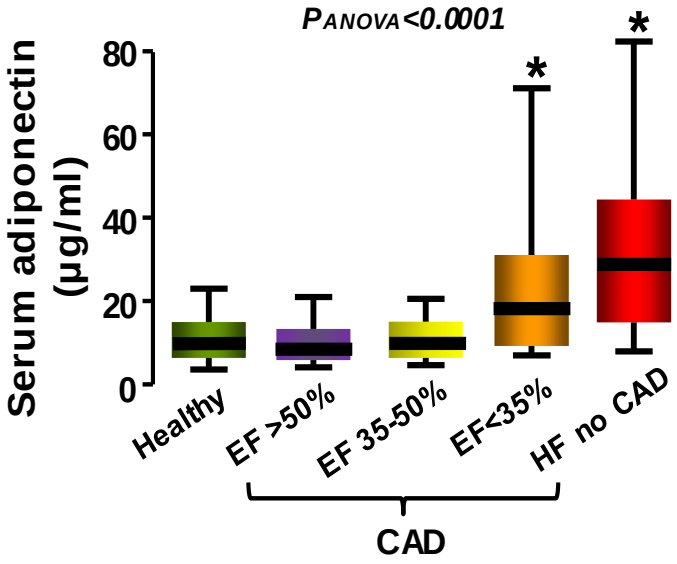
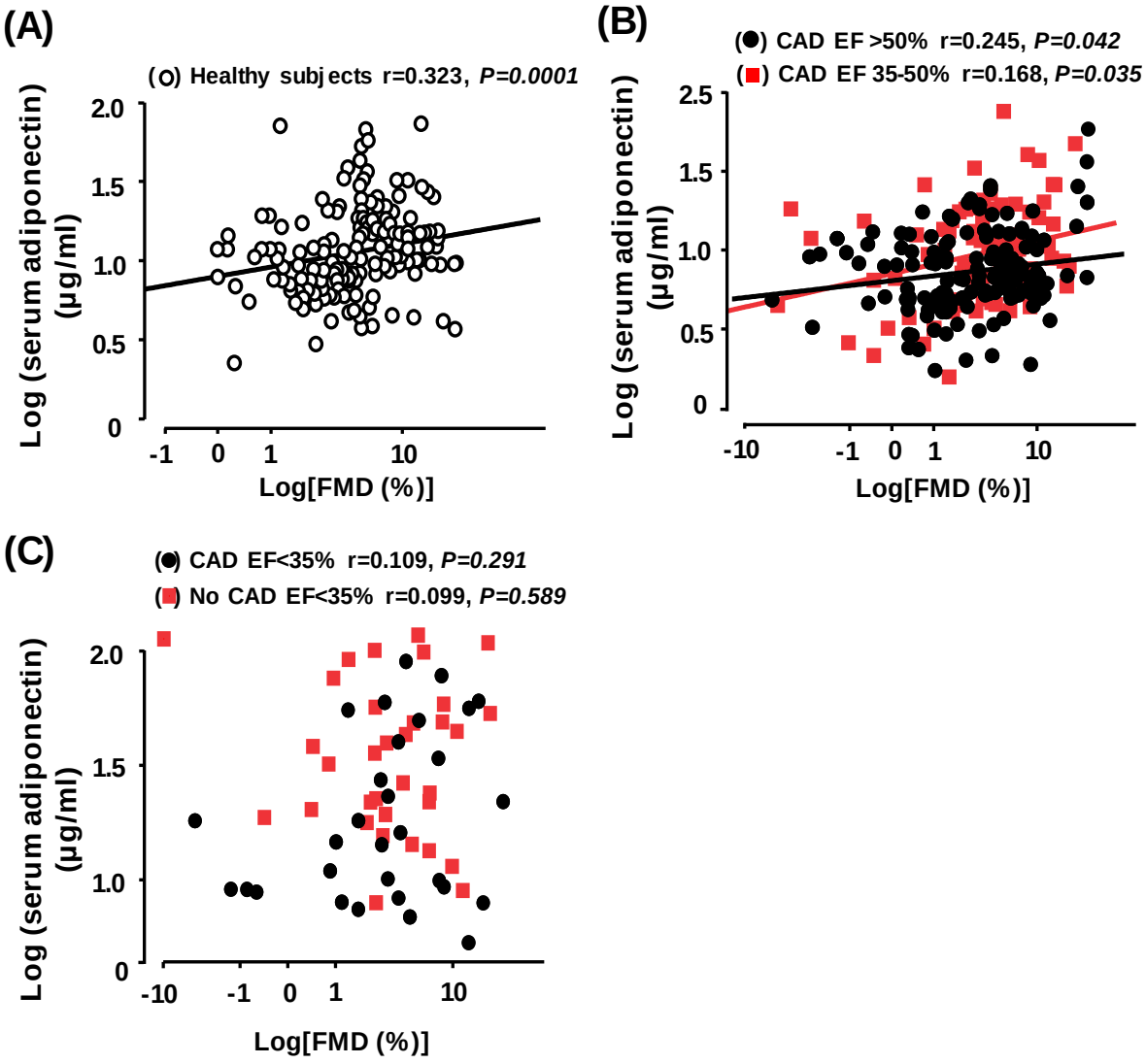


Figure 5.5: *Serum adiponectin levels were similar between healthy individuals and coronary artery disease (CAD) patients without heart failure (HF) (normal or mildly impaired ejection fraction (EF). However, patients with HF (EF<35%) had elevated serum adiponectin levels either in presence or absence of CAD. Table 5.1 shows n for each group. Values expressed as median [25th-75th percentile]. *P<0.05 vs healthy (individual comparisons Bonferroni post-hoc corrected).*

5.3.1.2 Heart failure, circulating adiponectin levels and endothelial function

In Chapter 3, I presented data showing a significant, independent correlation between circulating adiponectin levels and endothelial function in the Oxford CABG Bioresource Phase I population (Figure 3.4). After analysis of the cross-sectional study 1 presented in this chapter, I was able to duplicate this result in patients with advanced atherosclerosis and preserved LVEF (Figure 5.6, Panel B) and even more stronly in healthy subjects (Figure 5.6, Panel A). However, it was lost in patients with heart failure, either ischaemic or non-ischaemic (Figure 5.6, Panel C), suggesting that the pathophysiological changes caused by clinical heart failure are a major factor driving the circulating adiponectin pool.



9)

5.3.1.3 Determinants of circulating adiponectin in cardiovascular disease: role of BNP

Drawing on the results presented so far, and in order to uncover factors influencing serum adiponectin levels in patients with coronary atherosclerosis, I focused on a homogenous group of patients with CAD without evidence of heart failure undergoing CABG (study 2). In this cohort, I searched for predictors of serum adiponectin. In univariate analysis, there was significant correlation between log(serum adiponectin) and:

- age (r=0.179, P=0.009),
- BMI (r=-0.176, P=0.015),
- female gender (rho=0.183, P=0.007),
- dyslipidaemia (rho=-0.192, P=0.005) and
- type 2 diabetes (rho=-0.126, P=0.05).

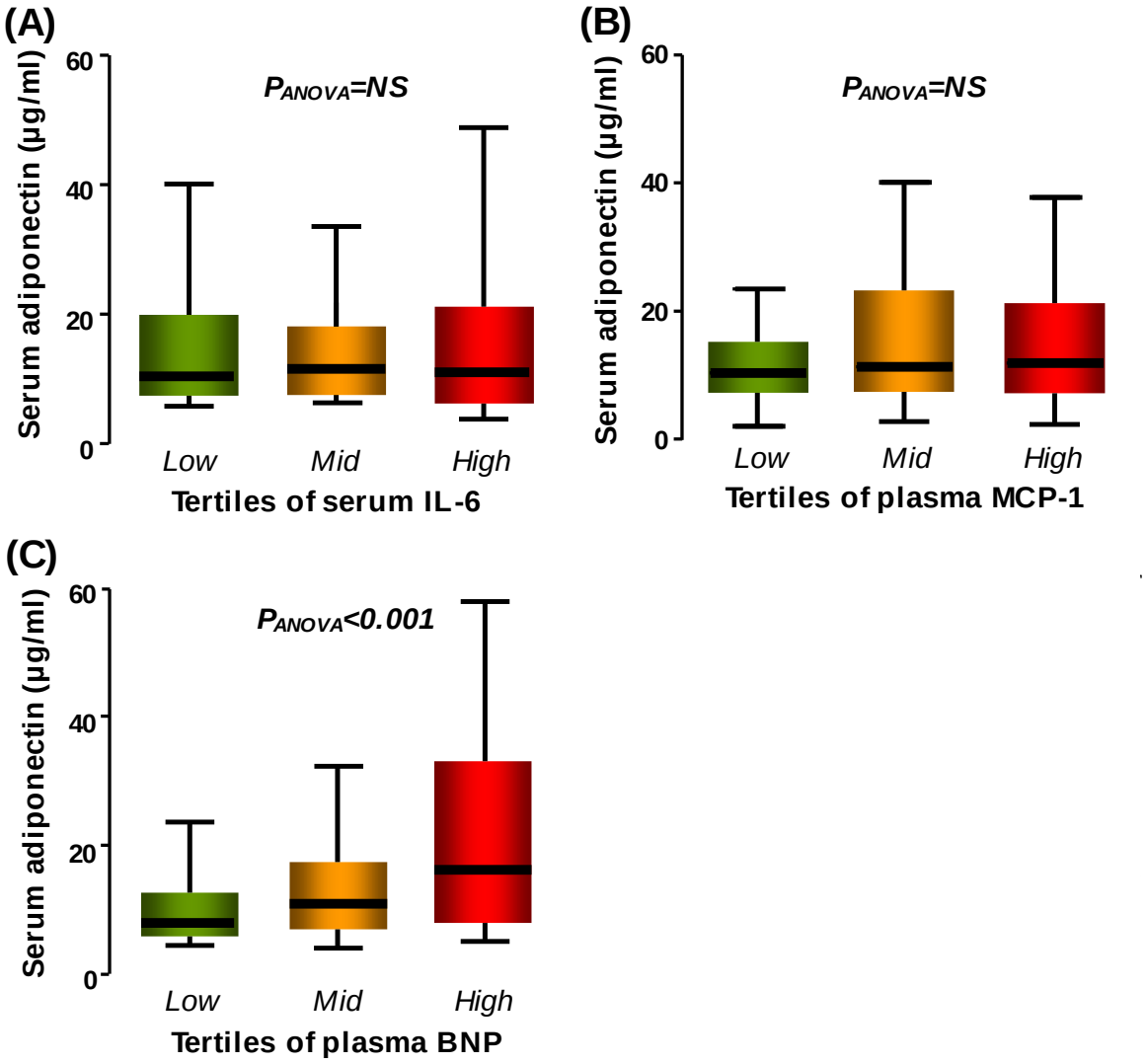
Importantly, log(serum adiponectin) was not correlated with log(plasma hsCRP) (r=-0.125, P=0.095) or log(serum IL-6) (r=0.089, P=0.239). In a multivariable model including the above variables, the independent predictors of log(serum adiponectin) were:

- age (β(SE): 0.007(0.003), P=0.006),
- female gender (β(SE): 0.131(0.059), P=0.028) and
- dyslipidaemia (β(SE): -0.128(0.048), P=0.008),

but not diabetes (β(SE): -0.101(0.054), P=0.062) or BMI (β(SE): -0.10(0.006), P=0.084).

Because this model only included demographic/anthropometric characteristics, I then searched for biomarkers that could predict serum adiponectin levels. Plasma levels of hsCRP were significantly elevated in CAD patients compared to healthy controls, and further increased in the presence of heart failure (Table 5.1). However, hsCRP (P=NS), interleukin-6 (IL-6) or plasma monocyte chemoattractant protein-1 (MCP-1) levels (Figure 5.7, Panels A&B) were not associated with serum adiponectin levels in univariate analysis.

Given the presumed links between BNP and adiponectin mentioned in the introductory paragraph of this chapter, plasma BNP levels in samples obtained from patients enrolled in Study 2 were quantified. I observed a significant association between log(plasma BNP) and log(serum adiponectin) (r=0.282, P<0.001, Figure 5.7, Panel C). When log(plasma BNP) was included into the multivariable model, it became clear that this was the strongest independent predictor of log(serum AdN) with (β(SE): 0.153(0.05), P=0.003), even in the absence of clinically evident heart failure. These results would seem to indicate that BNP plays a major role in determining adiponectin levels in the circulation, potentially through direct stimulating actions on human adipose tissue.



5.3.2 Human adipose tissue as a source of adiponectin

Following the previous observations, the logical next step would be to investigate whether plasma BNP levels are related to adiponectin synthesis in the adipose tissue sites available in the Oxford CABG Bioresource. However, before I could investigate this relationship, I needed to address the question of how human different adipose tissue depots contribute to the circulating adiponectin pool and what could be the determinants of adiponectin gene expression on a transcriptional level in human adipose tissue.

5.3.2.1 Contribution of distinct adipose tissue sites to circulating adiponectin levels

To explore the contribution of different adipose tissue sites to the circulating adiponectin pool, I performed qRT-PCR and used the adipose tissue explant culture method described in Chapter 2 to determine gene expression and release of adiponectin from subcutaneous (ScAT), mesothoracic (MtAT) and perivascular adipose tissue (PVAT) around the saphenous vein and internal mammary artery, in patients belonging to Study 2 – corresponding to a subset of Phase I Oxford CABG Bioresource population. I observed a significant, albeit weak, correlation between serum adiponectin levels and local adiponectin release/*ADIPOQ* gene expression in MtAT and ScAT, suggesting that total levels of this adipokine may be driven, at least in part, by these "remote" (non-perivascular) depots (Figure 5.8, Panels A-D). By contrast, circulating adiponectin was not related with either local adiponectin release/*ADIPOQ* gene expression in Peri-SV PVAT (Figure 5.8, Panels E&F) or *ADIPOQ* gene expression in Peri-IMA PVAT (r=0.072 P=0.602). This implies that different, potentially local, mechanisms control the expression and synthesis of adiponectin in perivascular adipose tissue. This result and the novel hypotheses generated from it are explored in detail in Chapter 6.

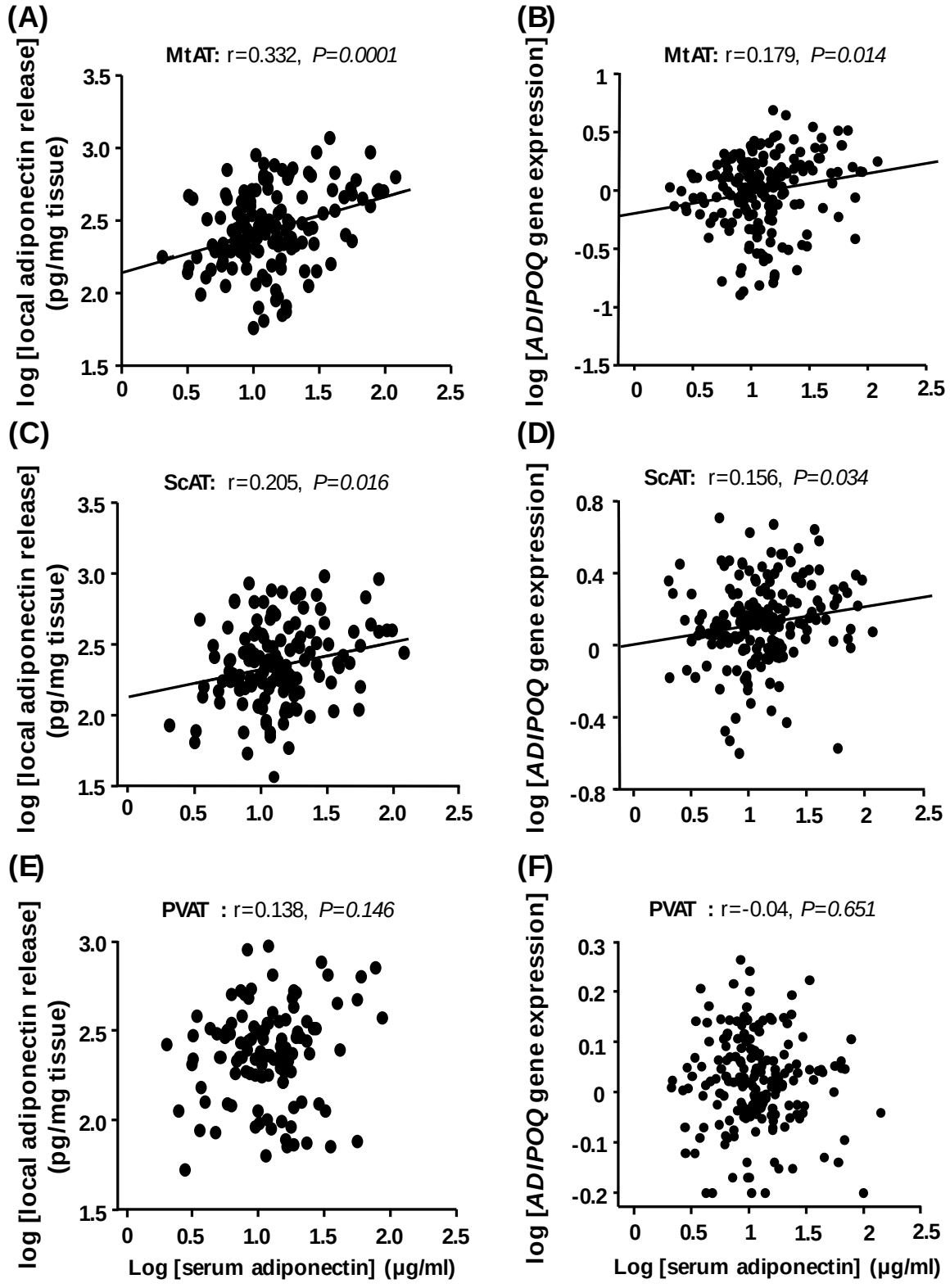


Figure 5.8: *Serum levels of adiponectin were significantly correlated with adiponectin release after 4 hours of ex vivo culture and ADIPOQ gene expression in mesothoracic (MtAT, Panels A and B) and subcutaneous (ScAT Panels C and D) but not perivascular (PVAT, Panels E and F) adipose tissue (n=258). Pearson's r correlation coefficients are presented.* ***(Margaritis et al. Circulation 2013;127(22):2209-21)***

5.3.2.2 *ADIPOQ* genetic variability and adiponectin gene expression in adipose tissue

The observations presented in the previous paragraph demonstrate an association between gene expression/release of adiponectin in certain depots and circulating adiponectin levels. However, despite the biological plausibility, they do not demonstrate causality. To document a causal relationship, I revisited the Mendelian randomization model utilised in Chapters 3&4. Having demonstrated that the additive effect of the rs 266717T and rs17366568G alleles is linked to higher serum adiponectin levels, I went on to document a similar relationship between these alleles and higher *ex vivo* release of adiponectin by MtAT (Figure 5.9, Panel A). However, echoing the observations regarding lack of association between serum adiponectin and expression/release in PVAT, I again failed to observe any relationship between the genetic model and adiponectin release from peri-SV PVAT (Figure 5.9, Panel B). This suggests that local factors in PVAT may overwhelm the influence of genetic variability on adiponectin expression. This is explored extensively in Chapter 6.

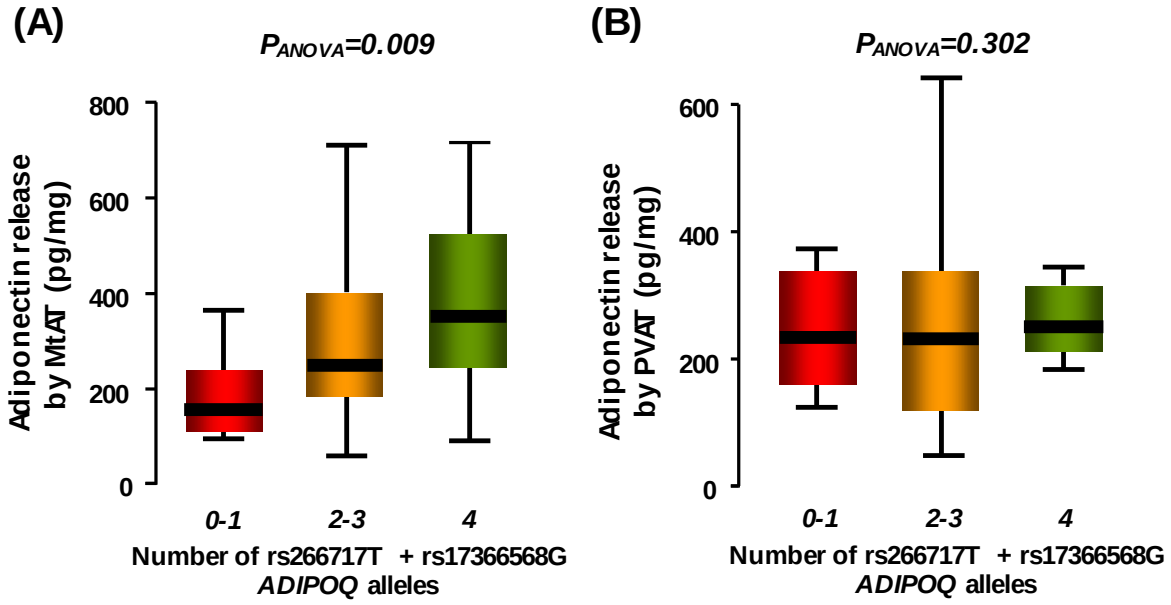


Figure 5.9: *The number of G alleles for rs17366568G and T alleles for rs266717 had an additive effect on adiponectin release by mesothoracic adipose tissue (MtAT, Panel A) but not perivascular adipose tissue surrounding the saphenous vein (PVAT, Panel B) (n=258). Values expressed as median [25th-75th percentiles].* ***(Margaritis et al. Circulation 2013;127(22):2209-21)***

5.3.2.3 Transcriptional control of adiponectin gene expression

The results presented in the previous paragraphs beget the question of how adiponectin synthesis is controlled on a transcriptional level and whether there are appreciable differences in the control mechanisms in distinct adipose tissue sites. The transcription factor PPARγ is a master regulator of adipogenesis and is known to regulate *ADIPOQ* gene expression in cell culture models[244]. To investigate whether this is relevant to human adipose tissue, I performed qRT-PCR to quantify gene expression of *PPARγ* gene. However, given that high gene expression is not necessarily linked to high activity of this transcription factor, I also quantified gene expression of *CD36*, a molecule that is known to be under the direct transcriptional control of PPARγ[245] and could therefore serve as a surrogate marker of PPARγ activity.

I observed a significant correlation between *PPARγ* and *ADIPOQ* gene expression in MtAT, ScAT, and femoral adipose tissue (FemAT) distant to the saphenous vein (Figure 5.10, Panels A-C). Importantly, the correlation between *PPARγ* and *ADIPOQ* gene expression was significantly stronger in FemAT compared to either ScAT (z-score:-3.846, P=0.00012) or ThAT (z-score:-0.513, P<0.00001). An even stronger association between *PPARγ* and *ADIPOQ* gene expression was observed in PVAT, either around the SV or the IMA (Figure 5.10, Panels D&E). In addition, I confirmed co-linearity between the expression of *PPARγ* and *CD36* gene expression in all three adipose tissue depots, validating the use of *PPARγ* gene expression as a surrogate marker of its activity. These results suggest that, despite the discordant findings presented previously regarding adiponectin expression/release in PVAT versus remote sites, *ADIPOQ* gene expression remains under the direct control of PPARγ in all types of human adipose studied in my project. They also generate the hypothesis that a strong activator of PPARγ may be driving expression of adiponectin in perivascular adipose tissue. This is investigated in Chapter 6.

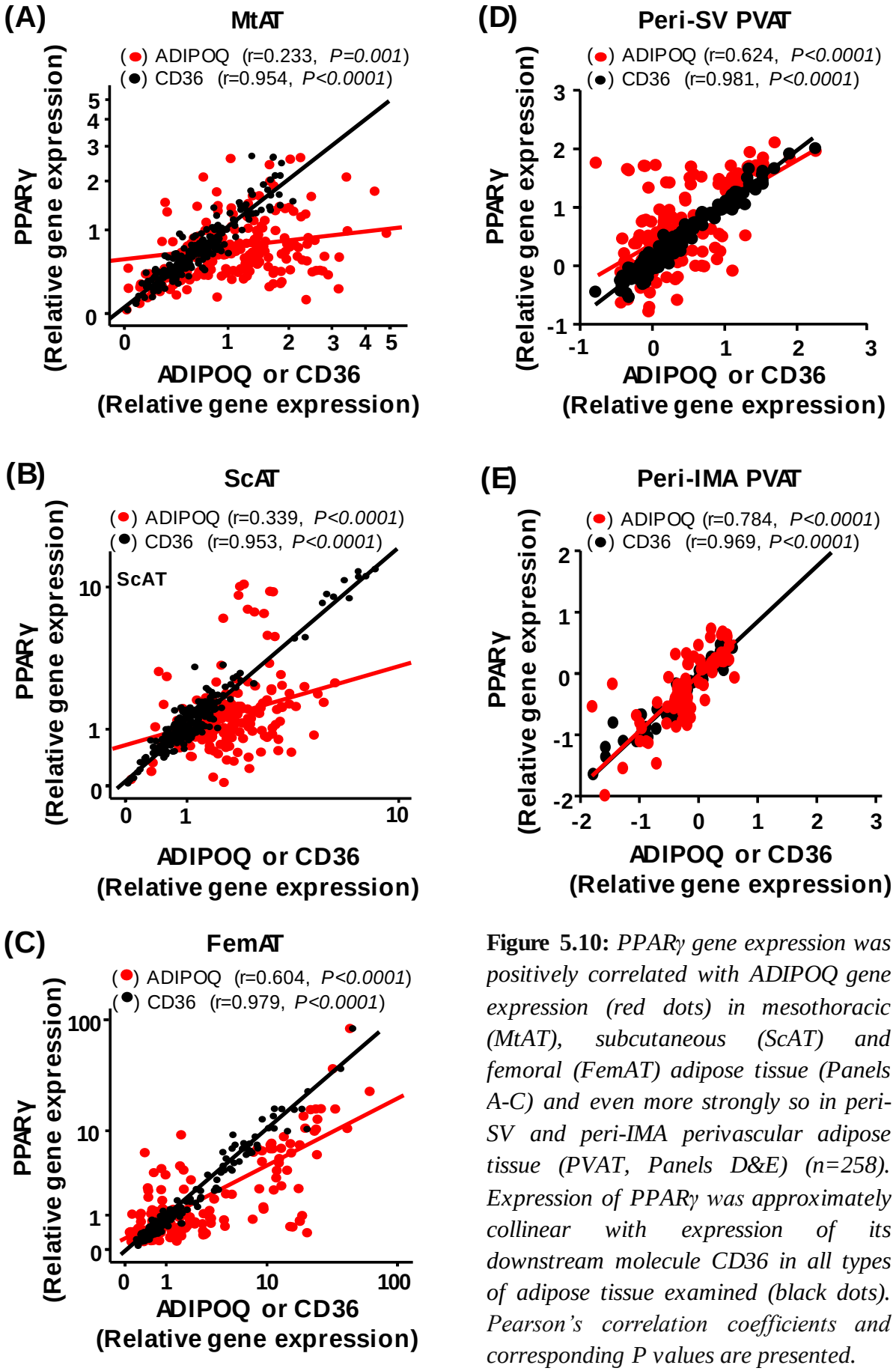


Figure 5.10: *PPARγ gene expression was positively correlated with ADIPOQ gene expression (red dots) in mesothoracic (MtAT), subcutaneous (ScAT) and femoral (FemAT) adipose tissue (Panels A-C) and even more strongly so in peri-SV and peri-IMA perivascular adipose tissue (PVAT, Panels D&E) (n=258). Expression of PPARγ was approximately collinear with expression of its downstream molecule CD36 in all types of adipose tissue examined (black dots). Pearson's correlation coefficients and corresponding P values are presented.*

5.3.3 BNP, inflammation & adiponectin synthesis in adipose tissue

In paragraph 5.3.1 I demonstrated that plasma BNP is a major determinant of circulating adiponectin levels. I also established in the previous paragraph that "remote" adipose tissue sites distant from major vessels, such as mesothoracic and subcutaneous, are potentially important sources of the adiponectin circulating in the bloodstream in humans. These observations gave birth to the hypothesis that BNP could have direct stimulating effects on adiponectin synthesis in these "remote" adipose tissue sites.

To investigate this hypothesis, I first examined the relationship between plasma levels of BNP and adiponectin gene expression/release from adipose tissue in patients from the Oxford CABG Bioresource Phase I, belonging to study 2 presented in this chapter. Indeed, plasma BNP was positively associated with both the expression (Figure 5.11, A-C) and release (Figure 5.11, D-F) of adiponectin from ScAT, MtAT and FemAT. This further supports the notion that in patients suffering from advanced atherosclerosis, circulating BNP is a key driver of adiponectin expression in adipose tissue and controls its release in the circulation even in the absence of clinically evident heart failure syndrome.

Interestingly, even though the classic inflammatory biomarkers (hsCRP and IL-6) were not significant predictors of circulating adiponectin, I observed that high levels of circulating IL-6 were linked to reduced gene expression and release of adiponectin in FemAT, but not in MtAT or ScAT (Figure 5.12). Similarly, circulating monocyte chemoattractant protein 1 (MCP-1) was inversely related with *ADIPOQ* gene expression and adiponectin protein release in FemAT, but not in MtAT or ScAT (Figure 5.13). These results suggest that, while BNP appears to be a universal driving force of adiponectin synthesis, there may be functional differences among the adipose tissue depots studied which could alter their responsiveness to other stimuli affecting adiponectin gene expression and release.

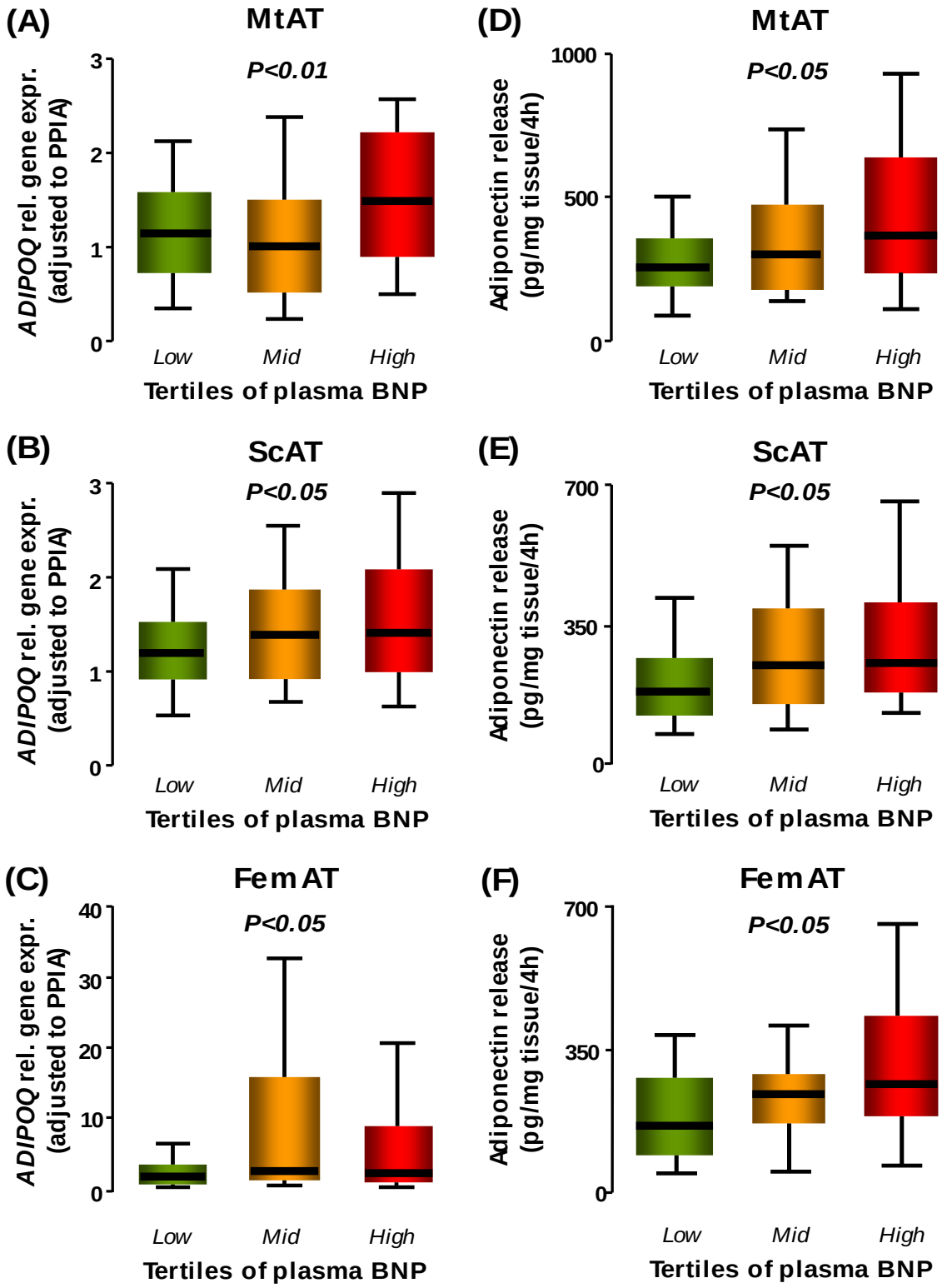


Figure 5.11: *Increased plasma brain natriuretic peptide (BNP) levels were related with higher gene expression of adiponectin (ADIPOQ) adjusted to cyclophilin (PPIA) in mesothoracic (MtAT, A), subcutaneous (ScAT, B) and femoral adipose tissue (FemAT, C). A similar association was observed with release of adiponectin in the supernatant after 4 hours' explant culture of these types of tissue (Panels D-F). Values expressed as median [25th-75th percentile] (n=258).* ***(Margaritis et al. ATVB 2014;34(9):2151-9)***

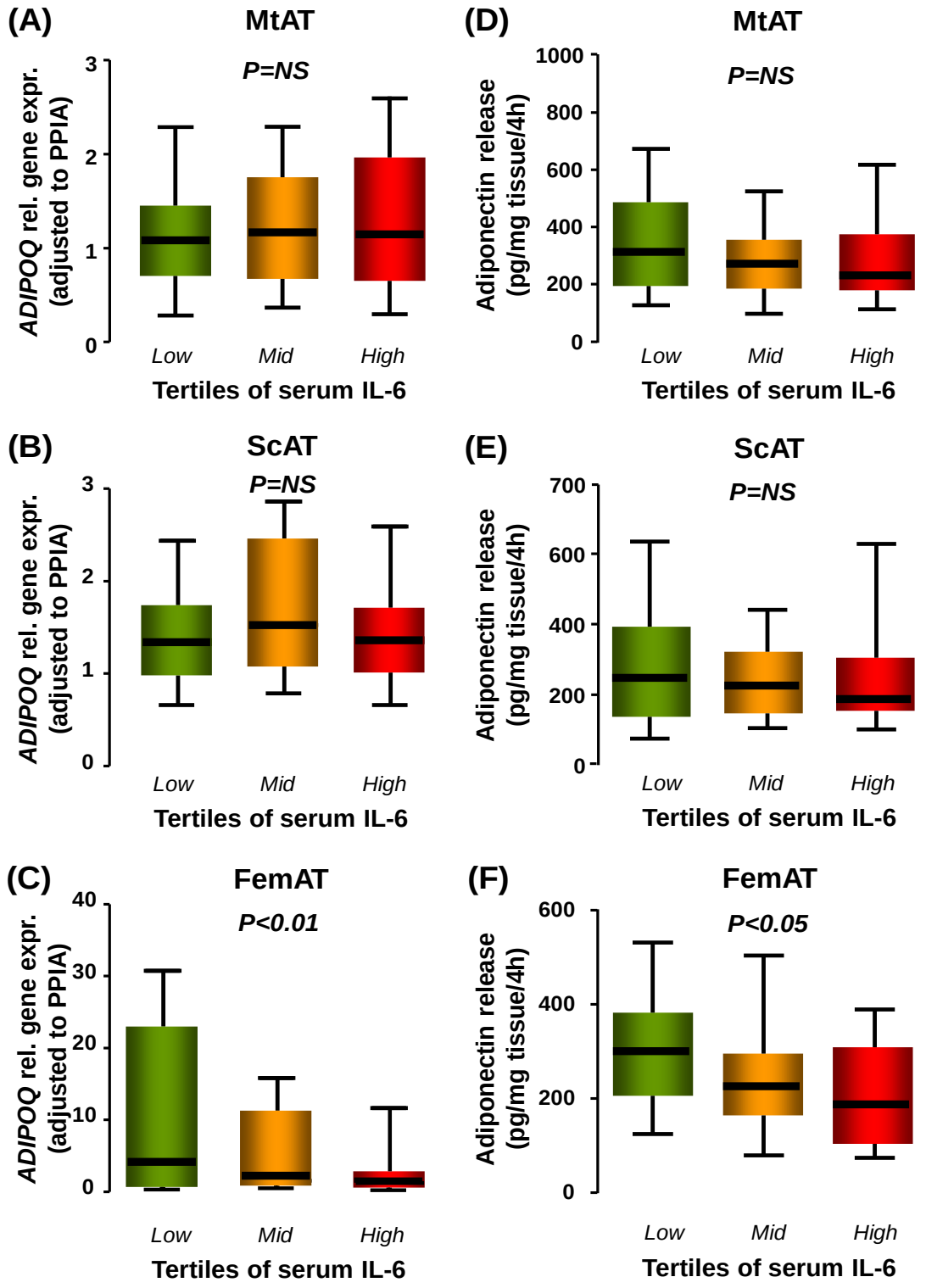


Figure 5.12: *Levels of serum interleukin-6 (IL-6) were not related with adiponectin (ADIPOQ) gene expression adjusted to cyclophilin (PPIA) (Panels A&B) or release (Panels D&E) from mesothoracic (MtAT) or subcutaneous (ScAT) adipose tissue in culture supernatant. Conversely, high levels of serum IL-6 were inversely related to gene expression and release of adiponectin from femoral adipose tissue in culture supernatant (FemAT, Panel C & F). Values expressed as median [25th-75th percentile] (n=258).* ***(Margaritis et al. ATVB 2014;34(9):2151-9)***

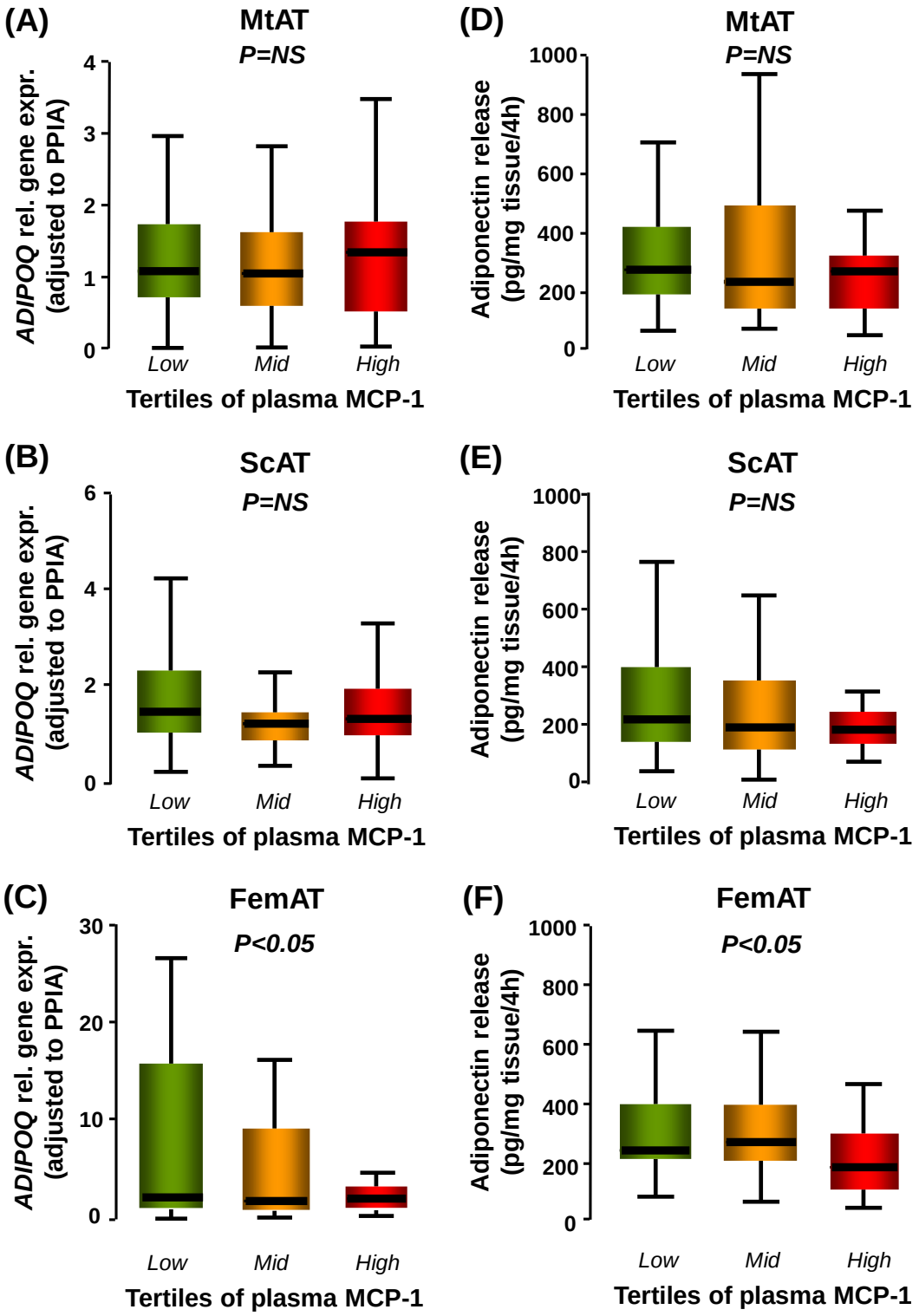


Figure 5.13: *Levels of plasma monocyte chemoattractant protein-1(MCP-1) were not related with adiponectin (ADIPOQ) gene expression adjusted to cyclophilin (PPIA) (Panels A&B) or release (Panels D&E) from mesothoracic (MtAT) or subcutaneous (ScAT) adipose tissue in culture supernatant. However, high levels of MCP-1 were inversely related to ADIPOQ gene expression and adiponectin release from femoral adipose tissue (FemAT, Panel C & F) in culture supernatant. Values expressed as median [25th-75th percentile] (n=258).* ***(Margaritis et al. ATVB 2014;34(9):2151-9)***

5.3.4 Direct effects of inflammatory cytokines & BNP on adiponectin synthesis in human adipose tissue: *ex vivo* culture model

The observations presented in the previous paragraph suggest existence of a regional variability in the responsiveness of distinct adipose tissue depots to inflammation and BNP; this subsequently produces a varied degree in the ability of these stimuli to affect adiponectin gene expression and release. However, the results shown are purely associations and do not necessarily reflect causality.

To establish direct effects of inflammatory cytokines and/or BNP on adiponectin synthesis in human adipose tissue, I employed an *ex vivo* adipose tissue culture model based on the adipose tissue explant culture method described in Chapter 2. I collected MtAT, ScAT and FemAT samples from n=13 patients undergoing CABG surgery, recruited in the AdipoRedox study (Study 3 presented in this chapter). In the lab, I incubated the samples in a paired manner with IL-6 (25 ng/mL) and tumour necrosis factor alpha (TNF-α 4 ng/mL) ± BNP (1 nmol/L) for 24 hours. At the end of the incubation period, I collected the adipose tissue and performed RNA extraction and qRT-PCR to quantify gene expression changes. I also collected the supernatant and quantified adiponectin release using ELISA, as described previously.

I found that exposure of human adipose tissue to inflammatory cytokines suppressed the expression of *PPARγ*, *CD36* and *ADIPOQ* genes in FemAT, resulting in a decrease in *ex vivo* adiponectin release; this effect was reversed by simultaneous incubation with BNP (Figure 5.14). However, MtAT and ScAT did not show any significant response to exogenous inflammatory stimulation, in relation to adiponectin release and expression of the above gene targets. These results complement the clinical association studies presented previously, confirming that FemAT appears to be more sensitive to inflammatory stimuli affecting adiponectin gene expression and release.

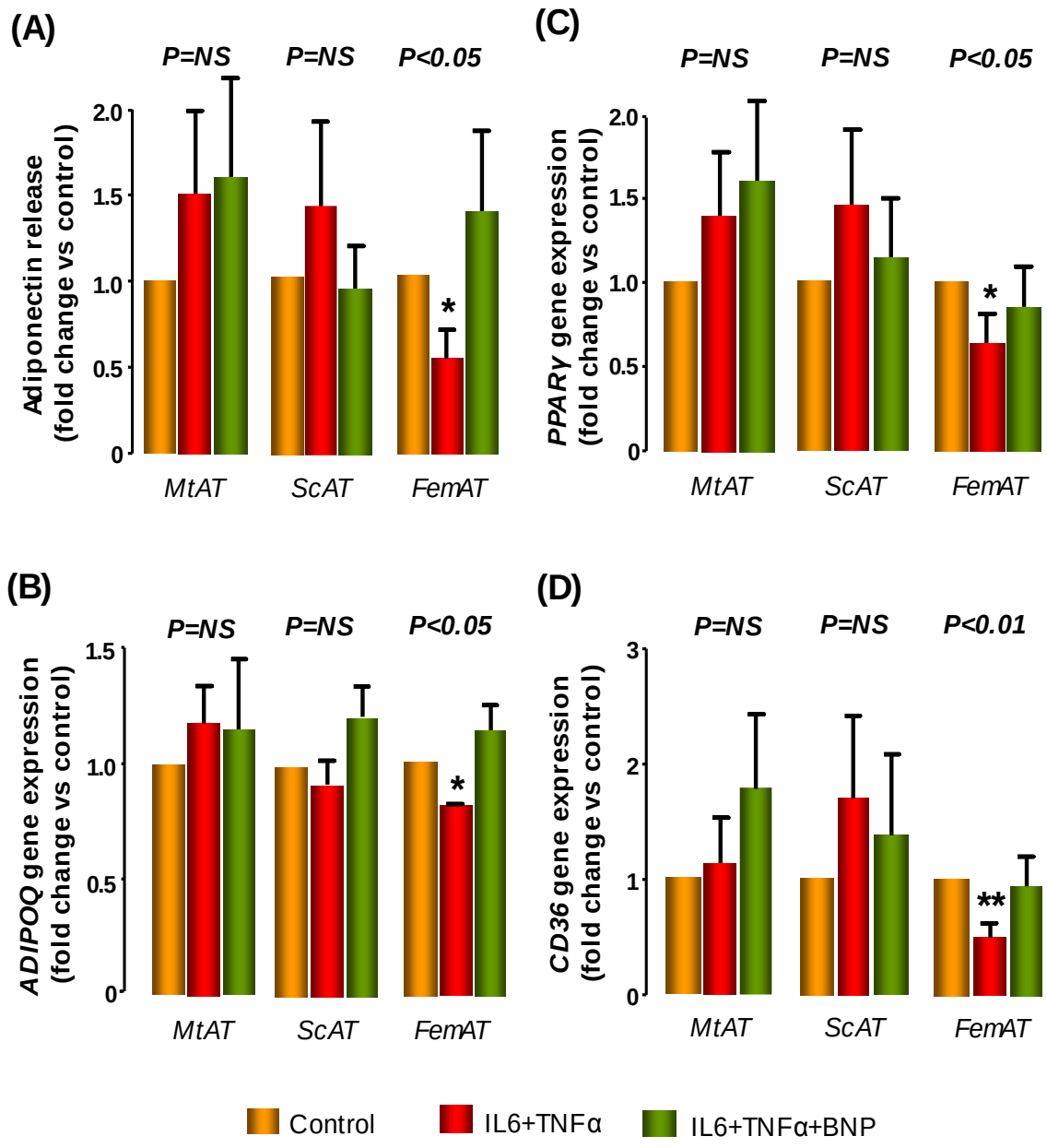


Figure 5.14: *Ex vivo incubation of femoral adipose tissue (FemAT) with interleukin-6 (IL-6, 25 ng/mL) and tumor necrosis factor-α (TNF-α, 4 ng/mL) for 24 hours significantly reduced the production of adiponectin (Panel A), as a consequence of reduced gene expression of ADIPOQ (Panel B) and PPARγ (Panel C). Gene expression of CD36, surrogate marker of PPARg activity, was also markedly reduced (Panel D). These effects were reversed by co-incubation with brain natriuretic peptide (BNP 1 nM) (Panels A to D). Importantly, mesothoracic (MtAT) and subcutaneous (ScAT) adipose tissue from the same patients did not respond to this inflammatory stimulation (Panels A to D). Values are expressed as mean ± SEM.*P<0.05, **P<0.01 vs. FemAT Control. n=13* ***(Margaritis et al. ATVB 2014;34(9):2151-9)***

5.3.5 Morphological/Functional differences of femoral versus mesothoracic and subcutaneous adipose tissue in humans

Given the discordant responses of distinct adipose tissue sites to inflammatory stimuli, I hypothesized that there may be morphological differences as well as differences in degree of inflammatory cell infiltration between FemAT and the other depots studied. To explore this hypothesis, I proceeded to examine the inflammatory cell infiltration profile and histological structure of human MtAT, ScAT and FemAT in more detail.

5.3.5.1 Inflammatory cell marker gene expression measurements in adipose tissue

Firstly, I performed gene expression studies in MtAT, ScAT and FemAT from patients enrolled in study 2 in this chapter, aiming to quantify expression of inflammatory cell markers. To this end I performed qRT-PCR to measure gene expression of CD68, a glycoprotein which binds to low density lipoprotein and is expressed in monocytes/macrophages[246]. I observed a 3-fold higher expression of *CD68* gene in MtAT compared to FemAT and a 2-fold higher expression in ScAT compared to FemAT (Figure 5.15, Panel A). Owing to the fact that CD68 is a general marker of macrophages and does not differentiate between M1 and M2 activated macrophages, I proceeded to quantify gene expression of *CCR7* (C-C chemokine receptor type 7 or CD107, marker of M1 macrophages) and *MRC1* (mannose receptor C type 1 or CD206, marker of M2 macrophages)[21]. I found that the *CCR7*/*MRC1* gene expression ratio in MtAT was ~3 fold higher than ScAT and ~5 fold higher than FemAT (Figure 5.15, Panel B). Given the interesting inverse association between serum IL-6 and adiponectin gene expression/release from FemAT (presented in Figure 5.12), I also quantified IL6-receptor (*IL6-R*) gene expression and found that this was significantly higher in FemAT compared to MtAT and ScAT (Figure 5.14, Panel C), suggesting a higher sensitivity of FemAT to the effects of this inflammatory cytokine.

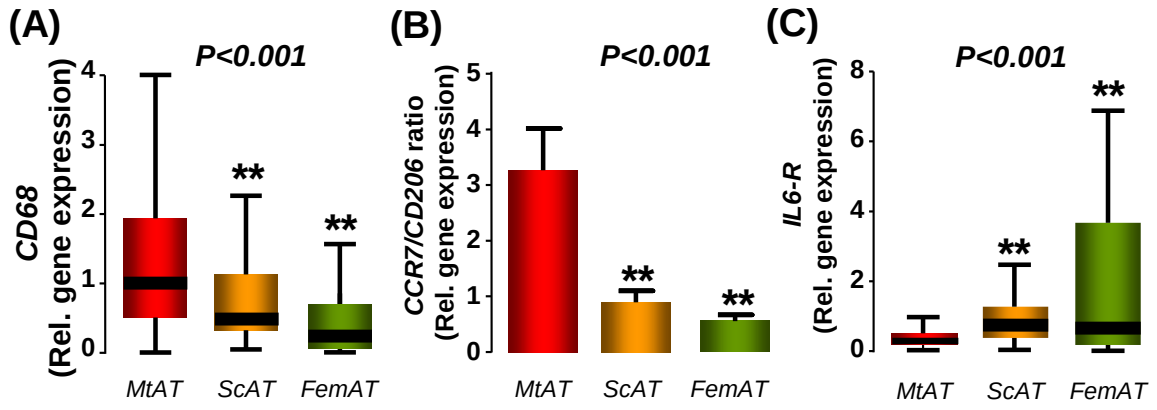


Figure 5.15: *There was significantly higher CD68 gene expression in mesothoracic (MtAT) compared to subcutaneous (ScAT) and femoral (FemAT) adipose tissue (Panel A) in paired samples from patients undergoing CABG surgery (n=258). Moreover, MtAT had a higher ratio of CCR7 (marker of M1 macrophages)/CD206 (marker of M2 macrophages) gene expression compared to ScAT & FemAT (**Panel B**). FemAT had higher expression of interleukin-6 receptor (IL6-R) compared to the other two depots (**Panel C**). Values are expressed as median [25th-75th percentile] for panels **A&C** or mean ± SEM for panel B. **P<0.01 vs MtAT* ***(Margaritis et al. ATVB 2014;34(9):2151-9)***

5.3.5.2 Immunohistochemistry of human adipose tissue

To confirm the aforementioned findings and to visualise the different adipose tissue sites examined to uncover potential morphological differences, I performed immunohistochemistry of MtAT, ScAT and FemAT sections from n=7 patients undergoing CABG surgery, using the technique described in this chapter. I initially stained for CD68 and observed significantly lower CD68+ macrophage infiltration in FemAT compared to ScAT (intermediate infiltration) and MtAT (highest infiltration) as demonstrated in Figure 5.16 (A & D-I). Interestingly, the average adipocyte cell size was significantly lower in MtAT compared to FemAT, with ScAT having intermediate-size adipocytes (Figure 5.16, B). I then assessed M1/M2 polarisation of macrophages by staining the sections for CD40 (surface marker of M1 macrophages) and CD206 (surface marker of M2 macrophages)[22]. I observed that the ratio of CD40+/CD206+ cells in MtAT was ~2 fold higher than ScAT and ~5 fold higher than FemAT (Figure 5.16, C & J-O), fully in keeping with the results obtained from the gene expression studies.

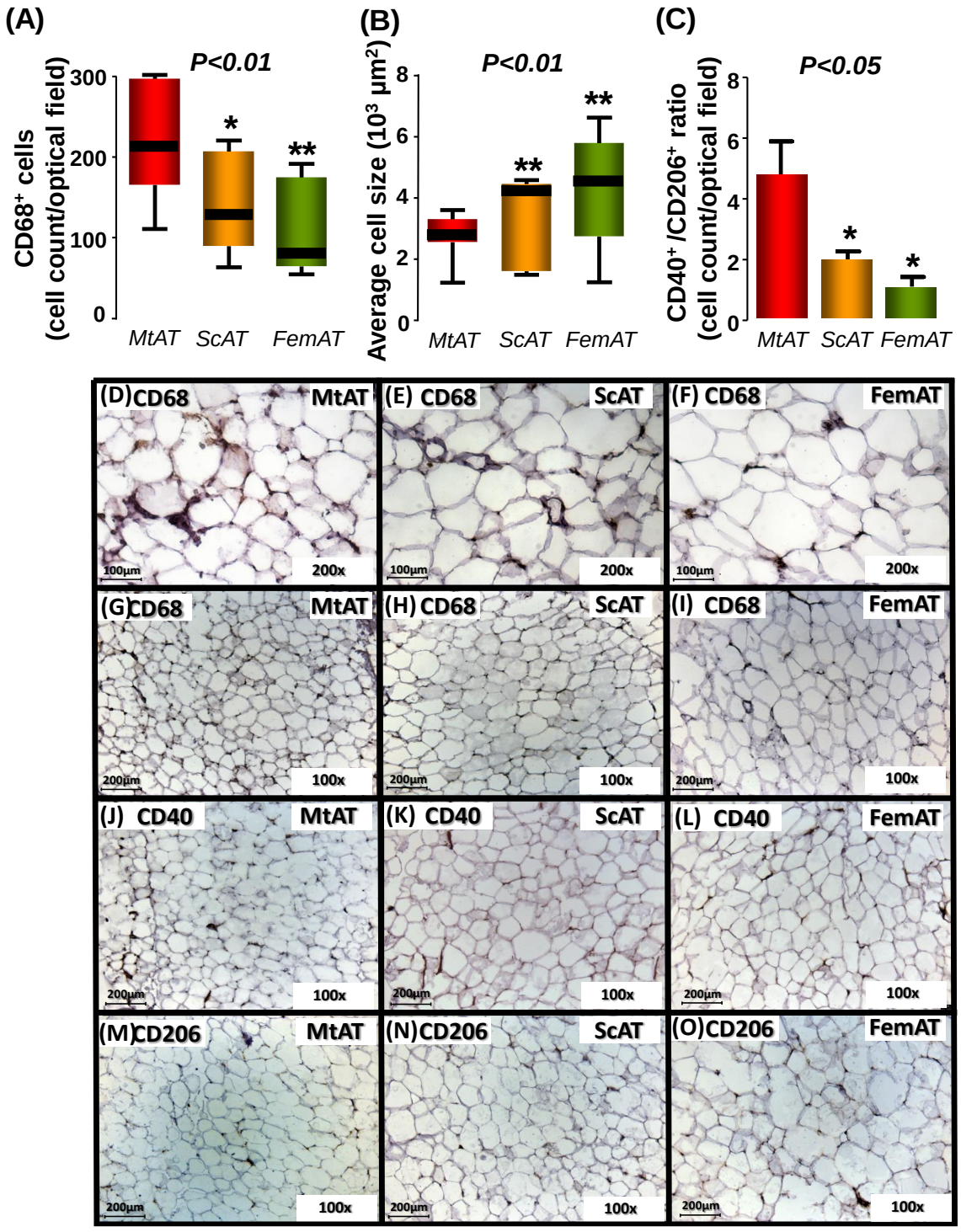


Figure 5.16: *In sections of paired human mesothoracic (MtAT), subcutaneous (ScAT) and femoral adipose tissue (FemAT) (n=7), staining for CD68 showed significantly higher count of CD68+ macrophages in MtAT compared to ScAT and FemAT (Panel A and images D-I). FemAT adipocytes were larger in size compared to the other depots (Panel B). The CD40+/CD206+ ratio (indicative of M1/M2 activated macrophages ratio) was significantly higher in MtAT compared to the other two depots. Values are expressed as median [25th-75th percentile] for panels A&B or mean ± SEM for panel C. *P<0.05, **P<0.01 vs MtAT* ***(Margaritis et al. ATVB 2014;34(9):2151-9)***

The results from the gene expression and immunohistochemistry experiments show that human FemAT from atherosclerotic patients exhibits reduced infiltration of CD68+ macrophages, with lower M1/M2 polarisation ratio. The reduced inflammatory state of this tissue, accompanied by an increased expression of IL-6 receptors, could explain its heightened sensitivity to exogenous inflammation, as documented in the ex vivo experiments in paragraph 5.3.4. Taken together, these results suggest that in human atherosclerosis a high degree of adipose tissue infiltration by macrophages in specific depots leads to a loss of response to variations of exogenous inflammation of PPARγ and as a consequence a loss of effects on its downstream signalling, as described by *CD36* and *ADIPOQ*.

5.4 Discussion

In this chapter I explored the mechanisms regulating adiponectin biosynthesis in patients with advanced coronary artery disease. I demonstrated that plasma BNP is the key determinant of serum levels of adiponectin and a major driver of adiponectin release from mesothoracic, subcutaneous and femoral adipose tissue of patients with ischemic heart disease. On the contrary, low-grade inflammation observed in CAD is not a significant regulator of circulating adiponectin in this population, as circulating inflammatory biomarkers predict *ADIPOQ* gene expression and release only in select adipose tissue depots with low infiltration with macrophages, such as femoral, but not in highly "inflamed" depots, such as mesothoracic. This could also be explained by the stronger effect of PPARγ signalling on the regulation of *ADIPOQ* gene expression in the femoral compared to other fat depots. By using an *ex vivo* model of human adipose tissue incubations, I demonstrated that only femoral (but not mesothoracic or subcutaneous) adipose tissue responds to exogenous inflammatory stimulation with IL-6 and TNF-α by suppressing PPARγ signalling and adiponectin expression/release. Importantly,

simultaneous exposure to BNP was able to reverse the effects of these inflammatory cytokines in femoral adipose tissue. These findings suggest that serum adiponectin levels are regulated by complex interactions between cytokines and BNP and the net effect is determined by the background disease state and the nature of the underlying inflammatory stimulus.

5.4.1 Adiponectin as a biomarker in cardiovascular disease

As reviewed in the Introduction chapter, large meta-analyses have demonstrated a clear link between high levels of adiponectin and reduced risk of prediabetes[247] and type 2 diabetes[109] in prospective cohorts of healthy individuals. However, despite its anti-atherogenic effects, the role of circulating adiponectin as a biomarker in cardiovascular disease is unclear, due to conflicting data on its clinical predictive value[248] . Although some early studies supported that higher adiponectin predicts low cardiovascular risk in healthy individuals,[192] elevated adiponectin levels have been associated with increased mortality in patients with heart failure.[243] To make matters even more confusing, in 2013 five different meta-analyses were published examining circulating adiponectin levels as a predictor of cardiovascular disease and stroke. One of them reported an association between high levels of adiponectin and lower risk of coronary heart disease in middle-aged men and women[249]. However, the other four studies failed to find a link between circulating adiponectin and incident coronary heart disease[250-253]; even worse, one of those studies also failed to find a link between adiponectin and stroke[250], whereas one study found a clear association between high adiponectin and higher risk of stroke[251] and the third found a higher risk for cardiovascular and total mortality in secondary prevention[252]. Importantly, in serial studies by Koh et al[254, 255] it was clearly demonstrated that conventional treatments (such as angiotensin converting enzyme inhibitors or statins) routinely used in patients with advanced atherosclerosis may also have a significant

impact on circulating adiponectin levels. Therefore, despite the beneficial metabolic, antioxidant and anti-atherosclerotic effects of adiponectin, its value as a biomarker is poorly understood and the mechanisms regulating its circulating levels are unclear.

Studies with cultured 3T3-L1 cells and human primary adipocytes have consistently shown that pro-inflammatory cytokines down-regulate adiponectin expression and release,[227] while in other studies natriuretic peptides (which are elevated in heart failure) have the opposite effect.[243] Despite these experimental findings, the net effect of systemic inflammation and BNP on adiponectin biosynthesis in adipose tissue from patients with ischemic heart disease is unclear.

In this chapter, I demonstrate that obesity (as evidenced by high BMI) is linked to reduced levels of adiponectin in the circulation in healthy subjects and patients with coronary atherosclerosis with preserved left ventricular function. However, this association is lost in patients with heart failure, even in the absence of coronary atherosclerosis. Indeed, I provide evidence that BNP is a strong driving force of adiponectin levels in the circulation. That is likely to be due to its function as a stimulus for adiponectin release from all adipose tissue depots (both *in vivo* and *ex vivo*), regulating levels of adiponectin in the circulation in patients with coronary atherosclerosis even in the absence of clinical heart failure. On the contrary, atherosclerosis-associated low grade inflammation was not related with changes in serum adiponectin levels in patients with coronary artery disease. Importantly, the correlation between circulating adiponectin and endothelial function observed in healthy individuals was weaker in patients with coronary atherosclerosis and was absent in the presence of heart failure. One possible explanation is that the value of circulating adiponectin as a biomarker in ischemic heart disease is confounded by the effect of circulating BNP as driving force of adiponectin synthesis. Another explanation for this finding is that in presence of advanced heart failure,

peripheral tissues exhibit adiponectin "resistance"; this is a mechanism which has been demonstrated in skeletal muscle[256] and adipose tissue[257] from patients with chronic heart failure.

My results, in combination with the literature presented, lead to the following conclusions. In disease-states such as obesity and type 2 diabetes, which are characterized by metabolic dysfunction but absence of myocardial dysfunction (as demonstrated by low BNP levels), low circulating adiponectin levels reveal the presence of a detrimental, pro-atherosclerotic, pro-inflammatory environment, which could increase the likelihood of adverse cardiovascular events in the future. On the other hand, in advanced cardiovascular disease states characterized by a failing myocardium which drives high BNP levels, adiponectin production in adipose tissue is increased as a "defence mechanism" in an attempt to protect the cardiovascular system. In these patients high adiponectin levels in the circulation flag the underlying advanced cardiovascular disease. However, the extent to which the potential beneficial effects conferred by adiponectin are successful in limiting the sequelae of a failing cardiovascular system is unclear.

5.4.2 Divergent characteristics of distinct human adipose tissue sites

In the last decades, it has been established that adipose tissue is not one uniform organ in the human body. Firstly, the identification of functioning brown adipose tissue in adults, as mentioned in Chapter 1, was a ground-breaking revelation in the study of adipose tissue biology in health and disease. Secondly, even among the different white adipose tissue depots, there exist significant structural and functional differences, which affect their biochemical behaviour. A number of studies have supported a beneficial, cardioprotective role for peripheral fat (pear-shaped adiposity) versus central, abdominal fat (apple-shaped adiposity)[258, 259]. Indeed, visceral adipose tissue has been shown to exhibit a heightened inflammatory state, associated with increased production of pro-

atherogenic adipokines[260]. A recent meta-analysis of 40 studies examining adipose tissue distribution and insulin resistance reported that visceral fat mass exhibited the strongest positive correlation with HOMA-IR, while there was no association of lower-extremity adipose tissue mass with insulin resistance[261]. In a study by Lee et al[262], the researchers employed CT to measure adipose tissue density (based on Hounsfield units) as a marker of inflammatory infiltration of this tissue. They found that abdominal adipose tissue exhibited lower density, suggesting increased inflammation. This was also associated with a profile of biomarkers suggestive of greater cardiometabolic risk, including lower adiponectin receptor expression.

In my clinical association studies, I found that adipose tissue sites which are "remote" from vessels (such as MtAT and ScAT) are associated with circulating adiponectin levels. Even though the expression of adiponectin in all adipose tissue depots examined was significantly related to plasma BNP levels, circulating levels of IL-6 and hsCRP were inversely related with *ADIPOQ* gene expression only in FemAT and not in MtAT or ScAT. Interestingly, I also noted that FemAT highly expresses IL6-R compared to MtAT and ScAT. By using immunohistochemistry, I demonstrated that MtAT and ScAT are highly infiltrated with macrophages shifted towards the M1 (proinflammatory) rather than M2 (resident) phenotype. My data suggests that "endogenous" inflammation of MtAT and ScAT may lead to down-regulation of IL-6R in these AT depots, which would explain their reduced responsiveness to exogenous inflammation, as demonstrated in the *ex vivo* experiments.

The results presented in this chapter lead to the conclusion that, while most adipose tissue depots contribute to the total circulating adiponectin pool, there are significant morphological and functional differences influencing the responsiveness of distinct adipose tissue sites to stimuli that affect adiponectin expression. Importantly, I presented

data showing that perivascular adipose tissue is not associated with circulating adiponectin levels. This observation would imply that PVAT displays unique properties with regards to adiponectin synthesis regulation. This is extensively explored in Chapter 6.

5.5 Conclusions

The degree of responsiveness of adipose tissue depots to inflammatory stimulation and BNP is reliant on the pre-existing inflammatory status of each depot. Obesity and low-grade inflammation reduce adiponectin levels in populations without significant cardiovascular disease and low plasma BNP. However, after the development of advanced cardiovascular disease adiponectin levels are no longer negatively controlled by low-grade inflammation, but they are driven upwards by circulating BNP levels. Therefore, high adiponectin levels in these populations "flag" the high levels of circulating BNP, explaining why high circulating adiponectin predicts (indirectly) worse clinical outcome in these populations. Interpretation of adiponectin as a biomarker should always take into account the underlying cardiovascular disease state.

Chapter 6

Cross-talk between perivascular adipose tissue and the vascular wall: the role of adiponectin

Chapter 6 explores the association between expression of adiponectin in perivascular adipose tissue and the redox state of the underlying vessel, and presents evidence for the existence of a reciprocal, two-way interaction between the aforementioned tissues.

6.1 Introduction

In the previous chapter, I presented evidence in favour of the notion that different adipose tissue sites in the human body have distinct biological behaviour. Perivascular adipose tissue (PVAT) is especially important to the development of atherosclerotic disease. Owing to its close proximity to the vascular wall, it has the potential to affect vascular homeostasis through paracrine mechanisms. The existing literature on the role of PVAT in human atherosclerosis is conflicting. Some studies support a detrimental role, by showing that increased volume of PVAT co-localizes with atherosclerotic plaques[167] and exhibits reduced differentiation and a heightened proinflammatory biochemical profile[168]. Other studies support a beneficial role, by demonstrating that PVAT displays anticontractile properties through paracrine diffusion of adiponectin[263], methyl palmitate[264] and hydrogen sulfide (H_2S)[265]. However, these protective anticontractile properties seem to be lost in obese humans due to hypertrophy of perivascular adipose tissue, causing local hypoxia, oxidative stress and inflammation[266]. It is unknown how PVAT is related to the oxidative status of the vessel it surrounds and whether the vessel itself could modify the biological behavior of its PVAT.

In Chapter 5, I showed that gene expression of adiponectin in PVAT was not related to serum levels of the adipokine, contrary to the other adipose tissue depots examined in

this project, which are located distally to large vessels (Figure 5.8). Similarly, the genetic variability of the *ADIPOQ* locus model, which was shown to influence serum adiponectin levels as well as its expression in mesothoracic adipose tissue (one of the "remote" adipose tissue depots) did not show any association with gene expression in PVAT. These observations would strongly suggest that local factors must affect the expression of adiponectin in PVAT and would appear to overwhelm the influence of genetic variability of the *ADIPOQ* locus in this specific adipose tissue depot.

In this chapter, I explore the relationship between adiponectin biosynthesis in PVAT and the redox state of the underling vessel and investigate the existence of a cross-talk between the human vascular wall and the adipose tissue surrounding it.

6.2 Methods

Sample collection, vascular superoxide measurements, biomarker measurements, Western immunoblotting, gene expression studies and statistical analysis were performed as described in the Methods chapter. No additional techniques were used in this chapter.

The study population in this chapter corresponds to the entire population of Phase I of the Oxford CABG Bioresource. Demographics can be seen in Table 3.1 of Chapter 3.

6.3 Results

6.3.1.1 Adiponectin expression in PVAT and vascular $O_2^{\cdot-}$ generation

Firstly, I sought to establish the relationship between expression of adiponectin in PVAT and the vascular redox state of the underlying vessel in humans. To this end I quantified the gene expression of adiponectin by qRT-PCR and also estimated the release of adiponectin from PVAT around the SV by using the adipose tissue explant culture model described in Chapter 2. Surprisingly I found that high vascular $O_2^{\cdot-}$ generation in

both SVs and IMAs was related to higher adiponectin expression in the PVAT surrounding the respective vessel (Figure 6.1, Panels A&B), as well as higher release of adiponectin from peri-SV PVAT (Figure 6.1, Panel C). This is the exact opposite association compared to the one observed between circulating adiponectin levels and vascular oxidative stress, where I showed that high levels of serum adiponectin were related to reduced $O_2^{\cdot -}$ generation in human vessels (results in Chapter 3, Figure 3.6, page 102).

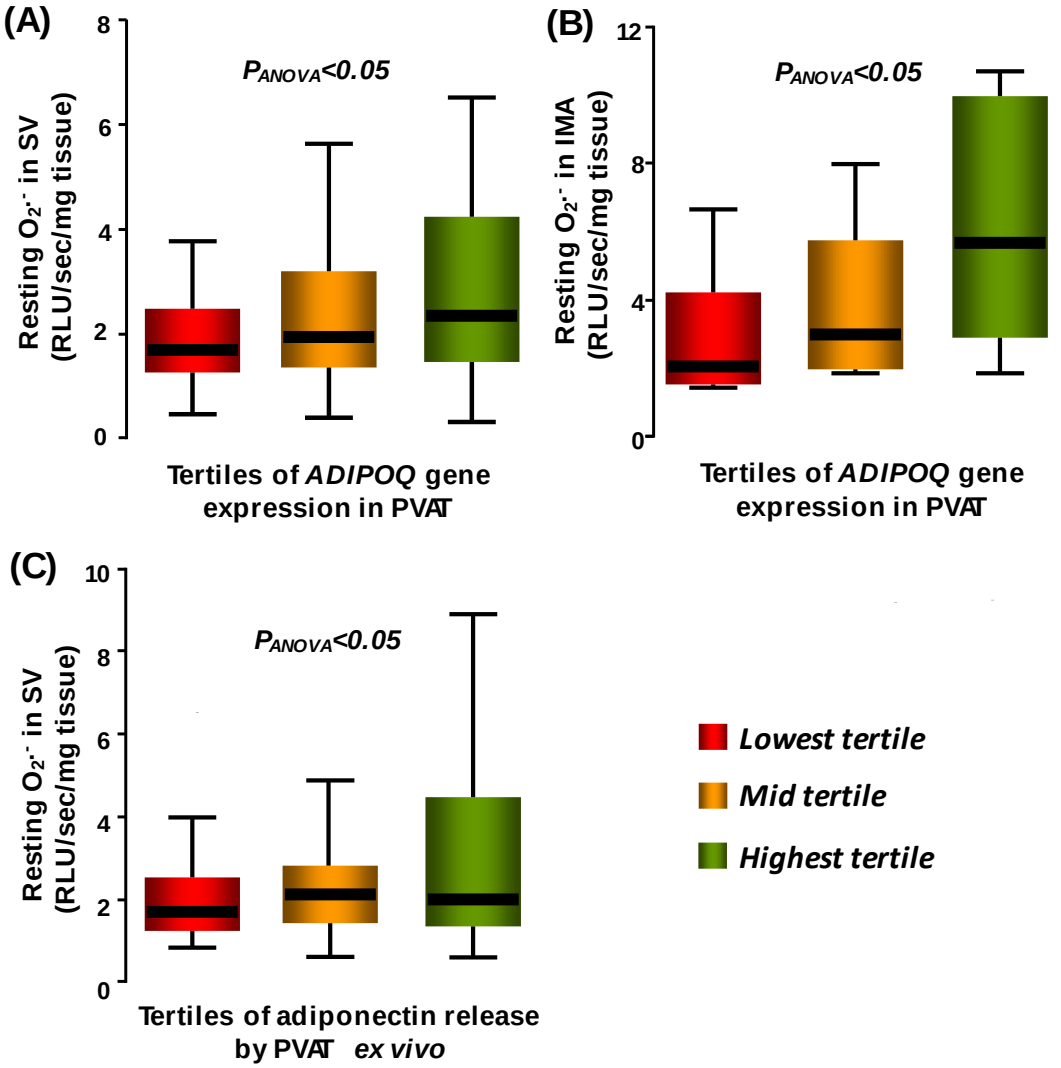


Figure 6.1: *High vascular superoxide ($O_2^{\cdot -}$) generation in saphenous veins (SV, n=244) and internal mammary artery (IMA, n=182) segments was related to higher adiponectin gene expression in the respective perivascular adipose tissue (PVAT) (Panels A & B). Similarly, higher ex vivo release of adiponectin from peri-SV PVAT supernatant (after 4-hour culture, Panel C, n=244) was also related with high $O_2^{\cdot -}$ in SVs. Values expressed as median [25^{th}-75^{th} percentile].* ***(Margaritis et al. Circulation 2013;127(22):2209-21)***

6.3.1.2 Adiponectin expression in PVAT and eNOS coupling

Continuing from the previous observations, I found that higher LNAME-inhibitable $O_2^{\cdot-}$ in both SVs and IMAs (indicative of more eNOS uncoupling) was related with higher *ADIPOQ* gene expression in the PVAT corresponding to these vessels (Figure 6.2, Panels A&B). Once again, these findings were compatible with increased local adiponectin synthesis and release observed in peri-SV PVAT from these patients (Figure 6.2, Panel C).

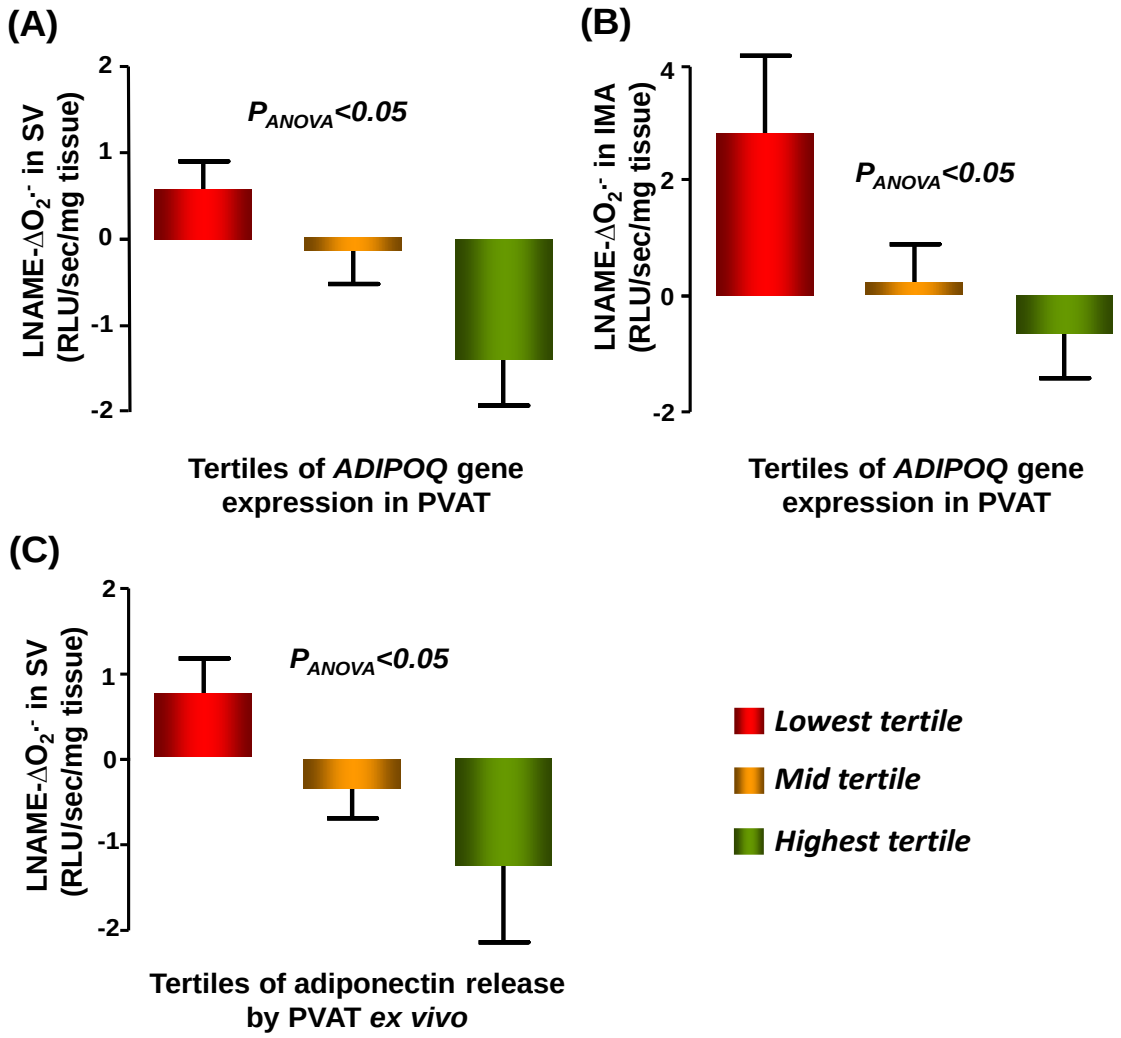


Figure 6.2: *Higher LNAME-inhibitable superoxide ($O_2^{\cdot-}$) in saphenous veins (SV, n=244) and internal mammary arteries (IMA, n=182), suggesting more uncoupled eNOS, was related to higher adiponetin gene expression in the respective perivascular adipose tissue (PVAT). Similarly, higher ex vivo release of adiponectin after 4-hour culture of peri-SV PVAT (Panel C, n=244) was related to greater LNAME-inhibitable vascular $O_2^{\cdot-}$ in human SVs. Values are expressed as mean ± SEM.* ***(Margaritis et al. Circulation 2013;127(22):2209-21)***

6.3.1.3 Adiponectin expression in PVAT and NADPH-oxidases activity

I then proceeded to examine the relationship between adiponectin gene expression in PVAT and NADPH-oxidases activity in the vascular wall. In keeping with the previous observations, I found that higher NADPH-stimulated $O_2^{\cdot -}$ generation in IMAs (indicative of higher NADPH-oxidases activity) was related with higher *ADIPOQ* gene expression in the PVAT surrounding the artery (Figure 6.3). These results are in stark contrast with the inverse association observed between circulating adiponectin levels and NADPH-stimulated $O_2^{\cdot -}$ generation in the IMA, initially presented in Chapter 3, Figure 3.7 and presented again below for comparison.

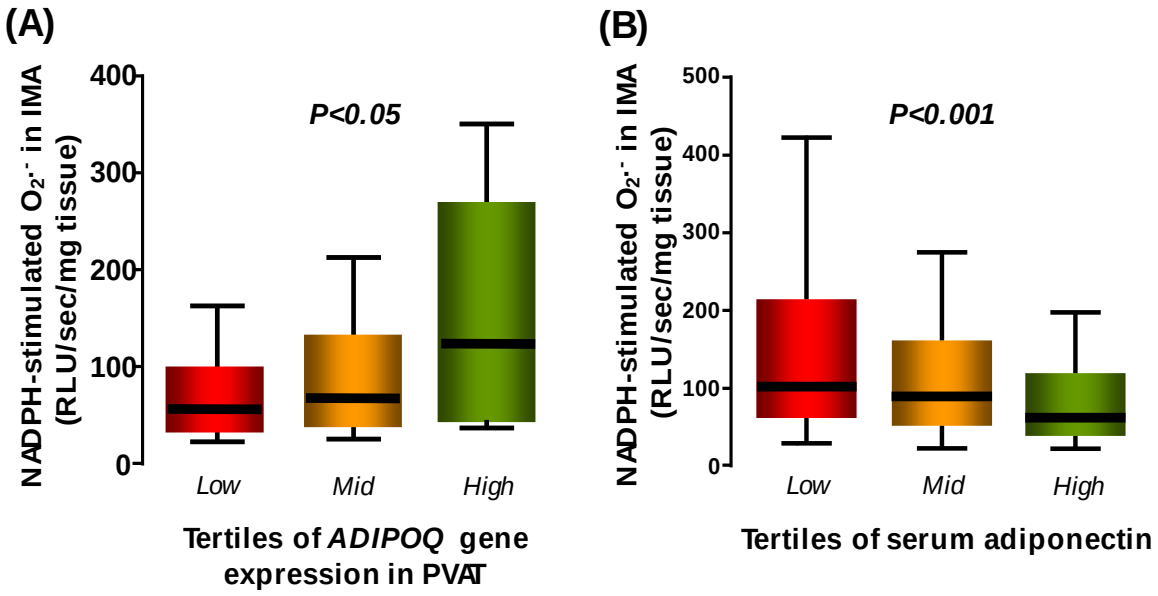


Figure 6.3 *High vascular NADPH-stimulated superoxide ($O_2^{\cdot -}$) generation in internal mammary artery (IMA) segments was related to higher adiponectin gene expression in perivascular adipose tissue (PVAT) (Panel A). On the contrary, high serum levels of adiponectin were related to reduced NADPH-stimulated $O_2^{\cdot -}$ generation in the IMA (Panel B) (n=182). Values are expressed as median [25^{th}-75^{th} percentile].* ***(Margaritis et al. Diabetes 2015;64(6):2207-19)***

6.3.2 "Local" versus "Remote" adipose tissue and vascular redox state

In Chapter 5, I demonstrated that gene expression and release of adiponectin from subcutaneous (ScAT) and mesothoracic (MtAT) adipose tissue displayed a small yet significant correlation with serum adiponectin levels (Figure 5.8). However, no such association was seen in PVAT. This generates the hypothesis that "remote" adipose tissue sites contribute to the serum adiponectin pool via endocrine effects, whereas the regulation of adiponectin expression in PVAT is regulated by local mechanisms. Given the unexpected correlation between high adiponectin gene expression in PVAT and high vascular oxidative stress, I proceeded to examine the association between adiponectin expression and release from ScAT and MtAT and vascular oxidative stress. I found that both adiponectin gene expression and release from subcutaneous (ScAT) and mesothoracic adipose tissue (MtAT) were inversely correlated with NADPH-stimulated $O_2\cdot^-$ generation in the IMA (Figure 6.4). This is in keeping with the suggestion that these adipose tissue depots are linked to the total circulating adiponectin pool and display inherently different biochemical behaviour compared to PVAT.

These seemingly conflicting findings pose an interpretative conundrum. One explanation would be that adiponectin released from PVAT has detrimental, pro-oxidant effects in the vasculature. However, I have already established the mechanisms through which adiponectin exerts protective, antiatherogenic effects, described in detail in Chapter 3, therefore this hypothesis is refuted by experimental evidence. The other explanation would be that these contrasting associations between adiponectin gene expression in different depots and vascular $O_2\cdot^-$ production reveal evidence of differential regulation of adiponectin synthesis between PVAT and "remote" adipose tissue sites, which are linked to circulating adiponectin levels, as shown in Chapter 5.

Based on my results so far, I hypothesized that high adiponectin expression in PVAT is caused by high oxidative stress in the underlying vessel. The increased levels of adiponectin released as a result would diffuse to the vascular wall and exert antioxidant effects, aiming to restore redox state balance. This could constitute a local, paracrine defence mechanism of PVAT against increased vascular oxidative stress in the underlying vessel.

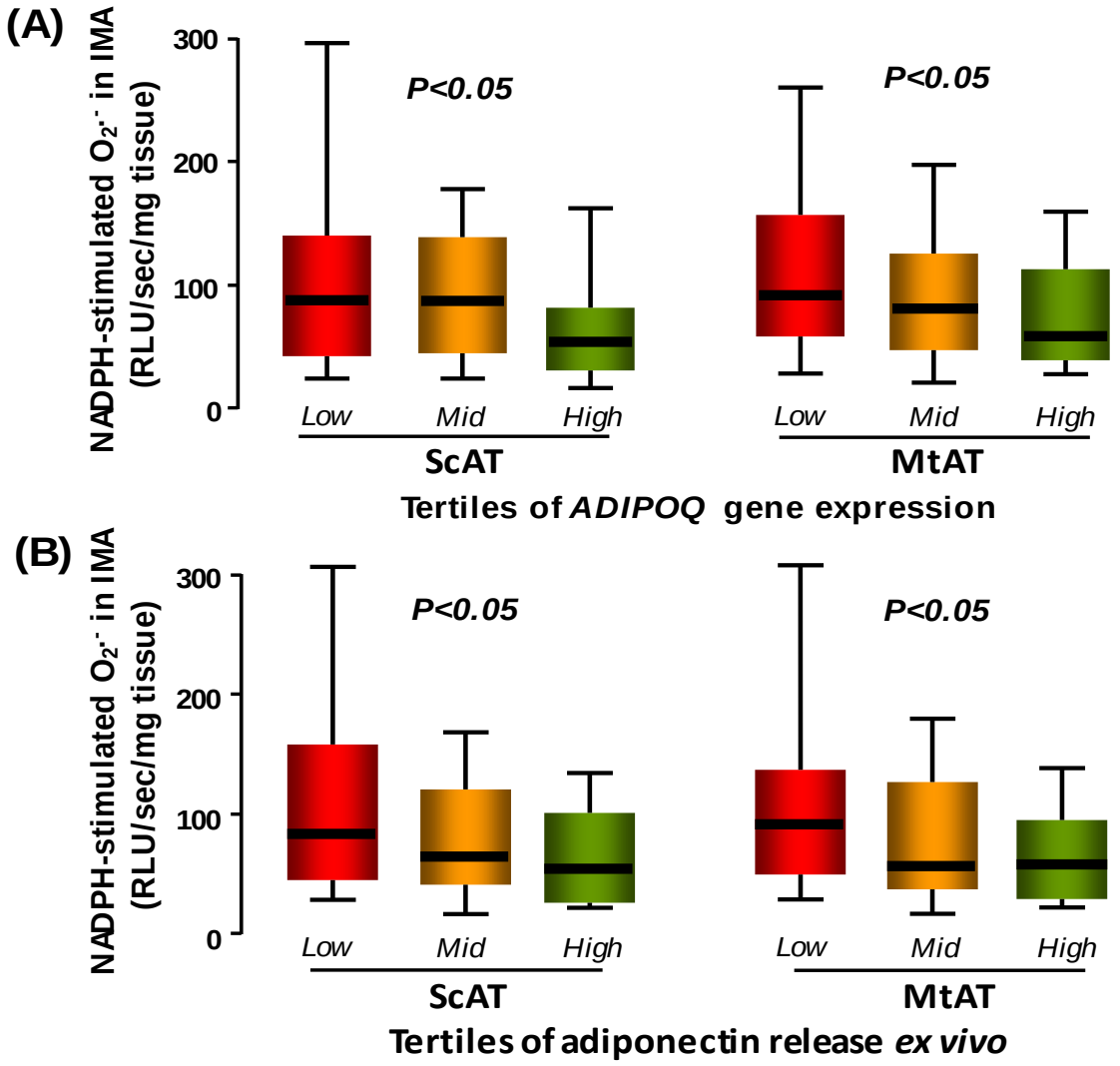


Figure 6.4 *High vascular NADPH-stimulated superoxide ($O_2^{\cdot -}$) generation in internal mammary artery (IMA) segments was related to lower adiponectin gene expression(A) and release (B) from subcutaneous (ScAT) and mesothoracic (MtAT) adipose tissue (Panel A). These observations are strikingly inverse to what was observed with regards to adiponectin expression in PVAT and NADPH-stimulated $O_2^{\cdot -}$ generation in the IMA (Figure 6.3, Panel A). Values are expressed as median [25^{th}-75^{th} percentile] (n=182).* ***(Margaritis et al. Diabetes 2015;64(6):2207-19)***

6.3.3 Exploring the existence of a "vessel-to-adipose tissue" signal

The presence of the "defence mechanism" such as the one described in the previous paragraph would necessitate the existence of a signal that would originate from the vascular wall and would be targeted at the perivascular adipose tissue. This signal would be able to trigger an up-regulation in adiponectin gene expression in PVAT, thus constituting the mediator of a "cross-talk" between PVAT and the vascular wall.

To establish proof-of-concept that such a communication indeed exists and is relevant to human vascular physiology, I designed the following experiment, presented in Figure 6.5. I collected pedicle IMA (IMA with its perivascular tissue) from patients recruited in the AdipoRedox study. In the lab, I carefully cut the IMA into segments and dissected the PVAT off a number of those segments, while maintaining it in others. I then proceeded to perform co-incubation experiments of PVAT with or without its respective IMA for 18 hours, as well as after stimulation of vascular NADPH-oxidases by using NADPH (100 μmol/L), or scavenging of superoxide radicals by using PEG-superoxide dismutase (SOD).

I found that removal of the underlying vascular tissue resulted into a ~50% reduction of *ADIPOQ* gene expression in PVAT, whereas stimulation of NADPH-oxidases led to even higher levels of adiponectin gene expression in PVAT. This was not due to direct effects of NADPH on PVAT (e.g. via effects on P2X receptors[267]), because incubation of PVAT + NADPH without the underlying vessel still led to a reduction in *ADIPOQ* gene expression. Importantly, scavenging $O_2^{\cdot -}$ with PEG-SOD not only prevented the NADPH-induced up-regulation of *ADIPOQ* gene, but it also resulted in its downregulation below the baseline (control) expression levels (PVAT+IMA). It is interesting to note that SOD works by converting $O_2^{\cdot -}$ to H_2O_2, therefore the high concentration of H_2O_2 generated seems to down-regulate adiponectin gene expression, as shown later in this thesis.

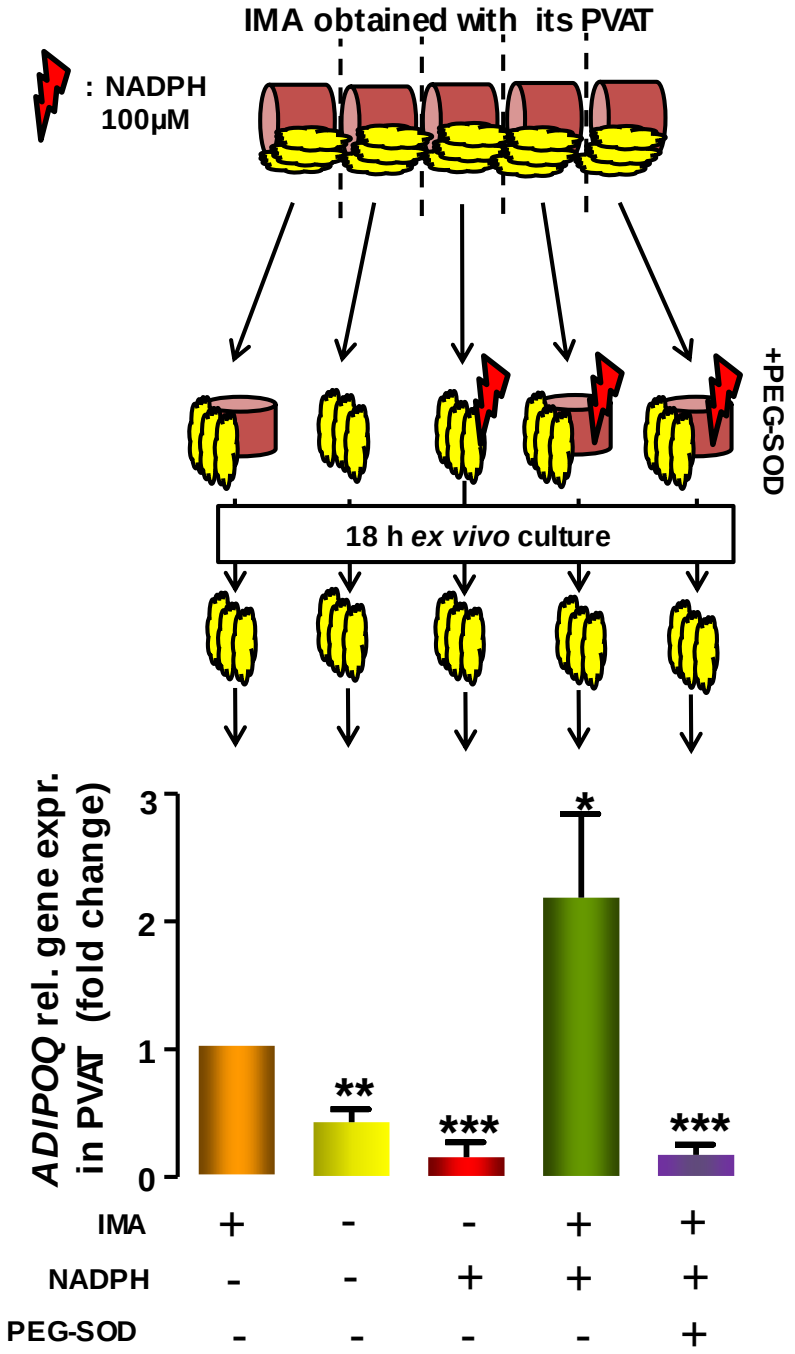


Figure 6.5: *Separation of perivascular adipose tissue (PVAT) from its underlying internal mammary artery (IMA) led to a reduction in ADIPOQ gene expression after 18 h incubation; conversely, stimulation of NADPH-oxidases–derived $O_2^{\cdot -}$ production by NADPH (100 µmol/L) significantly up-regulated ADIPOQ gene expression in PVAT (n=10). This was not through direct effects of NADPH on PVAT, as evidenced by a down-regulation of adiponectin gene expression in PVAT incubated with NADPH alone. This is further reinforced by the fact that scavenging of $O_2^{\cdot -}$ radicals with PEG-SOD prevented the up-regulation of ADIPOQ in PVAT after co-incubation with the underlying IMA and NADPH. Values are expressed as mean ± SEM. *P<0.05, **P<0.01, ***P<0.001 versus +IMA-NADPH-PEG-SOD* ***(Margaritis et al. Diabetes 2015;64(6):2207-19)***

These results demonstrate for the first time in humans that expression of adiponectin in perivascular adipose tissue can be regulated by changes in the oxidative stress status of the underlying vascular wall. They ultimately provide proof-of-concept evidence for the existence of a signal originating from the vascular wall targeting the PVAT, which has the ability to alter the biochemical behaviour of this adipose tissue site. Exploring the exact nature of this signal would be crucial in understanding the interactions between adipose tissue and the vascular wall in human disease.

6.3.4 Exploring the nature of the "vessel-to-adipose tissue" signal

In an attempt to define the nature of the aforementioned signal from the vascular wall to adipose tissue, I first hypothesized that free radicals themselves could potentially diffuse to PVAT from the vessel and trigger up-regulation of adiponectin. To explore this hypothesis, I collected PVAT surrounding the IMA and performed *ex vivo* incubations with hydrogen peroxide (H_2O_2 100 μmol/L for 16 hours) in order to simulate a high oxidative stress environment. Exposure of PVAT to H_2O_2 actually led to a significant reduction in *ADIPOQ* gene expression, without significantly affecting PPARγ gene expression (Figure 6.6), a result supported by the experiment presented in Figure 6.5.

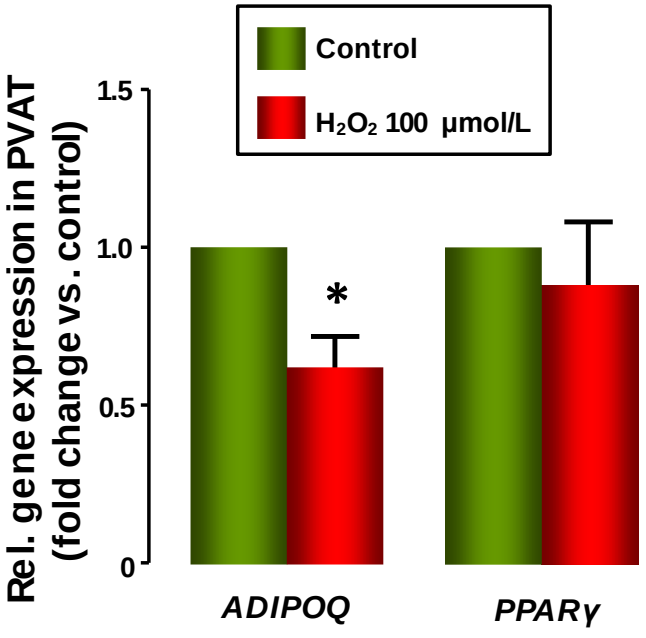


Figure 6.6: *Exposure of PVAT to hydrogen peroxide (H_2O_2 100 μmol/L) for 16 hours ex vivo led to reduction in ADIPOQ gene expression and no significant changes in PPARg gene expression. Values are expressed as mean ± SEM. *P<0.05 versus control.*

These results are not entirely unexpected. Direct exposure of adipose tissue to reactive oxygen species such as H_2O_2 and its associated radical $OH^{\cdot -}$ has been shown in the past to lead to a reduction in adiponectin gene expression[226] and this could not explain the results from the clinical association studies. Besides, free radicals by definition are extremely unstable moieties with very short half-life, rapidly reacting with proteins, lipid and DNA in a cellular setting; it would be highly unlikely that they would be able to reach perivascular adipose tissue from the vascular wall without first forming a more stable oxidation product.

This is precisely the premise on which I based my second hypothesis regarding the nature of the "vessel-to-adipose tissue" signal and proceeded to investigate the role of the lipid oxidation products 4-hydroxynonenal (4-HNE) and malonyldialdehyde (MDA) as potential candidate molecules. Both of these molecules are stable end-products of oxidation widely used as markers of systemic oxidative stress when measured in the circulation. Importantly, previous studies have shown that 4-HNE has the ability to up-regulate adiponectin gene expression in primary human adipocytes[244] and skeletal muscle cells[268]. However, their effects on human adipose tissue physiology, as well as their relationship to vascular oxidative stress, had not been examined before.

In order to recognise a molecule as the potential mediator of the cross-talk between adipose tissue and the vascular wall, two necessary conditions need to be shown experimentally. Firstly, increased oxidative stress in the vascular wall should be linked to increased production of the molecule from the vessel itself. Secondly, exposure of PVAT to the molecule should lead to a significant up-regulation of adiponectin expression. The existence of a molecule with the above properties could explain the observed positive associations between vascular oxidative stress and adiponectin gene expression in the surrounding PVAT, which were presented earlier in this chapter.

6.3.4.1 MDA & 4-HNE vascular content in conditions of high oxidative stress

To examine the first condition, I selected stored samples of SVs and IMAs obtained from patients demonstrating high or low vascular $O_2^{\cdot -}$ generation and estimated vascular 4-HNE protein adduct content by performing Western immunoblotting. I found that there was a good correlation between vascular $O_2^{\cdot -}$ and 4-HNE protein adducts in both SVs (r=0.720, P=0.042, n=11) and IMAs (r=0.489, P=0.039, n=18) (representative examples are shown in Figure 6.7). This suggests that there is increased production of 4-HNE in human arteries and veins in the presence of increased vascular oxidative stress.

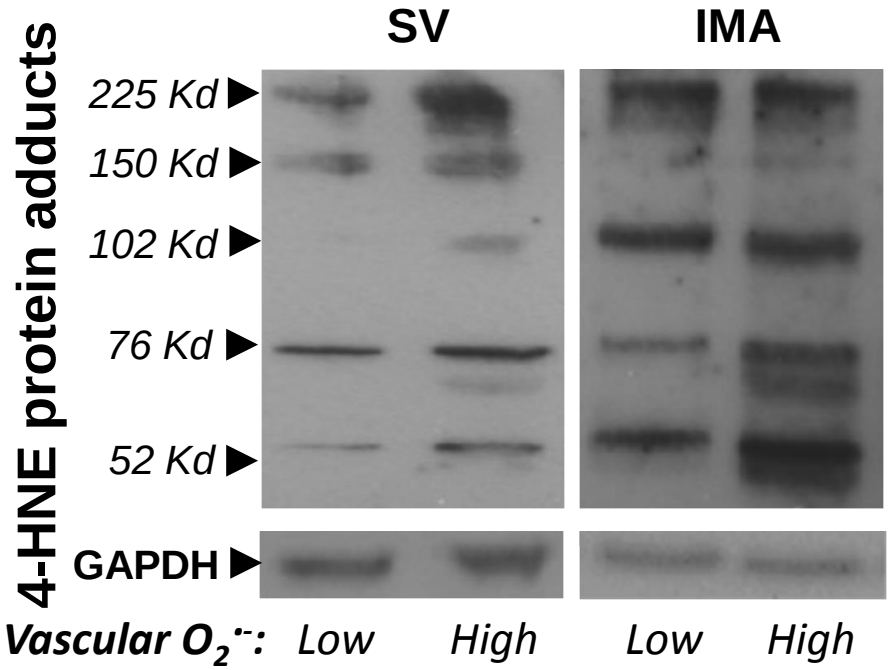


Figure 6.7: *The vascular content of 4-hydroxynonenal (4-HNE) protein adducts was evaluated in saphenous veins (SV) and internal mammary arteries (IMA) with known $O_2^{\cdot -}$ generation from patients in the Oxford CABG Bioresource. Representative blots for 4-HNE adducts in SVs with high (8.1 RLU/ Sec/mg) vs low (2.9 RLU/ Sec/mg) $O_2^{\cdot -}$ generation and IMAs with high (6.7 RLU/ Sec/mg) vs low (0.41 RLU/ Sec/mg) $O_2^{\cdot -}$ generation are presented.* ***(Margaritis et al. Circulation 2013;127(22):2209-21)***

Increased levels of 4-HNE protein adducts were also observed in human IMAs with higher NADPH-stimulated $O_2^{\cdot -}$ production, suggesting that NADPH-oxidase-derived $O_2^{\cdot -}$ is associated with increased production of 4-HNE in these vessels (Figure 6.8).

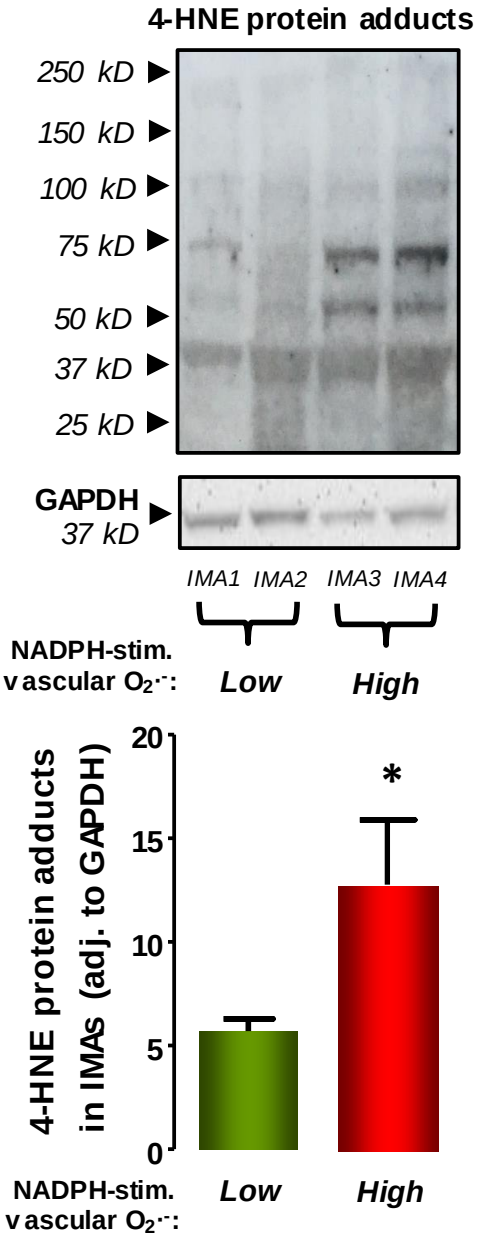


Figure 6.8: *Western immunoblotting for 4-hydroxy-nonenal (4-HNE) protein adducts revealed that internal mammary arteries (IMA) which demonstrate higher NADPH-stimulated $O_2^{\cdot -}$ exhibit higher levels of 4-HNE protein adducts. Representative blots from 4 patients out of n=9. Values are expressed as mean ± SEM. *P<0.05 vs low NADPH-stimulated $O_2^{\cdot -}$* ***(Margaritis et al. Diabetes 2015;64(6):2207-19)***

Similarly, IMAs obtained from patients with type 2 diabetes had higher levels of 4-HNE and MDA-protein adducts compared to patients without diabetes (Figure 6.9), in line with findings shown in Chapter 4 linking diabetes to increased vascular oxidative stress.

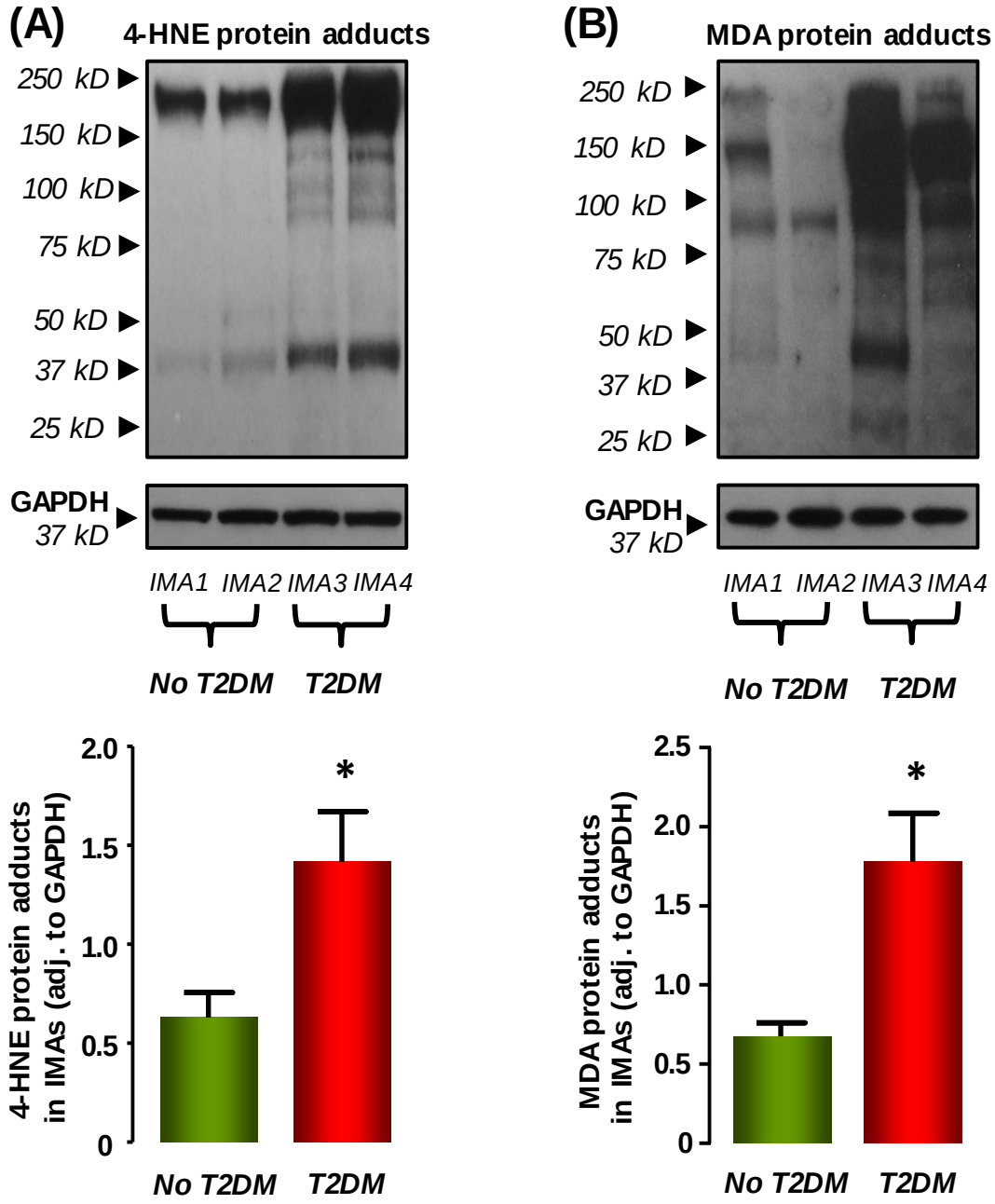


Figure 6.9: *Western blotting for 4-hydroxy-nonenal (4-HNE) and malonyldialdehyde (MDA) protein adducts revealed that internal mammary arteries (IMA) from patients with type 2 diabetes (T2DM) exhibit higher levels of 4-HNE (Panel A) and MDA (Panel B) protein adducts. Representative blots from 4 patients out of n=9. Values are expressed as mean ± SEM. *P<0.05 vs no T2DM.* ***(Margaritis et al. Diabetes 2015;64(6):2207-19)***

These findings lead to the conclusion that increased vascular oxidative stress (caused by diabetes or similar pro-atherogenic conditions) is linked to increased local vascular production of the oxidation products 4-HNE and MDA. Therefore, these molecules have the potential to be the "inside to outside – vessel to adipose tissue" signal linking vascular oxidative stress with up-regulation of *ADIPOQ* gene expression in PVAT.

6.3.4.2 Effects of MDA & 4-HNE on adiponectin gene expression in PVAT

Having established the link between vascular oxidative stress and increased production of MDA and 4-HNE, I proceeded to explore whether exposure of PVAT to these molecules has the ability to modify adiponectin gene expression in this depot. To this end, I first incubated PVAT samples obtained from the pedicle IMA of patients undergoing bypass surgery with MDA (1 mmol/L) for 16 hours and performed qRT-PCR. However, I was unable to find any significant effects of this molecule on adiponectin gene expression in PVAT (Figure 6.10).

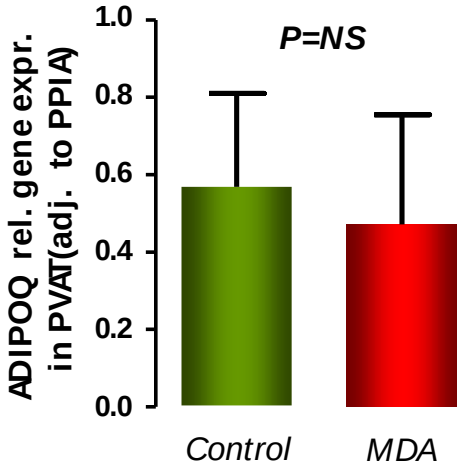


Figure 6.10: *Incubation of perivascular adipose tissue (PVAT) surrounding the internal mammary artery with MDA (1 mmol/L) for 16 hours ex vivo did not significantly alter the expression of adiponectin gene (ADIPOQ) (n=13). Values are expressed as mean ± SEM.* ***(Margaritis et al. Diabetes 2015;64(6):2207-19)***

I then proceeded to expose PVAT obtained around both the IMA and the SV with 4-HNE (30 μmol/L) for 16 hours and performed qRT-PCR. I found that 4-HNE led to a significant up-regulation of *ADIPOQ* gene expression in this adipose tissue depot (Figure 6.11, Panel A). This was accompanied by a parallel up-regulation of *PPARγ* gene expression (Figure 6.11, Panel B). Importantly, inhibition of PPARγ activity through use of the specific inhibitor T0070908 (10 μmol/L) prevented the effects of 4-HNE on *ADIPOQ* gene expression in PVAT.

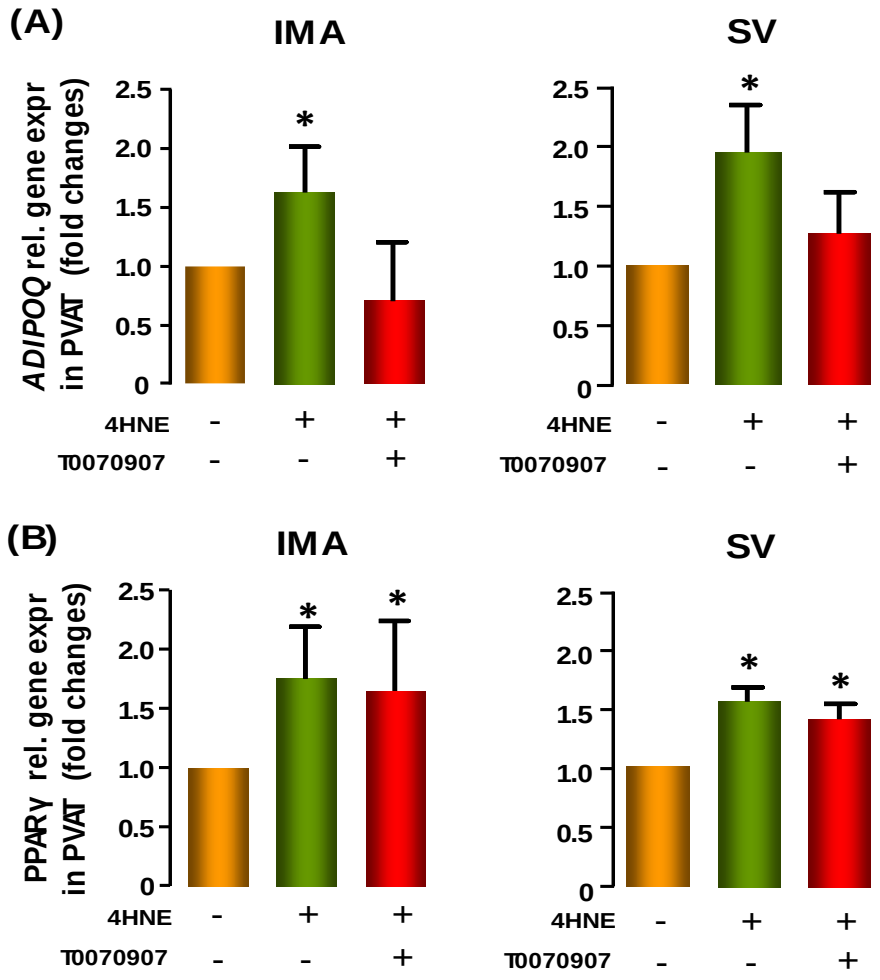


Figure 6.11: *Incubation of peri-IMA PVAT (n=11) and peri-SV PVAT (n=6) with 4-HNE 30 μM for 16hours led to up-regulation of ADIPOQ gene expression (Panel A), as well as PPAR-γ (Panel B). The effects of 4-HNE on ADIPOQ gene expression were prevented by the PPAR-γ activity inhibitor T0070907 (10 μM).Values are expressed as mean ± SEM.*P<0.05 versus control.* ***(Margaritis et al. Circulation 2013;127(22):2209-21; (Margaritis et al. Diabetes 2015;64(6):2207-19)***

The results from these experiments would suggest that 4-HNE fulfils both requirements in order to be recognised as a potential mediator in the cross-talk between the vascular wall and perivascular adipose tissue: its production is increased under conditions of vascular oxidative stress and it has the ability to up-regulate adiponectin gene expression in PVAT. The subsequent increase in adiponectin release would exert direct antioxidant effects in the vasculature, in an attempt to counter-act the pro-oxidant vascular microenvironment, by suppressing NADPH-oxidases activity and restoring eNOS coupling. This reciprocal, two-way interaction between perivascular adipose tissue and the vascular wall constitutes a novel paracrine defence mechanism against increased vascular oxidative stress.

6.4 Discussion

In this chapter, I presented my observations regarding a discordant relationship between vascular $O_2^{\cdot -}$ production and adiponectin expression in "remote" versus perivascular adipose tissue. My data suggest that increased vascular enzymatic production of $O_2^{\cdot -}$ is linked to increased adiponectin expression in PVAT, implying that its synthesis in this depot is driven by oxidative stress. I confirmed that the lipid oxidation product 4-HNE is present in increased quantities in the vascular wall under conditions of oxidative stress and it has the ability to up-regulate adiponectin expression in PVAT. The resulting increased adiponectin expression in PVAT would attempt to restore the vascular redox state, thus acting as a local paracrine defence mechanism against vascular oxidative stress.

6.4.1 Adiponectin expression in PVAT and vascular oxidative stress: a conundrum?

Reconciling the results from the clinical association studies and the *ex vivo* studies reveals an apparent loop paradox. My initial hypothesis for the existence of a PVAT-vessel reciprocal interaction was based on the antithesis between the association of high vascular oxidative stress with high adiponectin gene expression in PVAT and the known antioxidant effects of adiponectin. My results suggest that NADPH-oxidases and uncoupled eNOS lead to increased release of oxygen-derived free radicals, leading to higher production of 4-HNE. In turn, this up-regulates local adiponectin expression in PVAT in order to counteract the increased production of free radicals. However, if NADPH-oxidases are indeed successfully suppressed and eNOS is recoupled as a direct result of this locally increased adiponectin expression, then $O_2{\cdot}^-$ generation in the vascular wall should have been markedly decreased as a result and therefore increased $O_2{\cdot}^-$ release should never have been initially observed in the clinical cohort. As a consequence, I should never have been able to generate this hypothesis in the first place.

In fact, there are several explanations for this apparent paradox, which in no way invalidates the conclusions derived from my experiments. Firstly, it is not unreasonable to suggest that despite the existence of such a defence mechanism, this mechanism is obviously unable to fully suppress vascular $O_2{\cdot}^-$ generation in the studied vessels *in vivo*. More importantly, it is unknown whether in the absence of this mechanism, oxidative stress in the vascular wall would be even higher to what is quantified in my experiments. The extent to which perivascular adiponectin production is able to control redox state in the human vascular wall *in vivo* is hard to estimate, given the complexity of the mechanisms regulating vascular oxidative stress in humans.

Secondly, the vessels used in my thesis (the long saphenous veins and internal mammary artery) are inherently resistant to atherosclerosis. This is discussed in Chapter 7.

However, it can also be claimed that the existence of the proposed paracrine defence mechanism is a contributing factor to the known atherosclerosis resistance of these vessels. On the contrary, the PVAT surrounding the human coronary arteries has been shown to exhibit a high degree of inflammatory cell infiltration and a more undifferentiated phenotype[168]. Inflammatory changes to adipose tissue can lead to a loss of its protective anticontractile, antiatherogenic effects[266], partly mediated by suppressing adiponectin production. This could explain the failure of this protective mechanism to prevent coronary atherosclerosis in human disease.

6.4.2 The role of 4-HNE as a mediator of the cross-talk between PVAT and the vascular wall

My experiments highlighted the role of 4-hydroxynonenal as a mediator in the proposed interaction between adipose tissue and the vascular wall. 4-HNE is a 9 carbon-atom aldehyde with a double bond between atoms C2 and C3 conjugated to the head aldehyde group (C1) and a hydroxyl group at the C4 position (Figure 6.12). While the aldehyde group is hydrophilic, the nonpolar carbon chain from C5 to C9 is hydrophobic. This explains the preferential enrichment of the molecule in lipid-rich structures like membranes, as well as the capacity to cross the cellular membrane, which has been demonstrated before[269].

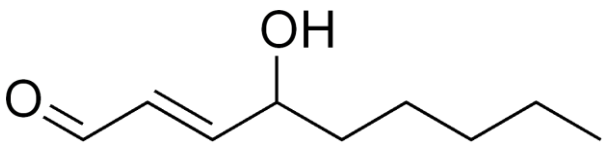


Figure 6.12: *Chemical structure of 4-HNE.*

4-HNE is a stable, end-product of ROS reaction with lipids containing polyunsaturated omega-6 acyl groups, such as linoleic or arachidonic acids. It can be formed both by enzymatic and non-enzymatic reactions and has been shown to act as a signalling molecule mediating cell-cycle processes/apoptosis, as well as interacting with a variety of other molecules modifying transcriptional pathways (e.g. AP-1, NF-kB, PPARs,

Akt and others)[270]. Previous literature has shown that 4-HNE has the ability to induce changes in gene expression in cells exposed to it extracellularly (e.g. changes in COX2)[271]. I now demonstrate for the first time in humans that increased oxidative stress in vascular tissue, caused by increased activity of pro-oxidant enzymes, is linked to increased production of 4-HNE, as evidenced by increased presence of 4-HNE protein adducts. I also show that 4-HNE has the ability to up-regulate adiponectin gene expression in human PVAT. Given that this molecule is able to cross the cellular membrane, I conclude that 4-HNE constitutes an inside-to-outside signal from the vessel to PVAT, with adiponectin being the counterpart to this interaction as an outside-to-inside signal from PVAT to the vessel.

6.4.3 The role of PVAT in atherosclerosis

The role of PVAT in atherosclerosis is a matter of considerable debate. On the one hand, there are a plethora of studies supporting a pro-inflammatory, pro-atherosclerotic role for this adipose tissue depot. Human pericoronary adipose tissue obtained from post-mortem samples from subjects who died from a non-atherosclerotic cause has been found to contain less differentiated adipocytes with a more inflammatory phenotype compared to subcutaneous and visceral adipose tissue from the same patients[168]. This heightened pro-inflammatory state is aggravated by the fact that PVAT is able to induce chemotaxis of peripheral leucocytes, namely macrophages and T-cells from the circulation[272]; in turn these inflammatory cells present in PVAT have been linked to increased myofibroblast recruitment/proliferation after balloon injury of porcine arteries, leading to vascular remodelling[273]. Similarly, in a mouse model of chronic inflammation, inflammation of PVAT was associated to increased matrix metalloproteinase (MMP)-mediated transforming growth factor-β production, resulting in neointima formation[274]. Additionally, human primary PVAT adipocytes have been shown to express and release

higher quantities of pro-angiogenic factors, such as thrombospondin-1, serpin-E1, MCP-1, acidic fibroblast growth factor, insulin-like growth factor-binding protein-3 and hepatocyte growth factor, compared with other adipocyte cell types[275]. Indeed, in humans, studies on post-mortem samples have shown that PVAT mass and infiltration with macrophages are significantly associated with atherosclerotic plaque size and composition in patients with atherosclerosis of the coronary arteries[276].

On the other hand, different studies would seem to suggest that PVAT can have effects which are beneficial to maintenance of vascular homeostasis. In a very important study by Chang et al[169], loss of PVAT in VSMC-specific PPARγ knock-out mice led to increased atherosclerosis after a high-fat diet, possibly through a loss of the protective thermogenic effects of PVAT in rodents. However, it is unclear whether such a mechanism would be applicable to human coronary atherosclerosis, given that pericoronary adipose tissue has been conclusively shown to be white adipose tissue and not brown[168]. Nevertheless, PVAT has a crucial role in maintaining vascular tone, by eliciting vasodilatory effects in both rat and human vessel rings[277,266]. Early studies showed that perivascular adipocytes produce a transferable adventitium-derived relaxing factor (ADRF) which causes relaxation of VSMCs through activation of potassium channels[278]. No single definitive ADRF has yet been identified: instead, several molecules and adipokines have been proposed as "ADRFs"; these include H_2S[265], palmitic acid methyl ester[264], prostacyclin[169], angiotensin 1-7[279] and adiponectin[263, 266]. An endothelium-independent mechanism involving activation of guanylyl cyclase by H_2O_2 has also been demonstrated[277]. However, these protective anti-contractile properties of PVAT seem to be lost in conditions linked to increased inflammation and hypoxia of adipose tissue, such as obesity[266] and metabolic syndrome[280]. Importantly, weight-loss

interventions in mice[281] and in humans, such as bariatric surgery[282], are able to reverse the obesity-induced phenotypical changes of PVAT and restore its anticontractile properties.

Overall, a vast amount of evidence supports an active role for PVAT in the regulation of vascular homeostasis in health and disease. Furthermore, it is evident that PVAT may be the potential source of a wide variety of adipocytokines with either protective or deleterious effects for vascular biology. Conversely, it is the balance between these two classes of adipokines that determines the net effects of PVAT on vascular biology. The characterization of the, yet miscellaneous, secretome of PVAT under different states of health or disease would therefore provide valuable insights into the pathophysiology of cardiometabolic disease.

My studies have demonstrated the existence of a novel role for perivascular adipose tissue in human physiology. Increased oxidative stress in the vascular wall causes elevated production of oxidation by-products, including 4-HNE. 4-HNE has the ability to up-regulate adiponectin gene expression in PVAT via a PPARγ-mediated pathway. Adiponectin, in turn, attempts to suppress oxidative stress, through the direct antioxidant mechanisms demonstrated in Chapter 3. This reciprocal, two-way interaction between PVAT and the vascular wall is summarized in Figure 6.12. By revealing the existence of this paracrine defence mechanism against oxidative stress, my results support the notion of a beneficial antioxidant effect of PVAT in human saphenous veins and internal mammary arteries.

6.5 Conclusions

Increased vascular oxidative stress leads to higher production of lipid oxidation products, such as 4-hydroxynonenal. 4-HNE has the ability to up-regulate adiponectin gene expression in perivascular adipose tissue. In turn, adiponectin has a direct antioxidant

effect in the vasculature, attempting to reduce the activity of pro-oxidant enzymes. This bi-directional interaction between adipose tissue and the vascular wall constitutes a newly-identified paracrine defence mechanism of the vascular wall against increased vascular oxidative stress (Figure 6.12).

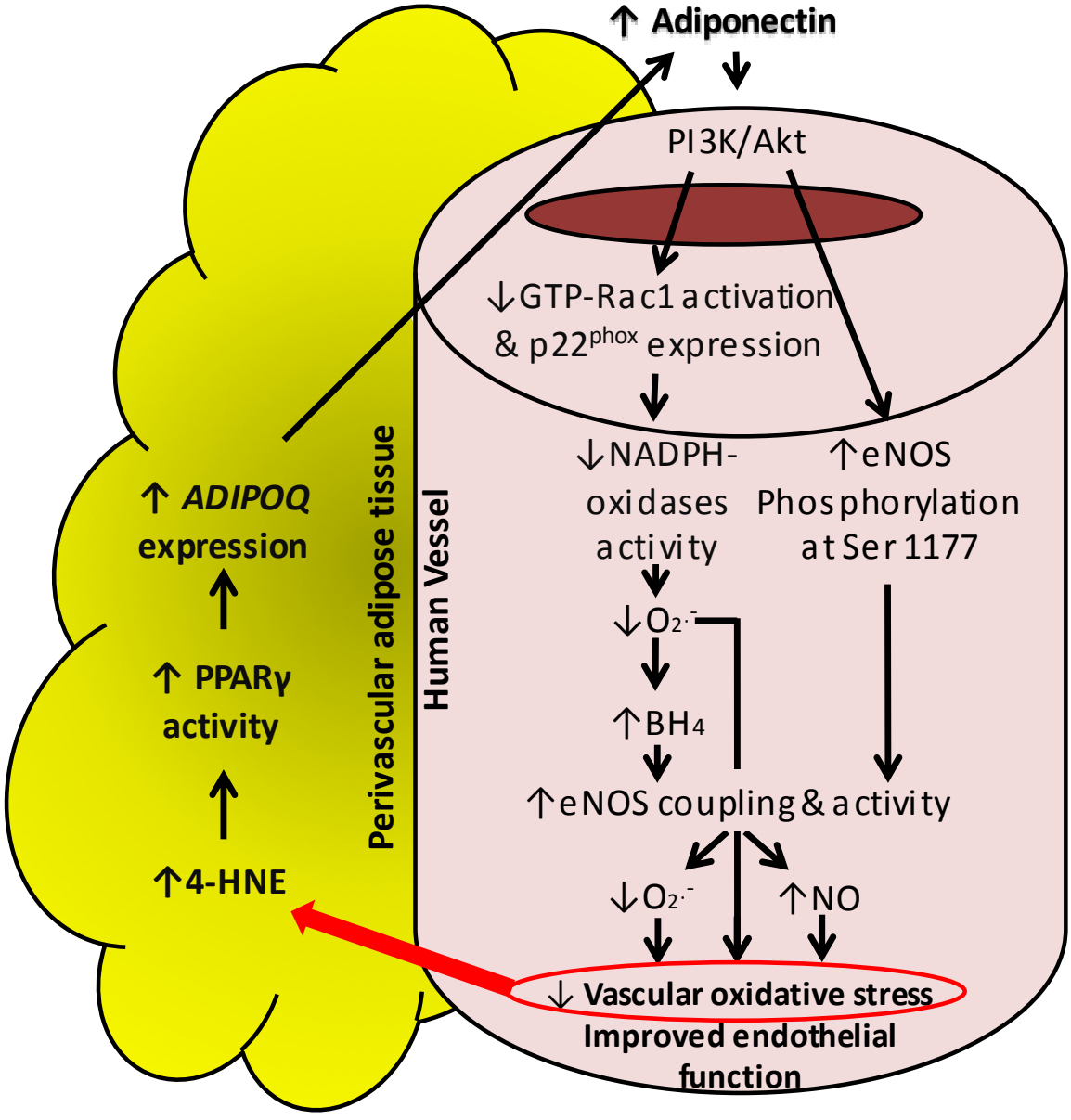


Figure 6.12: *The role of adipose tissue – vascular wall interactions in the regulation of human vascular redox state.*

Chapter 7
Study limitations

This chapter discusses potential limitations of my project and presents data from a small pilot study designed to address some of these limitations.

7.1 Use of saphenous veins

The vessels used throughout my thesis project (segment of the long saphenous vein and segment of a pedicle internal mammary artery) are well-known to be free from atherosclerotic disease. As a vein, the SV is exposed to a low pressure environment and displays innately different histological architecture compared to arteries.

To specifically address potential concerns regarding the use of a vein as a model system, I compared $O_2^{\cdot -}$ generation data from paired SVs and IMAs obtained from the same patients within the cohort. There was a strong, highly significant correlation between vascular $O_2^{\cdot -}$ generation in paired SVs and IMAs (R^2=0.43, P=0.0001). This can be explained by the fact that these vessels are obtained from patients with advanced coronary artery disease, displaying a systemic pro-oxidant, pro-inflammatory, pro-atherogenic environment arising from a combination of genetic, environmental and social risk factors.

Furthermore, all *ex vivo* mechanistic experiments were performed by using either both SVs and IMAs or IMAs alone, to ensure that they are relevant to human arterial physiology. The only experiments performed in SVs alone are the organ bath vasomotor studies. This is due to limited IMA tissue availability, which does not realistically allow for routine organ bath studies using these samples. That being said, the conclusions regarding endothelial function drawn on the basis of the *ex vivo* vasomotor studies are supported by *in vivo* measurements of flow-mediated dilatation of the brachial artery, which is also an accurate estimate of endothelial function.

In addition to the above, it is not unreasonable to claim that use of SVs as an experimental model is one of the best options available to study the mechanisms of human atherosclerotic disease. Firstly, it is obviously impossible to obtain actual coronary arteries from living patients. Cadaverous human coronary artery samples and their perivascular adipose tissue have been studied in the past[168], but such samples are clinically "dead" and are best used for histology and "snap-frozen sample" experiments; they certainly cannot be used for the complex, long-term incubation *ex vivo* experiments performed in my project. Secondly, as mentioned above, the SVs used in my thesis are obtained from patients with advanced atherosclerosis (critical coronary artery disease requiring bypass surgery). As such, they are chronically exposed to a systemic "pro-atherogenic" environment. On this basis, by studying these vessels we are able to understand the vascular biology of non-atherosclerotic vessels in a setting of "real life" atherosclerosis. Finally, given that the samples used constitute actual human vascular tissue, even if free from atherosclerosis, they provide a much closer approximation to human disease conditions than any *in vitro* cell culture or *in vivo* animal model ever could.

7.2 Lack of an atherosclerosis-free "control" group in the clinical cohort

A limitation of my study is the fact that my observations in the clinical cohort do not have an appropriate "control" group, i.e. a group of patients free from atherosclerosis. My study would potentially be much stronger if IMA and/or SV tissue could also have been obtained from human subjects without atherosclerosis, to allow direct comparison of human vascular biology in health and disease. However, "healthy" SVs are not harvested for any other type of surgery; conversely, surgical procedures that do involve SV harvesting (i.e. saphenectomy) do not provide access to "healthy" tissue, given that in those cases the SVs are the cause of the patient's disease (i.e. varicose veins) and their

physiology is highly abnormal. Similarly, there is no routine surgery that would provide access to internal mammary arteries. Given that IMAs are not harvested during valve surgery, access to these vessels in non-CABG patients is not possible.

Nevertheless, it could be claimed that obtaining adipose tissue samples from patients undergoing valve surgery and comparing that with tissue from patients undergoing bypass surgery would offer an attractive "control" sample from patients free from atherosclerosis. However, this would be impossible for PVAT: this tissue is firmly attached to the vascular wall of the IMA and it is not feasible to obtain it without harvesting the IMA (due to the possible risk of injuring the IMA and exposing the patient to higher perioperative risk). In my project, all IMAs studied are pedicle, harvested en bloc with their perivascular tissue, and separated in the lab under magnification.

In contrast, it is feasible to obtain subcutaneous and mesothoracic adipose tissue from patients undergoing valve repair/replacement who do not suffer from clinically significant coronary atherosclerosis. Indeed, as part of the AdipoRedox study, I obtained subcutaneous and mesothoracic adipose tissue from 29 patients undergoing such procedures. All of these patients had a preoperative coronary angiogram and clinically significant coronary artery disease was excluded prior to surgery. I performed biochemical measurements in serum/plasma and adiponectin gene expression in adipose tissue samples as described in Chapter 2 and proceeded to compare my results with the findings in the Oxford CABG Bioresource.

The demographic characteristics of this population are presented in Table 7.1 below, and are compared with the Oxford CABG Bioresource Phase I characteristics.

Table 7.1: Demographics of patients undergoing valve surgery compared to CABG patients

	Phase I Oxford CABG Bioresource	AdipoRedox patients undergoing valve surgery
Participants (n)	677	29
Age (years)	66.1±0.3	66.7±2.01
Males gender (%)	563 (83)	17(61)**
Hypertension, n (%)	465 (68)	17(61)
Hyperlipidaemia, n (%)	433 (64)	9(32)**
Diabetes mellitus, n (%)	221 (33)	2(7)**
Smoking (active/ex), n (%)	161/325 (24/48)	1/12(3.6/42.9)*
BMI (Kg/m^2)	27.6±0.17	26.0±0.7*
Cholesterol (mg/dl)	177.7±2.0	188.4±8.2
HDL (mg/dl)	38.6±0.5	42.3±1.8*
Triglycerides (mg/dl)	124[94-166]	100[74-137]*
Adiponectin (μg/ml)	10.1[1.2-28.7]	19.6[7.9-74.3]**
Medication (%)		
ACEi/ARBs	65	44*
Beta blockers	73	36**
Aspirin/clopidogrel	80	27**
Statins	76	36**

BMI: Body mass index; ACEi: Angiotensin converting enzyme inhibitors; ARBs: Angiotensin receptor blockers; *P<0.05; **P<0.01 vs CABG. Values presented as mean±SEM or median [25^{th}-75^{th} percentile].

Unsurprisingly these patients had a radically different risk factor profile for atherosclerosis compared to bypass patients. Even though patients in the two groups were of comparable age, there were a higher proportion of female, non-diabetic, non-

hyperlipidaemic individuals among patients undergoing valve surgery. There were also significant differences in the regular medications taken by these patients compared to patients with advanced atherosclerosis.

Serum levels of adiponectin as well as *ADIPOQ* gene expression in MtAT and ScAT were significantly higher in valve compared to CABG patients (Figure 7.1, Panels A-C). However, circulating adiponectin was extremely high (median value 19.6 μg/ml), and the values were comparable to those observed in patients with heart failure, as shown in Chapter 5. Therefore it is unclear whether patients having an operation for valvular heart disease can be used as "healthy controls" compared to patients undergoing CABG, at least when the aim is to study the physiology of adiponectin. To confirm that this is indeed the case, I quantified plasma brain natriuretic peptide (BNP) and observed that indeed, plasma BNP levels were 2-fold higher in patients undergoing valve surgery compared to CABG (Figure 7.1, Panel D). Interestingly, despite the absence of coronary artery disease and a more favourable risk profile, flow-mediated dilatation of the brachial artery and plasma MDA levels were not significantly different in valve patients compared to patients with coronary artery disease undergoing CABG (Figure 7.1, Panels E-F). This would imply presence of elevated levels of systemic oxidative stress and low-grade inflammation in these patients (both noted in patients within the heart failure spectrum as described in detail in Chapter 5). In any case, these results show that patients undergoing valve surgery cannot be used as a "healthy" control group in the context of my thesis project, due to significant differences in demographic/risk factor characteristics and a higher incidence of clinical heart failure, affecting the biology of adiponectin.

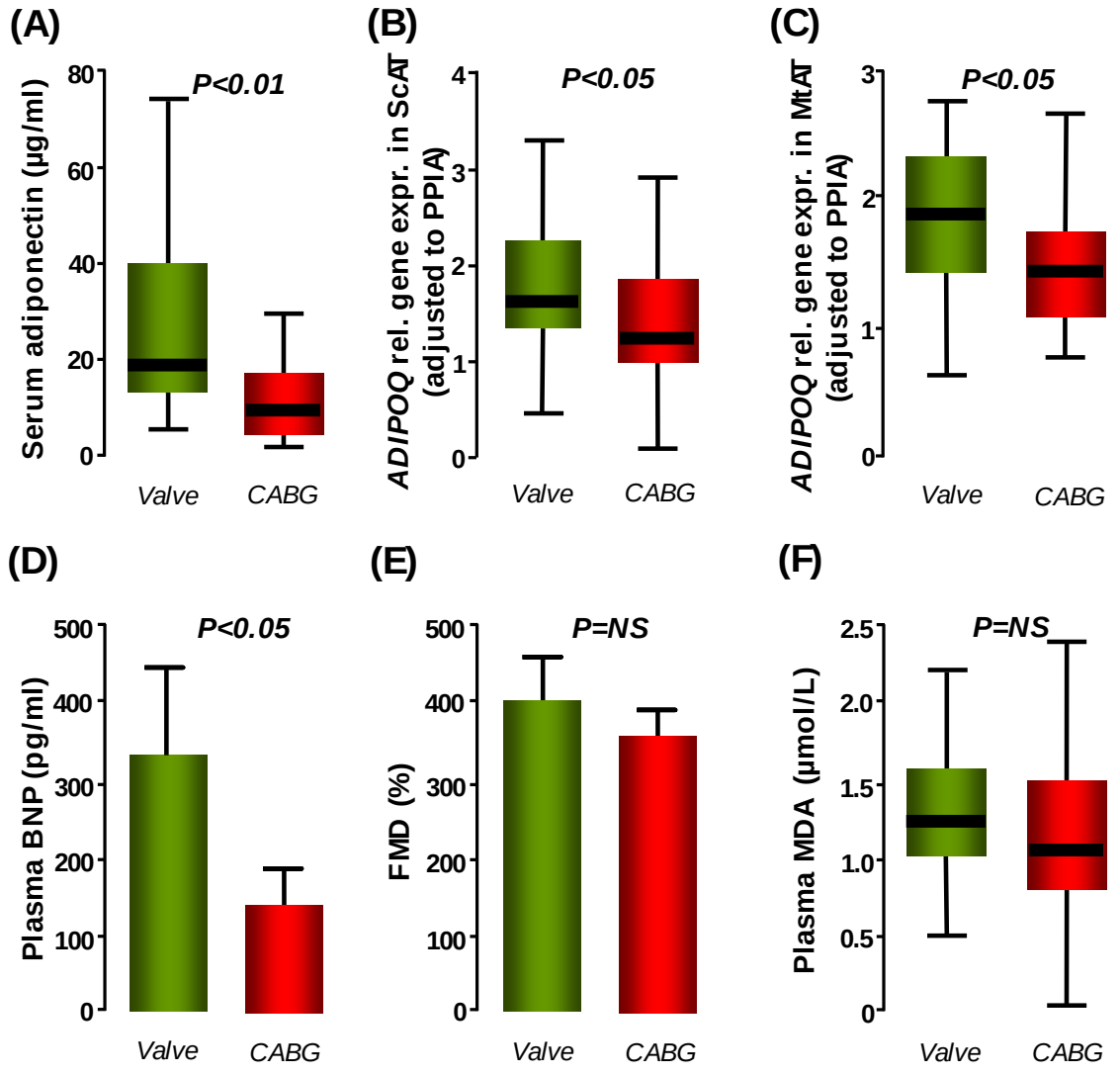


Figure 7.1: *N=29 patients undergoing valve replacement were recruited as candidate "control" subjects and compared with the Oxford CABG Bioresource Phase I cohort patients (n=677), who all had coronary artery disease. This "control" group had higher serum adiponectin levels (Panel A) and ADIPOQ gene expression in both subcutaneous (B, ScAT) and mesothoracic (C, MtAT) adipose tissue. However, valve patients had higher plasma brain natriuretic peptide (Panel D, BNP) and no significant differences in flow mediated dilatation (Panel E, FMD) or plasma malonylodialdehyde (Panel F, MDA). These findings suggest that the underlying pathology in patients undergoing valve surgery interferes with the mechanisms regulating adiponectin expression and vascular function, therefore they can't be used as "healthy controls" vs CABG patients. Values are expressed as median [25th-75th percentiles] (Panels A-C &F) or mean ± SEM (Panels D&E).*

Taking everything into consideration, the lack of a non-atherosclerotic control patient group does not detract from the value of my study results, because I do not rely purely on the clinical observations to draw mechanistic conclusions and causal relationships. It has been highlighted throughout my thesis that the associations observed in the clinical cohort do not demonstrate causality. Causal relationships have instead been shown through a Mendelian randomization study based on the genetic variability of the *ADIPOQ* locus, which largely eliminates the influence of environmental and social lifestyle risk factors. In addition, the *ex vivo* vascular tissue model uses a paired sample, same-patient source design, in which the only experimental condition differentiating the control from the intervention group is the intervention itself. The combination of these two experimental designs provides robust conclusions regarding causal relationships, even in the absence of a control group in the clinical cohort.

7.3 Other limitations

In Chapter 3, I demonstrated that incubation of vascular tissue with adiponectin 10 ug/ml for 6 hours did not lead to significant differences in protein expression of any subunits of NADPH-oxidases, although NOX5 was not examined. However, gene expression studies showed that $p22^{phox}$ gene expression was downregulated. This was the rationale for performing a longer incubation (18 hours), in order to detect a protein level change in $p22^{phox}$. It is therefore possible that an even longer incubation would lead to a demonstrable difference of other subunits of NADPH-oxidases as well, given the fact that detectable protein level changes would potentially require longer exposure to adiponectin. Similarly, in Chapter 4, in figure 4.9, while I did not detect differences in gene expression of adiponectin receptors in IMA tissue from diabetic vs. non-diabetic patients, it is possible that actual changes in protein level do exist, yet this was not tested experimentally.

Chapter 8
Discussion – Future work

This chapter presents the potential clinical and therapeutic value of the results documented in my thesis. It also highlights yet unanswered questions and discuss future work to investigate new hypotheses formed.

8.1 Clinical and therapeutic implications

8.1.1 Insights into the obesity "paradox"

The complexity of the role of adipose tissue in cardiovascular disease is highlighted by the so-called "obesity paradox". This term collectively summarizes the observation that moderately obese patients demonstrate, counterintuitively, lower overall complication and all-mortality rates compared to lean counterparts[283]. The obesity paradox has been documented by a wealth of clinical studies and under many metabolic & cardiovascular disease states including coronary artery disease, heart failure, peripheral arterial disease and arrhythmias[284]. In addition, amongst patients with type 2 diabetes mellitus and cardiovascular comorbidities, obese patients have been found to have lower mortality rates than lean individuals, whereas weight loss, and not weight gain, has been associated with increased morbidity and mortality rates [285]. Several hypotheses have attempted to explain this apparent paradox. Obese patients have been suggested to often be treated with more favourable medication regimens; on the other hand, decreased BMI in the context of advanced age and/or cardiovascular disease may reflect an overall malnutrition-cachexia-inflammation syndrome[284]. According to alternative theories it is believed that obesity may often been associated with increased muscle mass and better nutritional status that could elicit better metabolic responses in some circumstances[286]. This is depicted in recent studies that highlight the significance of "fitness over fatness"[283]. Furthermore, it is

reasonable to assume that the structural heterogeneity of different adipose tissue depots is associated with functional heterogeneity as well. Consequently, it may not obesity itself (as defined by global indices such as BMI) but rather the composition of adipose tissue in the body that affects the overall cardiometabolic effects of adipose tissue.

In any case, the existence of the obesity paradox profoundly demonstrates that our understanding about adipose tissue *in vivo* biology is still relatively poor. The results from my thesis shed some light into the unique structural and functional differences that characterize distinct adipose tissue depots. I have demonstrated that femoral adipose tissue exhibits reduced inflammatory infiltration and higher responsiveness to stimuli affecting adiponectin synthesis compared to mesothoracic and subcutaneous adipose tissue from the chest wall. This would lead credence to the theory of a beneficial effect of a gynecoid, "pear-shaped" adipose tissue distribution, linked to a more favourable adipokine profile in femoral and gluteal adipose tissue.

8.1.2 Adiponectin and adiponectin pathways as a therapeutic target

The results presented in my thesis provide evidence for the existence of direct antioxidant, atheroprotective effects of adiponectin in the human vasculature. As such, they lend strong support to the need for therapeutic interventions aimed at increasing adiponectin levels or targeting its downstream signalling pathways.

Lifestyle modifications play a major role in prevention of cardiovascular disease. As documented in my thesis, obesity and type 2 diabetes are strongly linked to reduced adiponectin levels. Smoking and lack of physical exercise have also been linked to hypoadiponectinaemia[287]. Interventions aimed at modifying these risk factors could form the cornerstone of a therapeutic approach targeting an increase in circulating adiponectin levels. Indeed, low circulating adiponectin in obese patients was increased via weight loss programs in diabetic and nondiabetic individuals[288] and in obese adolescents[289]. This was

accompanied by reduced levels of pro-inflammatory cytokines like TNFα and IL-6[290]. Similarly, moderately intense aerobic exercise leads to increased adiponectin levels only after one week of 2-3 exercise sessions[291]. Furthermore, adherence to a Mediterranean diet[292] and daily intake of fish or omega-3 supplementation[293] have also been linked to an increase in adiponectin levels.

Several pharmacological interventions already used in primary or secondary prevention of cardiovascular disease have also been linked to an increase in adiponectin levels. In my thesis, I provide evidence for the role of PPARγ as a universal regulator of adiponectin synthesis in all human adipose tissue depots examined. It comes as no surprise, therefore, that thiazolidinediones (glitazones), as PPARγ agonists, increase adiponectin levels in healthy, obese, and diabetic individuals[80]. Of course, the use of this class of medications requires caution due to increased risk of cardiovascular complications, as has been shown to be true especially in the case of rosiglitazone[294]. Nevertheless, glitazones provide a paradigm for successful pharmacological interventions in treating hypoadiponectinaemia.

Medications targeting the renin-angiotensin system have also been shown to significantly elevate circulating adiponectin and improve insulin sensitivity without affecting body adiposity[295]. Simultaneous administration of pioglitazone and candesartan to hypertensive diabetic patients significantly elevated baseline values of circulating HMW adiponectin[296]. A potential beneficial effect of angiotensin receptor blockers is increased differentiation of preadipocytes to mature adipocytes[297] via PPARγ[298]. Furthermore, telmisartan has been shown to enhance adiponectin sensitivity by up-regulating expression of AdipoR1 in experimental animal models[299].

In addition to the above agents, already well-established in our therapeutic arsenal against cardiovascular disease, attempts have been made at creating orally active

adiponectin receptor agonists. The first-in-class such molecule was ADP 355, described by Otvos et al in 2011[300]. ADP 355 is the lead peptidomimetic identified after peptide screening as an AdipoR1 and AdipoR2 agonist, with a higher affinity for AdipoR1. The researchers validated the synthetic peptide both *in vitro* and *in vivo* for cancer treatment in a mouse orthotopic human breast cancer xenograft model[300]. In 2013, Okada-Iwabu et al[301] reported in *Nature* the development of a small-molecule AdipoR agonist. Using both functional assays and single- & double-AdipoR1/2 knockout mice, the researchers identified an adiponectin receptor agonist –AdipoRon- with affinity for both receptors *in vivo*. They proceeded to demonstrate the efficacy of this compound by showing beneficial adiponectin-like effects in obese diabetic mice fed a high-fat diet: reduced liver and adipose tissue inflammation, diminished liver and skeletal muscle triglyceride content and increased antioxidant effects in adipose tissue, liver and muscle. The net effect was an improvement in glucose utilisation, increased insulin sensitivity and enhanced exercise tolerance, leading to increased life span of these mice[301]. This landmark study provided proof-of-concept that an adiponectin receptor agonist can achieve satisfactory oral bioavailability and reverse the pathophysiological consequences of obesity and diabetes.

Future work should focus both on clinical trials to validate the existing compounds and explore their safety and efficacy *in vivo* in humans, but also on the development of new compounds which could directly promote increased adiponectin synthesis in human adipose tissue. My thesis provides valuable insights into the mechanisms regulating adiponectin synthesis in distinct adipose tissue depots; the findings could form the basis of novel and exciting therapeutic approaches aimed at increased adiponectin levels in hypoadiponectinaemic states.

8.1.3 The importance of graft perivascular tissue in CABG surgery

In Chapter 7 I mention that the saphenous vein is a vessel that is free from atherosclerosis. While this is true when the vessel is in its *in vivo* anatomical location, it is important to note that use of saphenous veins as grafts in CABG surgery is plagued by disappointing rates of long-term graft patency. SV graft failure occurs in almost one in two grafts 5 to 10 years after surgery, with significant atheroma burden in the remaining grafts[302]. In some cohorts, up to 20% of SV grafts show clinically significant restenosis within just 1 year[303], in stark contrast to the excellent long-term patency rates of the LIMA (~95% patent in 5 years[303]).

Acute failure of the graft (within the first 6 weeks) is usually due to acute thrombosis; failure of the graft within the first year is due to intimal hyperplasia and neo-atherosclerosis is the cause of long-term graft failure[304]. The traditional technique of harvesting a long SV for use as graft in CABG, either open or endoscopic, involves separation of the SV from its perivascular tissue and distention of the vein with saline, to identify sites of discontinuity of the lumen. This leads to endothelial denuation and disturbs the normal vascular homeostatic mechanisms preserving vascular tone, contributing to vasospasm and endothelial dysfunction, which can trigger the process of atherogenesis[305].

Given these mechanisms contributing to graft failure, it has been hypothesized that preservation of perivascular tissue around the SV graft by using a no-touch, pedicle harvesting technique could potentially confer better patency and reduced failure rates. Indeed, small trials using no-touch techniques which harvest the SV en bloc with its perivascular adipose tissue have demonstrated long-term patency rates which approach those of the left IMA[306-309]. In mechanistic studies, the no-touch pedicle technique has been shown to confer improved NO bioavailability[310] and reduced vascular smooth muscle

cell activation[306]. In addition, one study highlighted the presence of leptin in SV graft PVAT after immunostaining, suggesting a beneficial role for PVAT-derived vasoactive molecules in preservation of vascular tone[311].

Fully in keeping with these observations, the conclusions from my thesis lead strong support to the notion that there exists a biological advantage in preserving perivascular adipose tissue around the SVs used as grafts in CABG surgery. I have demonstrated the existence of a reciprocal, two-way interaction between PVAT around the saphenous vein and the SV itself which acts as a defence mechanism against vascular oxidative stress. Adiponectin generated in PVAT could act on the underlying SV graft through paracrine or vasocrine signalling and exert its direct antioxidant effects. Indeed, the no-touch harvesting technique has been shown to preserve SV vasa vasorum[312], providing the anatomical basis to allow vasocrine signalling to take place. Given the pivotal role of oxidative stress in the development of atherosclerosis, any clinical intervention or change in practice that would reduce vascular production of reactive oxygen species could potentially protect against formation of neo-atherosclerosis. Of course, the existence of any real benefit can only be proven through randomized trials. My results highlight the need for large-scale trials to investigate this hypothesis and potentially lead to clinical practice-changing interventions.

8.2 Future work

8.2.1 Adiponectin in human health and disease

My work has shed light into the role of adiponectin in human vascular disease. I have established its antioxidant, antiatherogenic effects in the human vasculature and explored the complicated mechanisms regulating its synthesis in adipose tissue.

Several unanswered questions remain:

- A unified mechanism controlling adiponectin gene expression has not been clearly identified. While the role of PPARγ is crucial, it is possible that other transcription factors and regulatory mechanisms are involved. This can be explored using *ex vivo* experiments with pharmacological inhibitors of other transcription factors.
- The intracellular signalling pathways of adiponectin in human vascular tissue have not been explored. Even though I have demonstrated the central role of PI3K/Akt in mediating the effects of adiponectin, the exact mechanism leading to activation of this kinase system is unknown. Moreover, despite providing evidence for expression of all three known adiponectin receptors in human vascular tissue, it is unclear which ones contribute more to its anti-atherogenic effects and via which subcellular signalling pathways. This can be explored using a similar *ex vivo* experimental design as shown in my thesis, by using various pharmacological inhibitors of intracellular signalling molecules.
- Despite providing evidence of a PI3K/Akt-mediated down-regulation of $p22^{phox}$ gene expression by adiponectin, I have not identified the exact mechanism involved in this process. Similarly, it would be very interesting to investigate the effects of adiponectin on the human vascular transcriptome via microarray/gene chip analysis. This could identify novel adiponectin targets and uncover yet unknown effects of this adipokine.

- While 4-HNE and its adducts are potential mediators of the cross-talk between adipose tissue and the vascular wall, it is plausible that several other molecules released by the vascular wall could interact with PVAT. A metabolomic/lipidomic investigation of the vascular wall secretome could lead to identification of novel molecules with potential roles in a reciprocal two-way interaction between PVAT and human vessels.
- Even though I demonstrated that adiponectin has direct antioxidant effects, I did not include any function readouts that would show a direct beneficial effect of adiponectin in terms of improvement in endothelial function. One such experiment could be an organ bath vasomotor study of vascular tissue exposed to adiponectin, with/without pharmacological inhibitors.

8.2.2 The Oxford CABG Bioresource – Investigating novel adipokines

The cornerstone of my thesis project has been the Oxford CABG Bioresource. This unique tissue biobank can be used to investigate biological hypotheses relating to adipose tissue and cardiovascular disease. As such, the resources available can be utilized to explore the role of novel adipokines in human cardiovascular disease.

List of references

1. Barquera S, Pedroza-Tobias A, Medina C, Hernandez-Barrera L, Bibbins-Domingo K, Lozano R and Moran AE. Global Overview of the Epidemiology of Atherosclerotic Cardiovascular Disease. Archives of medical research. 2015;46:328-38.

2. Mendis S, Puska P, Norrving B, World Health Organization., World Heart Federation. and World Stroke Organization. Global atlas on cardiovascular disease prevention and control. Geneva: World Health Organization in collaboration with the World Heart Federation and the World Stroke Organization; 2011.

3. Antoniades C, Antonopoulos AS, Bendall JK and Channon KM. Targeting redox signaling in the vascular wall: from basic science to clinical practice. Curr Pharm Des. 2009;15:329-42.

4. Guzik TJ, Sadowski J, Kapelak B, Jopek A, Rudzinski P, Pillai R, Korbut R and Channon KM. Systemic regulation of vascular NAD(P)H oxidase activity and nox isoform expression in human arteries and veins. Arterioscler Thromb Vasc Biol. 2004;24:1614-20.

5. Antonopoulos AS, Lee R, Margaritis M and Antoniades C. Adiponectin as a Regulator of Vascular Redox State: Therapeutic Implications. Recent Pat Cardiovasc Drug Discov. 2011.

6. Deanfield JE, Halcox JP and Rabelink TJ. Endothelial function and dysfunction: testing and clinical relevance. Circulation. 2007;115:1285-95.

7. Frei B, Stocker R and Ames BN. Antioxidant defenses and lipid peroxidation in human blood plasma. Proc Natl Acad Sci U S A. 1988;85:9748-52.

8. Goldstein JL, Ho YK, Basu SK and Brown MS. Binding site on macrophages that mediates uptake and degradation of acetylated low density lipoprotein, producing massive cholesterol deposition. Proc Natl Acad Sci U S A. 1979;76:333-7.

9. Ishigaki Y, Oka Y and Katagiri H. Circulating oxidized LDL: a biomarker and a pathogenic factor. Curr Opin Lipidol. 2009;20:363-9.

10. Ishigaki Y, Katagiri H, Gao J, Yamada T, Imai J, Uno K, Hasegawa Y, Kaneko K, Ogihara T, Ishihara H, Sato Y, Takikawa K, Nishimichi N, Matsuda H, Sawamura T and Oka Y. Impact of plasma oxidized low-density lipoprotein removal on atherosclerosis. Circulation. 2008;118:75-83.

11. Kunsch C and Medford RM. Oxidative stress as a regulator of gene expression in the vasculature. Circulation research. 1999;85:753-66.

12. Shah AM and Channon KM. Free radicals and redox signalling in cardiovascular disease. Heart. 2004;90:486-7.

13. Channon KM and Guzik TJ. Mechanisms of superoxide production in human blood vessels: relationship to endothelial dysfunction, clinical and genetic risk factors. Journal of physiology and pharmacology : an official journal of the Polish Physiological Society. 2002;53:515-24.

14. Banfi B, Clark RA, Steger K and Krause KH. Two novel proteins activate superoxide generation by the NADPH oxidase NOX1. J Biol Chem. 2003;278:3510-3.

15. Lassegue B and Clempus RE. Vascular NAD(P)H oxidases: specific features, expression, and regulation. Am J Physiol Regul Integr Comp Physiol. 2003;285:R277-97.

16. Lassegue B, Sorescu D, Szocs K, Yin Q, Akers M, Zhang Y, Grant SL, Lambeth JD and Griendling KK. Novel gp91(phox) homologues in vascular smooth muscle cells : nox1 mediates angiotensin II-induced superoxide formation and redox-sensitive signaling pathways. Circulation research. 2001;88:888-94.

17. Briones AM, Tabet F, Callera GE, Montezano AC, Yogi A, He Y, Quinn MT, Salaices M and Touyz RM. Differential regulation of Nox1, Nox2 and Nox4 in vascular smooth muscle cells from WKY and SHR. Journal of the American Society of Hypertension : JASH. 2011;5:137-53.

18. Pandey D, Patel A, Patel V, Chen F, Qian J, Wang Y, Barman SA, Venema RC, Stepp DW, Rudic RD and Fulton DJ. Expression and functional significance of NADPH oxidase 5 (Nox5) and its splice variants in human blood vessels. American journal of physiology Heart and circulatory physiology. 2012;302:H1919-28.

19. Jones SA, O'Donnell VB, Wood JD, Broughton JP, Hughes EJ and Jones OT. Expression of phagocyte NADPH oxidase components in human endothelial cells. Am J Physiol. 1996;271:H1626-34.

20. Patterson C, Ruef J, Madamanchi NR, Barry-Lane P, Hu Z, Horaist C, Ballinger CA, Brasier AR, Bode C and Runge MS. Stimulation of a vascular smooth muscle cell NAD(P)H oxidase by thrombin. Evidence that p47(phox) may participate in forming this oxidase in vitro and in vivo. J Biol Chem. 1999;274:19814-22.

21. Brandes RP and Kreuzer J. Vascular NADPH oxidases: molecular mechanisms of activation. Cardiovasc Res. 2005;65:16-27.

22. Niu XL, Madamanchi NR, Vendrov AE, Tchivilev I, Rojas M, Madamanchi C, Brandes RP, Krause KH, Humphries J, Smith A, Burnand KG and Runge MS. Nox Activator 1. A Potential Target for Modulation of Vascular Reactive Oxygen Species in Atherosclerotic Arteries. Circulation.

23. Antonopoulos AS, Margaritis M, Verheule S, Recalde A, Sanna F, Herdman L, Psarros C, Nasrallah H, Coutinho P, Akoumianakis I, Brewer AC, Sayeed R, Krasopoulos G, Petrou M, Tarun A, Tousoulis D, Shah AM, Casadei B, Channon KM and Antoniades C. Mutual Regulation of Epicardial Adipose Tissue and Myocardial Redox State by PPAR-gamma/Adiponectin Signalling. Circulation research. 2016;118:842-55.

24. Stocker R and Keaney JF, Jr. Role of oxidative modifications in atherosclerosis. Physiol Rev. 2004;84:1381-478.

25. Gorlach A, Brandes RP, Nguyen K, Amidi M, Dehghani F and Busse R. A gp91phox containing NADPH oxidase selectively expressed in endothelial cells is a major source of oxygen radical generation in the arterial wall. Circulation research. 2000;87:26-32.

26. Rueckschloss U, Galle J, Holtz J, Zerkowski HR and Morawietz H. Induction of NAD(P)H oxidase by oxidized low-density lipoprotein in human endothelial cells: antioxidative potential of hydroxymethylglutaryl coenzyme A reductase inhibitor therapy. Circulation. 2001;104:1767-72.

27. Ray R, Murdoch CE, Wang M, Santos CX, Zhang M, Alom-Ruiz S, Anilkumar N, Ouattara A, Cave AC, Walker SJ, Grieve DJ, Charles RL, Eaton P, Brewer AC and Shah AM. Endothelial Nox4 NADPH oxidase enhances vasodilatation and reduces blood pressure in vivo. Arterioscler Thromb Vasc Biol. 2011;31:1368-76.

28. Forstermann U and Sessa WC. Nitric oxide synthases: regulation and function. European heart journal. 2012;33:829-37, 837a-837d.

29. Mount PF, Kemp BE and Power DA. Regulation of endothelial and myocardial NO synthesis by multi-site eNOS phosphorylation. J Mol Cell Cardiol. 2007;42:271-279.

30. Landmesser U, Hornig B and Drexler H. Endothelial function: a critical determinant in atherosclerosis? Circulation. 2004;109:II27-33.

31. Alp NJ, Mussa S, Khoo J, Cai S, Guzik T, Jefferson A, Goh N, Rockett KA and Channon KM. Tetrahydrobiopterin-dependent preservation of nitric oxide-mediated endothelial function in diabetes by targeted transgenic GTP-cyclohydrolase I overexpression. J Clin Invest. 2003;112:725-35.

32. Pacher P, Beckman JS and Liaudet L. Nitric oxide and peroxynitrite in health and disease. Physiol Rev. 2007;87:315-424.

33. Boger RH, Sydow K, Borlak J, Thum T, Lenzen H, Schubert B, Tsikas D and Bode-Boger SM. LDL cholesterol upregulates synthesis of asymmetrical dimethylarginine in human endothelial cells: involvement of S-adenosylmethionine-dependent methyltransferases. Circulation research. 2000;87:99-105.

34. Tran CT, Leiper JM and Vallance P. The DDAH/ADMA/NOS pathway. Atherosclerosis Supplements. 2003;4:33-40.

35. Antoniades C, Shirodaria C, Leeson P, Antonopoulos A, Warrick N, Van-Assche T, Cunnington C, Tousoulis D, Pillai R, Ratnatunga C, Stefanadis C and Channon KM. Association of plasma asymmetrical dimethylarginine (ADMA) with elevated vascular superoxide production and endothelial nitric oxide synthase uncoupling: implications for endothelial function in human atherosclerosis. European heart journal. 2009;30:1142-50.

36. Cardounel AJ, Xia Y and Zweier JL. Endogenous methylarginines modulate superoxide as well as nitric oxide generation from neuronal nitric-oxide synthase: differences in the effects of monomethyl- and dimethylarginines in the presence and absence of tetrahydrobiopterin. J Biol Chem. 2005;280:7540-9.

37. Scalera F, Borlak J, Beckmann B, Martens-Lobenhoffer J, Thum T, Tager M and Bode-Boger SM. Endogenous nitric oxide synthesis inhibitor asymmetric dimethyl L-arginine accelerates endothelial cell senescence. Arterioscler Thromb Vasc Biol. 2004;24:1816-22.

38. Boger RH, Maas R, Schulze F and Schwedhelm E. Asymmetric dimethylarginine (ADMA) as a prospective marker of cardiovascular disease and mortality--an update on patient populations with a wide range of cardiovascular risk. Pharmacological research : the official journal of the Italian Pharmacological Society. 2009;60:481-7.

39. Mueller CF, Laude K, McNally JS and Harrison DG. ATVB in focus: redox mechanisms in blood vessels. Arterioscler Thromb Vasc Biol. 2005;25:274-8.

40. Guzik TJ, West NE, Black E, McDonald D, Ratnatunga C, Pillai R and Channon KM. Vascular superoxide production by NAD(P)H oxidase: association with endothelial dysfunction and clinical risk factors. Circulation research. 2000;86:E85-90.

41. Kelley EE, Hock T, Khoo NK, Richardson GR, Johnson KK, Powell PC, Giles GI, Agarwal A, Lancaster JR, Jr. and Tarpey MM. Moderate hypoxia induces xanthine oxidoreductase activity in arterial endothelial cells. Free Radic Biol Med. 2006;40:952-9.

42. Zhang R, Brennan ML, Fu X, Aviles RJ, Pearce GL, Penn MS, Topol EJ, Sprecher DL and Hazen SL. Association between myeloperoxidase levels and risk of coronary artery disease. JAMA. 2001;286:2136-42.

43. Nicholls SJ and Hazen SL. Myeloperoxidase and cardiovascular disease. Arterioscler Thromb Vasc Biol. 2005;25:1102-11.

44. Hajer GR, van Haeften TW and Visseren FL. Adipose tissue dysfunction in obesity, diabetes, and vascular diseases. European heart journal. 2008;29:2959-71.

45. Duan SZ, Usher MG and Mortensen RM. Peroxisome proliferator-activated receptor-gamma-mediated effects in the vasculature. Circulation research. 2008;102:283-94.

46. Shimomura I, Shimano H, Korn BS, Bashmakov Y and Horton JD. Nuclear sterol regulatory element-binding proteins activate genes responsible for the entire program of unsaturated fatty acid biosynthesis in transgenic mouse liver. J Biol Chem. 1998;273:35299-306.

47. Barak Y, Nelson MC, Ong ES, Jones YZ, Ruiz-Lozano P, Chien KR, Koder A and Evans RM. PPAR gamma is required for placental, cardiac, and adipose tissue development. Mol Cell. 1999;4:585-95.

48. van Marken Lichtenbelt WD, Vanhommerig JW, Smulders NM, Drossaerts JM, Kemerink GJ, Bouvy ND, Schrauwen P and Teule GJ. Cold-activated brown adipose tissue in healthy men. N Engl J Med. 2009;360:1500-8.

49. Virtanen KA, Lidell ME, Orava J, Heglind M, Westergren R, Niemi T, Taittonen M, Laine J, Savisto NJ, Enerback S and Nuutila P. Functional brown adipose tissue in healthy adults. N Engl J Med. 2009;360:1518-25.

50. Lago F, Dieguez C, Gomez-Reino J and Gualillo O. Adipokines as emerging mediators of immune response and inflammation. Nat Clin Pract Rheumatol. 2007;3:716-24.

51. Scherer PE, Williams S, Fogliano M, Baldini G and Lodish HF. A novel serum protein similar to C1q, produced exclusively in adipocytes. J Biol Chem. 1995;270:26746-9.

52. Korner A, Wabitsch M, Seidel B, Fischer-Posovszky P, Berthold A, Stumvoll M, Bluher M, Kratzsch J and Kiess W. Adiponectin expression in humans is dependent on differentiation of adipocytes and down-regulated by humoral serum components of high molecular weight. Biochemical and biophysical research communications. 2005;337:540-50.

53. Liu Y, Chewchuk S, Lavigne C, Brule S, Pilon G, Houde V, Xu A, Marette A and Sweeney G. Functional significance of skeletal muscle adiponectin production, changes in animal models of obesity and diabetes, and regulation by rosiglitazone treatment. American journal of physiology Endocrinology and metabolism. 2009;297:E657-64.

54. Amin RH, Mathews ST, Alli A and Leff T. Endogenously produced adiponectin protects cardiomyocytes from hypertrophy by a PPARgamma-dependent autocrine mechanism. American journal of physiology Heart and circulatory physiology. 2010;299:H690-8.

55. Takahashi M, Arita Y, Yamagata K, Matsukawa Y, Okutomi K, Horie M, Shimomura I, Hotta K, Kuriyama H, Kihara S, Nakamura T, Yamashita S, Funahashi T and Matsuzawa Y. Genomic structure and mutations in adipose-specific gene, adiponectin. International journal of obesity and related metabolic disorders : journal of the International Association for the Study of Obesity. 2000;24:861-8.

56. Shapiro L and Scherer PE. The crystal structure of a complement-1q family protein suggests an evolutionary link to tumor necrosis factor. Current biology : CB. 1998;8:335-8.

57. Pajvani UB, Du X, Combs TP, Berg AH, Rajala MW, Schulthess T, Engel J, Brownlee M and Scherer PE. Structure-function studies of the adipocyte-secreted hormone Acrp30/adiponectin. Implications fpr metabolic regulation and bioactivity. J Biol Chem. 2003;278:9073-85.

58. Hattori Y, Hattori S, Akimoto K, Nishikimi T, Suzuki K, Matsuoka H and Kasai K. Globular adiponectin activates nuclear factor-kappaB and activating protein-1 and enhances angiotensin II-induced proliferation in cardiac fibroblasts. Diabetes. 2007;56:804-8.

59. Coppola A, Marfella R, Coppola L, Tagliamonte E, Fontana D, Liguori E, Cirillo T, Cafiero M, Natale S and Astarita C. Effect of weight loss on coronary circulation and adiponectin levels in obese women. International journal of cardiology. 2009;134:414-6.

60. Halberg N, Schraw TD, Wang ZV, Kim JY, Yi J, Hamilton MP, Luby-Phelps K and Scherer PE. Systemic fate of the adipocyte-derived factor adiponectin. Diabetes. 2009;58:1961-70.

61. Doran AC, Meller N, Cutchins A, Deliri H, Slayton RP, Oldham SN, Kim JB, Keller SR and McNamara CA. The helix-loop-helix factors Id3 and E47 are novel regulators of adiponectin. Circulation research. 2008;103:624-34.

62. Seo JB, Moon HM, Noh MJ, Lee YS, Jeong HW, Yoo EJ, Kim WS, Park J, Youn BS, Kim JW, Park SD and Kim JB. Adipocyte determination- and differentiation-dependent factor 1/sterol regulatory element-binding protein 1c regulates mouse adiponectin expression. J Biol Chem. 2004;279:22108-17.

63. Maeda N, Takahashi M, Funahashi T, Kihara S, Nishizawa H, Kishida K, Nagaretani H, Matsuda M, Komuro R, Ouchi N, Kuriyama H, Hotta K, Nakamura T, Shimomura I and Matsuzawa Y. PPARgamma ligands increase expression and plasma concentrations of adiponectin, an adipose-derived protein. Diabetes. 2001;50:2094-9.

64. Park SK, Oh SY, Lee MY, Yoon S, Kim KS and Kim JW. CCAAT/enhancer binding protein and nuclear factor-Y regulate adiponectin gene expression in adipose tissue. Diabetes. 2004;53:2757-66.

65. Soares AF, Guichardant M, Cozzone D, Bernoud-Hubac N, Bouzaidi-Tiali N, Lagarde M and Geloen A. Effects of oxidative stress on adiponectin secretion and lactate production in 3T3-L1 adipocytes. Free Radic Biol Med. 2005;38:882-9.

66. Fasshauer M, Klein J, Neumann S, Eszlinger M and Paschke R. Adiponectin gene expression is inhibited by beta-adrenergic stimulation via protein kinase A in 3T3-L1 adipocytes. FEBS Lett. 2001;507:142-6.

67. Yuan G, Chen X, Ma Q, Qiao J, Li R, Li X, Li S, Tang J, Zhou L, Song H and Chen M. C-reactive protein inhibits adiponectin gene expression and secretion in 3T3-L1 adipocytes. The Journal of endocrinology. 2007;194:275-81.

68. Ding Q, Ash C, Mracek T, Merry B and Bing C. Caloric restriction increases adiponectin expression by adipose tissue and prevents the inhibitory effect of insulin on circulating adiponectin in rats. The Journal of nutritional biochemistry. 2012;23:867-74.

69. Kern PA, Di Gregorio GB, Lu T, Rassouli N and Ranganathan G. Adiponectin expression from human adipose tissue: relation to obesity, insulin resistance, and tumor necrosis factor-alpha expression. Diabetes. 2003;52:1779-85.

70. Kotani K, Hazama A, Hagimoto A, Saika K, Shigeta M, Katanoda K and Nakamura M. Adiponectin and smoking status: a systematic review. Journal of atherosclerosis and thrombosis. 2012;19:787-94.

71. Mantzoros CS, Williams CJ, Manson JE, Meigs JB and Hu FB. Adherence to the Mediterranean dietary pattern is positively associated with plasma adiponectin concentrations in diabetic women. Am J Clin Nutr. 2006;84:328-35.

72. Simpson KA and Singh MA. Effects of exercise on adiponectin: a systematic review. Obesity. 2008;16:241-56.

73. Kopp HP, Krzyzanowska K, Mohlig M, Spranger J, Pfeiffer AF and Schernthaner G. Effects of marked weight loss on plasma levels of adiponectin, markers of chronic subclinical inflammation and insulin resistance in morbidly obese women. Int J Obes (Lond). 2005;29:766-71.

74. Aprahamian TR and Sam F. Adiponectin in cardiovascular inflammation and obesity. International journal of inflammation. 2011;2011:376909.

75. Shinmura K. Is adiponectin a bystander or a mediator in heart failure? The tangled thread of a good-natured adipokine in aging and cardiovascular disease. Heart failure reviews. 2010;15:457-66.

76. Siagris D, Vafiadis G, Michalaki M, Lekkou A, Starakis I, Makri M, Margaritis V, Christofidou M, Tsamandas AC and Labropoulou-Karatza C. Serum adiponectin in chronic hepatitis C and B. Journal of viral hepatitis. 2007;14:577-83.

77. Tsuchida A, Yamauchi T, Takekawa S, Hada Y, Ito Y, Maki T and Kadowaki T. Peroxisome proliferator-activated receptor (PPAR)alpha activation increases adiponectin receptors and reduces obesity-related inflammation in adipose tissue: comparison of activation of PPARalpha, PPARgamma, and their combination. Diabetes. 2005;54:3358-70.

78. Sharabi Y, Oron-Herman M, Kamari Y, Avni I, Peleg E, Shabtay Z, Grossman E and Shamiss A. Effect of PPAR-gamma agonist on adiponectin levels in the metabolic syndrome: lessons from the high fructose fed rat model. American journal of hypertension. 2007;20:206-10.

79. Choi KC, Lee SY, Yoo HJ, Ryu OH, Lee KW, Kim SM, Baik SH and Choi KM. Effect of PPAR-delta agonist on the expression of visfatin, adiponectin, and resistin in rat adipose tissue and 3T3-L1 adipocytes. Biochemical and biophysical research communications. 2007;357:62-7.

80. Yu JG, Javorschi S, Hevener AL, Kruszynska YT, Norman RA, Sinha M and Olefsky JM. The effect of thiazolidinediones on plasma adiponectin levels in normal, obese, and type 2 diabetic subjects. Diabetes. 2002;51:2968-74.

81. Antoniades C, Antonopoulos AS, Tousoulis D and Stefanadis C. Adiponectin: from obesity to cardiovascular disease. Obesity reviews : an official journal of the International Association for the Study of Obesity. 2009;10:269-79.

82. Heid IM, Henneman P, Hicks A, Coassin S, Winkler T, Aulchenko YS, Fuchsberger C, Song K, Hivert MF, Waterworth DM, Timpson NJ, Richards JB, Perry JR, Tanaka T, Amin N, Kollerits B, Pichler I, Oostra BA, Thorand B, Frants RR, Illig T, Dupuis J, Glaser B, Spector T, Guralnik J, Egan JM, Florez JC, Evans DM, Soranzo N, Bandinelli S, Carlson OD, Frayling TM, Burling K, Smith GD, Mooser V, Ferrucci L, Meigs JB, Vollenweider P, Dijk KW, Pramstaller P, Kronenberg F and van Duijn CM. Clear detection of ADIPOQ locus as the major gene for plasma adiponectin: results of genome-wide association analyses including 4659 European individuals. Atherosclerosis. 2010;208:412-20.

83. Hivert MF, Manning AK, McAteer JB, Florez JC, Dupuis J, Fox CS, O'Donnell CJ, Cupples LA and Meigs JB. Common variants in the adiponectin gene (ADIPOQ) associated with plasma adiponectin levels, type 2 diabetes, and diabetes-related quantitative traits: the Framingham Offspring Study. Diabetes. 2008;57:3353-9.

84. Morisaki H, Yamanaka I, Iwai N, Miyamoto Y, Kokubo Y, Okamura T, Okayama A and Morisaki T. CDH13 gene coding T-cadherin influences variations in plasma adiponectin levels in the Japanese population. Human mutation. 2012;33:402-10.

85. Fisher FM, McTernan PG, Valsamakis G, Chetty R, Harte AL, Anwar AJ, Starcynski J, Crocker J, Barnett AH, McTernan CL and Kumar S. Differences in adiponectin protein expression: effect of fat depots and type 2 diabetic status. Hormone and metabolic research = Hormon- und Stoffwechselforschung = Hormones et metabolisme. 2002;34:650-4.

86. Drolet R, Belanger C, Fortier M, Huot C, Mailloux J, Legare D and Tchernof A. Fat depot-specific impact of visceral obesity on adipocyte adiponectin release in women. Obesity. 2009;17:424-30.

87. Ding Q, Wang Z and Chen Y. Endocytosis of adiponectin receptor 1 through a clathrin- and Rab5-dependent pathway. Cell research. 2009;19:317-27.

88. Yamauchi T, Kamon J, Ito Y, Tsuchida A, Yokomizo T, Kita S, Sugiyama T, Miyagishi M, Hara K, Tsunoda M, Murakami K, Ohteki T, Uchida S, Takekawa S, Waki H, Tsuno NH, Shibata

Y, Terauchi Y, Froguel P, Tobe K, Koyasu S, Taira K, Kitamura T, Shimizu T, Nagai R and Kadowaki T. Cloning of adiponectin receptors that mediate antidiabetic metabolic effects. Nature. 2003;423:762-9.

89. Tanabe H, Fujii Y, Okada-Iwabu M, Iwabu M, Nakamura Y, Hosaka T, Motoyama K, Ikeda M, Wakiyama M, Terada T, Ohsawa N, Hato M, Ogasawara S, Hino T, Murata T, Iwata S, Hirata K, Kawano Y, Yamamoto M, Kimura-Someya T, Shirouzu M, Yamauchi T, Kadowaki T and Yokoyama S. Crystal structures of the human adiponectin receptors. Nature. 2015;520:312-6.

90. Antonopoulos AS, Margaritis M, Coutinho P, Shirodaria C, Psarros C, Herdman L, Sanna F, De Silva R, Petrou M, Sayeed R, Krasopoulos G, Lee R, Digby J, Reilly S, Bakogiannis C, Tousoulis D, Kessler B, Casadei B, Channon KM and Antoniades C. Adiponectin as a link between type 2 diabetes and vascular NADPH oxidase activity in the human arterial wall: the regulatory role of perivascular adipose tissue. Diabetes. 2015;64:2207-19.

91. Zhou L, Deepa SS, Etzler JC, Ryu J, Mao X, Fang Q, Liu DD, Torres JM, Jia W, Lechleiter JD, Liu F and Dong LQ. Adiponectin activates AMP-activated protein kinase in muscle cells via APPL1/LKB1-dependent and phospholipase C/Ca2+/Ca2+/calmodulin-dependent protein kinase kinase-dependent pathways. J Biol Chem. 2009;284:22426-35.

92. Yamauchi T, Nio Y, Maki T, Kobayashi M, Takazawa T, Iwabu M, Okada-Iwabu M, Kawamoto S, Kubota N, Kubota T, Ito Y, Kamon J, Tsuchida A, Kumagai K, Kozono H, Hada Y, Ogata H, Tokuyama K, Tsunoda M, Ide T, Murakami K, Awazawa M, Takamoto I, Froguel P, Hara K, Tobe K, Nagai R, Ueki K and Kadowaki T. Targeted disruption of AdipoR1 and AdipoR2 causes abrogation of adiponectin binding and metabolic actions. Nature medicine. 2007;13:332-9.

93. Mao X, Kikani CK, Riojas RA, Langlais P, Wang L, Ramos FJ, Fang Q, Christ-Roberts CY, Hong JY, Kim RY, Liu F and Dong LQ. APPL1 binds to adiponectin receptors and mediates adiponectin signalling and function. Nature cell biology. 2006;8:516-23.

94. Ryu J, Galan AK, Xin X, Dong F, Abdul-Ghani MA, Zhou L, Wang C, Li C, Holmes BM, Sloane LB, Austad SN, Guo S, Musi N, DeFronzo RA, Deng C, White MF, Liu F and Dong LQ. APPL1 potentiates insulin sensitivity by facilitating the binding of IRS1/2 to the insulin receptor. Cell reports. 2014;7:1227-38.

95. Holland WL, Miller RA, Wang ZV, Sun K, Barth BM, Bui HH, Davis KE, Bikman BT, Halberg N, Rutkowski JM, Wade MR, Tenorio VM, Kuo MS, Brozinick JT, Zhang BB, Birnbaum MJ, Summers SA and Scherer PE. Receptor-mediated activation of ceramidase activity initiates the pleiotropic actions of adiponectin. Nature medicine. 2011;17:55-63.

96. Ranscht B and Bronner-Fraser M. T-cadherin expression alternates with migrating neural crest cells in the trunk of the avian embryo. Development. 1991;111:15-22.

97. Hug C, Wang J, Ahmad NS, Bogan JS, Tsao TS and Lodish HF. T-cadherin is a receptor for hexameric and high-molecular-weight forms of Acrp30/adiponectin. Proc Natl Acad Sci U S A. 2004;101:10308-13.

98. Joshi MB, Philippova M, Ivanov D, Allenspach R, Erne P and Resink TJ. T-cadherin protects endothelial cells from oxidative stress-induced apoptosis. FASEB journal : official publication of the Federation of American Societies for Experimental Biology. 2005;19:1737-9.

99. Yoon MJ, Lee GY, Chung JJ, Ahn YH, Hong SH and Kim JB. Adiponectin increases fatty acid oxidation in skeletal muscle cells by sequential activation of AMP-activated protein kinase, p38 mitogen-activated protein kinase, and peroxisome proliferator-activated receptor alpha. Diabetes. 2006;55:2562-70.

100. Yamauchi T, Kamon J, Waki H, Terauchi Y, Kubota N, Hara K, Mori Y, Ide T, Murakami K, Tsuboyama-Kasaoka N, Ezaki O, Akanuma Y, Gavrilova O, Vinson C, Reitman ML, Kagechika H, Shudo K, Yoda M, Nakano Y, Tobe K, Nagai R, Kimura S, Tomita M, Froguel P and Kadowaki T. The fat-derived hormone adiponectin reverses insulin resistance associated with both lipoatrophy and obesity. Nature medicine. 2001;7:941-6.

101. Awazawa M, Ueki K, Inabe K, Yamauchi T, Kubota N, Kaneko K, Kobayashi M, Iwane A, Sasako T, Okazaki Y, Ohsugi M, Takamoto I, Yamashita S, Asahara H, Akira S, Kasuga M and Kadowaki T. Adiponectin enhances insulin sensitivity by increasing hepatic IRS-2 expression via a macrophage-derived IL-6-dependent pathway. Cell metabolism. 2011;13:401-12.

102. Liu Y, Turdi S, Park T, Morris NJ, Deshaies Y, Xu A and Sweeney G. Adiponectin corrects high-fat diet-induced disturbances in muscle metabolomic profile and whole-body glucose homeostasis. Diabetes. 2013;62:743-52.

103. Lin HV, Kim JY, Pocai A, Rossetti L, Shapiro L, Scherer PE and Accili D. Adiponectin resistance exacerbates insulin resistance in insulin receptor transgenic/knockout mice. Diabetes. 2007;56:1969-76.

104. Yamauchi T, Kamon J, Minokoshi Y, Ito Y, Waki H, Uchida S, Yamashita S, Noda M, Kita S, Ueki K, Eto K, Akanuma Y, Froguel P, Foufelle F, Ferre P, Carling D, Kimura S, Nagai R, Kahn BB and Kadowaki T. Adiponectin stimulates glucose utilization and fatty-acid oxidation by activating AMP-activated protein kinase. Nature medicine. 2002;8:1288-95.

105. Bjursell M, Ahnmark A, Bohlooly YM, William-Olsson L, Rhedin M, Peng XR, Ploj K, Gerdin AK, Arnerup G, Elmgren A, Berg AL, Oscarsson J and Linden D. Opposing effects of adiponectin receptors 1 and 2 on energy metabolism. Diabetes. 2007;56:583-93.

106. Liu Y, Michael MD, Kash S, Bensch WR, Monia BP, Murray SF, Otto KA, Syed SK, Bhanot S, Sloop KW, Sullivan JM and Reifel-Miller A. Deficiency of adiponectin receptor 2 reduces diet-induced insulin resistance but promotes type 2 diabetes. Endocrinology. 2007;148:683-92.

107. Brown JE, Conner AC, Digby JE, Ward KL, Ramanjaneya M, Randeva HS and Dunmore SJ. Regulation of beta-cell viability and gene expression by distinct agonist fragments of adiponectin. Peptides. 2010;31:944-9.

108. Dietze-Schroeder D, Sell H, Uhlig M, Koenen M and Eckel J. Autocrine action of adiponectin on human fat cells prevents the release of insulin resistance-inducing factors. Diabetes. 2005;54:2003-11.

109. Li S, Shin HJ, Ding EL and van Dam RM. Adiponectin levels and risk of type 2 diabetes: a systematic review and meta-analysis. JAMA. 2009;302:179-88.

110. Jiang Y, Owei I, Wan J, Ebenibo S and Dagogo-Jack S. Adiponectin levels predict prediabetes risk: the Pathobiology of Prediabetes in A Biracial Cohort (POP-ABC) study. BMJ open diabetes research & care. 2016;4:e000194.

111. Ouchi N, Ohishi M, Kihara S, Funahashi T, Nakamura T, Nagaretani H, Kumada M, Ohashi K, Okamoto Y, Nishizawa H, Kishida K, Maeda N, Nagasawa A, Kobayashi H, Hiraoka H, Komai N, Kaibe M, Rakugi H, Ogihara T and Matsuzawa Y. Association of hypoadiponectinemia with impaired vasoreactivity. Hypertension. 2003;42:231-4.

112. Matsuda M, Shimomura I, Sata M, Arita Y, Nishida M, Maeda N, Kumada M, Okamoto Y, Nagaretani H, Nishizawa H, Kishida K, Komuro R, Ouchi N, Kihara S, Nagai R, Funahashi T and Matsuzawa Y. Role of adiponectin in preventing vascular stenosis. The missing link of adipo-vascular axis. J Biol Chem. 2002;277:37487-91.

113. Okamoto Y, Kihara S, Ouchi N, Nishida M, Arita Y, Kumada M, Ohashi K, Sakai N, Shimomura I, Kobayashi H, Terasaka N, Inaba T, Funahashi T and Matsuzawa Y. Adiponectin reduces atherosclerosis in apolipoprotein E-deficient mice. Circulation. 2002;106:2767-70.

114. Yamauchi T, Kamon J, Waki H, Imai Y, Shimozawa N, Hioki K, Uchida S, Ito Y, Takakuwa K, Matsui J, Takata M, Eto K, Terauchi Y, Komeda K, Tsunoda M, Murakami K, Ohnishi Y, Naitoh T, Yamamura K, Ueyama Y, Froguel P, Kimura S, Nagai R and Kadowaki T. Globular

adiponectin protected ob/ob mice from diabetes and ApoE-deficient mice from atherosclerosis. J Biol Chem. 2003;278:2461-8.

115. Li CJ, Sun HW, Zhu FL, Chen L, Rong YY, Zhang Y and Zhang M. Local adiponectin treatment reduces atherosclerotic plaque size in rabbits. The Journal of endocrinology. 2007;193:137-45.

116. Ouchi N, Kihara S, Arita Y, Okamoto Y, Maeda K, Kuriyama H, Hotta K, Nishida M, Takahashi M, Muraguchi M, Ohmoto Y, Nakamura T, Yamashita S, Funahashi T and Matsuzawa Y. Adiponectin, an adipocyte-derived plasma protein, inhibits endothelial NF-kappaB signaling through a cAMP-dependent pathway. Circulation. 2000;102:1296-301.

117. Kobashi C, Urakaze M, Kishida M, Kibayashi E, Kobayashi H, Kihara S, Funahashi T, Takata M, Temaru R, Sato A, Yamazaki K, Nakamura N and Kobayashi M. Adiponectin inhibits endothelial synthesis of interleukin-8. Circulation research. 2005;97:1245-52.

118. Ouchi N, Kihara S, Arita Y, Maeda K, Kuriyama H, Okamoto Y, Hotta K, Nishida M, Takahashi M, Nakamura T, Yamashita S, Funahashi T and Matsuzawa Y. Novel modulator for endothelial adhesion molecules: adipocyte-derived plasma protein adiponectin. Circulation. 1999;100:2473-6.

119. Wulster-Radcliffe MC, Ajuwon KM, Wang J, Christian JA and Spurlock ME. Adiponectin differentially regulates cytokines in porcine macrophages. Biochemical and biophysical research communications. 2004;316:924-9.

120. Wolf AM, Wolf D, Rumpold H, Enrich B and Tilg H. Adiponectin induces the anti-inflammatory cytokines IL-10 and IL-1RA in human leukocytes. Biochemical and biophysical research communications. 2004;323:630-5.

121. Kumada M, Kihara S, Ouchi N, Kobayashi H, Okamoto Y, Ohashi K, Maeda K, Nagaretani H, Kishida K, Maeda N, Nagasawa A, Funahashi T and Matsuzawa Y. Adiponectin specifically increased tissue inhibitor of metalloproteinase-1 through interleukin-10 expression in human macrophages. Circulation. 2004;109:2046-9.

122. Ouchi N, Kihara S, Arita Y, Nishida M, Matsuyama A, Okamoto Y, Ishigami M, Kuriyama H, Kishida K, Nishizawa H, Hotta K, Muraguchi M, Ohmoto Y, Yamashita S, Funahashi T and Matsuzawa Y. Adipocyte-derived plasma protein, adiponectin, suppresses lipid accumulation and class A scavenger receptor expression in human monocyte-derived macrophages. Circulation. 2001;103:1057-63.

123. Tian L, Luo N, Klein RL, Chung BH, Garvey WT and Fu Y. Adiponectin reduces lipid accumulation in macrophage foam cells. Atherosclerosis. 2009;202:152-61.

124. Furukawa K, Hori M, Ouchi N, Kihara S, Funahashi T, Matsuzawa Y, Miyazaki A, Nakayama H and Horiuchi S. Adiponectin down-regulates acyl-coenzyme A:cholesterol acyltransferase-1 in cultured human monocyte-derived macrophages. Biochemical and biophysical research communications. 2004;317:831-6.

125. Chen H, Montagnani M, Funahashi T, Shimomura I and Quon MJ. Adiponectin stimulates production of nitric oxide in vascular endothelial cells. The Journal of biological chemistry. 2003;278:45021-6.

126. Hattori Y, Suzuki M, Hattori S and Kasai K. Globular adiponectin upregulates nitric oxide production in vascular endothelial cells. Diabetologia. 2003;46:1543-9.

127. Eid HM, Lyberg T, Arnesen H and Seljeflot I. Insulin and adiponectin inhibit the TNFalpha-induced ADMA accumulation in human endothelial cells: the role of DDAH. Atherosclerosis. 2007;194:e1-8.

128. Xi W, Satoh H, Kase H, Suzuki K and Hattori Y. Stimulated HSP90 binding to eNOS and activation of the PI3-Akt pathway contribute to globular adiponectin-induced NO production: vasorelaxation in response to globular adiponectin. Biochemical and biophysical research communications. 2005;332:200-5.

129. Lin LY, Lin CY, Su TC and Liau CS. Angiotensin II-induced apoptosis in human endothelial cells is inhibited by adiponectin through restoration of the association between endothelial nitric oxide synthase and heat shock protein 90. FEBS Lett. 2004;574:106-10.

130. Cao Y, Tao L, Yuan Y, Jiao X, Lau WB, Wang Y, Christopher T, Lopez B, Chan L, Goldstein B and Ma XL. Endothelial dysfunction in adiponectin deficiency and its mechanisms involved. J Mol Cell Cardiol. 2009;46:413-9.

131. Ouedraogo R, Gong Y, Berzins B, Wu X, Mahadev K, Hough K, Chan L, Goldstein BJ and Scalia R. Adiponectin deficiency increases leukocyte-endothelium interactions via upregulation of endothelial cell adhesion molecules in vivo. J Clin Invest. 2007;117:1718-26.

132. Ouedraogo R, Wu X, Xu SQ, Fuchsel L, Motoshima H, Mahadev K, Hough K, Scalia R and Goldstein BJ. Adiponectin suppression of high-glucose-induced reactive oxygen species in vascular endothelial cells: evidence for involvement of a cAMP signaling pathway. Diabetes. 2006;55:1840-6.

133. Kim JE, Song SE, Kim YW, Kim JY, Park SC, Park YK, Baek SH, Lee IK and Park SY. Adiponectin inhibits palmitate-induced apoptosis through suppression of reactive oxygen species in endothelial cells: involvement of cAMP/protein kinase A and AMP-activated protein kinase. The Journal of endocrinology. 2010;207:35-44.

134. Motoshima H, Wu X, Mahadev K and Goldstein BJ. Adiponectin suppresses proliferation and superoxide generation and enhances eNOS activity in endothelial cells treated with oxidized LDL. Biochemical and biophysical research communications. 2004;315:264-71.

135. Plant S, Shand B, Elder P and Scott R. Adiponectin attenuates endothelial dysfunction induced by oxidised low-density lipoproteins. Diabetes & vascular disease research. 2008;5:102-8.

136. Li R, Wang WQ, Zhang H, Yang X, Fan Q, Christopher TA, Lopez BL, Tao L, Goldstein BJ, Gao F and Ma XL. Adiponectin improves endothelial function in hyperlipidemic rats by reducing oxidative/nitrative stress and differential regulation of eNOS/iNOS activity. American journal of physiology Endocrinology and metabolism. 2007;293:E1703-8.

137. Cai XJ, Chen L, Li L, Feng M, Li X, Zhang K, Rong YY, Hu XB, Zhang MX, Zhang Y and Zhang M. Adiponectin inhibits lipopolysaccharide-induced adventitial fibroblast migration and transition to myofibroblasts via AdipoR1-AMPK-iNOS pathway. Mol Endocrinol. 24:218-28.

138. Deng G, Long Y, Yu YR and Li MR. Adiponectin directly improves endothelial dysfunction in obese rats through the AMPK-eNOS Pathway. Int J Obes (Lond). 34:165-71.

139. Kondo M, Shibata R, Miura R, Shimano M, Kondo K, Li P, Ohashi T, Kihara S, Maeda N, Walsh K, Ouchi N and Murohara T. Caloric restriction stimulates revascularization in response to ischemia via adiponectin-mediated activation of endothelial nitric-oxide synthase. J Biol Chem. 2009;284:1718-24.

140. Li R, Xu M, Wang X, Wang Y, Lau WB, Yuan Y, Yi W, Wei X, Lopez BL, Christopher TA, Wang XM and Ma XL. Reduced vascular responsiveness to adiponectin in hyperlipidemic rats-mechanisms and significance. J Mol Cell Cardiol. 2010.

141. Okui H, Hamasaki S, Ishida S, Kataoka T, Orihara K, Fukudome T, Ogawa M, Oketani N, Saihara K, Shinsato T, Shirasawa T, Mizoguchi E, Kubozono T, Ichiki H, Ninomiya Y, Matsushita T, Nakasaki M and Tei C. Adiponectin is a better predictor of endothelial function of the coronary artery than HOMA-R, body mass index, immunoreactive insulin, or triglycerides. International journal of cardiology. 2008;126:53-61.

142. Pischon T, Girman CJ, Hotamisligil GS, Rifai N, Hu FB and Rimm EB. Plasma adiponectin levels and risk of myocardial infarction in men. JAMA. 2004;291:1730-7.

143. Hashimoto N, Kanda J, Nakamura T, Horie A, Kurosawa H, Hashimoto T, Sato K, Kushida S, Suzuki M, Yano S, Iwai R, Takahashi H and Yoshida S. Association of hypoadiponectinemia in men with early onset of coronary heart disease and multiple coronary artery stenoses. Metabolism. 2006;55:1653-7.

144. Kumada M, Kihara S, Sumitsuji S, Kawamoto T, Matsumoto S, Ouchi N, Arita Y, Okamoto Y, Shimomura I, Hiraoka H, Nakamura T, Funahashi T, Matsuzawa Y and Osaka CADSGCad. Association of hypoadiponectinemia with coronary artery disease in men. Arterioscler Thromb Vasc Biol. 2003;23:85-9.

145. Arita Y, Kihara S, Ouchi N, Maeda K, Kuriyama H, Okamoto Y, Kumada M, Hotta K, Nishida M, Takahashi M, Nakamura T, Shimomura I, Muraguchi M, Ohmoto Y, Funahashi T and Matsuzawa Y. Adipocyte-derived plasma protein adiponectin acts as a platelet-derived growth factor-BB-binding protein and regulates growth factor-induced common postreceptor signal in vascular smooth muscle cell. Circulation. 2002;105:2893-8.

146. Wang Y, Lam KS, Xu JY, Lu G, Xu LY, Cooper GJ and Xu A. Adiponectin inhibits cell proliferation by interacting with several growth factors in an oligomerization-dependent manner. J Biol Chem. 2005;280:18341-7.

147. Kubota N, Terauchi Y, Yamauchi T, Kubota T, Moroi M, Matsui J, Eto K, Yamashita T, Kamon J, Satoh H, Yano W, Froguel P, Nagai R, Kimura S, Kadowaki T and Noda T. Disruption of adiponectin causes insulin resistance and neointimal formation. J Biol Chem. 2002;277:25863-6.

148. Terry RB, Stefanick ML, Haskell WL and Wood PD. Contributions of regional adipose tissue depots to plasma lipoprotein concentrations in overweight men and women: possible protective effects of thigh fat. Metabolism. 1991;40:733-40.

149. Lakka HM, Lakka TA, Tuomilehto J and Salonen JT. Abdominal obesity is associated with increased risk of acute coronary events in men. European heart journal. 2002;23:706-13.

150. See R, Abdullah SM, McGuire DK, Khera A, Patel MJ, Lindsey JB, Grundy SM and de Lemos JA. The association of differing measures of overweight and obesity with prevalent atherosclerosis: the Dallas Heart Study. J Am Coll Cardiol. 2007;50:752-9.

151. Tanko LB, Bagger YZ, Alexandersen P, Larsen PJ and Christiansen C. Peripheral adiposity exhibits an independent dominant antiatherogenic effect in elderly women. Circulation. 2003;107:1626-31.

152. Klein S, Fontana L, Young VL, Coggan AR, Kilo C, Patterson BW and Mohammed BS. Absence of an effect of liposuction on insulin action and risk factors for coronary heart disease. N Engl J Med. 2004;350:2549-57.

153. Okura T, Nakata Y, Yamabuki K and Tanaka K. Regional body composition changes exhibit opposing effects on coronary heart disease risk factors. Arterioscler Thromb Vasc Biol. 2004;24:923-9.

154. Gabriely I, Ma XH, Yang XM, Atzmon G, Rajala MW, Berg AH, Scherer P, Rossetti L and Barzilai N. Removal of visceral fat prevents insulin resistance and glucose intolerance of aging: an adipokine-mediated process? Diabetes. 2002;51:2951-8.

155. De Michele M, Panico S, Iannuzzi A, Celentano E, Ciardullo AV, Galasso R, Sacchetti L, Zarrilli F, Bond MG and Rubba P. Association of obesity and central fat distribution with carotid artery wall thickening in middle-aged women. Stroke. 2002;33:2923-8.

156. Morricone L, Donati C, Hassan T, Cioffi P and Caviezel F. Relationship of visceral fat distribution to angiographically assessed coronary artery disease: results in subjects with or without diabetes or impaired glucose tolerance. Nutr Metab Cardiovasc Dis. 2002;12:275-83.

157. Owens S, Gutin B, Ferguson M, Allison J, Karp W and Le NA. Visceral adipose tissue and cardiovascular risk factors in obese children. J Pediatr. 1998;133:41-5.

158. Goran MI and Gower BA. Relation between visceral fat and disease risk in children and adolescents. Am J Clin Nutr. 1999;70:149S-56S.

159. Gallagher D, Kelley DE, Yim JE, Spence N, Albu J, Boxt L, Pi-Sunyer FX and Heshka S. Adipose tissue distribution is different in type 2 diabetes. Am J Clin Nutr. 2009;89:807-14.

160. Motoshima H, Wu X, Sinha MK, Hardy VE, Rosato EL, Barbot DJ, Rosato FE and Goldstein BJ. Differential regulation of adiponectin secretion from cultured human omental and subcutaneous adipocytes: effects of insulin and rosiglitazone. The Journal of clinical endocrinology and metabolism. 2002;87:5662-7.

161. Tanko LB, Bruun JM, Alexandersen P, Bagger YZ, Richelsen B, Christiansen C and Larsen PJ. Novel associations between bioavailable estradiol and adipokines in elderly women with different phenotypes of obesity: implications for atherogenesis. Circulation. 2004;110:2246-52.

162. Gabrielsson BG, Johansson JM, Lonn M, Jernas M, Olbers T, Peltonen M, Larsson I, Lonn L, Sjostrom L, Carlsson B and Carlsson LM. High expression of complement components in omental adipose tissue in obese men. Obes Res. 2003;11:699-708.

163. Ohman MK, Shen Y, Obimba CI, Wright AP, Warnock M, Lawrence DA and Eitzman DT. Visceral adipose tissue inflammation accelerates atherosclerosis in apolipoprotein E-deficient mice. Circulation. 2008;117:798-805.

164. Cancello R, Tordjman J, Poitou C, Guilhem G, Bouillot JL, Hugol D, Coussieu C, Basdevant A, Bar Hen A, Bedossa P, Guerre-Millo M and Clement K. Increased infiltration of macrophages in omental adipose tissue is associated with marked hepatic lesions in morbid human obesity. Diabetes. 2006;55:1554-61.

165. Fontana L, Eagon JC, Trujillo ME, Scherer PE and Klein S. Visceral fat adipokine secretion is associated with systemic inflammation in obese humans. Diabetes. 2007;56:1010-3.

166. Chang L, Milton H, Eitzman DT and Chen YE. Paradoxical roles of perivascular adipose tissue in atherosclerosis and hypertension. Circulation journal : official journal of the Japanese Circulation Society. 2013;77:11-8.

167. Mazurek T, Zhang L, Zalewski A, Mannion JD, Diehl JT, Arafat H, Sarov-Blat L, O'Brien S, Keiper EA, Johnson AG, Martin J, Goldstein BJ and Shi Y. Human epicardial adipose tissue is a source of inflammatory mediators. Circulation. 2003;108:2460-6.

168. Chatterjee TK, Stoll LL, Denning GM, Harrelson A, Blomkalns AL, Idelman G, Rothenberg FG, Neltner B, Romig-Martin SA, Dickson EW, Rudich S and Weintraub NL. Proinflammatory phenotype of perivascular adipocytes: influence of high-fat feeding. Circulation research. 2009;104:541-9.

169. Chang L, Villacorta L, Li R, Hamblin M, Xu W, Dou C, Zhang J, Wu J, Zeng R and Chen YE. Loss of perivascular adipose tissue on peroxisome proliferator-activated receptor-gamma deletion in smooth muscle cells impairs intravascular thermoregulation and enhances atherosclerosis. Circulation. 2012;126:1067-78.

170. Shimokawa H, Ito A, Fukumoto Y, Kadokami T, Nakaike R, Sakata M, Takayanagi T, Egashira K and Takeshita A. Chronic treatment with interleukin-1 beta induces coronary intimal

lesions and vasospastic responses in pigs in vivo. The role of platelet-derived growth factor. J Clin Invest. 1996;97:769-76.

171. Yudkin JS, Eringa E and Stehouwer CD. "Vasocrine" signalling from perivascular fat: a mechanism linking insulin resistance to vascular disease. Lancet. 2005;365:1817-20.

172. Kwon HM, Sangiorgi G, Ritman EL, McKenna C, Holmes DR, Jr., Schwartz RS and Lerman A. Enhanced coronary vasa vasorum neovascularization in experimental hypercholesterolemia. J Clin Invest. 1998;101:1551-6.

173. Dikalov S, Griendling KK and Harrison DG. Measurement of reactive oxygen species in cardiovascular studies. Hypertension. 2007;49:717-27.

174. Munzel T, Afanas'ev IB, Kleschyov AL and Harrison DG. Detection of superoxide in vascular tissue. Arterioscler Thromb Vasc Biol. 2002;22:1761-8.

175. Faulkner K and Fridovich I. Luminol and lucigenin as detectors for O2. Free Radic Biol Med. 1993;15:447-51.

176. Afanas'ev IB. Lucigenin chemiluminescence assay for superoxide detection. Circ Res. 2001;89:E46.

177. Liochev SI and Fridovich I. Lucigenin (bis-N-methylacridinium) as a mediator of superoxide anion production. Arch Biochem Biophys. 1997;337:115-20.

178. Li Y, Zhu H, Kuppusamy P, Roubaud V, Zweier JL and Trush MA. Validation of lucigenin (bis-N-methylacridinium) as a chemilumigenic probe for detecting superoxide anion radical production by enzymatic and cellular systems. J Biol Chem. 1998;273:2015-23.

179. Kinugawa S, Post H, Kaminski PM, Zhang X, Xu X, Huang H, Recchia FA, Ochoa M, Wolin MS, Kaley G and Hintze TH. Coronary microvascular endothelial stunning after acute pressure overload in the conscious dog is caused by oxidant processes: the role of angiotensin II type 1 receptor and NAD(P)H oxidase. Circulation. 2003;108:2934-40.

180. Antoniades C, Van-Assche T, Shirodaria C, Diesch J, Antonopoulos AS, Lee J, Cunnington C, Tousoulis D, Stefanadis C, Casadei B, Taggart D, Channon KM and Leeson P. Preoperative sCD40L levels predict risk of atrial fibrillation after off-pump coronary artery bypass graft surgery. Circulation. 2009;120:S170-6.

181. Benov L, Sztejnberg L and Fridovich I. Critical evaluation of the use of hydroethidine as a measure of superoxide anion radical. Free Radic Biol Med. 1998;25:826-31.

182. Zhao H, Kalivendi S, Zhang H, Joseph J, Nithipatikom K, Vasquez-Vivar J and Kalyanaraman B. Superoxide reacts with hydroethidine but forms a fluorescent product that is distinctly different from ethidium: potential implications in intracellular fluorescence detection of superoxide. Free Radic Biol Med. 2003;34:1359-68.

183. Zhao H, Joseph J, Fales HM, Sokoloski EA, Levine RL, Vasquez-Vivar J and Kalyanaraman B. Detection and characterization of the product of hydroethidine and intracellular superoxide by HPLC and limitations of fluorescence. Proc Natl Acad Sci U S A. 2005;102:5727-32.

184. Pfaffl MW. A new mathematical model for relative quantification in real-time RT-PCR. Nucleic acids research. 2001;29:e45.

185. Antoniades C, Shirodaria C, Crabtree M, Rinze R, Alp N, Cunnington C, Diesch J, Tousoulis D, Stefanadis C, Leeson P, Ratnatunga C, Pillai R and Channon KM. Altered plasma versus vascular biopterins in human atherosclerosis reveal relationships between endothelial nitric oxide synthase coupling, endothelial function, and inflammation. Circulation. 2007;116:2851-9.

186. Katusic ZS. Vascular endothelial dysfunction: does tetrahydrobiopterin play a role? Am J Physiol Heart Circ Physiol. 2001;281:H981-6.

187. Milstien S and Katusic Z. Oxidation of tetrahydrobiopterin by peroxynitrite: implications for vascular endothelial function. Biochem Biophys Res Commun. 1999;263:681-4.

188. Chen CA, Druhan LJ, Varadharaj S, Chen YR and Zweier JL. Phosphorylation of endothelial nitric-oxide synthase regulates superoxide generation from the enzyme. The Journal of biological chemistry. 2008;283:27038-47.

189. Antoniades C, Bakogiannis C, Leeson P, Guzik TJ, Zhang MH, Tousoulis D, Antonopoulos AS, Demosthenous M, Marinou K, Hale A, Paschalis A, Psarros C, Triantafyllou C, Bendall J, Casadei B, Stefanadis C and Channon KM. Rapid, direct effects of statin treatment on arterial redox state and nitric oxide bioavailability in human atherosclerosis via tetrahydrobiopterin-mediated endothelial nitric oxide synthase coupling. Circulation. 2011;124:335-45.

190. Thanassoulis G and O'Donnell CJ. Mendelian randomization: nature's randomized trial in the post-genome era. Jama. 2009;301:2386-8.

191. Richards JB, Waterworth D, O'Rahilly S, Hivert MF, Loos RJ, Perry JR, Tanaka T, Timpson NJ, Semple RK, Soranzo N, Song K, Rocha N, Grundberg E, Dupuis J, Florez JC, Langenberg C, Prokopenko I, Saxena R, Sladek R, Aulchenko Y, Evans D, Waeber G, Erdmann J, Burnett MS, Sattar N, Devaney J, Willenborg C, Hingorani A, Witteman JC, Vollenweider P, Glaser B,

Hengstenberg C, Ferrucci L, Melzer D, Stark K, Deanfield J, Winogradow J, Grassl M, Hall AS, Egan JM, Thompson JR, Ricketts SL, Konig IR, Reinhard W, Grundy S, Wichmann HE, Barter P, Mahley R, Kesaniemi YA, Rader DJ, Reilly MP, Epstein SE, Stewart AF, Van Duijn CM, Schunkert H, Burling K, Deloukas P, Pastinen T, Samani NJ, McPherson R, Davey Smith G, Frayling TM, Wareham NJ, Meigs JB, Mooser V, Spector TD and Consortium G. A genome-wide association study reveals variants in ARL15 that influence adiponectin levels. PLoS genetics. 2009;5:e1000768.

192. Koenig W, Khuseyinova N, Baumert J, Meisinger C and Lowel H. Serum concentrations of adiponectin and risk of type 2 diabetes mellitus and coronary heart disease in apparently healthy middle-aged men: results from the 18-year follow-up of a large cohort from southern Germany. Journal of the American College of Cardiology. 2006;48:1369-77.

193. Ouchi N, Kobayashi H, Kihara S, Kumada M, Sato K, Inoue T, Funahashi T and Walsh K. Adiponectin stimulates angiogenesis by promoting cross-talk between AMP-activated protein kinase and Akt signaling in endothelial cells. The Journal of biological chemistry. 2004;279:1304-9.

194. Iwabu M, Yamauchi T, Okada-Iwabu M, Sato K, Nakagawa T, Funata M, Yamaguchi M, Namiki S, Nakayama R, Tabata M, Ogata H, Kubota N, Takamoto I, Hayashi YK, Yamauchi N, Waki H, Fukayama M, Nishino I, Tokuyama K, Ueki K, Oike Y, Ishii S, Hirose K, Shimizu T, Touhara K and Kadowaki T. Adiponectin and AdipoR1 regulate PGC-1alpha and mitochondria by Ca(2+) and AMPK/SIRT1. Nature. 2010;464:1313-9.

195. Liu Q, Gauthier MS, Sun L, Ruderman N and Lodish H. Activation of AMP-activated protein kinase signaling pathway by adiponectin and insulin in mouse adipocytes: requirement of acyl-CoA synthetases FATP1 and Acsl1 and association with an elevation in AMP/ATP ratio. FASEB journal : official publication of the Federation of American Societies for Experimental Biology. 2010;24:4229-39.

196. Lee MH, Klein RL, El-Shewy HM, Luttrell DK and Luttrell LM. The adiponectin receptors AdipoR1 and AdipoR2 activate ERK1/2 through a Src/Ras-dependent pathway and stimulate cell growth. Biochemistry. 2008;47:11682-92.

197. Kwon T, Kwon DY, Chun J, Kim JH and Kang SS. Akt protein kinase inhibits Rac1-GTP binding through phosphorylation at serine 71 of Rac1. The Journal of biological chemistry. 2000;275:423-8.

198. Fujita K, Maeda N, Sonoda M, Ohashi K, Hibuse T, Nishizawa H, Nishida M, Hiuge A, Kurata A, Kihara S, Shimomura I and Funahashi T. Adiponectin protects against angiotensin II-induced cardiac fibrosis through activation of PPAR-alpha. Arteriosclerosis, thrombosis, and vascular biology. 2008;28:863-70.

199. Essick EE, Ouchi N, Wilson RM, Ohashi K, Ghobrial J, Shibata R, Pimentel DR and Sam F. Adiponectin mediates cardioprotection in oxidative stress-induced cardiac myocyte remodeling. American journal of physiology Heart and circulatory physiology. 2011;301:H984-93.

200. Yamashita K, Kanzaki K, Hinauchi M, Fujishima T, Islam AT, Kitazawa C, Endo K and Yamanaka A. Changes of seasonal morph development induced by surgical operations in pupae of the large map butterfly Araschnia burejana Bermer (Lepidoptera: Nymphalidae). Journal of experimental zoology Part A, Ecological genetics and physiology. 2014;321:276-82.

201. Weiss R, Dziura J, Burgert TS, Tamborlane WV, Taksali SE, Yeckel CW, Allen K, Lopes M, Savoye M, Morrison J, Sherwin RS and Caprio S. Obesity and the metabolic syndrome in children and adolescents. The New England journal of medicine. 2004;350:2362-74.

202. Beatty AL, Zhang MH, Ku IA, Na B, Schiller NB and Whooley MA. Adiponectin is associated with increased mortality and heart failure in patients with stable ischemic heart disease: data from the Heart and Soul Study. Atherosclerosis. 2012;220:587-92.

203. Koh KK, Quon MJ, Han SH, Lee Y, Ahn JY, Kim SJ, Koh Y and Shin EK. Simvastatin improves flow-mediated dilation but reduces adiponectin levels and insulin sensitivity in hypercholesterolemic patients. Diabetes care. 2008;31:776-82.

204. Koh KK, Quon MJ, Han SH, Lee Y, Kim SJ, Park JB and Shin EK. Differential metabolic effects of pravastatin and simvastatin in hypercholesterolemic patients. Atherosclerosis. 2009;204:483-90.

205. Cerqueira FM, Brandizzi LI, Cunha FM, Laurindo FR and Kowaltowski AJ. Serum from calorie-restricted rats activates vascular cell eNOS through enhanced insulin signaling mediated by adiponectin. PloS one. 2012;7:e31155.

206. Saarikoski LA, Huupponen RK, Viikari JS, Marniemi J, Juonala M, Kahonen M and Raitakari OT. Adiponectin is related with carotid artery intima-media thickness and brachial flow-mediated dilatation in young adults--the Cardiovascular Risk in Young Finns Study. Ann Med. 2010;42:603-11.

207. Ran J, Xiong X, Liu W, Guo S, Li Q, Zhang R and Lao G. Increased plasma adiponectin closely associates with vascular endothelial dysfunction in type 2 diabetic patients with diabetic nephropathy. Diabetes research and clinical practice. 2010;88:177-83.

208. Guzik TJ, Mussa S, Gastaldi D, Sadowski J, Ratnatunga C, Pillai R and Channon KM. Mechanisms of increased vascular superoxide production in human diabetes mellitus: role of NAD(P)H oxidase and endothelial nitric oxide synthase. Circulation. 2002;105:1656-62.

209. Wang X, Hattori Y, Satoh H, Iwata C, Banba N, Monden T, Uchida K, Kamikawa Y and Kasai K. Tetrahydrobiopterin prevents endothelial dysfunction and restores adiponectin levels in rats. European journal of pharmacology. 2007;555:48-53.

210. Gao H, Fall T, van Dam RM, Flyvbjerg A, Zethelius B, Ingelsson E and Hagg S. Evidence of a causal relationship between adiponectin levels and insulin sensitivity: a Mendelian randomization study. Diabetes. 2013;62:1338-44.

211. Yaghootkar H, Lamina C, Scott RA, Dastani Z, Hivert MF, Warren LL, Stancakova A, Buxbaum SG, Lyytikainen LP, Henneman P, Wu Y, Cheung CY, Pankow JS, Jackson AU, Gustafsson S, Zhao JH, Ballantyne CM, Xie W, Bergman RN, Boehnke M, el Bouazzaoui F, Collins FS, Dunn SH, Dupuis J, Forouhi NG, Gillson C, Hattersley AT, Hong J, Kahonen M, Kuusisto J, Kedenko L, Kronenberg F, Doria A, Assimes TL, Ferrannini E, Hansen T, Hao K, Haring H, Knowles JW, Lindgren CM, Nolan JJ, Paananen J, Pedersen O, Quertermous T, Smith U, Consortium G, Consortium R, Lehtimaki T, Liu CT, Loos RJ, McCarthy MI, Morris AD, Vasan RS, Spector TD, Teslovich TM, Tuomilehto J, van Dijk KW, Viikari JS, Zhu N, Langenberg C, Ingelsson E, Semple RK, Sinaiko AR, Palmer CN, Walker M, Lam KS, Paulweber B, Mohlke KL, van Duijn C, Raitakari OT, Bidulescu A, Wareham NJ, Laakso M, Waterworth DM, Lawlor DA, Meigs JB, Richards JB and Frayling TM. Mendelian randomization studies do not support a causal role for reduced circulating adiponectin levels in insulin resistance and type 2 diabetes. Diabetes. 2013;62:3589-98.

212. Schnabel R, Messow CM, Lubos E, Espinola-Klein C, Rupprecht HJ, Bickel C, Sinning C, Tzikas S, Keller T, Genth-Zotz S, Lackner KJ, Munzel TF and Blankenberg S. Association of adiponectin with adverse outcome in coronary artery disease patients: results from the AtheroGene study. European heart journal. 2008;29:649-57.

213. Di Marco E, Gray SP, Chew P, Koulis C, Ziegler A, Szyndralewiez C, Touyz RM, Schmidt HH, Cooper ME, Slattery R and Jandeleit-Dahm KA. Pharmacological inhibition of NOX reduces atherosclerotic lesions, vascular ROS and immune-inflammatory responses in diabetic Apoe(-/-) mice. Diabetologia. 2014;57:633-42.

214. Guzik TJ and Harrison DG. Vascular NADPH oxidases as drug targets for novel antioxidant strategies. Drug discovery today. 2006;11:524-33.

215. Ghiselli A, Serafini M, Natella F and Scaccini C. Total antioxidant capacity as a tool to assess redox status: critical view and experimental data. Free Radic Biol Med. 2000;29:1106-14.

216. Berry EM and Kohen R. Is the biological antioxidant system integrated and regulated? Med Hypotheses. 1999;53:397-401.

217. Young IS. Measurement of total antioxidant capacity. J Clin Pathol. 2001;54:339.

218. Lee R, Margaritis M, Channon KM and Antoniades C. Evaluating oxidative stress in human cardiovascular disease: methodological aspects and considerations. Current medicinal chemistry. 2012;19:2504-20.

219. Geloneze B, Vasques AC, Stabe CF, Pareja JC, Rosado LE, Queiroz EC, Tambascia MA and Investigators B. HOMA1-IR and HOMA2-IR indexes in identifying insulin resistance and metabolic syndrome: Brazilian Metabolic Syndrome Study (BRAMS). Arquivos brasileiros de endocrinologia e metabologia. 2009;53:281-7.

220. Topsakal S, Yerlikaya E, Akin F, Kaptanoglu B and Erurker T. Relation with HOMA-IR and thyroid hormones in obese Turkish women with metabolic syndrome. Eating and weight disorders :EWD. 2012;17:e57-61.

221. Shao J, Yamashita H, Qiao L and Friedman JE. Decreased Akt kinase activity and insulin resistance in C57BL/KsJ-Leprdb/db mice. The Journal of endocrinology. 2000;167:107-15.

222. Dastani Z, Hivert MF, Timpson N, Perry JR, Yuan X, Scott RA, Henneman P, Heid IM, Kizer JR, Lyytikainen LP, Fuchsberger C, Tanaka T, Morris AP, Small K, Isaacs A, Beekman M, Coassin S, Lohman K, Qi L, Kanoni S, Pankow JS, Uh HW, Wu Y, Bidulescu A, Rasmussen-Torvik LJ, Greenwood CM, Ladouceur M, Grimsby J, Manning AK, Liu CT, Kooner J, Mooser VE, Vollenweider P, Kapur KA, Chambers J, Wareham NJ, Langenberg C, Frants R, Willems-Vandijk K, Oostra BA, Willems SM, Lamina C, Winkler TW, Psaty BM, Tracy RP, Brody J, Chen I, Viikari J, Kahonen M, Pramstaller PP, Evans DM, St Pourcain B, Sattar N, Wood AR, Bandinelli S, Carlson OD, Egan JM, Bohringer S, van Heemst D, Kedenko L, Kristiansson K, Nuotio ML, Loo BM, Harris T, Garcia M, Kanaya A, Haun M, Klopp N, Wichmann HE, Deloukas P, Katsareli E, Couper DJ, Duncan BB, Kloppenburg M, Adair LS, Borja JB, Wilson JG, Musani S, Guo X, Johnson T, Semple R, Teslovich TM, Allison MA, Redline S, Buxbaum SG, Mohlke KL, Meulenbelt I, Ballantyne CM, Dedoussis GV, Hu FB, Liu Y, Paulweber B, Spector TD,

Slagboom PE, Ferrucci L, Jula A, Perola M, Raitakari O, Florez JC, Salomaa V, Eriksson JG, Frayling TM, Hicks AA, Lehtimaki T, Smith GD, Siscovick DS, Kronenberg F, van Duijn C, Loos RJ, Waterworth DM, Meigs JB, Dupuis J, Richards JB, Voight BF, Scott LJ, Steinthorsdottir V, Dina C, Welch RP, Zeggini E, Huth C, Aulchenko YS, Thorleifsson G, McCulloch LJ, Ferreira T, Grallert H, Amin N, Wu G, Willer CJ, Raychaudhuri S, McCarroll SA, Hofmann OM, Segre AV, van Hoek M, Navarro P, Ardlie K, Balkau B, Benediktsson R, Bennett AJ, Blagieva R, Boerwinkle E, Bonnycastle LL, Bostrom KB, Bravenboer B, Bumpstead S, Burtt NP, Charpentier G, Chines PS, Cornelis M, Crawford G, Doney AS, Elliott KS, Elliott AL, Erdos MR, Fox CS, Franklin CS, Ganser M, Gieger C, Grarup N, Green T, Griffin S, Groves CJ, Guiducci C, Hadjadj S, Hassanali N, Herder C, Isomaa B, Jackson AU, Johnson PR, Jorgensen T, Kao WH, Kong A, Kraft P, Kuusisto J, Lauritzen T, Li M, Lieverse A, Lindgren CM, Lyssenko V, Marre M, Meitinger T, Midthjell K, Morken MA, Narisu N, Nilsson P, Owen KR, Payne F, Petersen AK, Platou C, Proenca C, Prokopenko I, Rathmann W, Rayner NW, Robertson NR, Rocheleau G, Roden M, Sampson MJ, Saxena R, Shields BM, Shrader P, Sigurdsson G, Sparso T, Strassburger K, Stringham HM, Sun Q, Swift AJ, Thorand B, Tichet J, Tuomi T, van Dam RM, van Haeften TW, van Herpt T, van Vliet-Ostaptchouk JV, Walters GB, Weedon MN, Wijmenga C, Witteman J, Bergman RN, Cauchi S, Collins FS, Gloyn AL, Gyllensten U, Hansen T, Hide WA, Hitman GA, Hofman A, Hunter DJ, Hveem K, Laakso M, Morris AD, Palmer CN, Rudan I, Sijbrands E, Stein LD, Tuomilehto J, Uitterlinden A, Walker M, Watanabe RM, Abecasis GR, Boehm BO, Campbell H, Daly MJ, Hattersley AT, Pedersen O, Barroso I, Groop L, Sladek R, Thorsteinsdottir U, Wilson JF, Illig T, Froguel P, van Duijn CM, Stefansson K, Altshuler D, Boehnke M, McCarthy MI, Soranzo N, Wheeler E, Glazer NL, Bouatia-Naji N, Magi R, Randall J, Elliott P, Rybin D, Dehghan A, Hottenga JJ, Song K, Goel A, Lajunen T, Doney A, Cavalcanti-Proenca C, Kumari M, Timpson NJ, Zabena C, Ingelsson E, An P, O'Connell J, Luan J, Elliott A, Roccasecca RM, Pattou F, Sethupathy P, Ariyurek Y, Barter P, Beilby JP, Ben-Shlomo Y, Bergmann S, Bochud M, Bonnefond A, Borch-Johnsen K, Bottcher Y, Brunner E, Bumpstead SJ, Chen YD, Chines P, Clarke R, Coin LJ, Cooper MN, Crisponi L, Day IN, de Geus EJ, Delplanque J, Fedson AC, Fischer-Rosinsky A, Forouhi NG, Franzosi MG, Galan P, Goodarzi MO, Graessler J, Grundy S, Gwilliam R, Hallmans G, Hammond N, Han X, Hartikainen AL, Hayward C, Heath SC, Hercberg S, Hillman DR, Hingorani AD, Hui J, Hung J, Kaakinen M, Kaprio J, Kesaniemi YA, Kivimaki M, Knight B, Koskinen S, Kovacs P, Kyvik KO, Lathrop GM, Lawlor DA, Le Bacquer O, Lecoeur C, Li Y, Mahley R, Mangino M, Martinez-Larrad MT, McAteer JB, McPherson R, Meisinger C, Melzer D, Meyre D, Mitchell BD, Mukherjee S, Naitza S, Neville MJ, Orru M, Pakyz R, Paolisso G, Pattaro C, Pearson D, Peden JF, Pedersen NL, Pfeiffer AF, Pichler I, Polasek O, Posthuma D, Potter SC, Pouta A, Province MA, Rice K, Ripatti S, Rivadeneira F, Rolandsson O, Sandbaek A, Sandhu M, Sanna S, Sayer AA, Scheet P, Seedorf U, Sharp SJ, Shields B, Sigurethsson G, Sijbrands EJ, Silveira A, Simpson L, Singleton A, Smith NL, Sovio U, Swift A, Syddall H,

Syvanen AC, Tonjes A, Uitterlinden AG, van Dijk KW, Varma D, Visvikis-Siest S, Vitart V, Vogelzangs N, Waeber G, Wagner PJ, Walley A, Ward KL, Watkins H, Wild SH, Willemsen G, Witteman JC, Yarnell JW, Zelenika D, Zethelius B, Zhai G, Zhao JH, Zillikens MC, Borecki IB, Meneton P, Magnusson PK, Nathan DM, Williams GH, Silander K, Bornstein SR, Schwarz P, Spranger J, Karpe F, Shuldiner AR, Cooper C, Serrano-Rios M, Lind L, Palmer LJ, Hu FBs, Franks PW, Ebrahim S, Marmot M, Wright AF, Stumvoll M, Hamsten A, Buchanan TA, Valle TT, Rotter JI, Penninx BW, Boomsma DI, Cao A, Scuteri A, Schlessinger D, Uda M, Ruokonen A, Jarvelin MR, Peltonen L, Mooser V, Musunuru K, Smith AV, Edmondson AC, Stylianou IM, Koseki M, Pirruccello JP, Chasman DI, Johansen CT, Fouchier SW, Peloso GM, Barbalic M, Ricketts SL, Bis JC, Feitosa MF, Orho-Melander M, Melander O, Li X, Cho YS, Go MJ, Kim YJ, Lee JY, Park T, Kim K, Sim X, Ong RT, Croteau-Chonka DC, Lange LA, Smith JD, Ziegler A, Zhang W, Zee RY, Whitfield JB, Thompson JR, Surakka I, Smit JH, Sinisalo J, Scott J, Saharinen J, Sabatti C, Rose LM, Roberts R, Rieder M, Parker AN, Pare G, O'Donnell CJ, Nieminen MS, Nickerson DA, Montgomery GW, McArdle W, Masson D, Martin NG, Marroni F, Lucas G, Luben R, Lokki ML, Lettre G, Launer LJ, Lakatta EG, Laaksonen R, Konig IR, Khaw KT, Kaplan LM, Johansson A, Janssens AC, Igl W, Hovingh GK, Hengstenberg C, Havulinna AS, Hastie ND, Harris TB, Haritunians T, Hall AS, Groop LC, Gonzalez E, Freimer NB, Erdmann J, Ejebe KG, Doring A, Dominiczak AF, Demissie S, de Faire U, Caulfield MJ, Boekholdt SM, Assimes TL, Quertermous T, Seielstad M, Wong TY, Tai ES, Feranil AB, Kuzawa CW, Taylor HA, Jr., Gabriel SB, Holm H, Gudnason V, Krauss RM, Ordovas JM, Munroe PB, Kooner JS, Tall AR, Hegele RA, Kastelein JJ, Schadt EE, Strachan DP, Reilly MP, Samani NJ, Schunkert H, Cupples LA, Sandhu MS, Ridker PM, Rader DJ and Kathiresan S. Novel loci for adiponectin levels and their influence on type 2 diabetes and metabolic traits: a multi-ethnic meta-analysis of 45,891 individuals. PLoS genetics. 2012;8:e1002607.

223. Lindberg S, Jensen JS, Pedersen SH, Galatius S, Frystyk J, Flyvbjerg A, Bjerre M and Mogelvang R. Low adiponectin levels and increased risk of type 2 diabetes in patients with myocardial infarction. Diabetes care. 2014;37:3003-8.

224. Lindberg S, Jensen JS, Bjerre M, Pedersen SH, Frystyk J, Flyvbjerg A, Galatius S, Jeppesen J and Mogelvang R. Adiponectin, type 2 diabetes and cardiovascular risk. European journal of preventive cardiology. 2015;22:276-83.

225. Dastani Z, Johnson T, Kronenberg F, Nelson CP, Assimes TL, Marz W and Richards JB. The shared allelic architecture of adiponectin levels and coronary artery disease. Atherosclerosis. 2013;229:145-8.

226. Kamigaki M, Sakaue S, Tsujino I, Ohira H, Ikeda D, Itoh N, Ishimaru S, Ohtsuka Y and Nishimura M. Oxidative stress provokes atherogenic changes in adipokine gene expression in 3T3-L1 adipocytes. Biochemical and biophysical research communications. 2006;339:624-32.

227. Wang B, Jenkins JR and Trayhurn P. Expression and secretion of inflammation-related adipokines by human adipocytes differentiated in culture: integrated response to TNF-alpha. American journal of physiology Endocrinology and metabolism. 2005;288:E731-40.

228. Yuan G, Jia J, Di L, Zhou L, Dong S, Ye J, Wang D, Yang L, Wang J, Li L, Yang Y, Mao C and Chen M. Effects of C-reactive protein on adipokines genes expression in 3T3-L1 adipocytes. Biochemical and biophysical research communications. 2012;424:462-8.

229. Tsuchihashi H, Yamamoto H, Maeda K, Ugi S, Mori T, Shimizu T, Endo Y, Hanasawa K and Tani T. Circulating concentrations of adiponectin, an endogenous lipopolysaccharide neutralizing protein, decrease in rats with polymicrobial sepsis. The Journal of surgical research. 2006;134:348-53.

230. Weiss R, Dufour S, Groszmann A, Petersen K, Dziura J, Taksali SE, Shulman G and Caprio S. Low adiponectin levels in adolescent obesity: a marker of increased intramyocellular lipid accumulation. The Journal of clinical endocrinology and metabolism. 2003;88:2014-8.

231. Yang WS, Lee WJ, Funahashi T, Tanaka S, Matsuzawa Y, Chao CL, Chen CL, Tai TY and Chuang LM. Plasma adiponectin levels in overweight and obese Asians. Obes Res. 2002;10:1104-10.

232. Hosogai N, Fukuhara A, Oshima K, Miyata Y, Tanaka S, Segawa K, Furukawa S, Tochino Y, Komuro R, Matsuda M and Shimomura I. Adipose tissue hypoxia in obesity and its impact on adipocytokine dysregulation. Diabetes. 2007;56:901-11.

233. Ye J, Gao Z, Yin J and He Q. Hypoxia is a potential risk factor for chronic inflammation and adiponectin reduction in adipose tissue of ob/ob and dietary obese mice. American journal of physiology Endocrinology and metabolism. 2007;293:E1118-28.

234. Oh DY, Morinaga H, Talukdar S, Bae EJ and Olefsky JM. Increased macrophage migration into adipose tissue in obese mice. Diabetes. 2012;61:346-54.

235. Lumeng CN, Bodzin JL and Saltiel AR. Obesity induces a phenotypic switch in adipose tissue macrophage polarization. J Clin Invest. 2007;117:175-84.

236. Fujisaka S, Usui I, Bukhari A, Ikutani M, Oya T, Kanatani Y, Tsuneyama K, Nagai Y, Takatsu K, Urakaze M, Kobayashi M and Tobe K. Regulatory mechanisms for adipose tissue M1 and M2 macrophages in diet-induced obese mice. Diabetes. 2009;58:2574-82.

237. Rizza S, Gigli F, Galli A, Micchelini B, Lauro D, Lauro R and Federici M. Adiponectin isoforms in elderly patients with or without coronary artery disease. Journal of the American Geriatrics Society. 2010;58:702-6.

238. Pilz S, Mangge H, Wellnitz B, Seelhorst U, Winkelmann BR, Tiran B, Boehm BO and Marz W. Adiponectin and mortality in patients undergoing coronary angiography. The Journal of clinical endocrinology and metabolism. 2006;91:4277-86.

239. Ozgen M, Koca SS, Dagli N, Balin M, Ustundag B and Isik A. Serum adiponectin and vaspin levels in rheumatoid arthritis. Archives of medical research. 2010;41:457-63.

240. Popa C, Netea MG, de Graaf J, van den Hoogen FH, Radstake TR, Toenhake-Dijkstra H, van Riel PL, van der Meer JW, Stalenhoef AF and Barrera P. Circulating leptin and adiponectin concentrations during tumor necrosis factor blockade in patients with active rheumatoid arthritis. The Journal of rheumatology. 2009;36:724-30.

241. Kistorp C, Faber J, Galatius S, Gustafsson F, Frystyk J, Flyvbjerg A and Hildebrandt P. Plasma adiponectin, body mass index, and mortality in patients with chronic heart failure. Circulation. 2005;112:1756-62.

242. Mikkelsen MM, Hansen TK, Gjedsted J, Andersen NH, Christensen TD, Hjortdal VE and Johnsen SP. Insulin resistance, adiponectin and adverse outcomes following elective cardiac surgery: a prospective follow-up study. Journal of cardiothoracic surgery. 2010;5:129.

243. Tsukamoto O, Fujita M, Kato M, Yamazaki S, Asano Y, Ogai A, Okazaki H, Asai M, Nagamachi Y, Maeda N, Shintani Y, Minamino T, Asakura M, Kishimoto I, Funahashi T, Tomoike H and Kitakaze M. Natriuretic peptides enhance the production of adiponectin in human adipocytes and in patients with chronic heart failure. Journal of the American College of Cardiology. 2009;53:2070-7.

244. Wang Z, Dou X, Gu D, Shen C, Yao T, Nguyen V, Braunschweig C and Song Z. 4-Hydroxynonenal differentially regulates adiponectin gene expression and secretion via activating PPARgamma and accelerating ubiquitin-proteasome degradation. Molecular and cellular endocrinology. 2012;349:222-31.

245. Nagy L, Tontonoz P, Alvarez JG, Chen H and Evans RM. Oxidized LDL regulates macrophage gene expression through ligand activation of PPARgamma. Cell. 1998;93:229-40.

246. Holness CL and Simmons DL. Molecular cloning of CD68, a human macrophage marker related to lysosomal glycoproteins. Blood. 1993;81:1607-13.

247. Lai H, Lin N, Xing Z, Weng H and Zhang H. Association between the level of circulating adiponectin and prediabetes: A meta-analysis. Journal of diabetes investigation. 2015;6:416-29.

248. Antoniades C, Mussa S, Shirodaria C, Lee J, Diesch J, Taggart DP, Channon KM and Leeson P. Relation of preoperative radial artery flow-mediated dilatation to nitric oxide bioavailability in radial artery grafts used in off-pump coronary artery bypass grafting. The American journal of cardiology. 2009;103:216-20.

249. Zhang H, Mo X, Hao Y, Huang J, Lu X, Cao J and Gu D. Adiponectin levels and risk of coronary heart disease: a meta-analysis of prospective studies. The American journal of the medical sciences. 2013;345:455-61.

250. Kanhai DA, Kranendonk ME, Uiterwaal CS, van der Graaf Y, Kappelle LJ and Visseren FL. Adiponectin and incident coronary heart disease and stroke. A systematic review and meta-analysis of prospective studies. Obesity reviews : an official journal of the International Association for the Study of Obesity. 2013;14:555-67.

251. Hao G, Li W, Guo R, Yang JG, Wang Y, Tian Y, Liu MY, Peng YG and Wang ZW. Serum total adiponectin level and the risk of cardiovascular disease in general population: a meta-analysis of 17 prospective studies. Atherosclerosis. 2013;228:29-35.

252. Sook Lee E, Park SS, Kim E, Sook Yoon Y, Ahn HY, Park CY, Ho Yun Y and Woo Oh S. Association between adiponectin levels and coronary heart disease and mortality: a systematic review and meta-analysis. Int J Epidemiol. 2013.

253. Wu Z, Cheng Y, Aung LH and Li B. Association between adiponectin concentrations and cardiovascular disease in diabetic patients: a systematic review and meta-analysis. PloS one. 2013;8:e78485.

254. Koh KK, Lim S, Choi H, Lee Y, Han SH, Lee K, Oh PC, Sakuma I, Shin EK and Quon MJ. Combination pravastatin and valsartan treatment has additive beneficial effects to simultaneously improve both metabolic and cardiovascular phenotypes beyond that of monotherapy with either drug in patients with primary hypercholesterolemia. Diabetes. 2013;62:3547-52.

255. Koh KK, Quon MJ, Han SH, Lee Y, Kim SJ and Shin EK. Atorvastatin causes insulin resistance and increases ambient glycemia in hypercholesterolemic patients. J Am Coll Cardiol. 2010;55:1209-16.

256. Van Berendoncks AM, Garnier A, Beckers P, Hoymans VY, Possemiers N, Fortin D, Martinet W, Van Hoof V, Vrints CJ, Ventura-Clapier R and Conraads VM. Functional adiponectin resistance at the level of the skeletal muscle in mild to moderate chronic heart failure. Circulation Heart failure. 2010;3:185-94.

257. Khan RS, Kato TS, Chokshi A, Chew M, Yu S, Wu C, Singh P, Cheema FH, Takayama H, Harris C, Reyes-Soffer G, Knoll R, Milting H, Naka Y, Mancini D and Schulze PC. Adipose tissue inflammation and adiponectin resistance in patients with advanced heart failure: correction after ventricular assist device implantation. Circulation Heart failure. 2012;5:340-8.

258. Bjorndal B, Burri L, Staalesen V, Skorve J and Berge RK. Different adipose depots: their role in the development of metabolic syndrome and mitochondrial response to hypolipidemic agents. Journal of obesity. 2011;2011:490650.

259. Wiklund P, Toss F, Weinehall L, Hallmans G, Franks PW, Nordstrom A and Nordstrom P. Abdominal and gynoid fat mass are associated with cardiovascular risk factors in men and women. The Journal of clinical endocrinology and metabolism. 2008;93:4360-6.

260. Ibrahim MM. Subcutaneous and visceral adipose tissue: structural and functional differences. Obesity reviews : an official journal of the International Association for the Study of Obesity. 2010;11:11-8.

261. Zhang M, Hu T, Zhang S and Zhou L. Associations of Different Adipose Tissue Depots with Insulin Resistance: A Systematic Review and Meta-analysis of Observational Studies. Scientific reports. 2015;5:18495.

262. Lee JJ, Pedley A, Hoffmann U, Massaro JM, Keaney JF, Jr., Vasan RS and Fox CS. Cross-Sectional Associations of Computed Tomography (CT)-Derived Adipose Tissue Density and Adipokines: The Framingham Heart Study. Journal of the American Heart Association. 2016;4:e002545.

263. Lynch FM, Withers SB, Yao Z, Werner ME, Edwards G, Weston AH and Heagerty AM. Perivascular adipose tissue-derived adiponectin activates BK(Ca) channels to induce anticontractile responses. American journal of physiology Heart and circulatory physiology. 2013;304:H786-95.

264. Lee YC, Chang HH, Chiang CL, Liu CH, Yeh JI, Chen MF, Chen PY, Kuo JS and Lee TJ. Role of perivascular adipose tissue-derived methyl palmitate in vascular tone regulation and pathogenesis of hypertension. Circulation. 2011;124:1160-71.

265. Beltowski J. Endogenous hydrogen sulfide in perivascular adipose tissue: role in the regulation of vascular tone in physiology and pathology. Canadian journal of physiology and pharmacology. 2013;91:889-98.

266. Greenstein AS, Khavandi K, Withers SB, Sonoyama K, Clancy O, Jeziorska M, Laing I, Yates AP, Pemberton PW, Malik RA and Heagerty AM. Local inflammation and hypoxia abolish the protective anticontractile properties of perivascular fat in obese patients. Circulation. 2009;119:1661-70.

267. Judkins CP, Sobey CG, Dang TT, Miller AA, Dusting GJ and Drummond GR. NADPH-induced contractions of mouse aorta do not involve NADPH oxidase: a role for P2X receptors. J Pharmacol Exp Ther. 2006;317:644-50.

268. Delaigle AM, Senou M, Guiot Y, Many MC and Brichard SM. Induction of adiponectin in skeletal muscle of type 2 diabetic mice: In vivo and in vitro studies. Diabetologia. 2006;49:1311-23.

269. Schwarzer E, Arese P and Skorokhod OA. Role of the lipoperoxidation product 4-hydroxynonenal in the pathogenesis of severe malaria anemia and malaria immunodepression. Oxidative medicine and cellular longevity. 2015;2015:638416.

270. Ayala A, Munoz MF and Arguelles S. Lipid peroxidation: production, metabolism, and signaling mechanisms of malondialdehyde and 4-hydroxy-2-nonenal. Oxidative medicine and cellular longevity. 2014;2014:360438.

271. Zarrouki B, Soares AF, Guichardant M, Lagarde M and Geloen A. The lipid peroxidation end-product 4-HNE induces COX-2 expression through p38MAPK activation in 3T3-L1 adipose cell. FEBS letters. 2007;581:2394-400.

272. Henrichot E, Juge-Aubry CE, Pernin A, Pache JC, Velebit V, Dayer JM, Meda P, Chizzolini C and Meier CA. Production of chemokines by perivascular adipose tissue: a role in the pathogenesis of atherosclerosis? Arterioscler Thromb Vasc Biol. 2005;25:2594-9.

273. Okamoto E, Couse T, De Leon H, Vinten-Johansen J, Goodman RB, Scott NA and Wilcox JN. Perivascular inflammation after balloon angioplasty of porcine coronary arteries. Circulation. 2001;104:2228-35.

274. Moe KT, Naylynn TM, Yin NO, Khairunnisa K, Allen JC, Wong MC, Chin-Dusting J and Wong P. Tumor necrosis factor-alpha induces aortic intima-media thickening via perivascular adipose tissue inflammation. Journal of vascular research. 2013;50:228-37.

275. Rittig K, Dolderer JH, Balletshofer B, Machann J, Schick F, Meile T, Kuper M, Stock UA, Staiger H, Machicao F, Schaller HE, Konigsrainer A, Haring HU and Siegel-Axel DI. The secretion pattern of perivascular fat cells is different from that of subcutaneous and visceral fat cells. Diabetologia. 2012;55:1514-25.

276. Verhagen SN, Vink A, van der Graaf Y and Visseren FL. Coronary perivascular adipose tissue characteristics are related to atherosclerotic plaque size and composition. A post-mortem study. Atherosclerosis. 2012;225:99-104.

277. Gao YJ, Lu C, Su LY, Sharma AM and Lee RM. Modulation of vascular function by perivascular adipose tissue: the role of endothelium and hydrogen peroxide. British journal of pharmacology. 2007;151:323-31.

278. Lohn M, Dubrovska G, Lauterbach B, Luft FC, Gollasch M and Sharma AM. Periadventitial fat releases a vascular relaxing factor. FASEB journal : official publication of the Federation of American Societies for Experimental Biology. 2002;16:1057-63.

279. Lee RM, Lu C, Su LY and Gao YJ. Endothelium-dependent relaxation factor released by perivascular adipose tissue. Journal of hypertension. 2009;27:782-90.

280. Marchesi C, Ebrahimian T, Angulo O, Paradis P and Schiffrin EL. Endothelial nitric oxide synthase uncoupling and perivascular adipose oxidative stress and inflammation contribute to vascular dysfunction in a rodent model of metabolic syndrome. Hypertension. 2009;54:1384-92.

281. Bussey CE, Withers SB, Aldous RG, Edwards G and Heagerty AM. Obesity-Related Perivascular Adipose Tissue Damage Is Reversed by Sustained Weight Loss in the Rat. Arterioscler Thromb Vasc Biol. 2016.

282. Aghamohammadzadeh R, Greenstein AS, Yadav R, Jeziorska M, Hama S, Soltani F, Pemberton PW, Ammori B, Malik RA, Soran H and Heagerty AM. Effects of bariatric surgery on human small artery function: evidence for reduction in perivascular adipocyte inflammation, and the restoration of normal anticontractile activity despite persistent obesity. J Am Coll Cardiol. 2013;62:128-35.

283. Sabik JF, 3rd, Lytle BW, Blackstone EH, Houghtaling PL and Cosgrove DM. Comparison of saphenous vein and internal thoracic artery graft patency by coronary system. The Annals of thoracic surgery. 2005;79:544-51; discussion 544-51.

284. Lavie CJ, De Schutter A and Milani RV. Healthy obese versus unhealthy lean: the obesity paradox. Nature reviews Endocrinology. 2015;11:55-62.

285. Hainer V and Aldhoon-Hainerova I. Obesity paradox does exist. Diabetes care. 2013;36 Suppl 2:S276-81.

286. Doehner W, Erdmann E, Cairns R, Clark AL, Dormandy JA, Ferrannini E and Anker SD. Inverse relation of body weight and weight change with mortality and morbidity in patients with type 2 diabetes and cardiovascular co-morbidity: an analysis of the PROactive study population. International journal of cardiology. 2012;162:20-6.

287. Florez H and Castillo-Florez S. Beyond the obesity paradox in diabetes: fitness, fatness, and mortality. Jama. 2012;308:619-20.

288. Al-Attas OS, Hussain T, Al-Daghri NM, De Rosas E, Kazmi U and Vinodson B. The relationship between a Mediterranean diet and circulating adiponectin levels is influenced by cigarette smoking. Journal of atherosclerosis and thrombosis. 2013;20:313-20.

289. Hotta K, Funahashi T, Arita Y, Takahashi M, Matsuda M, Okamoto Y, Iwahashi H, Kuriyama H, Ouchi N, Maeda K, Nishida M, Kihara S, Sakai N, Nakajima T, Hasegawa K, Muraguchi M, Ohmoto Y, Nakamura T, Yamashita S, Hanafusa T and Matsuzawa Y. Plasma concentrations of a novel, adipose-specific protein, adiponectin, in type 2 diabetic patients. Arteriosclerosis, thrombosis, and vascular biology. 2000;20:1595-9.

290. Balagopal P, George D, Yarandi H, Funanage V and Bayne E. Reversal of obesity-related hypoadiponectinemia by lifestyle intervention: a controlled, randomized study in obese adolescents. The Journal of clinical endocrinology and metabolism. 2005;90:6192-7.

291. Monzillo LU, Hamdy O, Horton ES, Ledbury S, Mullooly C, Jarema C, Porter S, Ovalle K, Moussa A and Mantzoros CS. Effect of lifestyle modification on adipokine levels in obese subjects with insulin resistance. Obesity research. 2003;11:1048-54.

291. Kriketos AD, Gan SK, Poynten AM, Furler SM, Chisholm DJ and Campbell LV. Exercise increases adiponectin levels and insulin sensitivity in humans. Diabetes care. 2004;27:629-30.

292. Fragopoulou E, Panagiotakos DB, Pitsavos C, Tampourlou M, Chrysohoou C, Nomikos T, Antonopoulou S and Stefanadis C. The association between adherence to the Mediterranean diet and adiponectin levels among healthy adults: the ATTICA study. The Journal of nutritional biochemistry. 2010;21:285-9.

293. Silva FM, de Almeida JC and Feoli AM. Effect of diet on adiponectin levels in blood. Nutrition reviews. 2011;69:599-612.

294. Gallagher AM, Smeeth L, Seabroke S, Leufkens HG and van Staa TP. Risk of death and cardiovascular outcomes with thiazolidinediones: a study with the general practice research database and secondary care data. PloS one. 2011;6:e28157.

295. Furuhashi M, Ura N, Higashiura K, Murakami H, Tanaka M, Moniwa N, Yoshida D and Shimamoto K. Blockade of the renin-angiotensin system increases adiponectin concentrations in patients with essential hypertension. Hypertension. 2003;42:76-81.

296. Suzuki H, Sakamoto M, Hayashi T, Iuchi H, Ohashi K, Isaka T, Sakamoto N, Kayama Y, Tojo K, Yoshimura M and Utsunomiya K. Effects of co-administration of candesartan with pioglitazone on inflammatory parameters in hypertensive patients with type 2 diabetes mellitus: a preliminary report. Cardiovascular diabetology. 2013;12:71.

297. Sharma AM, Janke J, Gorzelniak K, Engeli S and Luft FC. Angiotensin blockade prevents type 2 diabetes by formation of fat cells. Hypertension. 2002;40:609-11.

298. Schupp M, Janke J, Clasen R, Unger T and Kintscher U. Angiotensin type 1 receptor blockers induce peroxisome proliferator-activated receptor-gamma activity. Circulation. 2004;109:2054-7.

299. Guo Z, Zhang R, Li J and Xu G. Effect of telmisartan on the expression of adiponectin receptors and nicotinamide adenine dinucleotide phosphate oxidase in the heart and aorta in type 2 diabetic rats. Cardiovascular diabetology. 2012;11:94.

300. Otvos L, Jr., Haspinger E, La Russa F, Maspero F, Graziano P, Kovalszky I, Lovas S, Nama K, Hoffmann R, Knappe D, Cassone M, Wade J and Surmacz E. Design and development of a peptide-based adiponectin receptor agonist for cancer treatment. BMC biotechnology. 2011;11:90.

301. Okada-Iwabu M, Yamauchi T, Iwabu M, Honma T, Hamagami K, Matsuda K, Yamaguchi M, Tanabe H, Kimura-Someya T, Shirouzu M, Ogata H, Tokuyama K, Ueki K, Nagano T, Tanaka A, Yokoyama S and Kadowaki T. A small-molecule AdipoR agonist for type 2 diabetes and short life in obesity. Nature. 2013;503:493-9.

302. Fitzgibbon GM, Kafka HP, Leach AJ, Keon WJ, Hooper GD and Burton JR. Coronary bypass graft fate and patient outcome: angiographic follow-up of 5,065 grafts related to survival and reoperation in 1,388 patients during 25 years. Journal of the American College of Cardiology. 1996;28:616-26.

303. Motwani JG and Topol EJ. Aortocoronary saphenous vein graft disease: pathogenesis, predisposition, and prevention. Circulation. 1998;97:916-31.

304. Hassantash SA, Bikdeli B, Kalantarian S, Sadeghian M and Afshar H. Pathophysiology of aortocoronary saphenous vein bypass graft disease. Asian cardiovascular & thoracic annals. 2008;16:331-6.

305. Verma S, Lovren F, Pan Y, Yanagawa B, Deb S, Karkhanis R, Quan A, Teoh H, Feder-Elituv R, Moussa F, Souza DS and Fremes SE. Pedicled no-touch saphenous vein graft harvest limits vascular smooth muscle cell activation: the PATENT saphenous vein graft study. European journal of cardio-thoracic surgery : official journal of the European Association for Cardio-thoracic Surgery. 2014;45:717-25.

306. Souza DS, Dashwood MR, Tsui JC, Filbey D, Bodin L, Johansson B and Borowiec J. Improved patency in vein grafts harvested with surrounding tissue: results of a randomized study using three harvesting techniques. The Annals of thoracic surgery. 2002;73:1189-95.

307. Samano N, Geijer H, Liden M, Fremes S, Bodin L and Souza D. The no-touch saphenous vein for coronary artery bypass grafting maintains a patency, after 16 years, comparable to the left internal thoracic artery: A randomized trial. The Journal of thoracic and cardiovascular surgery. 2015;150:880-8.

308. Souza DS, Johansson B, Bojo L, Karlsson R, Geijer H, Filbey D, Bodin L, Arbeus M and Dashwood MR. Harvesting the saphenous vein with surrounding tissue for CABG provides long-term graft patency comparable to the left internal thoracic artery: results of a randomized longitudinal trial. The Journal of thoracic and cardiovascular surgery. 2006;132:373-8.

309. Tsui JC, Souza DS, Filbey D, Karlsson MG and Dashwood MR. Localization of nitric oxide synthase in saphenous vein grafts harvested with a novel "no-touch" technique: potential role of nitric oxide contribution to improved early graft patency rates. Journal of vascular surgery. 2002;35:356-62.

310. Dashwood MR, Dooley A, Shi-Wen X, Abraham DJ, Dreifaldt M and Souza DS. Perivascular fat-derived leptin: a potential role in improved vein graft performance in coronary artery bypass surgery. Interactive cardiovascular and thoracic surgery. 2011;12:170-3.

311. Dreifaldt M, Souza DS, Loesch A, Muddle JR, Karlsson MG, Filbey D, Bodin L, Norgren L and Dashwood MR. The "no-touch" harvesting technique for vein grafts in coronary artery bypass surgery preserves an intact vasa vasorum. The Journal of thoracic and cardiovascular surgery. 2011;141:145-50.

Appendix I

AdipoRedox Consent Form

CONSENT FORM (Version 7.1, Feb 2015)

Study Full Title	**Interactions between adipose tissue, vascular wall and myocardium in human atherosclerosis**
Patient ID	
Researchers	Prof Charalambos Antoniades (Tel 01865 228340)

Part A: General consent

Please initial box

1. I confirm that I have read and understand the information sheet (Version 7.1, Feb 2015) for the above study. I have had the opportunity to consider the information, ask questions and have had these answered satisfactorily. ☐

2. I understand that my participation is voluntary and that I am free to withdraw at any time without giving any reason, without my medical care or legal rights being affected. ☐

3. I understand that relevant sections of my medical notes and data collected during the study may be looked at by authorized individuals from the University of Oxford, from regulatory authorities or from the NHS Trust, where it is relevant to my taking part in this research. I permit these individuals access to my records. ☐

4. I understand that long term health outcome data will be collected by study investigators by securely accessing records held with the Health and Social Care Information Centre (HSCIC) and Office of National Statistics (ONS). I give permission for this. ☐

5. As part of the Research Study I understand that a study investigator will call me every other year (for ten years) by telephone to complete a brief questionnaire. ☐

6. I understand that ultrasound images, blood samples, samples of fat (adipose tissue), myocardial tissue and vascular tissue may be obtained during the bypass operation as part of this study. I also understand the images and samples may be stored in anonymised format as outlined in the information sheet and also for use in future ethically approved research and research publications. I give permission for this. I understand that my anonymised samples and/or data may be sent to other centers (including collaborators in UK or abroad and centers within the NIHR Bioresource). ☐

7. I understand that the treating surgical team will only be informed of the imaging findings if the results are relevant to my healthcare. I give permission for this. ☐

8. Applicable only to coronary bypass patients:

   (optional) I agree to undertake additional imaging (ultrasound/computed tomography angiography) at the follow up study visit. I understand that these examinations are performed exclusively for research purposes. ☐

9.. I agree to gift the images and samples taken for the purpose of the research study to the University of Oxford. If a commercial product were developed as a result of this study, I will not profit financially from such a product. ☐

10.. I agree to take part in the above study. ☐

11.. (optional) I agree to being contacted in the future to ask if I am interested in future related studies. ☐

Name of participant	Signature	Date

Name of person taking consent	Signature	Date

For researchers: original kept: copy given to participant (tick) ( ) ; copy inserted into medical notes ( )

Study Full Title	**Interactions between adipose tissue, vascular wall and myocardium in human atherosclerosis**
Patient ID	
Researchers	Prof Charalambos Antoniades (Tel 01865 221870)

Part B: Consent for genetic studies **Please initial box**

1. I understand that my DNA will be isolated and used in genetic research but that the results of these investigations will be used for research purposes only and will not be disclosed to me.

Name of participant	Signature	Date
Name of person taking consent	Signature	Date

For researchers: original kept: copy given to participant (tick) ( ) ; copy inserted into medical notes ( )

Appendix II

AdipoRedox Case Report Form

CASE REPORT FORM (AdipoRedOx 11/SC/0140)

INTERACTIONS BETWEEN ADIPOSE TISSUE, VASCULAR WALL AND MYOCARDIUM IN HUMAN ATHEROSCLEROSIS

CODE: **INITIALS:** **DATE:**

Demographics	
Age	
Gender (M/F)	
Ethnicity	
Hypertension / dur	
Hyperchol. / dur	
Diabetes mellitus / dur	
Smoker	
Family History	
LV function	
CCS	
NYHA class	
Previous MI	
Date of previous MI	
MI territories	
Number of VD	
LM	
LAD	
LCx	
RCA	
Previous PTCA	
PVD	
CVA / TIA	
Other Diseases	

Medication (type)	Dose

Measurements			
Weight (kg)		Height (cm)	
Waist (cm)		Hip (cm)	
Arm (cm)		Chest (cm)	
BP	/	HR	

Operative notes			
Operation		date	
Surgeon			
Euroscore		Off pump	
Clamp time		Bypass time	
N Vein grafts		LIMA	

Post-Operative notes			
Blood given		FFP given	
PLT given		Bleed in Hosp	
Days in CTCC		Days in CTW	
Days in hosp			
Ventilator (h)		Inotropes (d)	
AF in hosp		Day of AF	

Other post-operative notes

Echo data	
Surgical data	
NHS number	
Hospital number	
Other studies	
Adiporedox-CT	
Consent Copied	